



Universiteit  
Leiden  
The Netherlands

## **The RNA-binding protein Quaking in vascular health and disease**

Bruin, R.G. de

### **Citation**

Bruin, R. G. de. (2018, April 5). *The RNA-binding protein Quaking in vascular health and disease*. Retrieved from <https://hdl.handle.net/1887/60912>

Version: Not Applicable (or Unknown)

License: [Licence agreement concerning inclusion of doctoral thesis in the Institutional Repository of the University of Leiden](#)

Downloaded from: <https://hdl.handle.net/1887/60912>

**Note:** To cite this publication please use the final published version (if applicable).

Cover Page



Universiteit Leiden



The following handle holds various files of this Leiden University dissertation:

<http://hdl.handle.net/1887/60912>

**Author:** Bruin, R.G. de

**Title:** The RNA-binding protein Quaking in vascular health and disease

**Issue Date:** 2018-04-05

# The RNA-binding protein Quaking in vascular health and disease

R.G. de Bruin



The RNA-binding protein Quaking in vascular health and disease

ISBN: 978-94-028-0944-2

© R.G. de Bruin 2018

© Cover photograph: T.D. Matngelsen, USA, printed with permission

All rights are reserved. No part of this publication may be reproduced, stored in a retrieval system, or transmitted in any form or by any means, without permission of the copyright owners.

The research presented in this thesis was performed at the Eindhoven Laboratory of Experimental Vascular Medicine, Division of Nephrology, Department of Internal Medicine, Leiden University Medical Center, The Netherlands.

And the Lady Davis Institute for Medical Research, McGill University, Montréal, Canada.



# The RNA-binding protein Quaking in vascular health and disease

Proefschrift

ter verkrijging van  
de graad van Doctor aan de Universiteit Leiden  
op gezag van de Rector Magnificus prof. mr. C.J.J.M. Stolker  
volgens besluit van het College voor Promoties  
te verdedigen op donderdag 5 april 2018  
klokke 16.15 uur

door

Ruben Gosewinus de Bruin

geboren te 's-Gravenhage

in 1987

## Promotiecommissie

**Promotor** Prof. dr. A.J. van Zonneveld

**Copromotor** Dr. E.P. van der Veer

**Overige leden** Prof. Dr. A.J. Rabelink

Prof. Dr. P.H. Reitsma

Prof. Dr. D.E. Atsma

Prof. Dr. H. van Esch, Leuven University, Belgium

Prof. Dr. S. Richard, McGill University, Canada

dr. J.M. van Gils

## Financial support:

Medisch Specialistisch Bedrijf van het Groene Hart Ziekenhuis

Financial support by the Dutch Heart Foundation for the publication of this thesis is gratefully acknowledged

The cover of this thesis was generously provided by Thomas D. Mangelsen, <http://mangelsen.com>

*Opgedragen aan*  
*Dick Gosewinus de Bruin*



## Table of contents

<b>Chapter 1</b>	Preface: English and Dutch summary	9
<b>Chapter 2</b>	Scope of this thesis	13
<b>Chapter 3</b>	Introduction to cardiovascular disease and RNA biology	17
<b>Chapter 4</b>	The RNA-binding protein Quaking	29
<b>Chapter 5</b>	Emerging roles for RNA-binding proteins as effectors and regulators of cardiovascular disease <i>European Heart Journal 2016</i>	51
<b>Chapter 6</b>	Quaking, an RNA-Binding Protein, Is a Critical Regulator of Vascular Smooth Muscle Cell Phenotype <i>Circulation Research 2013</i>	77
<b>Chapter 7</b>	Quaking promotes monocyte differentiation into pro-atherogenic macrophages by controlling pre-mRNA splicing and gene expression <i>Nature Communications 2016</i>	105
<b>Chapter 8</b>	The RNA-binding protein quaking maintains endothelial barrier function and affects VE-cadherin and $\beta$ -catenin protein expression. <i>Scientific Reports 2016</i>	149
<b>Chapter 9</b>	Targeting Quaking ameliorates macrophage-induced renal interstitial fibrosis and induces alternative splicing of pre-mRNA transcripts in differentiated macrophages <i>Manuscript in preparation</i>	171
<b>Chapter 10</b>	Discussion & future directions	193
<b>Chapter 11</b>	Appendices	209
	Curriculum Vitae	
	Bibliography	
	Dankwoord	



# CHAPTER

Preface

1

## English summary

Within this thesis, several diseases central in the field of cardiovascular disease will be outlined. First, the central dogma of molecular biology, RNA biology in general, RNA (alternative)splicing and the role of RNA-binding proteins within these processes will be discussed to enhance the accessibility to non-molecular biologists (chapter 3). Subsequently, the current literature and insights into the RNA-binding protein Quaking will be outlined (chapter 4). Thereafter, a brief summary of the role of many distinct RNA-binding proteins (RBPs) in the cardiovascular system is provided, detailing their importance in the heart and cells of the blood vessels including endothelial cells, vascular smooth muscle cells and perivascular stromal cells (chapter 5). This review provides some historical and biological perspectives, while simultaneously highlighting many recent advances in our understanding of RBP function in cardiovascular health and disease.

Central to this thesis is the RBP called “Quaking”. This gene name was first coined in 1964 when a team of scientists in a renowned mouse-laboratory (Jackson Laboratories) encountered a shivering or “quaking” mouse with a tremor of the hind-quarters. By harnessing established and novel techniques, including RNA-sequencing, this thesis will describe the role of Quaking in vascular smooth muscle cells (chapter 6), monocytes/macrophages (chapters 7 and 9) and endothelial cells (chapter 8) within associated diseases such as vascular stenosis, atherosclerosis/inflammation and endothelial barrier function, respectively.

Collectively, Quaking can be described as a genome-wide governor of RNA-processing that results in the proper translation into functional proteins. The most prominent role of Quaking lies within the regulation of alternative splicing, facilitating the generation of a myriad of distinct proteins from a limited amount of genes. This ability to generate different proteins from the same gene marks a critical aspect of the human response to injury, as this process allows RBPs such as Quaking to improve or diminish how well a certain proteins work. Next to this, Quaking can influence how much of a given RNA will survive, where the RNA should be localised within the cell, and whether it should be translated into protein.

This thesis describes which RNA transcripts are under control of Quaking, which alternative transcripts are being generated through modulation by Quaking, while also describing the unique role for this protein in health and cardiovascular and renal disease.



## Nederlandse samenvatting

Binnen de hart- en vaatziekten vallen meerdere ziektebeelden waarvan de moleculaire en cellulaire pathofysiologie in dit proefschrift is onderzocht en beschreven. Inleidend wordt het centrale dogma van de moleculaire biologie, de diverse functies van RNA-bindende eiwitten in het algemeen en het proces van (alternatieve) splicing van RNA nader toegelicht om de leesbaarheid van dit proefschrift te bevorderen voor lezers die geen of weinig affiniteit hebben met de moleculaire biologie (hoofdstuk 3). In hoofdstuk 4 zal het RNA-bindende eiwit Quaking uitvoerig besproken worden. Vervolgens zal in hoofdstuk 5 beschreven worden welke RNA-bindende eiwitten tot op heden zijn onderzocht binnen cardiovasculaire ziektebeelden, met daarin vele voorbeelden van binnen het hart, het endotheel, de gladde spiercellen en de perivasculaire fibroblasten.

Centraal in dit proefschrift staat één RNA-bindend eiwit genaamd Quaking. Deze naam werd in 1964 voor het eerst genoemd toen enkele wetenschappers een “trillende muis”, vertaald naar het Angelsaksisch “a quaking mouse”, tegenkwamen in een gerenommeerd muizen-laboratorium (Jackson laboratories). Door gebruik te maken van gevestigde én nieuwe technologieën zoals RNA-sequencing, welke in de recente jaren het begrip van de cellulaire biologie exponentieel hebben doen toenemen, beschrijft dit proefschrift de rol van Quaking in gladde spiercellen (hoofdstuk 6), monocyten danwel macrofagen (hoofdstuk 7 en 9) en endotheelcellen (hoofdstuk 8) binnen gerelateerde ziektebeelden zoals vasculaire (re)stenose, aderverkalking, danwel inflammatie en de barrière functie van het endotheel.

Samenvattend kan de functie van Quaking beschreven worden als een eiwit dat genomwijd betrokken is bij het in goede banen lijden van het gehele traject van RNA naar functionele eiwitten. De meest prominente rol voor Quaking betreft de alternatieve splicing van RNA, een proces dat uiteindelijk voor een enorme diversiteit aan niet-coderende RNA's en eiwitten zorgt welke vele malen groter is dan het aantal genen dat een organisme heeft. Daarnaast bepaalt Quaking voor een deel de hoeveelheid van een target-RNA, de lokalisatie ervan binnen de cel én de vertaling van mRNA naar eiwit.

Dit proefschrift beschrijft onder andere welke RNA's onder invloed van Quaking staan, welke alternatieve transcripten worden aangemaakt dankzij Quaking en illustreert een unieke rol voor dit eiwit binnen het ontstaan van hart-, vaat- en nierziekten.



# CHAPTER

Scope of this thesis

# 2

## Scope of this thesis

Within this thesis, the function of the RNA-binding protein Quaking in the context of several inflammatory cardiovascular diseases has been investigated.

In **chapter 3**, an introduction and summary of the epidemiology, aetiology, risk factors and socio-economic impact of cardiovascular disease will be shortly outlined. Subsequently, the cellular mechanisms that lie at the basis of the pathophysiology of these diseases will be introduced. Thereafter, to enhance accessibility of this thesis to non-molecular biologists, the role of RNA-binding proteins in post-transcriptional regulation of RNA (with a focus on the process of alternative splicing) is discussed. **Chapter 4** encompasses a detailed review of the functional role of the RNA-binding protein Quaking, in embryonic and adult cardiovascular biology, along with an examination of the diverse (auto-)regulatory pathways that impinge on QKI protein isoform expression levels.

**Chapter 5** provides a historical perspective and detailed review of the current literature wherein the function of many RNA-binding proteins in both cardiac and vascular disease is described. Furthermore, we summarise how the latest technological advances and insights gained in RNA biology have ushered in a new era in RNA-based therapeutics that could facilitate the targeting of RBPs, and potentially the amelioration of cardiovascular disease.

A striking example of the profound impact that alternative splicing can have on the risk of vascular disease is provided in **chapter 6**. Here, we illustrate how QKI mediates the generation of two distinct Myocd protein isoforms that determine VSMC function in the setting of intimal hyperplasia, and demonstrate that diminishing QKI expression is an effective means of preventing excessive stenosis of arterial vessel upon damage.

As opposed to describing how a single alternative splicing event affects cellular homeostasis, **chapter 7** provides a genome-wide assessment of QKI-mediated post-transcriptional processing in monocytes and macrophages. In doing so, we have identified an important regulatory role for QKI in guiding the cellular properties of these inflammatory myeloid cells that accumulate in atherosclerotic lesions, and thereby gain a broader understanding of how these cells contribute to vascular disease and patient mortality worldwide. Moreover, using RNA-sequencing and splicing-sensitive microarray analyses, we could demonstrate a conserved mechanism by which QKI mediates alternative splicing in a position-dependent fashion.

Having focused on the regulatory role of QKI on RNA splicing in the previous chapters, **chapter 8** illustrates how QKI can also regulate mRNA translation (in endothelial cells). Using molecular techniques that assess the intricate process of mRNA translation into protein, we could identify that adequate expression and functionality of QKI is a prerequisite for the translation of the vascular-endothelial-cadherin and  $\beta$ -catenin mRNAs into functional proteins. Moreover, the functional consequences of destabilizing these transcripts and thereby the protein levels of their junctional proteins by targeting QKI strongly suggests a facilitatory role in the maintenance of a healthy endothelial monolayer and the maintenance of proper barrier function.

**Chapter 9** illustrates the consequences of monocyte- and macrophage-induced injury to the kidney, an inflammatory process that triggers the activation, proliferation and extracellular matrix production of perivascular cells. Using a recently developed conditional null allele of the *qki* locus, we could demonstrate that cell autonomous abrogation of QKI in monocytes and macrophages ameliorates the inflammatory damage within the kidney as evidenced by reduced renal interstitial fibrosis.

Collectively, this thesis details an upstream regulatory role for QKI in orchestrating the cellular response to disease-inducing stimuli in inflammatory vascular diseases such as intimal hyperplasia, atherosclerosis, endothelial dysfunction and kidney fibrosis. **In chapter 10**, these findings are evaluated in varying perspectives, which in keeping with 'scientific thought process' leads to a discussion that addresses several remaining questions that could be subject of further investigation.



# CHAPTER

Introduction to cardiovascular disease  
and RNA biology

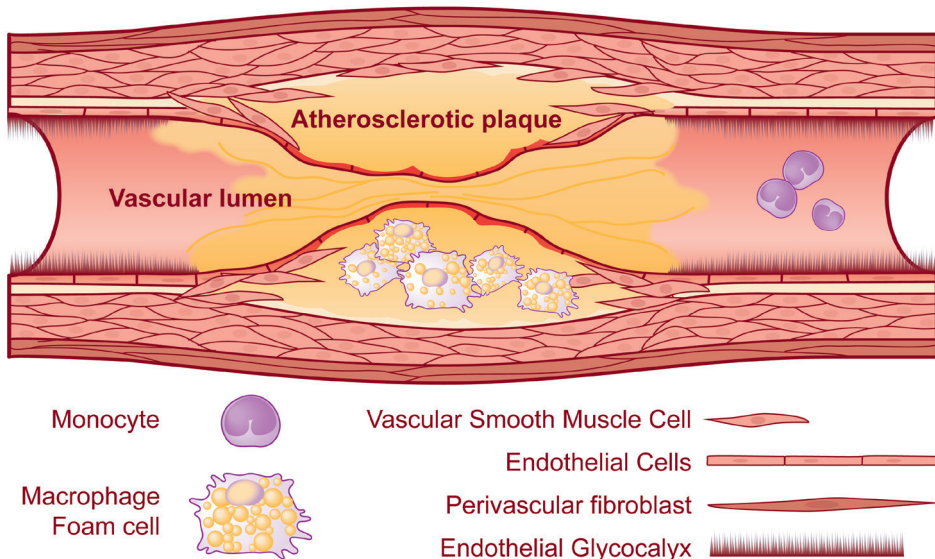
# 3

## Introduction

3

### Epidemiology, aetiology, risk factors and socio-economic impact of cardiovascular disease

Cardiovascular disease (CVD) encompasses the pathophysiology of a large variety of diseases that affect the heart and blood vessels throughout the human body. As defined by the World Health Organisation (WHO), roughly 80% of cardiovascular mortality is determined by the incidence of coronary heart disease and cerebral stroke, leading to an average of 14 million deaths worldwide on a yearly basis<sup>1,2</sup>. As a result of numerous technological and pharmacological advances, alongside increased efforts that focus on prevention, CVD mortality has been dramatically reduced. This diminution in prevalence is predominantly driven by decreased coronary heart disease and cerebral stroke as a result of increased standard of living in Europe<sup>3</sup> and the United States<sup>4,5</sup>. The most common pathophysiological process that drives this high mortality rate is atherosclerosis, a chronic progressive inflammatory disease of the vessel wall that affects the medium and large-sized arteries<sup>6</sup>. Atherosclerosis involves the accumulation of cholesterol deposits, proliferating smooth muscle cells and inflammatory cells in the intimal layer of the arterial wall, leading to the formation of atherosclerotic plaques that result in luminal narrowing and a fragile inner vessel lining<sup>7,8</sup>. Lesion progression and exacerbation can eventually trigger plaque rupture, leading to arterial occlusion and irreversible organ dysfunction as a result of hypoxia and ensuing tissue fibrosis<sup>9-11</sup>. The pathogenesis of atherosclerosis is illustrated in figure 1 (not to scale, adapted from<sup>12</sup>).





CVDs can roughly be divided in the most prevalent, macro-vascular diseases such as ischaemic heart disease, cerebral stroke, peripheral arterial disease and microvascular dysfunction; and the less prevalent diseases such as congenital heart disease, rheumatic heart disease, cardiomyopathies, cardiac valve disease and cardiac arrhythmias<sup>1,2</sup>. Moreover, a progressive decline in kidney function, termed chronic kidney disease (CKD) has also been proposed to be a vascular disease and is also causally involved by accelerating atherosclerosis development and progression<sup>13</sup>. Interestingly, the leading causes of CKD, hypertension and diabetes, are also prominent drivers of CVD<sup>14</sup>, further substantiating this intimate relationship between these two seemingly different diseases.

Numerous risk factors for the development of CVD have been extensively studied, including gender, hypertension, diabetes, smoking, degree of physical activity, obesity, hyperlipidaemia and diet. Other less known predisposing factors include standard of living, education level, air pollution, inherited predisposition and psychological factors<sup>1,2</sup>. Despite advances in the screening for these risk-factors, in combination with primary- and secondary prevention methods such as lipid lowering therapy and blood pressure regulation in developed countries, CVD prevalence remains high, and has in fact increased in recent years nationally and worldwide. More concerning is the projected further increase in the coming years in middle- and low-income countries<sup>5</sup>. This is widely being attributed to the alarming increase in the prevalence of obesity (and thus type 2 diabetes), but also the irreversibility of atherosclerotic or ischemic disease with currently available therapies<sup>15</sup>.

Furthermore, the large effect of a cardiovascular or cerebral event on life expectancy, quality of life, the disability adjusted life years (DALYs = the years lived with disability + years of life lost) and health-related productivity loss, are directly linked with CVD-associated increased healthcare costs. Although adequate data from low and middle income countries regarding health-related productivity loss and DALYs is sparse, recent analyses illustrate the growing problem of CVD on increasing healthcare costs worldwide and pinpoint CVD as the largest healthcare expenditure worldwide<sup>16,17</sup>. Illustrative of this is the fact that the United States spends the largest proportion of their gross domestic product (GDP) on healthcare in general as compared to other countries; more than 17% of the GDP in 2014. The annual costs attributed to the treatment of cardiovascular disease surmounts 320 billion US dollars, roughly 2.5% of the GDP, with similar numbers being observed in other developed countries, including the Netherlands (8-12% of the GDP on healthcare)<sup>18</sup>.

Therefore, to more effectively treat CVD, a better understanding of CVD pathophysiology is required in order to develop novel regenerative therapeutics that could improve the quality of life for CVD patients, while also reducing the financial burden on healthcare systems worldwide.

### How cellular phenotype drives cardiovascular disease

Driven by major technological advances, our understanding of the pathophysiology and cellular biology within CVD has exponentially increased in past decades. These advances not only include the development, but perhaps most importantly the general availability of research techniques such as polymerase chain reaction (PCR), microarrays, DNA/RNA sequencing, proteomics, cell/tissue culture techniques (including stem cell culture and differentiation), and high-power (fluorescence) microscopy that collectively enable the precise assessment of cellular changes upon disease triggers. As described in this thesis, the cardiovascular system encompasses many different cell types that are cooperatively involved in the reparative response upon cardiovascular damage. Cardiomyocytes for example, the primary constituent of the heart muscle, are required to rhythmically contract to ensure proper blood distribution throughout the body. Upon increased mechanical stress, e.g. by either pulmonary or arterial hypertension, cardiomyocytes undergo a phenotypic change known as hypertrophy, a collective volume increase that is designed to enhance contractility and ensure adequate blood propulsion<sup>19,20</sup>. However, the extent to which this compensatory mechanism can proceed is limited, and an excessive hypertrophic response is tightly coupled to heart failure. In contrast, severe ischemic injury to the heart leads to cardiomyocyte loss, and irreversible fibrosis of heart tissue caused by the activation, proliferation and production of extracellular matrix by tissue-resident fibroblasts<sup>21</sup>, collectively resulting in a dysfunctional myocardium. In the kidney, a similar pathophysiology process occurs upon (vascular) damage in the kidney, resulting in a progressive decline in kidney function due to the activation of perivascular fibroblasts<sup>22</sup>. Importantly, this again illustrates the pathophysiological overlap between cardiac and renal dysfunction.

Although many other cell types are implicated in the pathogenesis of atherosclerosis<sup>23,24</sup>, the activation and recruitment of monocytes to atherosclerotic plaques is central to both disease severity and progression<sup>25</sup>. Activation of these circulating immune cells at atheroprone sites in the vasculature triggers their adhesion to the vascular endothelium and migration to the sub-endothelial space. Here, in response to the local milieu they differentiate into macrophages<sup>26</sup>, where they locally phagocytose lipid particles and undergo a transformation into foam-cells. This generally results in their entrapment in the neointimal space<sup>7,27</sup>. Moreover, local proliferation within, but also perturbed emigration of macrophages from the atherosclerotic plaque has been implicated as a key determinant of atherosclerotic disease advancement<sup>27,28</sup>.

Within the setting of vascular injury, vascular smooth muscle cells (VSMCs) are important mediators of vascular repair. Residing in the medial layer of arteries, they normally provide vascular tone and regulate vascular diameter, thereby controlling blood pressure in concert with endothelial cells (ECs)<sup>29</sup>. In response to vascular injury, these contractile cells adopt a proliferative, synthetic highly hyperplastic phenotype that is involved in many vascular diseases, including atherosclerosis and restenosis upon arterial stenting, peripheral bypass grafting<sup>30</sup> or the creation of an arteriovenous fistula for hemodialysis<sup>31,32</sup>.

ECs line lumen of the vasculature throughout the body, contributing to vascular tone through nitric oxide production<sup>33,34</sup>, vascular barrier function<sup>35</sup> including the blood-brain barrier<sup>36</sup>, vascular stiffness<sup>37</sup>, leukocyte adhesion and diapedesis<sup>38</sup>, angiogenesis<sup>39</sup>, and hemostasis<sup>40</sup>. Alongside their mosaic patterning and phenotypic diversity of ECs in blood vessels, ECs also display organ-specific phenotypes<sup>41</sup>, as evidenced by ECs in the kidney which also facilitate the glomerular filtration barrier by forming fenestrae. This EC phenotype and the endothelial glycocalyx therein<sup>43</sup> is observed in no other organ<sup>42</sup>. More traditionally, ECs have predominantly been attributed critical roles in atherosclerosis, diabetes and hypertension<sup>44-46</sup>, as their dysfunction is tightly coupled with the development and progression of CVD. Collectively, given the diverse functions of ECs and their highly organ-specific phenotype, the function, adaptation and phenotype alteration upon organ damage is therefore also immensely diverse<sup>47</sup> and not fully understood.

### **The intricate path of DNA to RNA to protein expression**

It could be argued that in the past decades, few biological processes have been revised as extensively as the central dogma of molecular biology. First described by Francois Jacob and Jacques Monod in 1961, messenger RNA represented an intermediate between the information contained in our DNA and the proteins that these genetic sequences encode. To date, this relatively simplistic relationship between DNA and protein continues to be propagated due to its' conceptual clarity. In reality, this process is much more complex than common graphical representations, and has therefore been elaborated in figure 2, pinpointing the biology described within this thesis. As such, investigation of these manifold RNA processing events can increase our understanding of CVD pathophysiology.

Historically, the field of molecular biology has largely focused on transcriptional mechanisms, investigating proteins that drive the transcription of DNA into RNA. These proteins, known as transcription factors, bind to the promoter region that lies upstream of the transcriptional start site and drive the expression of a target gene. Importantly, the realisation that the transcriptional activity of genetic loci was not directly correlated with expression levels of the corresponding proteins led researchers to further investigate RNA expression levels, previously considered to serve as an intermediate between these two extremes. This led to the realization that RNA co-transcriptionally associates with RNA-binding proteins (RBPs) and non-protein coding RNAs, forming so-called heterogenous nuclear RiboNucleoProtein complexes (hnRNPs that facilitate subsequent RNA-processing<sup>48</sup>. Paradoxically, while only 2.94% of the total DNA sequence encodes for proteins in humans, a striking 74.7% of our DNA is actively transcribed into RNA by energy-dependant RNA-polymerases<sup>49</sup>. This marked investment of cellular energy resources into transcription suggests that alongside sequence that generates proteins, transcription the non-protein coding portions of our genome also contribute to our biological complexity.

*“This preservation of favourable variations and the rejection of injurious variations, I call Natural Selection. Variations neither useful nor injurious would not be affected by natural selection and would be left a fluctuating element.”*

Charles Darwin – 1859 <sup>50</sup>

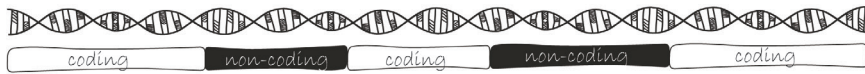
Following this theorem, the entry and expansion of non-protein coding DNA that is actively transcribed into RNA has been thought to be a favourable process as it coincides with the transition from the unicellular- to the multicellular world (and is highly conserved throughout species)<sup>51</sup>. Interestingly, protein domains involved in RNA metabolism (such as those involved in RNA methylation, polyadenylation and RNA degradation) are markedly conserved throughout bacteria, archaea and eukaryotes. As such, it has been suggested that the selective introduction of certain RNA-binding domains into eukaryotic proteins that regulate alternative splicing are in particular responsible for the existence of more complex life-forms such as vertebrates<sup>52,53</sup>.

In recent decades, major technological advances have, similar to the invention of the printing press during the cultural and scientific Renaissance starting in the 14th century, greatly facilitated our understanding of this ncDNA or “Junk DNA”<sup>54</sup>. While numerous conceptual advancements provided new insight into the complexity of our genome, it could be postulated that the development of Sanger sequencing marks the start of the RNAissance, as now it was possible to determine the exact nucleotide sequence that corresponds to a stretch of DNA. The further development of such techniques in laboratories worldwide, collectively resulted in the collaborative effort to fully map the human DNA sequence in 1990, also known as the Human Genome Project<sup>55</sup>. Officially completed in 2003, it was succeeded by the Encyclopedia of DNA Elements, or ENCODE project, that yielded an unprecedented collection of biological data pertaining to genomes from several species<sup>56</sup>. Whereas initial genome sequencing experiments focussed on protein-coding DNA, the so called transcriptional-tiling arrays and ensuing “exome sequencing” allowed for the investigation of the cellular “transcriptome” by mapping virtually all transcribed DNA. Moreover, this technique made it possible to accurately identify and quantitate coding and non-coding RNA sequences, including alternatively spliced RNAs.

# The central dogma of molecular biology

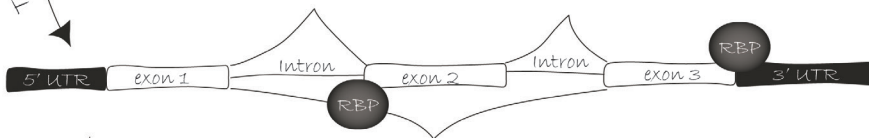
From

DNA



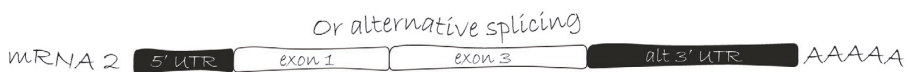
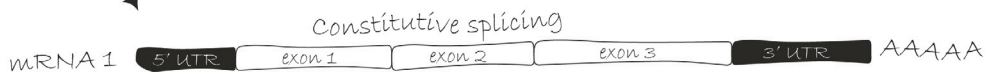
Transcription

to pre-mRNA



splicing

to mature mRNA through:



Translation

to Protein diversity



## An introduction to RNA splicing

The capacity of an organism to generate a multiplicity of distinct proteins from a single gene locus, as well as the ability to generate functional non-protein coding RNAs, has been proposed to determine organismal complexity. For example, the human- and the common roundworm (*Caenorhabditis elegans* or *C. elegans*) genome are both estimated to encode in the range of 20,000 distinct protein-coding genes. However, their total genomes differ immensely in size (3,2-Gigabases for humans vs 100-Megabases for *C. elegans*), suggesting that the expansion of non-protein coding DNA could assist in explaining the chasm in organismal complexity. When comparing these numbers amongst prokaryotes, eukaryotes, plants, invertebrates and vertebrates, this discrepancy becomes even more pronounced (as illustrated and discussed in <sup>51</sup>).

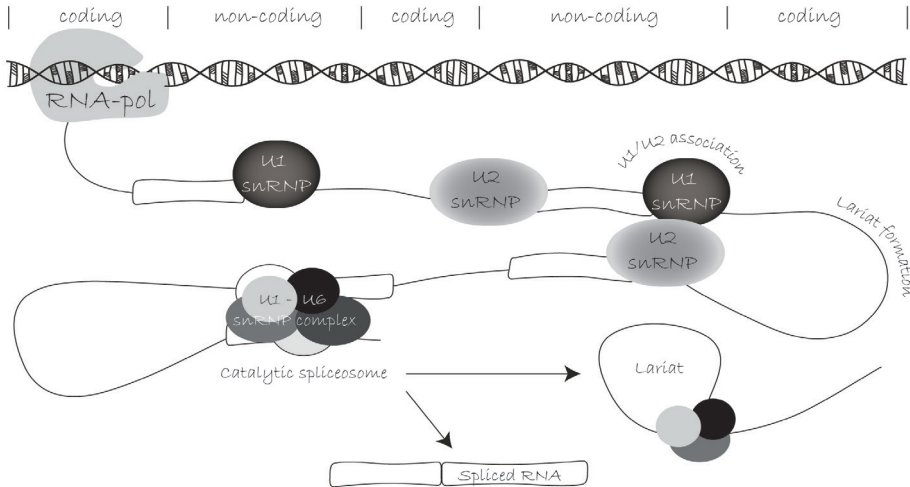
If one focuses on protein-coding genes, the initial RNA transcripts generated from these sequences harbours both protein-coding and non-protein-coding stretches, termed exons and introns respectively. After transcription, a highly regulated process termed splicing removes the introns, while simultaneous modifications to the 5' and 3' end of the transcript occur, yielding a protein coding messenger RNA (mRNA) and lariat(s) from the spliced intron(s). The human cellular infrastructure facilitates this alternative splicing of the pre-mRNAs in order to create on average 6.3 distinct mature mRNAs per gene that result in an average of 3.9 distinct protein isoforms from one single gene locus<sup>56</sup>. More recently, splicing has also been implicated in the generation of functional non-protein coding RNAs<sup>57</sup> and circular RNAs<sup>58</sup> that can be translated into formerly unknown micro-peptides<sup>59,60</sup>.

These aforementioned splicing reactions are catalysed in a dynamic RNA-protein complex termed the spliceosome. This complex exhibits enormous plasticity in target RNA recognition, a process that is affected by a variety of non-protein coding RNAs and associated RNA-binding proteins (RBPs) that are conferred with the capacity to physically interact with RNA in a sequence- or structure specific fashion<sup>48</sup>. Collectively, the spliceosome can pinpoint the exact nucleotide location of splicing-initiation and either enforce or repress splicing. This regulatory capacity can thereby mediate: 1) constitutive splicing, where all exons in a transcript are included; or 2) alternative splicing, where selected exons can be included or excluded in the final transcript. Other variations to mature-mRNA diversity induced by alternative splicing include alternative 5' or 3'splice sites of exons, alternative 5' or 3'UTRs, or intron retention<sup>61</sup>. A direct result of the increased number of sequenced human genes, and following completion of the human genome project in 2003, close examination of the human genomic sequence enabled researchers to identify repeating elements that flank protein coding exons<sup>62</sup>. These studies revealed that: 1) the exact definition of exon size was encoded in the DNA sequence, as defined by either 5' (GURAGU motif) or 3' (YAG motif) splice sites, where R is any purine and Y is any pyrimidine<sup>63</sup>; and 2) certain recurrent sequence motifs were present within and flanking the exon of interest (termed splicing regulatory elements: SREs)<sup>64-66</sup>. These sequences are termed either Exonic or Intronic Splicing Enhancers or Silencers (ESE/ESS or ISE/ISS, respectively).

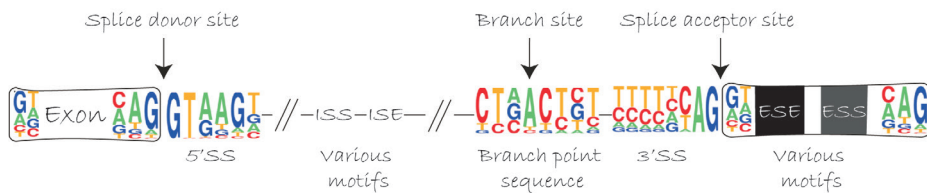
## Splicing regulation

3

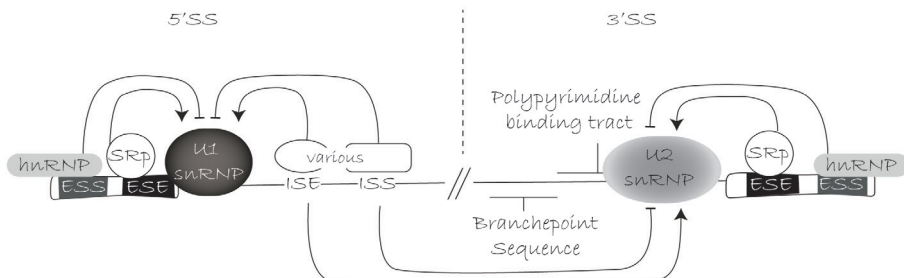
co-transcriptional spliceosome assembly



Splice site consensus sequence



## Regulation of alternative splicing





However, the implementation of bio-informatic approaches to predict alternative splicing patterns in a cell type-specific fashion based solely on the presence and sequence of these regulatory elements remains challenging. This is due to the fact that RBPs are differentially expressed in certain tissues as well as in health and disease states, gene abundance can impact RBP association with the target RNA, secondary structure of RNAs can impact splicing, or cryptic splicing enhancers/silencers at more distant sites from the alternative exon could impact the splice site usage<sup>48</sup>. These regulatory elements, as well as the process of splice-site selection are illustrated in figure 3 (adapted from <sup>63,67,68</sup>).

### **RNA-binding proteins and the recognition of target RNAs**

Approximately 80% of RBPs are ubiquitously expressed throughout human tissues. Recent estimates suggest that a striking 20% of the protein-coding transcriptome is mRNA encoding RBPs<sup>69</sup>. RBPs are typically categorised based on protein substructure, or their RNA-binding domain (RBD) that confers the capacity to interact with target RNAs. Common RBDs include the: 1) RNA-Recognition Motif (RRM); 2) DEAD-box helicases; 3) double-stranded RNA-binding domains; 4) zinc-finger domains; and 5) K-homology (KH) domains, which are extensively reviewed in <sup>69</sup>. Interestingly, these classical RBDs are modular and can be found in a variety of distinct RBPs that guide the recognition of their respective RNA targets. Moreover, many RBPs encode multiple distinct RBDs. The function of this modular design and sequence specificity of RBPs will be elaborated in the discussion of this thesis. Based on the presence of these RBDs, *in silico* analyses led to initial estimates of roughly 700 distinct RBPs <sup>70,71</sup> in humans, and their binding motifs showed remarkable evolutionary conservation with paralogs of other species<sup>52,72</sup>. The use of genome-wide RBP identifying techniques such as RNA-IP followed by mass spectrometry, and the validation and the assembly of multiple pre-existing databases, resulted in a census of roughly 1500 RBPs that now also includes numerous RBPs that do not possess canonical RBDs but instead contain intrinsically disordered regions that are responsible for RNA binding <sup>69,73,74</sup>. Experimental approaches that contributed to this comprehensive census of RBPs include the cross-linking and immunoprecipitation of RBPs bound to target RNAs. With this material, followed by next-generation sequencing (also known as CLIP-Seq or HITS-CLIP<sup>75</sup>), one can identify with single-nucleotide resolution the RBP binding sites. Recently developed variants of this technique are Photoactivatable Ribonucleoside-Enhanced Crosslinking<sup>76</sup> (PAR-CLIP), individual nucleotide-resolution cross-linking and immunoprecipitation<sup>77</sup> (iCLIP), and enhanced CLIP (eCLIP)<sup>78</sup>. Other methods to assess RNA-interacting partners rely on mass spectrometry to identify proteins associated to labelled and subsequently purified RNA. In depth comparison of technique methodology and validity has been elegantly reviewed previously<sup>79</sup>.



This expanding capacity to identify and validate RNA-RBP interactions, provided key insight into the sequence-specific binding properties of RBPs. The aforementioned high throughput technologies have facilitated major progress in generating a compendium of RNA-binding motifs for a significant number of RBPs amongst species<sup>80</sup>. Although these insights have greatly expanded our predictive capacities to determine the RNA targets of a RBP of interest within a cell-type, the *in silico* prediction of a certain RBP actually binding at a certain RNA, and the subsequent effect on RNA-processing *in vivo* remains challenging and will be further elaborated in the discussion of this thesis.

As previously mentioned, the majority of our DNA is actively transcribed into RNA. At present, many subclasses of transcribed RNA have been described that do not encode for proteins. These include long non-coding RNAs (lncRNAs), microRNAs (miRNAs), piwi-interacting RNAs (piRNAs), transfer RNAs (tRNAs), ribosomal RNAs (rRNAs), Small Cajal body-specific RNAs (scaRNAs), small nucleolar RNA (snoRNAs), small nuclear RNAs (snRNAs) and many others<sup>54</sup>. The subsequent routing within the cell, the processing and editing of these diverse RNA species encoded within our DNA, requires exact coordination to facilitate their cellular function. To a large extent, the assembly of ribonucleoprotein complexes (RNPs) co-transcriptionally determines initial RNA fate<sup>81</sup>. Therefore, RBPs orchestrate proper RNA processing by co-ordinating alternative splicing (as discussed below), secondary structure mRNA localisation, stability, and translation, as reviewed in<sup>82</sup>. Here below, the role the RBP Quaking plays in guiding these regulatory events will be discussed.



# CHAPTER

The RNA-binding protein Quaking

# 4

## The RNA-binding protein Quaking

*“Quaking is a new autosomal recessive mutant mouse with marked tremor of the hindquarters.”*

*Sidman et al. 1964 - Science<sup>83</sup>*

Based on the clear phenotype observed in the Quaking viable (qkv) mouse, QKI was initially attributed a sole role in the physiologic functioning of the nervous system. Indeed, Sidman and co-workers primarily demonstrated defective myelination of the central nervous system<sup>83</sup>, a phenotype that could also be observed in the peripheral nervous system<sup>84</sup>. Importantly, Kondo and co-workers investigated the QKI locus in qkv mice, and identified a megabase deletion in the promoter region that not only markedly reduces QKI expression, but also prevents expression of parkin (PARK2) and parkin co-regulated gene (PACRG). Nonetheless, the mouse still generally serves as a reliable model for in vivo studies into the consequences of perturbed QKI expression. Indeed, many studies focused on the biochemical and lipid composition of the qkv brain to evaluate this myelination defect<sup>85-96</sup> along with electron/light microscopy studies<sup>97-99</sup>. Erroneously, diminished QKI levels were also deemed to be responsible for the sterility of homozygous qkv male mice<sup>100,101</sup>, albeit that subsequent studies by Lorenzetti and co-workers uncovered that this was instead the result of decreased Parkin expression<sup>102</sup>.

The development of molecular biological technologies such as PCR enabled researchers to analyse how QKI deficiency, as observed in the qkv mouse, triggered a myelination-defect in the central and peripheral nervous system. An early study in 1985 pointed towards a role for QKI in guiding alternative RNA processing, resulting in two RNA transcripts of the protamine 1 RNA, in this situation a product of alternative adenylation<sup>101</sup>. Subsequent analysis of gene expression identified a pivotal role for QKI in the regulation of expression levels of proteolipid protein (PLP), basic protein (BP), and myelin-associated glycoprotein (MAG) RNAs<sup>103</sup>. The first indication that QKI also functions as a regulator of RNA-splicing was published by Fujita and co-workers, who discovered that a reduction of QKI led to defective splicing of the myelin-associated glycoprotein pre-mRNA<sup>104</sup>. Interestingly, this shift was subsequently demonstrated to attenuate translation of the alternative mRNA-encoded isoform<sup>104</sup>. Alongside a role in regulating transcript stability and splicing, Barbarese were the first to identify a critical role for QKI in guiding the localization of RNA molecules within the cell, as oligodendrocytes derived from qkv mice were characterized by perturbed distribution of the MBP mRNA in the processes and instead a cell body retention<sup>105</sup>. Collectively, these studies highlight an important role for QKI in myelination of the nervous system, and have greatly contributed to our understanding of the protein QKI in general. In the last two decades however, QKI has also been implicated in stem-cell biology, inflammation, schizophrenia, 6q terminal deletions and numerous cancers. Given some excellent reviews on the role of QKI in all of these diseases<sup>106-108</sup>, this will not be discussed in within this thesis.

### Quaking in cardiovascular embryogenesis

A first glimpse regarding a potential role for QKI outside the nervous system was published in 1988, following the generation of ethylnitrosurea (ENU)-induced QKI mutations in mice. The resultant embryos showed early developmental arrest on day 9, prompting researchers to investigate whether defective QKI protein was causal for this striking phenotype. These initial studies demonstrated a variety of structural abnormalities, but most prominent were developmental defects of the brain, haemorrhaging in the mesencephalon and in one embryo a strikingly enlarged heart with pericardial effusion<sup>109</sup>. Interestingly, given that myelination of the nervous system occurs post-natally in mice, the embryonic death 9 days post-fertilization suggested that a non-neurological pathway is responsible for the observed lethality<sup>109</sup>. Nearly a decade later, strong QKI expression was also reported in mouse lung, heart and testis, alongside the liver, spleen, kidney and ovary<sup>110</sup>, suggesting at the tissue-level that QKI is ubiquitously expressed. Subsequent studies by Tanaka and colleagues using whole-mount RNA in situ hybridization in zebrafish embryos revealed QKI expression in the cardiac sac and pectoral fin buds at hatching, and in earlier developmental stages within the mesoderm<sup>111</sup>, namely primordial cells that give rise to e.g. vascular smooth muscle, cardiac muscle or skeletal muscle, but also the kidneys, connective tissue and the endothelium. Interestingly, red- and white blood cells, including monocytes and tissue-residing macrophages such as microglia and Kupffer cells, are derived from the embryonic mesoderm<sup>112</sup> putting forth the hypothesis that QKI could be involved in all mesoderm-derived cellular lineages.

The striking evolutionary conservation of QKI homologs in many species<sup>113</sup>, such as *Caenorhabditis elegans* (*C. Elegans*), *Drosophila melanogaster* (*D. melanogaster*) and *Xenopus laevis*, have furthermore increased our understanding of the protein QKI in the cardiovascular system. One such example is the *D. melanogaster* homolog of QKI, termed held-out-wings (HOW) that was described to affect the cardiovascular system. Initially attributed to perturb flying and wing-position by obstructing muscle differentiation<sup>114</sup>, Zaffran et al. described similar defects in muscle differentiation that resulted in altered cardiac heart rate and myoblast contractile activity<sup>115</sup>. Notably, both studies confirmed a strong mesodermal and cardiac HOW expression. These findings were further corroborated by Zorn & Krieg who, based on experimental assessment of the in vitro RNA-binding capacity of *Xenopus* Quaking (Xqua), were the first to suggest that QKI binds to RNA targets as homodimers. Moreover, they also demonstrated distinct subcellular localization of the Xqua proteins and pinpoint the region of the nuclear localization signal<sup>116</sup>. Subsequently, the report by Kondo et al. in 1999 not only describes the genomic organization of the mouse qk locus, but also provides the first conclusive evidence that the QKI proteins are ubiquitously expressed in all assessed tissues using novel antibodies that selectively recognized QKI-5 and QKI-6 in lung, heart, liver, spleen, kidney muscle, testis and uterus<sup>117</sup>.

As previously mentioned, given that embryonic lethality is induced before myelination starts, Noveroske undertook an in depth assessment of the cardiovascular link with premature death. They concluded that QKI is expressed at the interface between the yolk sac endoderm and the mesodermal site where blood islands develop, the site where endothelial cells and blood cells form during embryogenesis<sup>118</sup>. Moreover, they showed that defective vascular remodelling coincided with the time of embryonic death. The pericardial effusions observed in developing QKI deficient embryos led to a more exact investigation of the vascular anatomy, revealing disorganised endothelial, smooth muscle, and pericyte alignment 9.5 days after fertilization. Of particular interest was the pronounced decreased in size and branching of the arteries together with the inability of perivascular cells to surround newly forming vessels<sup>118</sup>. The multifactorial and complex nature of the vascular defect (perturbations in endothelial, perivascular and endodermal cell function) prevented the authors from pinpointing causality. However, shortly thereafter, it was shown that 1) QKI is expressed in both ECs and VSMCs during embryogenesis (along with cardiomyocytes, endocardium, gut epithelial cells, and striated muscle); and 2) VSMC differentiation in particular is selectively perturbed in an in vitro angiogenesis assay, suggesting that this defect is responsible for the observed embryonic lethality in *qk* deficient mice<sup>119</sup>. Contrasting evidence was later provided in 2006, suggesting that the abrogation of QKI expression in the visceral endoderm is responsible by altering the production of secreted proteins that are required for vascular patterning, such as alpha-Fetoprotein, claudin-7 and retinaldehyde dehydrogenase 2. Moreover, expression levels of the pivotal angiogenesis inducer VEGF-A were not altered at the mRNA-level but were markedly reduced at the protein levels in the yolk sac of the *qk*-deficient embryos<sup>120</sup>. A subsequent study supported these findings by illustrating that QKI regulates the expression of secreted angiogenic proteins such as VEGF-A, bFGF and PDGF, thereby affecting in vitro angiogenesis in murine embryonic endothelial cells (MEECs)<sup>121</sup>. Based on these observations, we postulate that the vascular malformations in QKI deficient mouse embryos likely represent a combinatorial effect ECs, VSMCs and visceral endoderm defects. Further studies using conditional QKI knockout mice might reveal more information regarding this lethal phenotype.

### **Quaking in the adult vasculature of mice and men**

Up to this point, studies investigating QKI focused solely on cardiovascular development based on embryonic and/or neonatal defects and mechanisms. Chapter 3 of this thesis represents the first report that demonstrates a role for QKI in the adult vasculature and vascular disease<sup>122</sup>. The pivotal role in VSMC differentiation was recently further corroborated<sup>123</sup>. Moreover, chapter 5 confirms a critical role for QKI in adult human and mouse endothelial cells<sup>124</sup> that was further supported and elaborated on by a comprehensive report showing a pivotal role for QKI EC differentiation, neovascularization, and angiogenesis<sup>125</sup>.

Although the field of QKI-mediated RNA processing in cancer has progressed rapidly, reports addressing the role of QKI in the physiology of haematopoiesis and myeloid cell differentiation are limited. Indeed, early studies already indicated reduced numbers of red blood cells in mouse embryo blood islands<sup>118</sup>, while recent work has indeed confirmed a role for QKI in erythropoiesis<sup>126</sup>. Interestingly, red blood cells are derived from the same common myeloid progenitor as monocytes/macrophages, eosinophils, neutrophils, basophils and platelets<sup>127</sup>, of which the differentiation has been described to be based on the activity of CCAAT/enhancer-binding protein (C/EBP)  $\alpha$  and PU.1<sup>128</sup>, transcription factors that in turn have both been suggested to transcriptionally induce QKI expression<sup>122,129</sup>. This interesting coupling between transcriptional and post-transcriptional gene regulation however that has not yet been properly investigated. In contrast to previous studies that have assessed the effects of QKI on myeloid cell differentiation by single target gene target approaches<sup>129,130</sup>, chapter 4 of this thesis illustrates the genome-wide implications of QKI on mRNA expression and pre-mRNA splicing in mouse and human monocytes & macrophages<sup>122</sup>. The identification that QKI mediates circular RNA formation<sup>58</sup> resulted in further analysis of our datasets by others and yielded distinct differences in circular RNA expression<sup>131</sup>. Although the exact mechanism remains unknown, translational efforts recently pinpointed single nucleotide polymorphisms near the QKI locus to be predictive for myocardial infarction and coronary heart disease<sup>132</sup>.

Collectively, while QKI was initially solely ascribed a pivotal function in the myelination of the nervous system, an extensive body of evidence now exists that firmly establishes QKI as a central governor of RNA fate in numerous tissues and disease states, including the pathophysiology of cardiovascular diseases as detailed in this thesis.

## Structural properties and genomic architecture of the Quaking proteins

*“If you want to study function, study structure”*  
*Francis Crick 1988*<sup>133</sup>

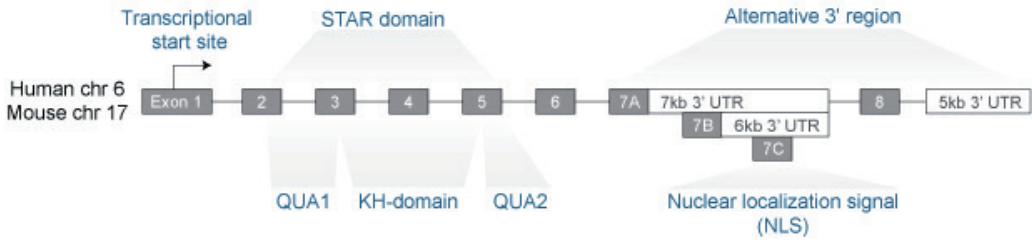
4

Most illustrative of this statement is the ancient study of anatomy which draws conclusions on organ function based on the appearance and localization of the organs, a practice dating back as far as the Egyptian civilization in 1600 BC with the Edwin Smith Surgical Papyrus<sup>134</sup>. Moreover, extensive insight into the function of QKI has been gained by carefully examining structural properties of the QKI locus, the pre-encoded (pre-)mRNAs, and distinct protein isoforms that will be highlighted next, these are also illustrated in the figure on the right.

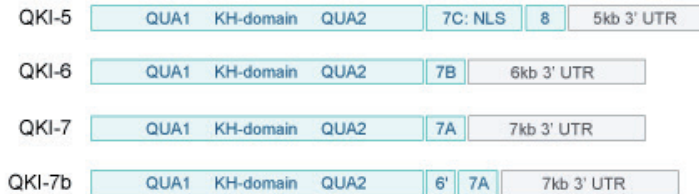
Ebersole and co-workers were the first to provide a detailed report on the genomic organization and protein architecture of QKI, and based on their studies also proposed that QKI interacts with target RNAs through the central KH-domain<sup>110</sup>. Located on mouse chromosome 17 and human chromosome 6, transcription from the qki gene locus encodes a pre-mRNA that through extensive alternative splicing leads to the generation of four distinct mature mRNAs of 5, 6 or 7 kilobases in length (termed qki-5, qki-6, qki-7 and qki-7b respectively), where splicing in the 3'-end of said transcript is exclusively responsible for transcript diversity<sup>110,135</sup>. These unique QKI mRNA transcripts give rise to multiple QKI protein isoforms, each containing an identical N-terminal KH-domain (termed Signal Transduction and Activators of RNA, or “STAR-family” proteins)<sup>136</sup>, and unique C-termini as a result of the aforementioned alternative splicing of the QKI pre-mRNA. These transcripts encode the QKI-5, QKI-6, QKI-7 and QKI-7b isoforms<sup>117</sup>, as well as the recently identified QKI-6b (in astrocytes)<sup>137,138</sup>. QKI-5 harbours a strong nuclear localization signal in the C-terminal region, resulting in nuclear enrichment of this protein isoform throughout tissues<sup>139</sup>, while QKI-6 and QKI-7 have been reported to be restricted to the cellular cytoplasm. Of note, our studies provide evidence that QKI-6 can also be detected, and potentially enriched in the nuclear spliceosome of VSMCs<sup>140</sup>. The functionality of this distinct subcellular localization has been demonstrated previously, resulting in nuclear retention of mRNAs<sup>141</sup>, perturbed shuttling of mRNAs to the cellular periphery<sup>105</sup> or sequestering mRNA to stress granules<sup>142</sup> upon a reduction of QKI, thereby effectively inhibiting translation of protein coding-RNAs. Moreover, augmentation of QKI expression levels, in particular of QKI-6, has been shown to rescue the defective myelination in qkv mice<sup>143</sup>. Unfortunately, genome-wide studies investigating QKI-mediated distribution of RNA targets within the cell are technically challenging and at present have not been published. The presence of the QUA1 and QUA2 protein domains that flank the KH-domain add another level of functional complexity to QKI<sup>110</sup> as crystal structure-based studies have pinpointed these domains to be responsible for the homo- or heterodimerization of the distinct QKI isoforms<sup>116,144-146</sup>. The pleiotropic properties of QKI as described above raise the question how QKI selectively recognizes its targets and how the expression and activity of QKI are regulated at the transcriptional, post-transcriptional and post-translational level.



## Genomic organization of the quaking locus



## Protein isoforms



## Unique C-terminal amino acid sequences

QKI-5: GAVATKVRRHDMRVHPYQRIVTADRAATG N (NLS is underlined)

QKI-6: GMAFPTKG

QKI-7: EWIEPMP DIS

QKI-7b: VVLSQRKAK NSRTVLTEPSS DLNLTNA

all mouse proteins

## Target RNA recognition by QKI

Initial experiments that assessed the RNA motif specifically bound by QKI resulted in the identification of a high-affinity bipartite binding motif containing a core-site (ACUAA) and a secondary half-site (UAAY) separated by 1-20 random nucleotides, termed the Quaking-Response-Element (in short QRE, annotated as: ACUAA-N(1-20)-UAAY)<sup>147,148</sup>. Later studies confirmed the importance of the core binding motif ACUAA in particular, but failed to demonstrate the necessity of a proximal UAAY motif, potentially due to the experimental approach<sup>76,80</sup>. Moreover, it has been suggested that other STAR-proteins, including GLD-1, SAM68 and SLM-2, all recognise bipartite motifs<sup>148</sup>. Evolutionarily conserved amongst the STAR-proteins is the KH-domain, which in prokaryotes consists of a combination of at least three  $\beta$ -sheets and three  $\alpha$ -helices ordered into a  $\beta\alpha\alpha\beta\alpha$  configuration<sup>149</sup>. This creates a binding groove that can spatially accommodate four nucleotides. Interestingly, a comparison of the binding motifs of several KH-domain containing-proteins yielded a wide variety of distinct RNA-binding motifs, showing dissimilarity even between two KH-domains within the same RBP. The RBP Nova e.g. binds UCAC, SF1 binds UAAC, hnRNPk binds TCCC, PCP2

binds CCCT, NusA (KH nr 1) binds AGAA, NusA (KH nr 2) binds CAAU and FBP (KH nr 3) binds ATTC and KH nr 4 binds TTTT<sup>149</sup>.

Although KH-domain containing proteins are less promiscuous in recognizing RNA species as compared to other RBD-containing proteins, this raises the question as to how the KH-domain of QKI is conferred with the capacity to specifically recognise the previously reported 6 nucleotide ACUAAY core motif. In contrast to QKI, which harbours only one KH-domain, other KH-domain containing RBPs have enhanced sequence specificity by either including repetitive KH-domains within the same protein, or by adding another subtype of RBD<sup>149</sup>. Previously, it has been proposed that SF1, a STAR family member that harbours but one KH-domain, yet recognizes a seven-nucleotide UACUAAC motif, does so by extending the binding groove into another  $\alpha$ -helix (namely  $\beta\alpha\alpha\beta\beta\alpha$ ) which is encoded in the QUA2 domain<sup>150</sup>. QKI also harbours this QUA2 domain, and could represent the means by which motif-specificity is extended, but also includes the dimerization-facilitating QUA1 domain<sup>139,145</sup>. Importantly, QKI dimerization confers the capacity to the secondary motif (UAAY) in close physical proximity to the core site (ACUAAY), and is likely responsible for the high sequence specificity of QKI<sup>147,148</sup>. The possibilities that 1) two distinct RNAs could be in complex with two dimerized QKI isoforms, or 2) that the secondary motif is brought in proximity by the secondary structure of the target RNA, however can also not be excluded, but has yet to be demonstrated. Interestingly, the KH-domain harbours the inherent property that it can also bind single stranded DNA (ssDNA), as it fails to possess the capacity to discriminate between the phosphate backbone of DNA versus RNA (the presence versus absence of one -OH group)<sup>151</sup>. However, the potential DNA-binding capacity of QKI also has yet to be investigated.

### Transcriptional regulation of the qki locus

Although few studies have specifically investigated the transcriptional regulation of the QKI locus, a large majority of studies investigating the consequences of altered QKI expression have shown the protein to be expressed in various tissues. Despite evidence that QKI is broadly expressed, the initial dysmyelination defect triggered a false assumption that QKI is only expressed, and perhaps relevant, in the nervous system. However, given the widespread expression of QKI at the RNA level, it suggests that constitutive transcription of the qki locus by transcription factors is likely occurring and that the protein is relevant in numerous cell types and tissues. Indeed, our studies detail abundant expression of QKI at the RNA level. This is likely driven by a strikingly high GC-content<sup>124</sup> and resultant high frequency of Cytosine-phosphate-Guanine islands (CpG; extracted from<sup>152</sup>) proximal to the transcriptional start site. This is in keeping with the notion that the majority of housekeeping genes contain CpG islands in their promotor regions<sup>153</sup>. However, CpG islands can also be methylated, which is known to induce gene silencing. To our knowledge, DNA methyltransferases have yet to be shown to affect the QKI promoter. It is important to note that this ubiquitous expression of QKI RNA does not entail that cell type-specific transcription factors could not be involved in specifically enhancing QKI transcription. Evidence supporting this

concept is the binding of KLF4 to the QKI promoter in VSMCs<sup>154</sup>, and the induction of QKI expression transcriptionally in hematopoietic progenitor cells by C/EBP $\alpha$ <sup>129</sup>. Furthermore, p53, a potent tumour suppressor, has been shown to directly interact with the QKI promoter, thereby influencing QKI protein levels and a role in cancer biology<sup>155</sup>. Nonetheless, remarkably little is known about the factors responsible for the apparent constitutive transcription of QKI, and the regulation of the QKI locus.

### Post-transcriptional regulation of the QKI (pre-)mRNA

Alongside the myriad of factors responsible for driving transcription from the QKI locus, the resultant QKI pre-mRNA is subsequently extensively regulated post-transcriptionally. In particular, alternative splicing of the QKI pre-mRNA generates distinct transcripts that encode unique protein isoforms, including a truncated RNA-binding KH-domain of which the exact function and tissue-specific expression profile is not yet known<sup>117</sup>. Fagg & Ares Jr. have recently shown QKI splicing is auto-regulatory, wherein QKI-5 plays a pivotal role in mediating QKI protein isoform balance<sup>156</sup>. Furthermore, bioinformatic analyses of the mature QKI mRNA 3'-UTR uncovered great evolutionary conservation and enrichment for interaction with targeting miRNAs. The predicted binding of 57% of all miRNAs in fact places the QKI mRNA as one of the top-ranked coding genes in the human genome (11th highest)<sup>136</sup>. Interestingly, an enrichment of myocardial, microvascular, endothelium and immune cell specific miRNA binding sites was identified, pointing towards a pivotal role for QKI in regulating cardiovascular biology and inflammation. Indeed, several recent studies have illustrated microRNA-based regulation of QKI expression, including miRNA-214<sup>121,123,157</sup>, miRNA-155<sup>158</sup> and miRNA-143-3p<sup>159</sup>.

### Post-translational modifications of the QKI protein

Following translation, several studies have identified post-translational modifications to QKI that influence function. Indeed, the protein architecture harbours several C-terminal tyrosine residues that have been found to be susceptible to post-translational modification<sup>110</sup>. Zhang and co-workers discovered that the Src-PTK- and FYN-mediated phosphorylation of these tyrosine residues inhibits the RNA-binding capacity of QKI to the MBP mRNA, both *in vitro* and *in vivo*<sup>160</sup>. Other studies in *D. melanogaster* showed that MAP/ERK-dependant phosphorylation at the QUA1 domain induces a conformational shift in this region that in turn enhances QKI dimerization and subsequent RNA target binding<sup>161</sup>. This is consistent with the finding that the introduction of point mutations in this region can fully abrogate the RNA-binding capacity of QKI<sup>146</sup>. Lastly, two studies detail the methylation of the QKI protein by protein-arginine-methyl-transferase 1 (PRMT1) at arginine residues, but do not comment on the functionality of this modification<sup>162,163</sup>. As such, the consequences of these post-translational modifications on QKI function remain poorly understood, and more research could provide novel insight into how this biology could be modulated to enhance or attenuate QKI activity.

### Catalytic and inhibitory mechanisms that mediate QKI function

So far we have discussed the inherent properties of QKI that influence protein expression and function. In a biological context however, QKI is embedded in heterogenous protein/RNA complexes involving a variety of other proteins and RBPs that can either inhibit or catalyse QKI-mediated RNA-processing events. Indeed, QKI appears to harbour a SH3-like domain that facilitates protein-protein interactions that enable it to play a role in intracellular signalling<sup>110,160</sup>. Using a yeast two-hybrid assay to identify QKI-interacting proteins, QKI was shown to associate with many other proteins, including RBPs such as RBFOX1, RBPMS, RBM9, RBM14, RBM24, PTBP1/2 (proteins that bind the polypyrimidine tract in intronic sequences) and HNRNP-K, but also DNA-interacting factors such as PAX6, THAP1 and SETDB1<sup>164</sup>. The role of QKI in the potential coupling of transcriptional and post-transcriptional processes have to our knowledge not yet been investigated.

Given this striking association with RBPs, including the presence of QKI in the human spliceosome<sup>165</sup>, QKI is likely competing with other RBPs for binding to target RNAs. Indeed, it has been demonstrated that QKI and PTB control overlapping splicing regulatory networks in muscle differentiation in the absence of competition for the ACUAA motif<sup>166</sup>. However, Hall and co-workers have also elegantly shown that the RNA-binding capacity of QKI, SF1, SAM68 and several other proteins are highly dependent on the same ACUAA motif, clearly illustrating direct competition for this nucleotide sequence<sup>166</sup>. In these studies, QKI also associated with CSTF2, a RBP involved in 3'-end cleavage and polyadenylation of mRNA species, pinpointing another role for QKI in mediating RNA processing. Lastly, recent studies have pinpointed SLM-2 (or KHDRBS3) as an RBP that also interacts with the ACUAA motif<sup>80</sup>.

Another means of impacting QKI-mediated regulation of target RNAs is the direct competition of ncRNA species for access to ACUAA motifs. For this, miRNAs and lncRNAs that bind to ACUAA motifs (or in the proximity of) can prevent QKI from controlling RNA fate<sup>149</sup>. For RBPs such as Pumilio 1 and Pumilio 2 this competition for RNA targets has already been illustrated<sup>167</sup>. Early studies investigating interactions between QKI and RNA targets showed a strikingly enhanced affinity and preference for linear RNA as compared to folded RNA upon adopting a secondary structure<sup>147</sup>. In theory, other RBPs or ncRNA species that induce this secondary structure shielding of the QRE could affect the susceptibility to QKI-mediated regulation, but this has not yet been definitively demonstrated. Computational analyses of PAR-CLIP data further indicates that QKI binding sites are indeed enriched in regions of RNA with little to no secondary structure (Hilal Kazan, personal communication).

Conversely, a therapeutic possibility for targeting RBPs such as QKI could be the sequestration or saturation of the protein itself by flooding the cell with ncRNA species that in turn would prohibit the RBP of interest from exerting effects on RNA fate, such as splicing in the case of QKI. Physiologic evidence of this phenomenon is known, as the lncRNA Gomafu (or MIAT) harbours >14 ACUAA repeats, and has been found to inhibit QKI function as evidenced by aberrant QKI-mediated splicing patterns upon overexpression of Gomafu<sup>168</sup>. This implies that saturating a cell with artificially synthesised RNAs containing ACUAA repeats, could potentially inhibit QKI activity in vivo.

## References

- 1 World-Health-Organisation. <http://www.who.int>, (2016).
- 2 Mendis, S., Puska, P. & Norrving, B. Global atlas on cardiovascular disease prevention and control. (World Health Organization, 2011).
- 3 Townsend, N. et al. Cardiovascular disease in Europe: epidemiological update 2016. *European heart journal*, ehw334 (2016).
- 4 Benjamin, E. J. et al. Heart Disease and Stroke Statistics-2017 Update: A Report From the American Heart Association. *Circulation*, doi:10.1161/CIR.0000000000000485 (2017).
- 5 Kelly, B. B. & Fuster, V. Promoting cardiovascular health in the developing world: a critical challenge to achieve global health. (National Academies Press, 2010).
- 6 Libby, P. Mechanisms of acute coronary syndromes and their implications for therapy. *New England Journal of Medicine* 368, 2004-2013 (2013).
- 7 Chistiakov, D. A., Bobryshev, Y. V. & Orekhov, A. N. Macrophage-mediated cholesterol handling in atherosclerosis. *J Cell Mol Med* 20, 17-28, doi:10.1111/jcmm.12689 (2016).
- 8 Lacolley, P., Regnault, V., Nicoletti, A., Li, Z. & Michel, J.-B. The vascular smooth muscle cell in arterial pathology: a cell that can take on multiple roles. *Cardiovascular research* 95, 194-204 (2012).
- 9 Tedgui, A. & Mallat, Z. Cytokines in atherosclerosis: pathogenic and regulatory pathways. *Physiological reviews* 86, 515-581, doi:10.1152/physrev.00024.2005 (2006).
- 10 Ross, R. Atherosclerosis--an inflammatory disease. *The New England journal of medicine* 340, 115-126, doi:10.1056/NEJM199901143400207 (1999).
- 11 Mills, B., Robb, T. & Larson, D. Intimal hyperplasia: slow but deadly. *Perfusion* 27, 520-528 (2012).
- 12 de Bruin, R. G., Rabelink, T. J., van Zonneveld, A. J. & van der Veer, E. P. Emerging roles for RNA-binding proteins as effectors and regulators of cardiovascular disease. *European heart journal* 38, 1380-1388 (2016).
- 13 Gansevoort, R. T. et al. Chronic kidney disease and cardiovascular risk: epidemiology, mechanisms, and prevention. *Lancet* 382, 339-352, doi:10.1016/S0140-6736(13)60595-4 (2013).
- 14 Levey, A. S. & Coresh, J. Chronic kidney disease. *The Lancet* 379, 165-180 (2012).
- 15 Davies, A. R., Smeeth, L. & Grundy, E. M. D. Contribution of changes in incidence and mortality to trends in the prevalence of coronary heart disease in the UK: 1996-2005. *European heart journal* 28, 2142-2147, doi:10.1093/eurheartj/ehm272 (2007).
- 16 Chaker, L. et al. The global impact of non-communicable diseases on macro-economic productivity: a systematic review. *European Journal of Epidemiology* 30, 357-395, doi:10.1007/s10654-015-0026-5 (2015).
- 17 Muka, T. et al. The global impact of non-communicable diseases on healthcare spending and national income: a systematic review. *Eur J Epidemiol* 30, 251-277, doi:10.1007/s10654-014-9984-2 (2015).
- 18 World-Health-Organisation. <http://apps.who.int/nha/database>.
- 19 Ziaeian, B. & Fonarow, G. C. Epidemiology and aetiology of heart failure. *Nat Rev Cardiol* 13, 368-378, doi:10.1038/nrcardio.2016.25 (2016).
- 20 Frey, N., Luedde, M. & Katus, H. A. Mechanisms of disease: hypertrophic cardiomyopathy

- thy. *Nat Rev Cardiol* 9, 91-100 (2012).
- 21 Weber, K. T., Sun, Y., Bhattacharya, S. K., Ahokas, R. A. & Gerling, I. C. Myofibroblast-mediated mechanisms of pathological remodelling of the heart. *Nat Rev Cardiol* 10, 15-26 (2013).
- 22 Zeisberg, M. & Neilson, E. G. Mechanisms of tubulointerstitial fibrosis. *J Am Soc Nephrol* 21, 1819-1834, doi:10.1681/ASN.2010080793 (2010).
- 23 Tabas, I., García-Cardena, G. & Owens, G. K. Recent insights into the cellular biology of atherosclerosis. *The Journal of Cell Biology* 209, 13-22, doi:10.1083/jcb.201412052 (2015).
- 24 Galkina, E. & Ley, K. Immune and inflammatory mechanisms of atherosclerosis. *Annual review of immunology* 27, 165-197 (2009).
- 25 Hilgendorf, I., Swirski, F. K. & Robbins, C. S. Monocyte fate in atherosclerosis. *Arteriosclerosis, thrombosis, and vascular biology* 35, 272-279, doi:10.1161/ATVBAHA.114.303565 (2015).
- 26 Murray, P. J. & Wynn, T. A. Protective and pathogenic functions of macrophage subsets. *Nature reviews. Immunology* 11, 723-737, doi:10.1038/nri3073 (2011).
- 27 Van Gils, J. M. et al. The neuroimmune guidance cue netrin-1 promotes atherosclerosis by inhibiting the emigration of macrophages from plaques. *Nature immunology* 13, 136-143 (2012).
- 28 Robbins, C. S. et al. Local proliferation dominates lesional macrophage accumulation in atherosclerosis. *Nature medicine* 19, 1166-1172, doi:10.1038/nm.3258 (2013).
- 29 Owens, G. K., Kumar, M. S. & Wamhoff, B. R. Molecular regulation of vascular smooth muscle cell differentiation in development and disease. *Physiological reviews* 84, 767-801 (2004).
- 30 de Vries, M. R., Simons, K. H., Jukema, J. W., Braun, J. & Quax, P. H. Vein graft failure: from pathophysiology to clinical outcomes. *Nature Reviews Cardiology* 13, 451-470 (2016).
- 31 Wong, C. Y. et al. Vascular remodeling and intimal hyperplasia in a novel murine model of arteriovenous fistula failure. *Journal of vascular surgery* 59, 192-201 e191, doi:10.1016/j.jvs.2013.02.242 (2014).
- 32 Roy-Chaudhury, P. et al. Neointimal hyperplasia in early arteriovenous fistula failure. *Am J Kidney Dis* 50, 782-790, doi:10.1053/j.ajkd.2007.07.019 (2007).
- 33 Furchgott, R. F., Cherry, P. D., Zawadzki, J. V. & Jothianandan, D. Endothelial cells as mediators of vasodilation of arteries. *Journal of cardiovascular pharmacology* 6 Suppl 2, S336-343 (1984).
- 34 Gryglewski, R. J., Palmer, R. M. & Moncada, S. Superoxide anion is involved in the breakdown of endothelium-derived vascular relaxing factor. *Nature* 320, 454-456, doi:10.1038/320454a0 (1986).
- 35 Trani, M. & Dejana, E. New insights in the control of vascular permeability: vascular endothelial-cadherin and other players. *Current opinion in hematology* 22, 267-272 (2015).
- 36 Zhao, Z., Nelson, A. R., Betsholtz, C. & Zlokovic, B. V. Establishment and dysfunction of the blood-brain barrier. *Cell* 163, 1064-1078 (2015).
- 37 Huveneers, S., Daemen, M. J. & Hordijk, P. L. Between Rho(k) and a hard place: the relation between vessel wall stiffness, endothelial contractility, and cardiovascular dis



- ease. *Circulation research* 116, 895-908, doi:10.1161/CIRCRESAHA.116.305720 (2015).
- 38 Vestweber, D. How leukocytes cross the vascular endothelium. *Nature Reviews Immunology* (2015).
- 39 Carmeliet, P. & Jain, R. K. Molecular mechanisms and clinical applications of angiogenesis. *Nature* 473, 298-307 (2011).
- 40 Versteeg, H. H., Heemskerk, J. W., Levi, M. & Reitsma, P. H. New fundamentals in hemostasis. *Physiological reviews* 93, 327-358 (2013).
- 41 Rafii, S., Butler, J. M. & Ding, B.-S. Angiocrine functions of organ-specific endothelial cells. *Nature* 529, 316-325, doi:10.1038/nature17040 (2016).
- 42 Satchell, S. C. & Braet, F. Glomerular endothelial cell fenestrations: an integral component of the glomerular filtration barrier. *American Journal of Physiology - Renal Physiology* 296, F947-F956, doi:10.1152/ajprenal.90601.2008 (2009).
- 43 Dane, M. J. et al. Glomerular endothelial surface layer acts as a barrier against albumin filtration. *The American journal of pathology* 182, 1532-1540 (2013).
- 44 Gimbrone, M. A. & García-Cardeña, G. Endothelial cell dysfunction and the pathobiology of atherosclerosis. *Circulation research* 118, 620-636 (2016).
- 45 Shi, Y. & Vanhoutte, P. M. Macro- and Microvascular Endothelial Dysfunction in Diabetes. *Journal of Diabetes* (2017).
- 46 Mordi, I., Mordi, N., Delles, C. & Tzemos, N. Endothelial dysfunction in human essential hypertension. *Journal of hypertension* 34, 1464-1472 (2016).
- 47 Dejana, E., Hirschi, K. K. & Simons, M. The molecular basis of endothelial cell plasticity. *Nature communications* 8, 14361 (2017).
- 48 Fu, X. D. & Ares, M., Jr. Context-dependent control of alternative splicing by RNA-binding proteins. *Nature reviews. Genetics* 15, 689-701, doi:10.1038/nrg3778 (2014).
- 49 Djebali, S. et al. Landscape of transcription in human cells. *Nature* 489, 101 (2012).
- 50 Darwin, C., Adler, M. J. & Hutchins, R. M. . The origin of species by means of natural selection.
- 51 Mattick, J. S. The central role of RNA in human development and cognition. *FEBS letters* 585, 1600-1616 (2011).
- 52 Anantharaman, V., Koonin, E. V. & Aravind, L. Comparative genomics and evolution of proteins involved in RNA metabolism. *Nucleic acids research* 30, 1427-1464 (2002).
- 53 Kornblihtt, A. R. et al. Alternative splicing: a pivotal step between eukaryotic transcription and translation. *Nature reviews Molecular cell biology* 14, 153-165 (2013).
- 54 Cech, T. R. & Steitz, J. A. The noncoding RNA revolution-trashing old rules to forge new ones. *Cell* 157, 77-94, doi:10.1016/j.cell.2014.03.008 (2014).
- 55 Collins, F. S., Morgan, M. & Patrinos, A. The Human Genome Project: lessons from large-scale biology. *Science* 300, 286-290 (2003).
- 56 Consortium, E. P. An integrated encyclopedia of DNA elements in the human genome. *Nature* 489, 57-74 (2012).
- 57 Quinn, J. J. & Chang, H. Y. Unique features of long non-coding RNA biogenesis and function. *Nature Reviews Genetics* 17, 47-62 (2016).
- 58 Conn, S. J. et al. The RNA binding protein quaking regulates formation of circRNAs. *Cell* 160, 1125-1134 (2015).
- 59 Legnini, I. et al. Circ-ZNF609 is a circular RNA that can be translated and functions in myogenesis. *Molecular cell* (2017).



- 60 Pamudurti, N. R. et al. Translation of circRNAs. *Molecular cell* (2017).
- 61 Bruce Alberts, A. J., Julian Lewis, David Morgan, Martin Raff, Keith Roberts, Peter Walter. . *Molecular Biology of the Cell*.
- 62 Zhang, M. Q. Statistical Features of Human Exons and Their Flanking Regions. *Human molecular genetics* 7, 919-932, doi:10.1093/hmg/7.5.919 (1998).
- 63 Padgett, R. A. New connections between splicing and human disease. *Trends Genet* 28, 147-154, doi:10.1016/j.tig.2012.01.001 (2012).
- 64 Robberson, B. L., Cote, G. J. & Berget, S. M. Exon definition may facilitate splice site selection in RNAs with multiple exons. *Molecular and cellular biology* 10, 84-94 (1990).
- 65 Kuo, H. C., Nasim, F. H. & Grabowski, P. J. Control of alternative splicing by the differential binding of U1 small nuclear ribonucleoprotein particle. *Science* 251, 1045-1050 (1991).
- 66 Zhang, X. H., Leslie, C. S. & Chasin, L. A. Dichotomous splicing signals in exon flanks. *Genome Res* 15, 768-779, doi:10.1101/gr.3217705 (2005).
- 67 Matera, A. G. & Wang, Z. A day in the life of the spliceosome. *Nature reviews. Molecular cell biology* 15, 108-121, doi:10.1038/nrm3742 (2014).
- 68 Matlin, A. J., Clark, F. & Smith, C. W. Understanding alternative splicing: towards a cellular code. *Nature reviews. Molecular cell biology* 6, 386-398, doi:10.1038/nrm1645 (2005).
- 69 Gerstberger, S., Hafner, M. & Tuschl, T. A census of human RNA-binding proteins. *Nature Reviews Genetics* 15, 829-845 (2014).
- 70 Galante, P. A. et al. A comprehensive in silico expression analysis of RNA binding proteins in normal and tumor tissue; identification of potential players in tumor formation. *RNA biology* 6, 426-433 (2009).
- 71 Cook, K. B., Kazan, H., Zuberi, K., Morris, Q. & Hughes, T. R. RBPDB: a database of RNA-binding specificities. *Nucleic acids research* 39, D301-308, doi:10.1093/nar/gkq1069 (2011).
- 72 Ray, D. et al. Rapid and systematic analysis of the RNA recognition specificities of RNA-binding proteins. *Nat Biotechnol* 27, 667-670, doi:10.1038/nbt.1550 (2009).
- 73 Castello, A. et al. Insights into RNA biology from an atlas of mammalian mRNA-binding proteins. *Cell* 149, doi:10.1016/j.cell.2012.04.031 (2012).
- 74 Baltz, A. G. et al. The mRNA-bound proteome and its global occupancy profile on protein-coding transcripts. *Molecular cell* 46, 674-690 (2012).
- 75 Darnell, R. B. HITS-CLIP: panoramic views of protein-RNA regulation in living cells. *Wiley interdisciplinary reviews. RNA* 1, 266-286, doi:10.1002/wrna.31 (2010).
- 76 Hafner, M. et al. Transcriptome-wide identification of RNA-binding protein and microRNA target sites by PAR-CLIP. *Cell* 141, 129-141, doi:10.1016/j.cell.2010.03.009 (2010).
- 77 Huppertz, I. et al. iCLIP: protein-RNA interactions at nucleotide resolution. *Methods* 65, 274-287, doi:10.1016/j.ymeth.2013.10.011 (2014).
- 78 Van Nostrand, E. L. et al. Robust transcriptome-wide discovery of RNA-binding protein binding sites with enhanced CLIP (eCLIP). *Nature methods* 13, 508-514 (2016).
- 79 McHugh, C. A., Russell, P. & Guttman, M. Methods for comprehensive experimental identification of RNA-protein interactions. *Genome biology* 15, 203 (2014).
- 80 Ray, D. et al. A compendium of RNA-binding motifs for decoding gene regulation. *Nature* 499, 172-177, doi:10.1038/nature12311 (2013).

- 81 Lee, S. R. & Lykke-Andersen, J. Emerging roles for ribonucleoprotein modification and remodeling in controlling RNA fate. *Trends in cell biology* 23, 504-510 (2013).
- 82 Gerstberger, S., Hafner, M. & Tuschl, T. A census of human RNA-binding proteins. *Nature Reviews Genetics* (2014).
- 83 Sidman, R. L., Dickie, M. M. & Appel, S. H. Mutant mice (quaking and jimpy) with deficient myelination in the central nervous system. *Science* 144, 309-311 (1964).
- 84 Larocque, D. et al. The QKI-6 and QKI-7 RNA binding proteins block proliferation and promote Schwann cell myelination. *PloS one* 4, e5867 (2009).
- 85 Baumann, N., Jacque, C., Pollet, S. & Harpin, M. L. [Biochemical study of the "Quaking" mutation in the mouse. Analysis of lipids and fatty acids of the brain]. *Comptes rendus hebdomadaires des seances de l'Academie des sciences. Serie D: Sciences naturelles* 264, 2953-2956 (1967).
- 86 Baumann, N. A., Jacque, C. M., Pollet, S. A. & Harpin, M. L. Fatty acid and lipid composition of the brain of a myelin deficient mutant, the "quaking" mouse. *Eur J Biochem* 4, 340-344 (1968).
- 87 Hogan, E. L. & Joseph, K. C. Composition of cerebral lipids in murine leucodystrophy: the quaking mutant. *Journal of neurochemistry* 17, 1209-1214 (1970).
- 88 Jacque, C., Bourre, J. M., Moreno, P. & Baumann, N. [Study of cerebral lipids in "quaking" mice during myelinization]. *Comptes rendus hebdomadaires des seances de l'Academie des sciences. Serie D: Sciences naturelles* 271, 798-801 (1970).
- 89 Jacque, C., Bourre, J. M., Moreno, P. & Baumann, N. [Fatty acid composition of total lipids and cerebrosides of the brain in normal and Quaking mice as a function of age]. *Biochimie* 53, 1121-1124 (1971).
- 90 Jacque, C. M., Harpin, M. L. & Baumann, N. A. Brain lipid analysis of a myelin deficient mutant, the "quaking" mouse. *Eur J Biochem* 11, 218-224 (1969).
- 91 Kostic, D., Nussbaum, J. L. & Neskovic, N. [Cerebral gangliosides of the 2 mutants "Quaking" and "Jimpy"]. *Acta medica lugoslavica* 24, 20-26 (1970).
- 92 Kurtz, D. J. & Kanfer, J. N. Cerebral acid hydrolase activities: comparison in "quaking" and normal mice. *Science* 168, 259-260 (1970).
- 93 Neskovic, N., Nussbaum, J. L. & Mandel, P. [The galactosyl-sphingosine transferase of quaking mutant mouse brain]. *Comptes rendus hebdomadaires des seances de l'Academie des sciences. Serie D: Sciences naturelles* 269, 1125-1128 (1969).
- 94 Neskovic, N., Nussbaum, J. L. & Mandel, P. A study of glycolipid metabolism in myelination disorder of Jimpy and Quaking mice. *Brain research* 21, 39-53 (1970).
- 95 Pollet, S., Bourre, J. M. & Baumann, N. [Study of the de novo biosynthesis of fatty acids in the brain of normal, quaking and heterozygotic for quaking mice]. *Comptes rendus*

- hebdomadaires des seances de l'Academie des sciences. Serie D: Sciences naturelles 268, 2146-2149 (1969).
- 96 Reasor, M. J. & Kanfer, J. N. Alterations of the sphingolipid composition in the brains of the "quaking" mouse and the "jimpy" mouse. *Life sciences* 8, 1055-1060 (1969).
- 97 Russell, D. H. & Meier, H. Alterations in the accumulation patterns of polyamines in brains of myelin-deficient mice. *Journal of neurobiology* 6, 267-275, doi:10.1002/neu.480060303 (1975).
- 98 Suzuki, K. & Zagoren, J. C. Focal axonal swelling in cerebellum of quaking mouse: light and electron microscopic studies. *Brain research* 85, 38-43 (1975).
- 99 Watanabe, I. & Bingle, G. J. Dysmyelination in "quaking" mouse. Electron microscopic study. *Journal of neuropathology and experimental neurology* 31, 352-369 (1972).
- 100 Bennett, W. I., Gall, A. M., Southard, J. L. & Sidman, R. L. Abnormal spermiogenesis in quaking, a myelin-deficient mutant mouse. *Biology of reproduction* 5, 30-58 (1971).
- 101 Hecht, N. B., Bower, P. A., Kleene, K. C. & Distel, R. J. Size changes of protamine 1 mRNA provide a molecular marker to monitor spermatogenesis in wild-type and mutant mice. *Differentiation; research in biological diversity* 29, 189-193 (1985).
- 102 Lorenzetti, D., Bishop, C. E. & Justice, M. J. Deletion of the Parkin coregulated gene causes male sterility in the quakingviable mouse mutant. *Proceedings of the National Academy of Sciences of the United States of America* 101, 8402-8407 (2004).
- 103 Konat, G., Trojanowska, M., Gantt, G. & Hogan, E. L. Expression of myelin protein genes in quaking mouse brain. *J Neurosci Res* 20, 19-22, doi:10.1002/jnr.490200104 (1988).
- 104 Fujita, N. et al. The large isoform of myelin-associated glycoprotein is scarcely expressed in the quaking mouse brain. *Journal of neurochemistry* 55, 1056-1059 (1990).
- 105 Barbarese, E. Spatial distribution of myelin basic protein mRNA and polypeptide in quaking oligodendrocytes in culture. *J Neurosci Res* 29, 271-281, doi:10.1002/jnr.490290302 (1991).
- 106 Chénard, C. A. & Richard, S. New implications for the QUAKING RNA binding protein in human disease. *Journal of neuroscience research* 86, 233-242 (2008).
- 107 Darbelli, L. & Richard, S. Emerging functions of the Quaking RNA-binding proteins and link to human diseases. *Wiley interdisciplinary reviews. RNA* 7, 399-412, doi:10.1002/wrna.1344 (2016).
- 108 Volk, T. & Artzt, K. Post-Transcriptional Regulation by STAR Proteins: Control of RNA Metabolism in Development and Disease. Vol. 693 (Springer Science & Business Media, 2011).
- 109 Justice, M. J. & Bode, V. C. Three ENU-induced alleles of the murine quaking locus are recessive embryonic lethal mutations. *Genetical research* 51, 95-102 (1988).
- 110 Ebersole, T. A., Chen, Q., Justice, M. J. & Artzt, K. The quaking gene product necessary in embryogenesis and myelination combines features of RNA binding and signal transduction proteins. *Nature genetics* 12, 260-265 (1996).
- 111 Tanaka, H., Abe, K. & Kim, C.-H. Cloning and expression of the quaking gene in the zebrafish embryo. *Mechanisms of development* 69, 209-213 (1997).
- 112 Schoenwolf, G. C., Bleyl, S. B., Brauer, P. R. & Francis-West, P. H. *Larsen's human embryology*. (Elsevier Health Sciences, 2014).
- 113 Zorn, A. M. et al. Remarkable sequence conservation of transcripts encoding amphibian

- and mammalian homologues of quaking, a KH domain RNA-binding protein. *Gene* 188, 199-206 (1997).
- 114 Baehrecke, E. H. who encodes a KH RNA binding protein that functions in muscle development. *Development* 124, 1323-1332 (1997).
- 115 Zaffran, S., Astier, M., Gratecos, D. & Sémériva, M. The held out wings (how) *Drosophila* gene encodes a putative RNA-binding protein involved in the control of muscular and cardiac activity. *Development* 124, 2087-2098 (1997).
- 116 Zorn, A. M. & Krieg, P. A. The KH domain protein encoded by quaking functions as a dimer and is essential for notochord development in *Xenopus* embryos. *Genes & development* 11, 2176-2190 (1997).
- 117 Kondo, T. et al. Genomic organization and expression analysis of the mouse *qkl* locus. *Mammalian Genome* 10, 662-669 (1999).
- 118 Noveroske, J. K. et al. Quaking is essential for blood vessel development. *Genesis* 32, 218-230 (2002).
- 119 Li, Z. et al. Defective smooth muscle development in *qkl*-deficient mice. *Development, growth & differentiation* 45, 449-462 (2003).
- 120 Bohnsack, B. L., Lai, L., Northrop, J. L., Justice, M. J. & Hirschi, K. K. Visceral endoderm function is regulated by quaking and required for vascular development. *Genesis* 44, 93-104 (2006).
- 121 van Mil, A. et al. MicroRNA-214 inhibits angiogenesis by targeting Quaking and reducing angiogenic growth factor release. *Cardiovascular research* 93, 655-665, doi:10.1093/cvr/cvs003 (2012).
- 122 de Bruin, R. G. et al. Quaking promotes monocyte differentiation into pro-atherogenic macrophages by controlling pre-mRNA splicing and gene expression. *Nature communications* 7, 10846, doi:10.1038/ncomms10846 (2016).
- 123 Wu, Y. et al. MicroRNA-214 regulates smooth muscle cell differentiation from stem cells by targeting RNA-binding protein QKI. *Oncotarget* 8, 19866 (2017).
- 124 de Bruin, R. G. et al. The RNA-binding protein quaking maintains endothelial barrier function and affects VE-cadherin and  $\beta$ -catenin protein expression. *Scientific Reports* 6, 21643 (2016).
- 125 Cochrane, A. et al. Quaking Is a Key Regulator of Endothelial Cell Differentiation, Neovascularization, and Angiogenesis. *STEM CELLS* 35, 952-966 (2017).
- 126 Wang, F. et al. The RNA-binding protein QKI5 regulates primary miR-124-1 processing via a distal RNA motif during erythropoiesis. *Cell research* (2017).
- 127 Orkin, S. H. & Zon, L. I. Hematopoiesis: an evolving paradigm for stem cell biology. *Cell* 132, 631-644 (2008).
- 128 Rosmarin, A. G., Yang, Z. & Resendes, K. K. Transcriptional regulation in myelopoiesis: Hematopoietic fate choice, myeloid differentiation, and leukemogenesis. *Experimental hematology* 33, 131-143 (2005).
- 129 Fu, H. et al. The RNA-binding protein QKI5 is a direct target of C/EBP $\alpha$  and delays macrophage differentiation. *Mol Biol Cell* 23, 1628-1635, doi:10.1091/mbc.E11-05-0412 (2012).
- 130 Wang, S. et al. miR-29a promotes scavenger receptor A expression by targeting QKI (quaking) during monocyte-macrophage differentiation. *Biochemical and biophysical research communications* 464, 1-6 (2015).

- 131 Gaffo, E., Bonizzato, A., Kronnie, G. t. & Bortoluzzi, S. CirComPara: A Multi-Method Comparative Bioinformatics Pipeline to Detect and Study circRNAs from RNA-seq Data. *Non-Coding RNA* 3, 8 (2017).
- 132 Dehghan, A. et al. Genome-wide association study for incident myocardial infarction and coronary heart disease in prospective cohort studies: the CHARGE consortium. *PloS one* 11, e0144997 (2016).
- 133 Watson, J. D. & Crick, F. H. C. Molecular Structure of Nucleic Acids: A Structure for Deoxyribose Nucleic Acid. *Nature* 171, 737-738 (1953).
- 134 Feldman, R. P. & Goodrich, J. T. The edwin smith surgical papyrus. *Child's Nervous System* 15, 281-284 (1999).
- 135 Mezquita, J., Pau, M. & Mezquita, C. Four isoforms of the signal-transduction and RNA-binding protein QKI expressed during chicken spermatogenesis. *Molecular reproduction and development* 50, 70-78 (1998).
- 136 Artzt, K. & Wu, J. I. in *Post-Transcriptional Regulation by STAR Proteins* 1-24 (Springer, 2010).
- 137 Farnsworth, B. et al. QKI6B mRNA levels are upregulated in schizophrenia and predict GFAP expression. *Brain research*, doi:<https://doi.org/10.1016/j.brainres.2017.05.027>.
- 138 Radomska, K. J. et al. RNA-binding protein QKI regulates Glial fibrillary acidic protein expression in human astrocytes. *Human molecular genetics* 22, 1373-1382 (2013).
- 139 Wu, J., Zhou, L., Tonissen, K., Tee, R. & Artzt, K. The quaking I-5 protein (QKI-5) has a novel nuclear localization signal and shuttles between the nucleus and the cytoplasm. *Journal of Biological Chemistry* 274, 29202-29210 (1999).
- 140 van der Veer, E. P. et al. Quaking, an RNA-binding protein, is a critical regulator of vascular smooth muscle cell phenotype. *Circulation research* 113, 1065-1075, doi:10.1161/CIRCRESAHA.113.301302 (2013).
- 141 Larocque, D. et al. Nuclear retention of MBP mRNAs in the quaking viable mice. *Neuron* 36, 815-829 (2002).
- 142 Wang, Y. et al. The QKI-6 RNA binding protein localizes with the MBP mRNAs in stress granules of glial cells. *PloS one* 5, e12824 (2010).
- 143 Zhao, L., Tian, D., Xia, M., Macklin, W. B. & Feng, Y. Rescuing qkV dysmyelination by a single isoform of the selective RNA-binding protein QKI. *Journal of Neuroscience* 26, 11278-11286 (2006).
- 144 Teplova, M. et al. Structure–function studies of STAR family Quaking proteins bound to their in vivo RNA target sites. *Genes & development* 27, 928-940 (2013).
- 145 Beuck, C., Qu, S., Fagg, W. S., Ares, M. & Williamson, J. R. Structural analysis of the quaking homodimerization interface. *Journal of molecular biology* 423, 766-781 (2012).
- 146 Chen, T. & Richard, S. Structure-function analysis of Qk1: a lethal point mutation in mouse quaking prevents homodimerization. *Molecular and cellular biology* 18, 4863-4871 (1998).
- 147 Galarneau, A. & Richard, S. Target RNA motif and target mRNAs of the Quaking STAR protein. *Nature structural & molecular biology* 12, 691-698, doi:10.1038/nsmb963 (2005).
- 148 Galarneau, A. & Richard, S. The STAR RNA binding proteins GLD-1, QKI, SAM68 and SLM-2 bind bipartite RNA motifs. *BMC molecular biology* 10, 47, doi:10.1186/1471-2199-10-47 (2009).

- Cléry, A. & Allain, F. H.-T. From structure to function of rna binding domains. (2013).
- Liu, Z. et al. Structural basis for recognition of the intron branch site RNA by splicing factor 1. *Science* 294, 1098-1102 (2001).
- Braddock, D. T., Louis, J. M., Baber, J. L., Levens, D. & Clore, G. M. Structure and dynamics of KH domains from FBP bound to single-stranded DNA. *Nature* 415, 1051-  
http://dbcat.cgm.ntu.edu.tw/.
- Deaton, A. M. & Bird, A. CpG islands and the regulation of transcription. *Genes & development* 25, 1010-1022 (2011).
- Shankman, L. S. et al. KLF4-dependent phenotypic modulation of smooth muscle cells has a key role in atherosclerotic plaque pathogenesis. *Nature medicine* 21, 628-637, doi:10.1038/nm.3866 (2015).
- Chen, A.-J. et al. STAR RNA-binding protein Quaking suppresses cancer via stabilization of specific miRNA. *Genes & development* 26, 1459-1472 (2012).
- Fagg, W. S. & Ares, M. Autogenous Cross-Regulation Of Quaking mRNA Processing And Translation Balances Quaking Functions In Splicing And Translation. *bioRxiv*, doi:10.1101/127936 (2017).
- Irie, K., Tsujimura, K., Nakashima, H. & Nakashima, K. MicroRNA-214 Promotes Dendritic Development by Targeting the Schizophrenia-associated Gene Quaking (Qki). *Journal of Biological Chemistry* 291, 13891-13904 (2016).
- He, B. et al. MicroRNA-155 promotes the proliferation and invasion abilities of colon cancer cells by targeting quaking. *Molecular medicine reports* 11, 2355-2359 (2015).
- He, Z. et al. MiR-143-3p functions as a tumor suppressor by regulating cell proliferation, invasion and epithelial-mesenchymal transition by targeting QKI-5 in esophageal squamous cell carcinoma. *Molecular Cancer* 15, 51 (2016).
- Zhang, Y. et al. Tyrosine phosphorylation of QKI mediates developmental signals to regulate mRNA metabolism. *The EMBO journal* 22, 1801-1810 (2003).
- Nir, R., Grossman, R., Paroush, Z. e. & Volk, T. Phosphorylation of the Drosophila melanogaster RNA-binding protein HOW by MAPK/ERK enhances its dimerization and activity. *PLoS genetics* 8, e1002632 (2012).
- Coûté, J., Boulanger, M.-C., Bedford, M. T. & Richard, S. Sam68 RNA binding protein is an in vivo substrate for protein arginine N-methyltransferase 1. *Molecular biology of the cell* 14, 274-287 (2003).
- Weimann, M. et al. A Y2H-seq approach defines the human protein methyltransferase interactome. *Nature methods* 10, 339-342 (2013).
- Lim, J. et al. A protein-protein interaction network for human inherited ataxias and disorders of Purkinje cell degeneration. *Cell* 125, 801-814 (2006).
- Hegele, A. et al. Dynamic protein-protein interaction wiring of the human spliceosome. *Molecular cell* 45, 567-580 (2012).
- Hall, M. P. et al. Quaking and PTB control overlapping splicing regulatory networks during muscle cell differentiation. *Rna* 19, 627-638 (2013).
- HafezQorani, S. et al. Modeling the combined effect of RNA-binding proteins and microRNAs in post-transcriptional regulation. *Nucleic acids research* 44, e83-e83 (2016).
- Barry, G. et al. The long non-coding RNA Gomafu is acutely regulated in response to neuronal activation and involved in schizophrenia-associated alternative splicing. *Molecular psychiatry* 19, 486-494 (2014).







# CHAPTER

# 5

Emerging roles for RNA-binding  
proteins as effectors and regulators  
of cardiovascular disease

*European Heart Journal 2016*

**Collaborative effort by:**

Ruben G. de Bruin, Ton J. Rabelink, Anton Jan van Zonneveld  
and Eric P. van der Veer

**Abstract**

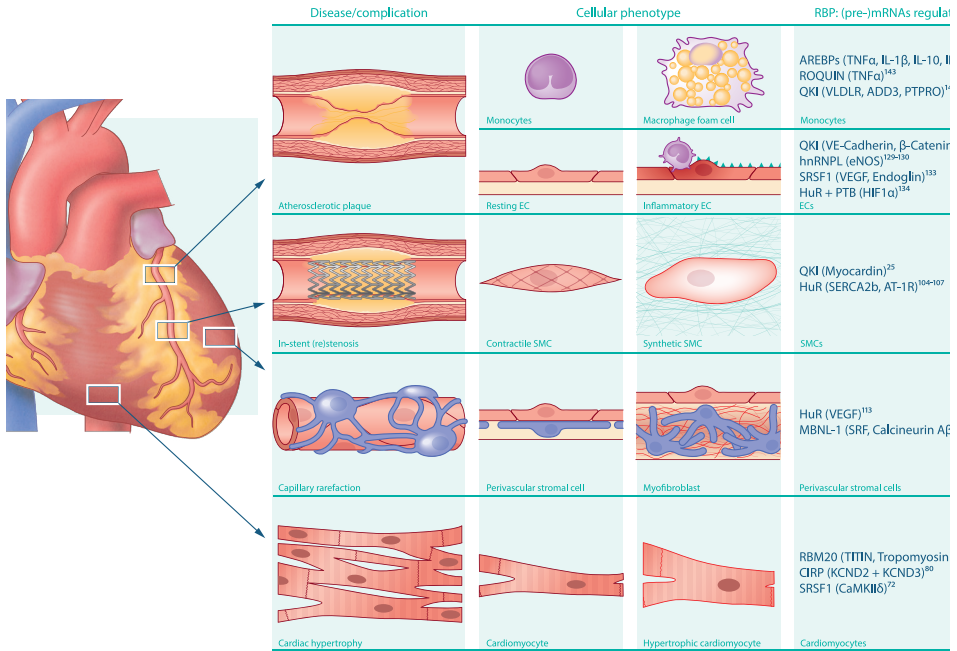
The cardiovascular system comprises multiple cell types that possess the capacity to modulate their phenotype in response to acute or chronic injury. Transcriptional and post-transcriptional mechanisms play a key role in the regulation of remodelling and regenerative responses to damaged cardiovascular tissues. Simultaneously, insufficient regulation of cellular phenotype is tightly coupled with the persistence and exacerbation of cardiovascular disease. Recently, RNA-binding proteins such as Quaking, HuR, Muscleblind, and SRSF1 have emerged as pivotal regulators of these functional adaptations in the cardiovascular system by guiding a wide-ranging number of posttranscriptional events that dramatically impact RNA fate, including alternative splicing, stability, localization and translation. Moreover, homozygous disruption of RNA-binding protein genes is commonly associated with cardiac- and/or vascular complications. Here, we summarize the current knowledge on the versatile role of RNA-binding proteins in regulating the transcriptome during phenotype switching in cardiovascular health and disease. We also detail existing and potential DNA- and RNA-based therapeutic approaches that could impact the treatment of cardiovascular disease in the future.

## Introduction

The modulation of cellular phenotype is intimately intertwined with organ function, repair upon injury, and the pathophysiology of disease.<sup>1–4</sup> The cardiovascular system possesses numerous cell types, such as vascular smooth muscle cells (VSMCs), endothelial cells (ECs), monocytes and macrophages and cardiomyocytes, that are conferred with the capacity to undergo phenotypic switches in response to acute or chronic injury that serve to limit tissue damage and restore proper cardiovascular function.<sup>3,5,6</sup> However, these reparative cellular phenotypes can also drive the onset, persistence, and exacerbation of cardiovascular disease (CVD; Figure 1). An example of this phenomenon is the pre-stenotic fibroproliferative response of medial VSMCs as a result of endothelial denudation of the coronary artery after percutaneous coronary interventions or in coronary artery bypass grafts due to procedure-related stress factors.<sup>3,7–9</sup> In contrast to VSMCs, the cardiomyocyte adaptation to injury is characterized by an increase in cell size (hypertrophy), enhancement of protein synthesis, and more pronounced organization of the sarcomere.<sup>10</sup> Another class of environment-induced phenotypic switches that are critical in CVD pathogenesis are inflammatory cells. In particular, the differentiation of monocyte subsets into various highly plastic macrophage phenotypes profoundly impacts atherosclerotic lesion development and progression.<sup>5,11–14</sup>

Despite the knowledge that cellular phenotype switching is pivotal for CVD development, the treatment of CVD has primarily focused on combating proteins responsible for generating unfavourable lipid profiles. An excellent clinical example of this biology is represented by statins, which aside from their lipid-lowering capacity, skew ECs to an atheroprotective phenotype by promoting their anti-inflammatory and anti-thrombotic properties. Mechanistically, statins transcriptionally repress NF- $\kappa$ B signalling<sup>15</sup> while simultaneously inducing shear-responsive transcription factor Krüppel-Like Factor 2 (KLF2), driving expression of anti-inflammatory markers such as thrombomodulin and eNOS.<sup>16,17</sup> Simultaneously, statins activate microRNA (miRNA) expression profiles that are essential for the maintenance of EC health by enhancing transcription and activity of anti-apoptotic and proangiogenic AKT signalling pathways.<sup>18,19</sup> Therefore, adaptations in cellular function in disease settings are associated with dynamic changes at the transcriptional and post-transcriptional levels, suggesting that therapeutic targeting of factors that drive these processes could shift cellular phenotype from a disease-advancing to a regenerative state (Figure 1).<sup>20–22</sup>

RNA-binding proteins (RBPs) are rapidly emerging as pivotal players in this biological script, as they are intimately involved in co-ordinating all aspects of (patho)physiological RNA processing and gene expression.<sup>22–25</sup> In the past decade, extensive work has elucidated the sequence to which many of these RBPs bind,<sup>26–31</sup> enabling one to identify putative RNA species specifically targeted by individual RBPs. Importantly, this knowledge, when coupled with the recent development of sophisticated delivery methods<sup>32</sup> for RNA-based therapeutics,<sup>33,34</sup>



### The RNAissance: new insights into genomic complexity

Remarkably, the human and roundworm genomes (and other less complex organisms) encode similar numbers of genes (approximately 20 000),<sup>35</sup> indicating that the number of encoded genes does not directly determine organismal complexity. In the slipstream of the development and utilization of revolutionary tools that enabled scientists and clinicians to sequence (human) genomes and transcriptomes, came the realization that organismal complexity evolved with an increased capacity to regulate gene expression at the posttranscriptional level. Following the human genome project, attempts to better understand our genome culminated in the Encyclopaedia of DNA Elements (ENCODE), a project designed to identify the 'functional elements' in the human genome.<sup>36</sup> This worldwide collaborative effort exponentially expanded our understanding of regulatory elements in our genome that affect human health and disease, and divided the genome more definitively into protein-coding and nonprotein-coding transcribed portions of our genomic DNA.<sup>36</sup> Previously, it was established that about 1.2% of the human genome codes for protein-encoding mRNA precursors, whereas an astounding majority contains information allowing for the generation of a large variety of non-protein-coding RNA species, including microRNAs (miRs), long non-coding RNAs, piwi-interacting RNAs, small nucleolar RNAs, and small nuclear RNAs.<sup>37,38</sup> These non-protein-coding RNAs are widely considered to control the activation or repression of gene expression in response to, e.g. developmental and environmental cues such as aging, metabolic stress, cancer and inflammation,<sup>39–44</sup> whereas the cellular functions of an extensive list of other non-protein-coding RNA species are currently unclear. This review will focus on the regulatory role of RBPs and events they catalyse, as the biology on non-coding RNAs in CVD has been detailed in numerous outstanding reviews.<sup>38,44–48</sup>

### RNA-binding proteins: directors of post-transcriptional regulation

Concomitant with their transcription, nascent pre-mRNA molecules are covered with a myriad of RBPs that collectively form ribonucleoprotein structures (RNPs). The dynamic formation of these RNPs determines all facets of RNA fate, including splicing, stability, cellular localization, and rate of translation (Figure 2). It is estimated that the human genome encodes more than 700 RBPs.<sup>26</sup> These RBPs have been divided into families based on evolutionarily conserved RNA-binding motifs that confer the capacity to bind target RNAs in a sequence-specific fashion.<sup>28,29,49,50</sup> RBPs interact with target (pre-)mRNAs at the 5'- and 3'-untranslated regions (UTRs), as well as at non-coding (intronic) and coding (exonic) regions. Importantly, the region to which a given RBP binds on a target (pre-)mRNA generally influences the event that is catalysed, illustrating how these proteins dynamically and spatially impact gene expression (Figure 2). Finally, RBPs serve as global and cell-type-specific regulators of gene expression, where competition for access to target RNAs is determined by expression levels of individual RBPs in health and disease.<sup>51–53</sup>

Given that splicing of pre-mRNAs markedly impacts mature mRNA fate and the protein repertoire in healthy and diseased cells, it is important to provide a brief overview of splicing biology. Firstly, pre-mRNAs containing sequence encoding protein generally require RBP-guided excision of intronic sequences by (i) constitutive splicing;

and/or (ii) alternative splicing, which when combined can lead to functionally distinct mature mRNAs.<sup>52,54,55</sup> Splicing requires the dynamic assembly of RBPs into the spliceosome, a highly organized intra-nuclear structure consisting of RBPs and small RNA complexes, called heterogeneous ribonucleoprotein particles (hnRNPs).<sup>55–57</sup> The spliceosome also plays a central role in alternative splicing,<sup>52</sup> as the binding of RBPs to consensus sequences proximal to exons limits spliceosomal accessibility to 50- and/or 30-splice junctions, promoting the formation of splice variants (Figure 2).<sup>20,23,52,54</sup> ‘Alternative’ splicing occurs in an estimated 80–90% of protein-coding genes, with recent estimates indicating that this process is responsible for generating more than 200 000 unique protein-coding transcripts in humans.<sup>58</sup> Interestingly, although the core spliceosomal proteins are expressed in almost all individual cell types, including anucleate platelets,<sup>59</sup> it is the differential expression and modifiable activity of RBPs that has been pinpointed as defining tissue-specific splicing patterns.<sup>20,54,60</sup> Clinically relevant examples of alternatively spliced transcripts that influence CVD risk are Troponin T,<sup>61</sup> SERCA2a/b,<sup>62</sup> and CETP.<sup>63</sup>

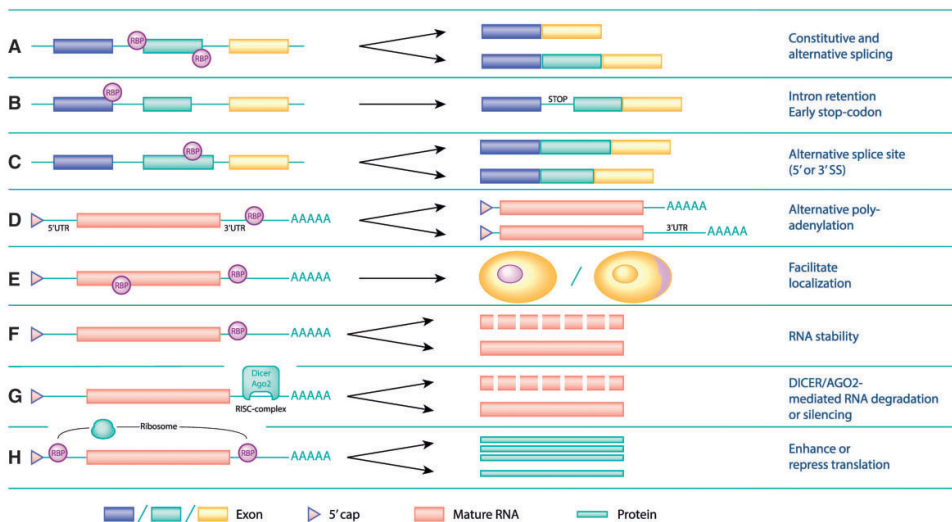


**Figure 2 | RNA-binding proteins (RBPs) serve as critical effectors and regulators of RNA fate by guiding gene expression post-transcriptionally.** The spatial interaction of RBPs with RNA species impacts the post-transcriptional event catalysed, be it: modifications of pre-mRNAs that alter mature mRNA composition including splicing (A–C) and alternative polyadenylation (D); subcellular localization (E); RNA stability (F, G); or ribosome-mediated translation of mature mRNAs (H). By co-ordinating these events, RBPs are intimately involved in determining the cellular transcriptome, and thereby impact cellular phenotype and function in health and disease settings.

RNA-binding proteins are also critically involved in embryonic development of the cardiovascular system.<sup>64</sup> The Mouse Genome Information (MGI) database provides a comprehensive list of reported gene ‘knockout’ mice and their associated phenotypes.<sup>65–67</sup> Our assessment of this database uncovered a significant proportion of mice with defects in cardiac- and/or vascular development as a result of validated RBP loss (Table 1). As foetal gene expression or splicing programmes are often recapitulated in adult disease settings,<sup>68</sup> we elected to analyse the relative expression, extracted from

publically available data sets deposited in the NCBI Geo dataset server, of validated RBPs in several specialized cell-types of the cardiovascular system. This analysis clearly illustrates that a vast number of RBPs are abundantly expressed and display cell-type-specific expression profiles (Figure 3, see Supplementary material online, Figure S1 and Table S1). The heatmap in Figure 3 clearly shows the expression levels of individual RBPs discussed in the review, whereas Supplementary material online, Figure S1 shows the relative expression of more than 300 RBPs in numerous cell-types relevant in CVD (Supplementary material online, Table S1 provides all the raw data used to generate these heatmaps).

Here below, we will focus on some of the more recent developments and insights into RBP biology gained primarily from human and mouse studies. Collectively, they illustrate the versatility of RBPs in regulating key aspects of cardiovascular health and disease.

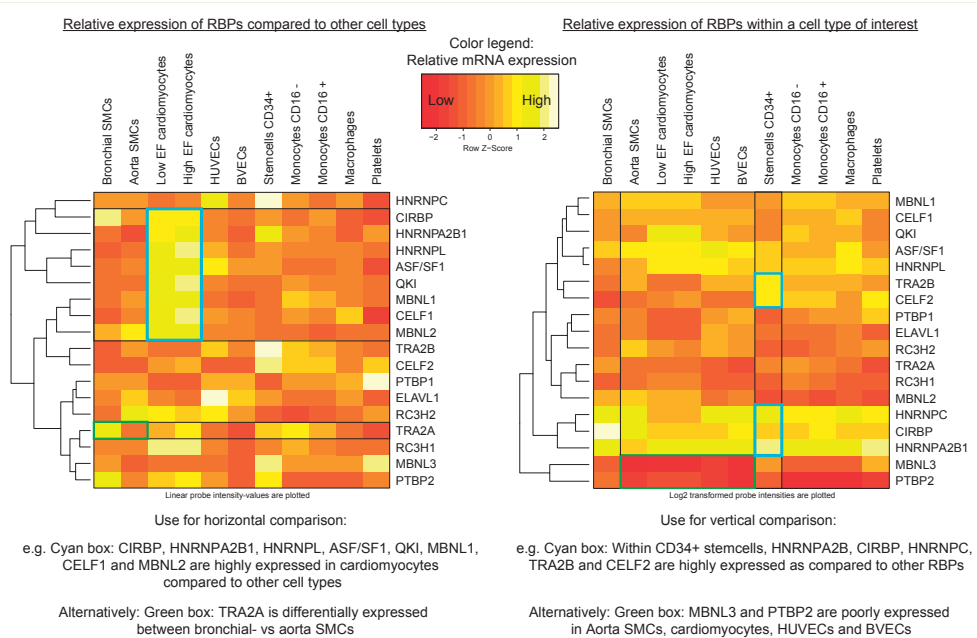


**Figure 3 | RNA-binding protein (RBP) expression levels in various healthy and diseased vascular cells.** Heatmap depicting relative expression levels 317 RBPs in various cell types that are associated with cardiovascular health and disease. Red and white shading depict low and high relative mRNA expression levels, respectively. The heatmap was generated using online available data sets (NCBI Geo dataset server) which were all run on Affymetrix GeneChipVR Human Genome U133 Plus 2.0 arrays to allow inter-array comparison (data set references as follows: bronchial SMCs;<sup>161</sup> aortic SMCs;<sup>162</sup> low and high EF cardiomyocytes;<sup>163</sup> HUVECs;<sup>164</sup> BVECs; CD34+stem cells;<sup>165</sup> CD16- and CD16+ monocytes;<sup>166</sup> macrophages;<sup>167</sup> platelets<sup>168</sup>). The data were subjected to robust multi-array averaging (RMA) for normalization using the Affymetrix expression console. Subsequently, RNA-binding proteins were selected by cross-referencing the online RBP-database as published by Ray et al.,<sup>29</sup> whereafter either linear or Log2-transformed probe-intensities were plotted using R-studio software including the gplots algorithm for heatmap generation.

**Table 1** RNA-binding protein deficiencies in mice resulting in vascular and/or cardiac developmental defects (pre- and post-natal)

RBP	Binding domain	MGI ID	Phenotype description	References
<b>Vascular phenotype</b>				
QKI	KH	3033861	Lack of SMAA in blood vessel, vascular remodelling incomplete, decreased complexity of brain vasculature, abnormal heart morphology, pericardial effusion, irregular vitelline artery	98
ANKRD17	KH	1932101	Haemorrhages, impaired vascular smooth muscle cell development, impaired vascular integrity, and growth retardation	169
SHARPIN	RanBP ZF	1856699	Perturbed angiogenesis, tortuous dilated capillaries in dermis	170
ZFP36	CCCH ZF	2652418	Reduced blood pressure, vascular inflammation, reduced relaxation upon acetylcholine, EC dysfunction	171, 172
ZFP36L2	CCCH ZF	4360890	Overt gastrointestinal haemorrhage, decreased leucocyte number	173
G3BP1	RRM	3604716	Intracranial haemorrhaging	174
HNRNPD	RRM	3693617	Kidney haemorrhage, altered macrophage function	175
MSI1	RRM	2450917	Intracerebral haemorrhage	176
ELAV1/HuR	RRM	5316082	Decreased angiogenesis after hind limb ischaemia, abnormal placental labyrinth vasculature	177, 178
TRA2B	RRM	4450921	No vasculogenesis	179
UHMK1	RRM	3832867	Accelerated neointima and more VSMCs after femoral wire injury	180
PABPC4	RRM	4364054	Decreased circulating cholesterol, HDL, and free fatty acid levels	181
<b>Cardiac phenotype</b>				
PPARGC1A	RRM	3511352	Increased or decreased heart weight, accelerated cardiac dysfunction after aortic constriction, decreased cardiac output, decreased heart rate	182, 183
RCAN2	RRM	3641543	No cardiac hypertrophy upon phenylephrin/angiotensin II infusions, protection against volume overload, increased myocardial damage after ischaemia reperfusion injury	184
SRSF2	RRM	3036846	Extensive fibrosis, myofibril disarray, dilated cardiomyopathy evident after 5 weeks, decreased ventricle muscle contractility	185
PPARGC1B	RRM	3757705	Decreased heart rate elevation after dobutamine	186
SRSF1	RRM	3766573	Hypoplastic pulmonary trunk, signs of tetralogy of fallot complex, ventricular septal defects, overriding aortic valve, transposition of great arteries, suppulmonary stenosis	187
SPEN	RRM	2667509	Defects in the formation of the cardiac septum and muscle	188

**Table 1 | RNA-binding protein deficiency is associated with cardiovascular developmental defects.** Defective vascular and cardiac development as a result of RBP loss in various mouse models are detailed in this table. The RBPs have been grouped based on their RNA-binding domains for clarity. Data were obtained from the Mouse Genome Information (MGI) database from Jackson Laboratories and RBP knockout mice were selected by cross-referencing the online RBP database as published by Ray et al.<sup>29</sup> Human RBP names were extracted from [http://cisbp-rna.ccrb.utoronto.ca/bulk\\_archive.php](http://cisbp-rna.ccrb.utoronto.ca/bulk_archive.php) (1 December 2016), thereafter cross-referenced with the MP:0005385 mammalian phenotype 'cardiovascular phenotype system' from the MGI database to screen for a CVD defect.

## RNA-binding proteins in cardiomyocytes: preserving heart function and aiding in post-natal heart remodelling

Insight into the differential expression of RBPs in the adult heart and their critical regulatory role in cardiomyocyte pathophysiology has in part been derived from studies assessing alternative splicing patterns during foetal heart development<sup>69–71</sup> and the discovery that cardiomyocyte dysfunction is associated with a reversion to foetal mRNAs and protein isoforms.<sup>68</sup> In fact, foetal transcripts of key sarcomeric genes, including cardiac troponin T, cardiac troponin I, myosin heavy chain 7, and filamin C-c were found to be enriched in the setting of human ischaemic cardiomyopathy, idiopathic dilated cardiomyopathy (DCM) and aortic stenosis. Of note, in these aortic stenosis samples, patient inclusion was based on high or low ejection fraction (EF <50%), prompting the authors to postulate that splicing defects could precede heart



dysfunction.<sup>72</sup> Interestingly, RBPs have also been found to critically regulate splicing during cardiac remodelling postnatally.<sup>69,73</sup> The RBPs Celf1 and Muscleblind1 (MBNL) were found to guide alternative splicing patterns in mice required immediately after birth for the effective organization of transverse tubules and calcium handling.<sup>69</sup> Further along the developmental timeline, Serine/ Arginine-Rich Splicing Factor 1 (SRSF1; also known as ASF/SF2) was found to guide the alternative splicing patterns required for maintaining electrical conductivity in mouse cardiomyocytes during juvenile to adult transition, where in particular defects in CaMKIId splicing resulted in severe excitation–contraction coupling defects, triggering a hypercontractile phenotype.<sup>73</sup>

In the adult heart, changes in splicing patterns have also been shown to perturb cardiomyocyte function. The expression levels of several crucial splicing factors (SF1, ZRSR2, SRSF4, and SRSF5) are potently repressed in dysfunctional, low EF cardiomyocytes, and display tight correlations with high EF cardiomyocytes (see Supplementary material online, Figure S1). Other studies have identified that a reduction in expression levels of RNA-binding motif protein 20 (RBM20; or MATR3) can lead to DCM in humans. RBM20 is most abundantly expressed in the human heart.<sup>74–76</sup> Common single nucleotide polymorphisms (SNPs) in a RBM20 exonal hotspot were found to significantly associate with an increased risk of DCM due to altered RBM20 expression in humans.<sup>74,75</sup> This finding enabled Guo et al.<sup>77</sup> to discover that these genetic variants impair RBP20 function in rats, directly affecting the splicing of a myriad of pre-mRNAs involved in ion homeostasis, sarcomere organization, and diastolic function, such as titin, tropomyosin I, and PDZ- and LIM-domain 5. Genome-wide analyses of RBM20 RNA targets revealed that the protein represses splicing by binding introns proximal to alternatively spliced exons. These studies nicely illustrate how RBPs can orchestrate pre-mRNA processing, thereby serving as molecular switches in gene networks with essential cardiac functions.

The arrhythmias and dilated cardiomyopathies observed in type I myotonic dystrophy (DM1) also illustrate how dysregulated splicing can be causal for heart disease. Recently, expansion of CUG trinucleotides in the 3' UTR of the DM protein kinase mRNA was found to result in the nuclear retention of the mRNA in affected human cardiomyocytes.<sup>78</sup> Using genetically modified mice that similarly accumulate nuclear CUG-repeat-containing DM mRNAs, this CUG-repeat expansion was found to trigger sequestration of the RBPs CUG-binding protein 1 and CUG-binding protein 2, impairing their ability to participate in splicing programmes required for the maintenance of physiological cardiomyocyte function.<sup>78</sup>

Alongside splicing, RBPs also critically control mRNA transcript abundance and translation of mature mRNAs into protein. For example, expression (and splicing) of the voltage-gated sodium channel SCN5A has recently been described to be regulated by the RBP MBNL1 in cardiomyocytes,<sup>79,80</sup> whereas the RBP PCBP2 was found to inhibit angiotensin II-induced hypertrophy of cardiomyocytes by promoting GPR56 mRNA degradation.<sup>81</sup> Finally, a short QTc interval and abbreviated action potential were observed in cardiomyocytes derived from cold-inducible RNA-bind-

ing protein (CIRP)-deficient rats.<sup>82</sup> This phenotype was triggered by an increased transient outward potassium current due to decreased translation of the KCND2 and KCND3 mRNAs. CIRP binding to mature RNAs enhanced the translation of these essential ion channel subunits, illustrating how loss of this RBP is causal for defective voltage-gated potassium channel function and reduced bioelectric activity in mammalian hearts.<sup>82</sup>

Collectively, these studies define an important co-ordinating role for RBPs in foetal, juvenile, and adult hearts, while also demonstrating how altered RBP levels can impact cardiac function in health and disease.

### **RNA-binding proteins in vascular smooth muscle cells and perivascular stromal cells: governors of cellular phenotype and function**

Upon vascular injury, VSMCs undergo a well-established phenotypic shift from a contractile to a fibroproliferative, migratory state (Figure 1). This physiological response aids in repair of damaged vessels.<sup>3</sup> This VSMC-mediated damage response aids in the resolution of initial damage,<sup>3,5</sup> but is also tightly linked with pathophysiological situations including coronary artery disease, vascular(re)stenosis, atherosclerosis, and peripheral arterial disease.<sup>83–85</sup> Surprisingly, the RBPs that co-ordinate vital splicing events in genes involved in this phenotype switch, such as SM-myosin heavy chain,<sup>86</sup> myosin light chain kinase,<sup>87,88</sup> smoothelin,<sup>89,90</sup> tropomyosin,<sup>91,92</sup> (meta)vinculin,<sup>93</sup> calponin,<sup>94</sup> and caldesmon,<sup>95,96</sup> are largely unknown.

Studies investigating the consequences of knockout of the RBP Quaking (QKI) revealed an embryonic lethal phenotype.<sup>97–99</sup> In keeping with the aforementioned frequent developmental defects in the cardiac and vascular systems of RBP knockout mice, QKI<sup>-/-</sup> mice displayed an inability to form vitelline vessels, along with defects in pericyte ensheathment of nascent vessels and pericardial effusion.<sup>97–99</sup> More recently, QKI was found to play a critical role in the human, adult vasculature,<sup>25</sup> where VSMC dedifferentiation in response to vessel injury was associated with increased QKI protein levels. This augmentation of QKI enhanced the direct interaction with the Myocardin pre-mRNA (Myocd), driving an alternative splicing event that alters Myocd protein balance to a distinct isoform (named Myocd\_v1) that activates proliferative gene expression profiles in VSMCs [via serum response factor (SRF) and myocyte enhancing factor 2-binding domains].<sup>25,100–102</sup> After injury resolution in mice, QKI protein levels subside and Myocd reverts to an isoform that solely interacts with SRF (Myocd\_v3), enhancing expression of contractile apparatus proteins and the restoration of VSMC contractile function.<sup>25</sup> Interestingly, the well-established role of Myocd in the human heart, and abundant expression of QKI in cardiomyocytes (Figure 3), suggests that QKI could similarly regulate cardiomyocyte-mediated remodelling of the heart following injury.

Increased expression of the RBP HuR was also observed in the setting of neointimal hyperplasia, vein graft specimens, and fibromuscular dysplasias of the human kidney, which all represent clinical manifestations of enhanced VSMC proliferation.<sup>103</sup> Furthermore, HuR was found to stimulate VSMC-mediated vasoconstriction, as the

interaction of this stabilizing RBP with the 30 UTR of the sarco/endoplasmic reticulum Ca<sup>2+</sup>pump (SERCA2b)<sup>104</sup> and angiotensin receptor type 1 (AT-1R) mRNAs enhanced Ca<sup>2+</sup>influx and angiotensin II binding, respectively.<sup>105–107</sup> Interestingly, Paukku et al.<sup>107</sup> identified that subjects with type 2 diabetes-associated hyperinsulinaemia have increased HuR protein levels, leading to enhanced AT-1R protein levels in VSMCs. This provided novel mechanistic insight into factors that increase CVD risk in patients with type II diabetes, namely via activation of the renin–angiotensin–aldosterone system.<sup>107</sup> Given the considerable attention gained for the combinatorial use of angiotensin-converting enzyme-inhibitors with AT-1R blockade for the effective management of blood pressure,<sup>108,109</sup> these studies collectively illustrate how RBPs intracellularly impact VSMC-mediated vasoconstriction by determining cell-surface availability of the angiotensin receptor.

In keeping with the central role that perivascular stromal cells play in ensheathing nascent microvessels and stabilizing existing microvessels, it is critical for these cells to regulate the expression of cell–cell adhesion proteins, along with growth factors that stimulate the maintenance of these interactions.<sup>110,111</sup> Moreover, it is well-established that CVD is associated with the disappearance of microvessels (microvessel rarefaction), as a result of progressive perivascular stromal cell loss that is associated with a pro-fibrotic phenotypic shift to a myofibroblastic state.<sup>112</sup> This phenotypic conversion is tightly coupled with capillary destabilization, pathological angiogenesis, and ultimately microvascular rarefaction. Several RBPs have been intimately linked with maintenance of EC–perivascular stromal cell interactions, or mediating a shift to the destabilizing myofibroblast phenotype, including HuR, which was found to drive excessive angiogenesis by stabilizing the vascular endothelial growth factor (VEGF) mRNA.<sup>113</sup> Muscleblind (MBNL-1) was also shown to bind to the 3'UTR of the SRF mRNA, enhancing expression of this transcription factor that guides perivascular stromal cells differentiation into myofibroblasts in mice.<sup>114</sup> Moreover, MBNL-1 was also found to directly influence alternative splicing of calcineurin Ab<sup>114</sup>, a protein phosphatase that activates T-cell-mediated responses to injury. Importantly, the resultant constitutively active Calcineurin Ab1 isoform was found to be enriched in both mouse cardiac fibroblasts<sup>114</sup> and cardiomyocytes after myocardial infarction (MI).<sup>115</sup>

These findings suggest that CVD progression could be limited by developing strategies that target RBPs such as HuR, MBNL-1, and QKI or splicing events mediated by these proteins, with the goal of rendering VSMCs quiescent.

## RNA-binding proteins in endothelial cells: alternating between function and dysfunction

The activation of ECs by inflammatory stimuli triggers endothelial dysfunction and accelerates CVD onset.<sup>116,117</sup> This pro-atherogenic state is greatly increased in patients with risk factors such as diabetes, renal failure, hypercholesterolaemia, and high blood pressure. Statins have proved to effectively ameliorate endothelial dysfunction in combination with their lipid-lowering effects.<sup>16</sup>

Similar to VSMCs, ECs play a critical role in regulating vascular tone, as EC activation is tightly coupled with a decrease in nitric oxide (NO) bio-availability that triggers vasoconstriction.<sup>118–120</sup> The expression and activity of eNOS, the main enzyme responsible for synthesizing free NO by ECs, is modulated by the shear-responsive and atheroprotective transcription factor KLF2.<sup>17,121–124</sup> KLF2 mediates these effects by binding to the promoter region of shear-responsive genes, including the RBPs QKI and HuR.<sup>125,126</sup> Further evidence that RBPs directly impact eNOS expression, and thereby activity, has been derived from computational analyses<sup>27,28</sup> and experimental studies investigating RBP function in human ECs. Another means by which RBPs impact eNOS biology is through hnRNP L, a protein that by co-ordinating eNOS pre-mRNA alternative splicing triggers the generation of a truncated, dominant negative eNOS isoform.<sup>127,128</sup> Despite evidence indicating that these alternative eNOS isoforms affect NO production, the pathophysiological relevance and consequences on EC function in patients with CVD are at present unknown. Nonetheless, these studies pinpoint an important role for RBPs in maintaining the quiescent EC phenotype.

Another hallmark of the healthy endothelium is the maintenance of barrier function, which requires the formation of tightly linked adherens junctions on adjacent ECs, ensuring the low permeability of the vessel to circulating solutes, proteins, and cells. Strikingly, reports regarding the post-transcriptional regulation of adherens junction proteins are limited. Recently, we discovered that the RBP QKI is highly expressed in quiescent human ECs *in vivo*, and that the specific abrogation of this RBP markedly impaired the capacity to form a high-resistance endothelial monolayer in human ECs and in mice.<sup>125</sup> Mechanistically, QKI appears to be essential for maintaining barrier function by interacting with quaking response elements in the 3'UTRs of mature *b*-catenin and VE-cadherin mRNAs, ensuring sufficient translation to restrict vascular permeability.<sup>125</sup>

RNA-binding proteins have also been implicated in the posttranscriptional regulation of several other vital EC-derived factors, including VEGF,<sup>129,130</sup> endoglin,<sup>131</sup> and HIF1 $\alpha$ -<sup>132</sup>. Along with pivotal roles in tumour-accelerating angiogenesis,<sup>133–135</sup> changes in the abundance and splicing of these pre-mRNAs have also been linked with the development of CVD. An isoform of RBP76 (DRBP76/NF90) was found to bind to the 3'UTR of the VEGF mRNA, enhancing VEGF production by human ECs,<sup>130</sup> whereas changes in SRSF1 levels in senescent ECs altered VEGF and endoglin pre-mRNA splicing.<sup>131</sup> More recently, a pivotal role for HuR in guiding angiogenesis has been strengthened based on the finding that it enhances translation of the human VEGF mRNA<sup>129</sup> while also working in unison with polypyrimidine

tract binding protein (PTB) to enhance translation of HIF1 $\alpha$  by binding to distinct sites on the human HIF1 $\alpha$  mRNA, namely the 5'- and 3'UTRs, respectively.<sup>132</sup> Although the mechanism by which these factors drive CVD is incompletely understood, a potential explanation linking their established role in cancer biology and CVD is that they could stimulate the formation of vasa vasorum in large vessels. This could accelerate lesion formation as it enhances the supply of essential nutrients and pro-atherogenic factors to sites of vessel injury.

### **RNA-binding proteins in monocytes and macrophages: coordinating inflammatory responses to injury**

In acute and chronic disease settings, circulating monocytes are exposed to diverse stimuli that generally triggers their activation into pro-inflammatory phenotype,<sup>136,137</sup> followed by their homing to sites of tissue injury and differentiation into macrophages. As cellular differentiation is tightly coupled with the dynamic regulation of mRNA stability, splicing patterning, and mRNA localization, RBPs are ideally positioned to post-transcriptionally co-ordinate events that determine monocyte and macrophage function. Indeed, AU-rich element binding proteins (ARE-BPs) have long been known to tightly control the expression of a plethora of cytokines and chemokines in monocytes and macrophages, including TNF- $\alpha$ , GM-CSF, M-CSF, IL-1 $\beta$ , IL-6, IL-10, and IFN- $\gamma$ .<sup>138</sup> The RBP-mRNA interaction at AREs encoded in the 3'UTR of these target (pre-) mRNAs<sup>139</sup> triggers rapid mRNA decay.<sup>140</sup> More recently, diversification of cytokine-regulating RBPs was made with the discovery that the Roquin RBPs specifically bind to stem-loop structures [termed constitutive decay elements (CDEs)] in the 3'UTR of target mRNAs in mice.<sup>141</sup> The 3'UTR of mouse TNF- $\alpha$  mRNA contains such a CDE, conferring Roquin with the capacity to bind to and destabilize the mRNA. Importantly, although these experiments were performed in mice, interaction of the human Roquin-1 and -2 isoforms with an mRNA containing a CDE was recently confirmed by X-ray crystallography.<sup>142</sup> As such, in concert with ARE-BPs, Roquins are likely responsible for ensuring a limited window of TNF- $\alpha$  expression in response to tissue injury in humans. These studies indicate that the induction, as opposed to targeting of certain RBPs, could serve as a novel approach for repressing the inflammatory component of atherosclerosis.<sup>143</sup>

Very recently, four SNPs were identified proximal to the QKI locus, revealing a nominally significant association with incident MI and coronary heart disease (CHD).<sup>144</sup> This two-stage full genome-wide association studies (GWAS) analysis of more than 64 000 individuals (with 3898 MI cases and 5465 CHD cases) pinpointed QKI as a novel predictive locus for incident CHD in prospective studies.<sup>144</sup> Although the authors did not detail the pathophysiological mechanism for this association, the recent discovery that QKI mRNA and protein are induced in macrophages of advanced human plaques, and that depletion of QKI protein in primary human monocytes significantly impaired: (i) monocyte adhesion and migration, (ii) differentiation into pro-inflammatory macrophages, and (iii) foam cell formation *in vitro* and *in vivo*, suggest that this RBP plays a central role in guiding inflammatory processes that accelerate CHD. Transcriptome analysis of monocytes and macrophages derived from a unique QKI haploinsufficient individual suggests that this phenotypic conversion is reliant on QKI-mediated changes in pre-mRNA splicing and mRNA transcript abundance.<sup>145</sup>

Collectively, these studies indicate that RBPs such as QKI can post-transcriptionally guide pro-inflammatory macrophage identity and function.

### **Therapeutic targeting of RNA binding protein-mediated events: harnessing the power of RNA regulation in human disease**

Strategies geared towards augmenting gene expression represent a powerful means of correcting decreases in the abundance of transcripts that encode proteins required to limit disease progression. Recently, adenoviral-associated virus (AAV) vectors have regained their status as a plausible means of achieving this therapeutic goal,<sup>146</sup> as these minimally immunogenic and non-integrative vectors can increase expression levels of selected genes by infecting both dividing and non-dividing cardiac cells based on the existence of several viral serotypes, whereas their small size allows for the efficient delivery to the myocardium via coronary arteries.<sup>146,147</sup> Alternatively, retrograde delivery into the coronary sinus and a surgical recirculation method have recently been implemented to enhance cardiomyocyte expression of SERCA2a in pigs and sheep, respectively. More recently, AAV has also been used to drive exogenous expression of heme oxygenase 1<sup>148</sup> and VEGF-B<sup>149</sup> in pigs and dogs, respectively.

These pre-emptive studies effectively limited cardiac ischaemia<sup>148</sup> and tachy-pacing induced heart failure,<sup>149</sup> respectively. Attempts to treat established CVD using AAV in the form of Mydica (Celladon; now Eiger Biopharmaceuticals) initially yielded promising results for SERCA2a enzymatic replacement therapy in clinical trials.<sup>150</sup> However, the Phase IIb clinical trial failure of Mydica is being attributed to an inability of the AAV to deeply penetrate the myocardial tissue mass, indicating that direct intramyocardial injection or coronary sinus delivery method could increase the likelihood of success in the future.<sup>150</sup> Importantly, AAVs could also be tailored to specifically encode beneficial splice variants of genes, such as the full-length SCN5A splice variant (as opposed to the truncated SCN5A splice variant), which could limit arrhythmias by maintaining cardiac Na currents and thereby electric conduction velocity in the heart.<sup>79,151</sup> Furthermore, the introduction of promoter regions that induce expression solely in response to injury could broaden the applicability of AAVs as a means of correcting decreased cardioprotective gene expression in a spatiotemporal fashion.

To combat increases in inflammatory and fibroproliferative gene expression commonly observed in CVD, short-interfering RNA-based approaches are currently being extensively employed in the (pre-)clinical forum (see RNA-based clinical trial review<sup>34</sup>). As their safety profile and mechanism by which they function are well-established, these could represent an excellent means of ameliorating RBP expression, although the hierarchical positioning of these proteins as global regulators of the transcriptome could elicit undesirable off-target effects. Therefore, computational mining of transcriptomic databases in cardiovascular centres worldwide could uncover splice variants that are enriched in diverse cardiovascular complications, enabling the design of small interfering RNAs (siRNAs) that could specifically target disease advancing splice variants (thereby reducing production of encoded protein isoforms), representing a novel and highly effective means of targeting in a cell type-specific fashion. Although several methods are currently being employed to deliver siRNAs in humans,<sup>34</sup> the development of lipid-based formulations for the effective transport of siRNAs,

miRNAs and antagomiRs is regarded as essential for the broad applicability of RNA-based therapeutic approaches in the clinical setting, and has been prioritized by the pharmaceutical industry.<sup>32</sup>

Aberrant splicing, as a result of genetic mutations that alter either RBP function or the splice sites these proteins recognize, is becoming increasingly recognized as a major contributor to human disease, including CVD.<sup>152–154</sup> The use of antisense oligonucleotides (AONs) to correct these RNA-based defects has been applied extensively at the drug developmental level,<sup>33,155</sup> conferring the capacity to skip one or more exons or restore/disrupt the transcript reading frame (Figure 2).<sup>155,156</sup> Importantly, these biotools have gained widespread attention as a result of their therapeutic potential for Duchenne's muscular dystrophy (drisapersen and eteplersen; GlaxoSmithKline plc. and Sarepta Therapeutics Inc., respectively) and spinal muscular atrophy (nusinersen; Ionis Pharmaceuticals & Biogen Inc.). Of note, eteplersen has recently been granted accelerated FDA approval whereas nusinersen filing for FDA approval is imminent. Despite these successes in correcting splicing dysregulation in rare genetic diseases, ventures into the cardiovascular field are limited. This is particularly surprising given the identification of numerous CVD-associated splicing events, such as troponin T in cardiomyocytes,<sup>157</sup> oxidized low-density lipoprotein receptor 1 in macrophages,<sup>154</sup> VEGF in ECs,<sup>158</sup> and myocardin in VSMCs.<sup>25</sup> Recently, an AON-based approach was used to correct the A-band truncating mutation of Ser14450fsX4 in exon 326 of titin,<sup>159</sup> a protein that plays a critical role in sarcomere organization and passive elasticity in cardiomyocytes. Importantly, missense mutations in human titin, including truncations as described above,<sup>159</sup> have been found to responsible for 25% of familial DCM cases and 18% of sporadic DCM cases. By forcing excision of exon 326 in patient-specific cardiomyocytes ex vivo, myofibril assembly was improved, and similar studies with the truncation-correcting AON in mice revealed a correction of DCM phenotype.<sup>159</sup> Further evidence that AONs could represent a potent means of limiting CVD progression can be found in their recent application to correct autoimmunity in mice as a result of defective NLRP3.<sup>160</sup> Interestingly, the inflammasome protein complex plays a critical role in promoting cytokine maturation and inflammation in myeloid cells, including macrophages. As such, the in vivo correction of an alternative splice acceptor site<sup>160</sup> (as detailed in Figure 2) in macrophages by Thygesen et al. represents an important step towards similar AON-based interventions in human myeloid cells, and potential therapeutic application in humans.

Collectively, the continued development of DNA- and RNA-based approaches designed to alter the transcriptome could result in the generation of novel therapies that harness RBP-mediated processes, and significantly impact the treatment of CVD in the future.



## Conclusions and future perspectives

In conclusion, cells undergo functional adaptations at sites of injury that serve to limit tissue damage and restore proper tissue function and structure. These remodelling and regenerative responses in affected cells are tightly coupled with dynamic changes in gene expression patterns that necessitate RBPs to determine the fate of nascent RNAs. In doing so, RBPs have emerged as potent effectors and regulators of cellular function in (patho)physiological settings. In light of our expanding insight into the diversity and complexity of protein-coding and non-protein-coding RNA transcripts, as well as the critical role played by an ever-expanding number of RBPs involved in processing these transcripts, our understanding of the human genome has broadened significantly. Importantly, this 'RNAissance' has unleashed a revolution in drug development, leading to numerous RNA-based therapies that are currently being explored in diverse pre-clinical animal studies and clinical trials. The potential inclusion of these novel therapeutic modalities could represent an important broadening of our medical arsenal in combating CVD in the 21st century.

## Permissions

The authors do hereby declare that all illustrations and figures in the manuscript are entirely original and do not require reprint permission. Supplementary material  
Supplementary material is available at European Heart Journal online.

## Funding

Netherlands Institute for Regenerative Medicine research grants (FES0908) to R.G.B. and E.P.V. Funding to pay the Open Access publication charges for this article was provided by the Department of Internal Medicine, Leiden University Medical Center.

**Conflict of interest:** none declared.

Supplementary material is available at European Heart Journal online.



## References

1. Gonzalez DM, Medici D. Signaling mechanisms of the epithelial-mesenchymal transition. *Sci Signal* 2014;7:re8.
2. Ritzel RM, Patel AR, Grenier JM, Crapser J, Verma R, Jellison ER, McCullough LD. Functional differences between microglia and monocytes after ischemic stroke. *J Neuroinflammation* 2015;12:106.
3. Owens GK, Kumar MS, Wamhoff BR. Molecular regulation of vascular smooth muscle cell differentiation in development and disease. *Physiol Rev* 2004;84:767–801.
4. Bijkerk R, de Bruin RG, van Solingen C, Duijs JM, Kobayashi K, van der Veer EP, ten Dijke P, Rabelink TJ, Goumans MJ, van Zonneveld AJ. MicroRNA-155 functions as a negative regulator of RhoA signaling in TGF-beta-induced endothelial to mesenchymal transition. *Microna* 2012;1:2–10.
5. Ross R. Atherosclerosis—an inflammatory disease. *N Engl J Med* 1999;340:115–126.
6. Robbins CS, Hilgendorf I, Weber GF, Theurl I, Iwamoto Y, Figueiredo JL, Gorbato R, Sukhova GK, Gerhardt LM, Smyth D, Zavitz CC, Shikatani EA, Parsons M, van Rooijen N, Lin HY, Husain M, Libby P, Nahrendorf M, Weissleder R, Swirski FK. Local proliferation dominates lesion macrophage accumulation in atherosclerosis. *Nat Med* 2013;19:1166–1172.
7. Holmes DR Jr, Taggart DP. Revascularization in stable coronary artery disease: a combined perspective from an interventional cardiologist and a cardiac surgeon. *Eur Heart J* 2016;37:1873–1882.
8. Siontis GC, Stefanini GG, Mavridis D, Siontis KC, Alfonso F, Perez-Vizcaino MJ, Byrne RA, Kastrati A, Meier B, Salanti G, Juni P, Windecker S. Percutaneous coronary interventional strategies for treatment of in-stent restenosis: a network meta-analysis. *Lancet* 2015;386:655–664.
9. Zargham R. Preventing restenosis after angioplasty: a multistage approach. *Clin Sci* 2008;114:257–264.
10. Ahuja P, Sdek P, MacLellan WR. Cardiac myocyte cell cycle control in development, disease, and regeneration 2007;87:521–544.
11. Tedgui A, Mallat Z. Cytokines in atherosclerosis: pathogenic and regulatory pathways. *Physiol Rev* 2006;86:515–581.
12. Hilgendorf I, Swirski FK, Robbins CS. Monocyte fate in atherosclerosis. *Arterioscler Thromb Vasc Biol* 2015;35:272–279.
13. Murray PJ, Wynn TA. Protective and pathogenic functions of macrophage subsets. *Nat Rev Immunol* 2011;11:723–737.
14. Chistiakov DA, Bobryshev YV, Orekhov AN. Macrophage-mediated cholesterol handling in atherosclerosis. *J Cell Mol Med* 2016;20:17–28.
15. Beckman JA, Creager MA. The nonlipid effects of statins on endothelial function. *Trends Cardiovasc Med* 2006;16:156–162.
16. Parmar KM, Nambudiri V, Dai G, Larman HB, Gimbrone MA Jr, Garcia-Cardena G. Statins exert endothelial atheroprotective effects via the KLF2 transcription factor. *J Biol Chem* 2005;280:26714–26719.
17. Sen-Banerjee S, Mir S, Lin Z, Hamik A, Atkins GB, Das H, Banerjee P, Kumar A, Jain MK. Kruppel-like factor 2 as a novel mediator of statin effects in endothelial cells. *Circulation* 2005;112:720–726.
18. Fish JE, Santoro MM, Morton SU, Yu S, Yeh R-F, Wythe JD, Ivey KN, Bruneau BG, Stainier DY, Srivastava D. miR-126 regulates angiogenic signaling and vascular integrity. *Dev Cell* 2008;15:272–284.
19. van Solingen C, Seghers L, Bijkerk R, Duijs JM, Roeten MK, van Oeveren-Rietdijk AM, Baelde HJ, Monge M, Vos JB, de Boer HC, Quax PH, Rabelink TJ, van Zonneveld AJ. An tagomir-mediated silencing of endothelial cell specific microRNA-126 impairs ischemia-induced angiogenesis. *J Cell Mol Med* 2009;13:1577–1585.
20. de Klerk E, T Hoen PA. Alternative mRNA transcription, processing, and translation: insights from RNA sequencing. *Trends Genet* 2015;31:128–139.
21. Wahlestedt C. Targeting long non-coding RNA to therapeutically upregulate gene expression. *Nat Rev Drug Discov* 2013;12:433–446.
22. Kafasla P, Skliris A, Kontoyiannis DL. Post-transcriptional coordination of immunological responses by RNA-binding proteins. *Nat Immunol* 2014;15:492–502.
23. Neelamraju Y, Hashemikhabir S, Janga SC. The human RBPome: from genes and proteins to

- human disease. *J Proteomics* 2015;127:61–70.
24. Sheng JJ, Jin JP. Gene regulation, alternative splicing, and posttranslational modification of troponin subunits in cardiac development and adaptation: a focused review. *Front Physiol* 2014;5:165.
  25. van der Veer EP, de Bruin RG, Kraaijeveld AO, de Vries MR, Bot I, Pera T, Segers FM, Trompet S, van Gils JM, Roeten MK, Beckers CM, van Santbrink PJ, Janssen A, van Solingen C, Swildens J, de Boer HC, Peters EA, Bijkerk R, Rousch M, Doop M, Kuiper J, Schaliij MJ, van der Wal AC, Richard S, van Berkel TJ, Pickering JG, Hiemstra PS, Goumans MJ, Rabelink TJ, de Vries AA, Quax PH, Jukema JW, Biessen EA, van Zonneveld AJ. Quaking, an RNA-binding protein, is a critical regulator of vascular smooth muscle cell phenotype. *Circ Res* 2013;113:1065–1075.
  26. Beckmann BM, Horos R, Fischer B, Castello A, Eichelbaum K, Alleaume AM, Schwarzl T, Curk T, Foehr S, Huber W, Krijgsveld J, Hentze MW. The RNA-binding proteomes from yeast to man harbour conserved enigmRBPs. *Nature Commun* 2015;6:10127.
  27. Kazan H, Ray D, Chan ET, Hughes TR, Morris Q. RNAcontext: a new method for learning the sequence and structure binding preferences of RNA-binding proteins. *PLoS Comput Biol* 2010;6:e1000832.
  28. Ray D, Kazan H, Chan ET, Pena Castillo L, Chaudhry S, Talukder S, Blencowe BJ, Morris Q, Hughes TR. Rapid and systematic analysis of the RNA recognition specificities of RNA-binding proteins. *Nat Biotechnol* 2009;27:667–670.
  29. Ray D, Kazan H, Cook KB, Weirauch MT, Najafabadi HS, Li X, Gueroussov S, Albu M, Zheng H, Yang A, Na H, Irimia M, Matzat LH, Dale RK, Smith SA, Yarosh CA, Kelly SM, Nabet B, Meenas D, Li W, Laishram RS, Qiao M, Lipshitz HD, Piano F, Corbett AH, Carstens RP, Frey BJ, Anderson RA, Lynch KW, Penalva LO, Lei EP, Fraser AG, Blencowe BJ, Morris QD, Hughes TR. A compendium of RNA-binding motifs for decoding gene regulation. *Nature* 2013;499:172–177.
  30. Galarneau A, Richard S. Target RNA motif and target mRNAs of the quaking STAR protein. *Nat Struct Mol Biol* 2005;12:691–698.
  31. Galarneau A, Richard S. The STAR RNA binding proteins GLD-1, QKI, SAM68 and SLM-2 bind bipartite RNA motifs. *BMC Mol Biol* 2009;10:47.
  32. Yin H, Kanasty RL, Eltoukhy AA, Vegas AJ, Dorkin JR, Anderson DG. Non-viral vectors for gene-based therapy. *Nat Rev Genet* 2014;15:541–555.
  33. Aartsma-Rus A. New momentum for the field of oligonucleotide therapeutics. *Mol Ther* 2016;24:193–194.
  34. Kanasty R, Dorkin JR, Vegas A, Anderson D. Delivery materials for siRNA therapeutics. *Nat Mater* 2013;12:967–977.
  35. Hillier LW, Coulson A, Murray JI, Bao Z, Sulston JE, Waterston RH. Genomics in *C. elegans*: so many genes, such a little worm. *Genome Res* 2005;15:1651–1660.
  36. Consortium EP. An integrated encyclopedia of DNA elements in the human genome. *Nature* 2012;489:57–74.
  37. Hube F, Francastel C. Mammalian introns: when the junk generates molecular diversity. *Int J Mol Sci* 2015;16:4429–4452.
  38. Esteller M. Non-coding RNAs in human disease. *Nat Rev Genet* 2011;12:861–874.
  39. Archer K, Broskova Z, Bayoumi AS, Teoh JP, Davila A, Tang Y, Su H, Kim IM. Long non-coding RNAs as master regulators in cardiovascular diseases. *Int J Mol Sci* 2015;16:23651–23667.
  40. Dey BK, Mueller AC, Dutta A. Long non-coding RNAs as emerging regulators of differentiation, development, and disease. *Transcription* 2014;5:e944014.
  41. Earls LR, Westmoreland JJ, Zakharenko SS. Non-coding RNA regulation of synaptic plasticity and memory: implications for aging. *Ageing Res Rev* 2014;17:34–42.
  42. Haemmerle M, Gutschner T. Long non-coding RNAs in cancer and development: where do we go from here?. *Int J Mol Sci* 2015;16:1395–1405.
  43. Smolle E, Haybaeck J. Non-coding RNAs and lipid metabolism. *Int J Mol Sci* 2014;15:13494–13513.
  44. Thum T, Condorelli G. Long noncoding RNAs and microRNAs in cardiovascular pathophysiology. *Circ Res* 2015;116:751–762.
  45. Boon RA, Jae N, Holdt L, Dimmeler S. Long noncoding RNAs: from clinical genetics to therapeutic Targets?. *J Am Coll Cardiol* 2016;67:1214–1226.
  46. Elzenaar I, Pinto YM, van Oort RJ. MicroRNAs in heart failure: new targets in disease management. *Clin Pharmacol Ther* 2013;94:480–489.

47. Marian AJ. Recent developments in cardiovascular genetics and genomics. *Circ Res* 2014;115:e11–e17.
48. Elia L, Condorelli G. RNA (Epi)genetics in cardiovascular diseases. *J Mol Cell Cardiol* 2015;89:11–16.
49. Lunde BM, Moore C, Varani G. RNA-binding proteins: modular design for efficient function. *Nat Rev Mol Cell Biol* 2007;8:479–490.
50. Weyn-Vanhenhenryck SM, Zhang C. mCarts: genome-wide prediction of clustered sequence motifs as binding sites for RNA-binding proteins. *Methods Mol Biol* 2016;1421:215–226.
51. Corcoran DL, Georgiev S, Mukherjee N, Gottwein E, Skalsky RL, Keene JD, Ohler U. PARalyzer: definition of RNA binding sites from PAR-CLIP short-read sequence data. *Genome Biol* 2011;12:R79.
52. Fu XD, Ares M Jr. Context-dependent control of alternative splicing by RNA-binding proteins. *Nat Rev Genet* 2014;15:689–701.
53. Hafner M, Landthaler M, Burger L, Khorshid M, Hausser J, Berninger P, Rothballer A, Ascano M Jr, Jungkamp AC, Munschauer M, Ulrich A, Wardle GS, Dewell S, Zavolan M, Tuschl T. Transcriptome-wide identification of RNA-binding protein and microRNA target sites by PAR-CLIP. *Cell* 2010;141:129–141.
54. Wang ET, Sandberg R, Luo S, Khrebukova I, Zhang L, Mayr C, Kingsmore SF, Schroth GP, Burge CB. Alternative isoform regulation in human tissue transcriptomes. *Nature* 2008;456:470–476.
55. Will CL, Luhrmann R. Spliceosome structure and function. *Cold Spring Harb Perspect Biol* 2011;3:1–25.
56. Wahl MC, Luhrmann R. SnapShot: spliceosome dynamics I. *Cell* 2015;161:1474–14e1.
57. Wahl MC, Will CL, Luhrmann R. The spliceosome: design principles of a dynamic RNP machine. *Cell* 2009;136:701–718.
58. Hu Z, Scott HS, Qin G, Zheng G, Chu X, Xie L, Adelson DL, Oftedal BE, Venugopal P, Babic M, Hahn CN, Zhang B, Wang X, Li N, Wei C. Revealing missing human protein isoforms based on Ab Initio prediction, RNA-seq and proteomics. *Sci Rep* 2015;5:10940.
59. Denis MM, Tolley ND, Bunting M, Schwertz H, Jiang H, Lindemann S, Yost CC, Rubner FJ, Albertine KH, Swoboda KJ, Fratto CM, Tolley E, Kraiss LW, McIntyre TM, Zimmerman GA, Weyrich AS. Escaping the nuclear confines: signal-dependent pre-mRNA splicing in anucleate platelets. *Cell* 2005;122:379–391.
60. Mortazavi A, Williams BA, McCue K, Schaeffer L, Wold B. Mapping and quantifying mammalian transcriptomes by RNA-Seq. *Nat Methods* 2008;5:621–628.
61. Anderson PA, Greig A, Mark TM, Malouf NN, Oakeley AE, Ungerleider RM, Allen PD, Kay BK. Molecular basis of human cardiac troponin T isoforms expressed in the developing, adult, and failing heart. *Circ Res* 1995;76:681–686.
62. Wuytack F, van den Bosch L, Ver Heyen M, Baba-Aissa F, Raeymaekers L, Casteels R. Regulation of alternative splicing of the SERCA2 pre-mRNA in muscle. *Ann N Y Acad Sci* 1998;853:372–375.
63. Yang TP, Agellon LB, Walsh A, Breslow JL, Tall AR. Alternative splicing of the human cholesteryl ester transfer protein gene in transgenic mice. Exon exclusion modulates gene expression in response to dietary or developmental change. *J Biol Chem* 1996;271:12603–12609.
64. Blech-Hermoni Y, Ladd AN. RNA binding proteins in the regulation of heart development. *Int J Biochem Cell Biol* 2013;45:2467–2478.
65. Bult CJ, Krupke DM, Begley DA, Richardson JE, Neuhauser SB, Sundberg JP, Eppig JT. Mouse Tumor Biology (MTB): a database of mouse models for human cancer. *Nucleic Acids Res* 2015;43:D818–D824.
66. Eppig JT, Blake JA, Bult CJ, Kadin JA, Richardson JE. The Mouse Genome Database (MGD): facilitating mouse as a model for human biology and disease. *Nucleic Acids Res* 2015;43:D726–D736.
67. Smith CM, Finger JH, Hayamizu TF, McCright IJ, Xu J, Berghout J, Campbell J, Corbani LE, Forthofer KL, Frost PJ, Miers D, Shaw DR, Stone KR, Eppig JT, Kadin JA, Richardson JE, Ringwald M. The mouse Gene Expression Database (GXD): 2014 update. *Nucleic Acids Res* 2014;42:D818–D824.
68. Verma SK, Deshmukh V, Liu P, Nutter CA, Espejo R, Hung ML, Wang GS, Yeo GW, Kuyumcu-Martinez MN. Reactivation of fetal splicing programs in diabetic hearts is mediated by protein kinase C signaling. *J Biol Chem* 2013;288:35372–35386.

69. Giudice J, Xia Z, Wang ET, Scavuzzo MA, Ward AJ, Kalsotra A, Wang W, Wehrens XH, Burge CB, Li W, Cooper TA. Alternative splicing regulates vesicular trafficking genes in cardiomyocytes during postnatal heart development. *Nat Commun* 2014;5:3603.
70. Kalsotra A, Xiao X, Ward AJ, Castle JC, Johnson JM, Burge CB, Cooper TA. A postnatal switch of CELF and MBNL proteins reprograms alternative splicing in the developing heart. *Proc Natl Acad Sci U S A* 2008;105:20333–20338.
71. Olson EN. Gene regulatory networks in the evolution and development of the heart. *Science* 2006;313:1922–1927.
72. Kong SW, Hu YW, Ho JW, Ikeda S, Polster S, John R, Hall JL, Bisping E, Pieske B, dos Remedios CG, Pu WT. Heart failure-associated changes in RNA splicing of sarcomere genes. *Circ Cardiovasc Genet* 2010;3:138–146.
73. Xu X, Yang D, Ding JH, Wang W, Chu PH, Dalton ND, Wang HY, Bermingham JR, Jr., Ye Z, Liu F, Rosenfeld MG, Manley JL, Ross J Jr, Chen J, Xiao RP, Cheng H, Fu XD. ASF/ SF2-regulated CaMKII $\delta$  alternative splicing temporally reprograms excitation-contraction coupling in cardiac muscle. *Cell* 2005;120:59–72.
74. Brauch KM, Karst ML, Herron KJ, de Andrade M, Pellikka PA, Rodeheffer RJ, Michels VV, Olson TM. Mutations in ribonucleic acid binding protein gene cause familial dilated cardiomyopathy. *J Am Coll Cardiol* 2009;54:930–941.
75. Li D, Morales A, Gonzalez-Quintana J, Norton A, Siegfried JD, Hofmeyer M, Hershberger RE. Identification of novel mutations in RBM20 in patients with dilated cardiomyopathy. *Clin Transl Sci* 2010;3:90–97.
76. Maatz H, Jens M, Liss M, Schafer S, Heinig M, Kirchner M, Adami E, Rintisch C, Dauksaite V, Radke MH, Selbach M, Barton PJ, Cook SA, Rajewsky N, Gotthardt M, Landthaler M, Hubner N. RNA-binding protein RBM20 represses splicing to orchestrate cardiac pre-mRNA processing. *J Clin Invest* 2014;124:3419–3430.
77. Guo W, Schafer S, Greaser ML, Radke MH, Liss M, Govindarajan T, Maatz H, Schulz H, Li S, Parrish AM, Dauksaite V, Vakeel P, Klaassen S, Gerull B, Thierfelder L, Regitz-Zagrosek V, Hacker TA, Saue KW, Dec GW, Ellinor PT, MacRae CA, Spallek B, Fischer R, Perrot A, Ozcelik C, Saar K, Hubner N, Gotthardt M. RBM20, a gene for hereditary cardiomyopathy, regulates titin splicing. *Nat Med* 2012;18:766–773.
78. Wang GS, Kearney DL, De Biasi M, Taffet G, Cooper TA. Elevation of RNA-binding protein CUGBP1 is an early event in an inducible heart-specific mouse model of myotonic dystrophy. *J Clin Invest* 2007;117:2802–2811.
79. Freyermuth F, Rau F, Kokunai Y, Linke T, Sellier C, Nakamori M, Kino Y, Arandel L, Jollet A, Thibault C, Philipps M, Vicaire S, Jost B, Udd B, Day JW, Duboc D, Wahbi K, Matsumura T, Fujimura H, Mochizuki H, Deryckere F, Kimura T, Nukina N, Ishiura S, Lacroix V, Campan-Fournier A, Navratil V, Chautard E, Auboeuf D, Horie M, Imoto K, Lee KY, Swanson MS, Lopez de Munain A, Inada S, Itoh H, Nakazawa K, Ashihara T, Wang E, Zimmer T, Furling D, Takahashi MP, Charlet-Berguerand N. Splicing misregulation of SCN5A contributes to cardiac-conduction delay and heart arrhythmia in myotonic dystrophy. *Nat Commun* 2016;7:11067.
80. Zhou A, Greener I, Xie A, Shi G, Yang K-C, Liu H, Rutledge C, Dudley S. mRNA stability proteins regulate human cardiac sodium channel expression. *Circulation* 2014;130:A15892–A15892.
81. Zhang Y, Si Y, Ma N, Mei J. The RNA-binding protein PCBP2 inhibits Ang II-induced hypertrophy of cardiomyocytes through promoting GPR56 mRNA degradation. *Biochem Biophys Res Commun* 2015;464:679–684.
82. Li J, Xie D, Huang J, Lv F, Shi D, Liu Y, Lin L, Geng L, Wu Y, Liang D. Cold-inducible RNA-binding protein regulates cardiac repolarization by targeting transient outward potassium channels. *Circ Res* 2015;116:1655–1659.
83. Agema W, Jukema J, Pimstone S, Kastelein J. Genetic aspects of restenosis after percutaneous coronary interventions; towards more tailored therapy. *Eur Heart J* 2001;22:2058–2074.
84. Lee T, Safdar N, Mistry MJ, Wang Y, Chauhan V, Campos B, Munda R, Cornea V, Roy-Chaudhury P. Preexisting venous calcification prior to dialysis vascular access surgery. *Semin Dial* 2012;25:592–595.
85. Mitchell RN, Libby P. Vascular remodeling in transplant vasculopathy. *Circ Res* 2007;100:967–978.
86. Nagai R, Kuro-O M, Babij P, Periasamy M. Identification of two types of smooth muscle myosin heavy chain isoforms by cDNA cloning and immunoblot analysis. *J Biol Chem* 1989;264:9734–

87. Lenz S, Lohse P, Seidel U, Arnold H. The alkali light chains of human smooth and nonmuscle myosins are encoded by a single gene. Tissue-specific expression by alternative splicing pathways. *J Biol Chem* 1989;264:9009–9015.
88. Nabeshima Y, Nonomura Y, Fujii-Kuriyama Y. Nonmuscle and smooth muscle myosin light chain mRNAs are generated from a single gene by the tissuespecific alternative RNA splicing. *J Biol Chem* 1987;262:10608–10612.
89. van Eys GJ, Vo<sup>o</sup>ller MC, Timmer ED, Wehrens XH, Small JV, Schalken JA, Ramaekers FC, van der Loop FT. Smoothelin expression characteristics: development of a smooth muscle cell in vitro system and identification of a vascular variant. *Cell Struct Funct* 1997;22:65–72.
90. Rensen S, Thijssen V, De Vries C, Doevendans P, Detera-Wadleigh S, Van Eys G. Expression of the smoothelin gene is mediated by alternative promoters. *Cardiovasc Res* 2002;55:850–863.
91. Ruiz-Opazo N, Nadal-Ginard B. Alpha-tropomyosin gene organization. Alternative splicing of duplicated isotype-specific exons accounts for the production of smooth and striated muscle isoforms. *J Biol Chem* 1987;262:4755–4765.
92. Wieczorek DF, Smith C, Nadal-Ginard B. The rat alpha-tropomyosin gene generates a minimum of six different mRNAs coding for striated, smooth, and nonmuscle isoforms by alternative splicing. *Mol Cell Biol* 1988;8:679–694.
93. Byrne B, Kaczorowski Y, Coutu M, Craig S. Chicken vinculin and meta-vinculin are derived from a single gene by alternative splicing of a 207-base pair exon unique to meta-vinculin. *J Biol Chem* 1992;267:12845–12850.
94. Strasser P, Gimona M, Moessler H, Herzog M, Small JV. Mammalian calponin. *FEBS Lett* 1993;330:13–18.
95. Humphrey MB, Herrera-Sosa H, Gonzalez G, Lee R, Bryan J. Cloning of cDNAs encoding human caldesmons. *Gene* 1992;112:197–204.
96. Sobue K, Sellers J. Caldesmon, a novel regulatory protein in smooth muscle and nonmuscle actomyosin systems. *J Biol Chem* 1991;266:12115–12118.
97. Justice MJ, Bode VC. Three ENU-induced alleles of the murine quaking locus are recessive embryonic lethal mutations. *Genet Res* 1988;51:95–102.
98. Li Z, Takakura N, Oike Y, Imanaka T, Araki K, Suda T, Kaname T, Abe K, Yamamura K. Defective smooth muscle development in qkl-deficient mice. *Dev Growth Differ* 2003;45:449–
99. Noveroske JK, Lai L, Gaussin V, Northrop JL, Nakamura H, Hirschi KK, Justice MJ. Quaking is essential for blood vessel development. *Genesis* 2002;32:218–230.
100. Creemers EE, Sutherland LB, Oh J, Barbosa AC, Olson EN. Coactivation of MEF2 by the SAP domain proteins myocardin and MASTR. *Molecular Cell* 2006;23:83–96.
101. Ilagan RM, Genheimer CW, Quinlan SF, Guthrie KI, Sangha N, Ramachandranair S, Kelley RW, Presnell SC, Basu J, Ludlow JW. Smooth muscle phenotypic diversity is mediated through alterations in myocardin gene splicing. *J Cell Physiol* 2011;226:2702–2711.
102. Miano JM. Myocardin in biology and disease. *J Biomed Res* 2015;29:3–19.
103. Pullmann R Jr, Juhaszova M, Lopez de Silanes I, Kawai T, Mazan-Mamczarz K, Halushka MK, Gorospe M. Enhanced proliferation of cultured human vascular smooth muscle cells linked to increased function of RNA-binding protein HuR. *J Biol Chem* 2005;280:22819–22826.
104. Misquitta CM, Chen T, Grover AK. Control of protein expression through mRNA stability in calcium signalling. *Cell Calcium* 2006;40:329–346.
105. Nickenig G, Michaelsen F, Muller C, Berger A, Vogel T, Sachinidis A, Vetter H, Bohm M. Destabilization of AT(1) receptor mRNA by calreticulin. *Circ Res* 2002;90:53–58.
106. Pende A, Contini L, Sallo R, Passalacqua M, Tanveer R, Port JD, Lotti G. Characterization of RNA-binding proteins possibly involved in modulating human AT 1 receptor mRNA stability. *Cell Biochem Funct* 2008;26:493–501.
107. Paukku K, Backlund M, De Boer RA, Kalkkinen N, Kontula KK, Lehtonen JY. Regulation of AT1R expression through HuR by insulin. *Nucleic Acids Res* 2012;40:5250–5261.
108. Claggett B, Packer M, McMurray JJ, Swedberg K, Rouleau J, Zile MR, Jhund P, Lefkowitz M, Shi V, Solomon SD. Estimating the long-term treatment benefits of Sacubitril–Valsartan. *N Engl J Med* 2015;373:2289–2290.
109. Schmieder RE, Hilgers KF, Schlaich MP, Schmidt BM. Renin-angiotensin system and cardiovascular risk. *Lancet* 2007;369:1208–1219.
110. Kramann R, Schneider RK, DiRocco DP, Machado F, Fleig S, Bondzie PA, Henderson JM, Ebert BL, Humphreys BD. Perivascular Gli1<sup>+</sup> progenitors are key contributors to injury-induced organ fibrosis. *Cell Stem Cell* 2015;16:51–66.

111. Pu KM, Sava P, Gonzalez AL. Microvascular targets for anti-fibrotic therapeutics. *Yale J Biol Med* 2013;86:537–554.
112. Howard CM, Baudino TA. Dynamic cell-cell and cell-ECM interactions in the heart. *J Mol Cell Cardiol* 2014;70:19–26.
113. Amadio M, Scapagnini G, Lupo G, Drago F, Govoni S, Pascale A. PKC $\beta$ etall/ HuR/VEGF: a new molecular cascade in retinal pericytes for the regulation of VEGF gene expression. *Pharmacol Res* 2008;57:60–66.
114. Davis J, Salomonis N, Ghearing N, Lin SC, Kwong JQ, Mohan A, Swanson MS, Molkentin JD. MBNL1-mediated regulation of differentiation RNAs promotes myofibroblast transformation and the fibrotic response. *Nat Commun* 2015;6:10084.
115. Felkin LE, Narita T, Germack R, Shintani Y, Takahashi K, Sarathchandra P, Lopez-Olaneta MM, Gomez-Salinerio JM, Suzuki K, Barton PJ, Rosenthal N, Lara-Pezzi E. Calcineurin splicing variant calcineurin Abeta1 improves cardiac function after myocardial infarction without inducing hypertrophy. *Circulation* 2011;123:2838–2847.
116. Ganz P, Hsue PY. Endothelial dysfunction in coronary heart disease is more than a systemic process. *Eur Heart J* 2013;34:2025–2027.
117. Huvenneers S, Daemen MJ, Hordijk PL. Between Rho(k) and a hard place: the relation between vessel wall stiffness, endothelial contractility, and cardiovascular disease. *Circ Res* 2015;116:895–908.
118. Gryglewski RJ, Palmer RM, Moncada S. Superoxide anion is involved in the breakdown of endothelium-derived vascular relaxing factor. *Nature* 1986;320:454–456.
119. De Caterina R, Libby P, Peng HB, Thannickal VJ, Rajavashisth TB, Gimbrone MA Jr, Shin WS, Liao JK. Nitric oxide decreases cytokine-induced endothelial activation. Nitric oxide selectively reduces endothelial expression of adhesion molecules and proinflammatory cytokines. *J Clin Invest* 1995;96:60–68.
120. Alexander LM, Kutz JL, Kenney WL. Tetrahydrobiopterin increases NO-dependent vasodilation in hypercholesterolemic human skin through eNOS coupling mechanisms. *Am J Physiol Regul Integr Comp Physiol* 2013;304:R164–R169.
121. Dekker RJ, Boon RA, Rondaij MG, Kragt A, Volger OL, Elderkamp YW, Meijers JC, Voorberg J, Pannekoek H, Horrevoets AJ. KLF2 provokes a gene expression pattern that establishes functional quiescent differentiation of the endothelium. *Blood* 2006;107:4354–4363.
122. Dekker RJ, van Soest S, Fontijn RD, Salamanca S, de Groot PG, VanBavel E, Pannekoek H, Horrevoets AJ. Prolonged fluid shear stress induces a distinct set of endothelial cell genes, most specifically lung Kruppel-like factor (KLF2). *Blood* 2002;100:1689–1698.
123. Gimbrone MA Jr, Nagel T, Topper JN. Biomechanical activation: an emerging paradigm in endothelial adhesion biology. *J Clin Invest* 1997;99:1809–1813.
124. SenBanerjee S, Lin Z, Atkins GB, Greif DM, Rao RM, Kumar A, Feinberg MW, Chen Z, Simon DI, Lusinskas FW, Michel TM, Gimbrone MA Jr, Garcia-Cardena G, Jain MK. KLF2 is a novel transcriptional regulator of endothelial proinflammatory activation. *J Exp Med* 2004;199:1305–1315.
125. de Bruin RG, van der Veer EP, Prins J, Lee DH, Dane MJ, Zhang H, Roeten MK, Bijkerk R, de Boer HC, Rabelink TJ. The RNA-binding protein quaking maintains endothelial barrier function and affects VE-cadherin and  $\beta$ -catenin protein expression. *Sci Rep* 2016;6.
126. Rhee WJ, Ni CW, Zheng Z, Chang K, Jo H, Bao G. HuR regulates the expression of stress-sensitive genes and mediates inflammatory response in human umbilical vein endothelial cells. *Proc Natl Acad Sci U S A* 2010;107:6858–6863.
127. Hui J, Stangl K, Lane WS, Bindereif A. HnRNP L stimulates splicing of the eNOS gene by binding to variable-length CA repeats. *Nat Struct Biol* 2003;10:33–37.
128. Lorenz M, Hewing B, Hui J, Zepp A, Baumann G, Bindereif A, Stangl V, Stangl K. Alternative splicing in intron 13 of the human eNOS gene: a potential mechanism for regulating eNOS activity. *FASEB J* 2007;21:1556–1564.
129. Osera C, Martindale JL, Amadio M, Kim J, Yang X, Moad CA, Indig FE, Govoni S, Abdelmohsen K, Gorospe M, Pascale A. Induction of VEGFA mRNA translation by CoCl<sub>2</sub> mediated by HuR. *RNA Biol* 2015;12:1121–1130.
130. Vumbaca F, Phoenix KN, Rodriguez-Pinto D, Han DK, Claffey KP. Doublestranded RNA-binding protein regulates vascular endothelial growth factor mRNA stability, translation, and breast cancer angiogenesis. *Mol Cell Biol* 2008;28:772–783.
131. Blanco FJ, Bernabeu C. Alternative splicing factor or splicing factor-2 plays a key role in intron



- retention of the endoglin gene during endothelial senescence. *Aging Cell* 2011;10:896–907.
132. Galban S, Kuwano Y, Pullmann R Jr, Martindale JL, Kim HH, Lai A, Abdelmohsen K, Yang X, Dang Y, Liu JO, Lewis SM, Holcik M, Gorospe M. RNA-binding proteins HuR and PTB promote the translation of hypoxia-inducible factor 1 $\alpha$ . *Mol Cell Biol* 2008;28:93–107.
133. de Brot S, Ntekim A, Cardenas R, James V, Allegrucci C, Heery DM, Bates DO, Odum N, Persson JL, Mongan NP. Regulation of vascular endothelial growth factor in prostate cancer. *Endocr Relat Cancer* 2015;22:R107–R123.
134. Mamlouk S, Wielockx B. Hypoxia-inducible factors as key regulators of tumor inflammation. *Int J Cancer* 2013;132:2721–2729.
135. Seon BK, Haba A, Matsuno F, Takahashi N, Tsujie M, She X, Harada N, Uneda S, Tsujie T, Toi H, Tsai H, Haruta Y. Endoglin-targeted cancer therapy. *Curr Drug Deliv* 2011;8:135–143.
136. Geissmann F, Manz MG, Jung S, Sieweke MH, Merad M, Ley K. Development of monocytes, macrophages, and dendritic cells. *Science* 2010;327:656–661.
137. Ziegler-Heitbrock L, Ancuta P, Crowe S, Dalod M, Grau V, Hart DN, Leenen PJ, Liu Y-J, MacPherson G, Randolph GJ. Nomenclature of monocytes and dendritic cells in blood. *Blood* 2010;116:e74–e80.
138. Anderson P. Post-transcriptional control of cytokine production. *Nat Immunol* 2008;9:353–359.
139. Chen C-Y, Gherzi R, Ong S-E, Chan EL, Rajmakers R, Pruijn GJ, Stoecklin G, Moroni C, Mann M, Karin M. AU binding proteins recruit the exosome to degrade ARE-containing mRNAs. *Cell* 2001;107:451–464.
140. Shaw G, Kamen R. A conserved AU sequence from the 3' untranslated region of GM-CSF mRNA mediates selective mRNA degradation. *Cell* 1986;46:659–667.
141. Leppke K, Schott J, Reitter S, Poetz F, Hammond MC, Stoecklin G. Roquin promotes constitutive mRNA decay via a conserved class of stem-loop recognition motifs. *Cell* 2013;153:869–880.
142. Sakurai S, Ohto U, Shimizu T. Structure of human Roquin-2 and its complex with constitutive-decay element RNA. *Acta Crystallogr F Struct Biol Commun* 2015;71:1048–1054.
143. Libby P, Hansson GK. Inflammation and immunity in diseases of the arterial tree: players and layers. *Circ Res* 2015;116:307–311.
144. Dehghan A, Bis JC, White CC, Smith AV, Morrison AC, Cupples LA, Trompet S, Chasman DI, Lumley T, Vo"lker U. Genome-wide association study for incident myocardial infarction and coronary heart disease in prospective cohort studies: the CHARGE consortium. *PloS One* 2016;11:e0144997.
145. de Bruin RG, Shiue L, Prins J, de Boer HC, Singh A, Fagg WS, van Gils JM, Duijs JM, Katzman S, Kraaijeveld AO, Bohringer S, Leung WY, Kielbasa SM, Donahue JP, van der Zande PH, Sijbom R, van Alem CM, Bot I, van Kooten C, Jukema JW, Van Esch H, Rabelink TJ, Kazan H, Biessen EA, Ares M Jr, van Zonneveld AJ, van der Veer EP. Quaking promotes monocyte differentiation into pro-atherogenic macrophages by controlling pre-mRNA splicing and gene expression. *Nat Commun* 2016;7:10846.
146. Hammoudi N, Ishikawa K, Hajjar RJ. Adeno-associated virus-mediated gene therapy in cardiovascular disease. *Curr Opin Cardiol* 2015;30:228–234.
147. Hinkel R, Trenkwalder T, Kupatt C. Gene therapy for ischemic heart disease. *Expert Opin Biol Ther* 2011;11:723–737.
148. Hinkel R, Lange P, Petersen B, Gottlieb E, Ng JK, Finger S, Horstkotte J, Lee S, Thormann M, Knorr M, El-Aouni C, Boekstegers P, Reichart B, Wenzel P, Niemann H, Kupatt C. Heme oxygenase-1 gene therapy provides cardioprotection via control of post-ischemic inflammation: an experimental study in a preclinical pig model. *J Am Coll Cardiol* 2015;66:154–165.
149. Woitek F, Zentilin L, Hoffman NE, Powers JC, Ottiger I, Parikh S, Kulczycki AM, Hurst M, Ring N, Wang T, Shaikh F, Gross P, Singh H, Kolpakov MA, Linke A, Houser SR, Rizzo V, Sabri A, Madesh M, Giacca M, Recchia FA. Intracoronary cytoprotective gene therapy: a study of VEGF-B167 in a pre-clinical animal model of dilated cardiomyopathy. *J Am Coll Cardiol* 2015;66:139–153.
150. Yla-Herttuala S. Gene therapy for heart failure: back to the bench. *Mol Ther* 2015;23:1551–1560.
151. Gao G, Dudley SC Jr. SCN5A splicing variants and the possibility of predicting heart failure-associated arrhythmia. *Expert Rev Cardiovasc Ther* 2013;11:117–119.
152. van den Hoogenhof MM, Pinto YM, Creemers EE. RNA Splicing: Regulation and Dysregulation in the Heart. *Circ Res* 2016;118:454–468.
153. Lin J, Hu Y, Nunez S, Foulkes AS, Cieply B, Xue C, Gerelus M, Li W, Zhang H, Rader DJ, Musunuru K, Li M, Reilly MP. Transcriptome-wide analysis reveals modulation of human macrophage inflammatory phenotype through alternative splicing. *Arterioscler Thromb Vasc Biol*

- 2016;36:1434–1437.
154. Tejedor JR, Tilgner H, Iannone C, Guigo R, Valcarcel J. Role of six single nucleotide polymorphisms, risk factors in coronary disease, in OLR1 alternative splicing. *RNA* 2015;21:1187–1202.
  155. Aartsma-Rus A. Overview on AON design. *Methods Mol Biol* 2012;867:117–129.
  156. Siva K, Covello G, Denti MA. Exon-skipping antisense oligonucleotides to correct missplicing in neurogenetic diseases. *Nucleic Acid Therapeutics* 2014;24:69–86.
  157. Thierfelder L, Watkins H, MacRae C, Lamas R, McKenna W, Vosberg HP, Seidman JG, Seidman CE. Alpha-tropomyosin and cardiac troponin T mutations cause familial hypertrophic cardiomyopathy: a disease of the sarcomere. *Cell* 1994;77:701–712.
  158. Azimi-Nezhad M. Vascular endothelial growth factor from embryonic status to cardiovascular pathology. *Rep Biochem Mol Biol* 2014;2:59–69.
  159. Gramlich M, Pane LS, Zhou Q, Chen Z, Murgia M, Schotterl S, Goedel A, Metzger K, Brade T, Parotta E, Schaller M, Gerull B, Thierfelder L, Aartsma-Rus A, Labeit S, Atherton JJ, McGaughan J, Harvey RP, Sinnecker D, Mann M, Laugwitz KL, Gawaz MP, Moretti A. Antisense-mediated exon skipping: a therapeutic strategy for titin-based dilated cardiomyopathy. *EMBO Mol Med* 2015;7:562–576.
  160. Thygesen SJ, Sester DP, Cridland SO, Wilton SD, Stacey KJ. Correcting the NLRP3 inflammation some deficiency in macrophages from autoimmune NZB mice with exon skipping antisense oligonucleotides. *Immunol Cell Biol* 2016;94:520–524.
  161. Bosse Y, Maghni K, Hudson TJ. 1 $\alpha$ ,25-dihydroxy-vitamin D3 stimulation of bronchial smooth muscle cells induces autocrine, contractility, and remodeling processes. *Physiol Genomics* 2007;29:161–168.
  162. Rao DA, Eid RE, Qin L, Yi T, Kirkiles-Smith NC, Tellides G, Pober JS. Interleukin (IL)-1 promotes allogeneic T cell intimal infiltration and IL-17 production in a model of human artery rejection. *J Exp Med* 2008;205:3145–3158.
  163. Kaneda R, Takada S, Yamashita Y, Choi YL, Nonaka-Sarukawa M, Soda M, Misawa Y, Isomura T, Shimada K, Mano H. Genome-wide histone methylation profile for heart failure. *Genes Cells* 2009;14:69–77.
  164. Schmolke M, Viemann D, Roth J, Ludwig S. Essential impact of NF-kappaB signaling on the H5N1 influenza A virus-induced transcriptome. *J Immunol* 2009;183:5180–5189.
  165. Pellagatti A, Cazzola M, Giagounidis A, Perry J, Malcovati L, Della Porta MG, Jadersten M, Killick S, Verma A, Norbury CJ, Hellstrom-Lindberg E, Wainscoat JS, Boultonwood J. Deregulated gene expression pathways in myelodysplastic syndrome hematopoietic stem cells. *Leukemia* 2010;24:756–764.
  166. Ancuta P, Liu KY, Misra V, Wacleche VS, Gosselin A, Zhou X, Gabuzda D. Transcriptional profiling reveals developmental relationship and distinct biological functions of CD16b and CD16- monocyte subsets. *BMC Genomics* 2009;10:403.
  167. Smith JA, Barnes MD, Hong D, DeLay ML, Inman RD, Colbert RA. Gene expression analysis of macrophages derived from ankylosing spondylitis patients reveals interferon-gamma dysregulation. *Arthritis Rheum* 2008;58:1640–1649.
  168. Raghavachari N, Xu X, Harris A, Villagra J, Logun C, Barb J, Solomon MA, Suffredini AF, Danner RL, Kato G, Munson PJ, Morris SM Jr, Gladwin MT. Amplified expression profiling of platelet transcriptome reveals changes in arginine metabolic pathways in patients with sickle cell disease. *Circulation* 2007;115:1551–1562.
  169. Hou SC, Chan LW, Chou YC, Su CY, Chen X, Shih YL, Tsai PC, Shen CK, Yan YT. Ankrd17, an ubiquitously expressed ankyrin factor, is essential for the vascular integrity during embryo genesis. *FEBS Lett* 2009;583:2765–2771.
  170. HogenEsch H, Gijbels MJ, Offerman E, van Hooft J, van Bakkum DW, Zurcher C. A spontaneous mutation characterized by chronic proliferative dermatitis in C57BL mice. *Am J Pathol* 1993;143:972–982.
  171. Bollmann F, Wu Z, Oelze M, Siuda D, Xia N, Henke J, Daiber A, Li H, Stumpo DJ, Blackshear PJ, Kleinert H, Pautz A. Endothelial dysfunction in tristetraprolindeficient mice is not caused by enhanced tumor necrosis factor- $\alpha$  expression. *J Biol Chem* 2014;289:15653–15665.
  172. Phillips K, Kedersha N, Shen L, Blackshear PJ, Anderson P. Arthritis suppressor genes TIA-1 and TTP dampen the expression of tumor necrosis factor  $\alpha$ , cyclooxygenase 2, and inflammatory arthritis. *Proc Natl Acad Sci U S A* 2004;101:2011–2016.



173. Stumpo DJ, Broxmeyer HE, Ward T, Cooper S, Hangoc G, Chung YJ, Shelley WC, Richfield EK, Ray MK, Yoder MC, Aplan PD, Blackshear PJ. Targeted disruption of Zfp36l2, encoding a CCCH tandem zinc finger RNA-binding protein, results in defective hematopoiesis. *Blood* 2009;114:2401–2410.
174. Zekri L, Chebli K, Tourriere H, Nielsen FC, Hansen TV, Rami A, Tazi J. Control of fetal growth and neonatal survival by the RasGAP-associated endoribonuclease G3BP. *Mol Cell Biol* 2005;25:8703–8716.
175. Lu JY, Sadri N, Schneider RJ. Endotoxic shock in AUF1 knockout mice mediated by failure to degrade proinflammatory cytokine mRNAs. *Genes Dev* 2006;20:3174–3184.
176. Sakakibara S, Nakamura Y, Yoshida T, Shibata S, Koike M, Takano H, Ueda S, Uchiyama Y, Noda T, Okano H. RNA-binding protein Musashi family: roles for CNS stem cells and a subpopulation of ependymal cells revealed by targeted disruption and antisense ablation. *Proc Natl Acad Sci U S A* 2002;99:15194–15199.
177. Katsanou V, Milatos S, Yiakouvakis A, Sgantzis N, Kotsoni A, Alexiou M, Harokopos V, Aidinis V, Hemberger M, Kontoyiannis DL. The RNA-binding protein Elavl1/HuR is essential for placental branching morphogenesis and embryonic development. *Mol Cell Biol* 2009;29:2762–2776.
178. Zhang J, Modi Y, Yarovsky T, Yu J, Collinge M, Kyriakides T, Zhu Y, Sessa WC, Pardi R, Bender JR. Macrophage beta2 integrin-mediated, HuR-dependent stabilization of angiogenic factor-encoding mRNAs in inflammatory angiogenesis. *Am J Pathol* 2012;180:1751–1760.
179. Mende Y, Jakubik M, Riessland M, Schoenen F, Rossbach K, Kleinridders A, Kohler C, Buch T, Wirth B. Deficiency of the splicing factor Sfrs10 results in early embryonic lethality in mice and has no impact on full-length SMN/Smn splicing. *Human Mol Genet* 2010;19:2154–2167.
180. Langenickel TH, Olive M, Boehm M, San H, Crook MF, Nabel EG. KIS protects against adverse vascular remodeling by opposing stathmin-mediated VSMC migration in mice. *J Clin Invest* 2008;118:3848–3859.
181. Koscielny G, Yaikhom G, Iyer V, Meehan TF, Morgan H, Atienza-Herrero J, Blake A, Chen CK, Easty R, Di Fenza A, Fiegel T, Griffiths M, Horne A, Karp NA, Kurbatova N, Mason JC, Matthews P, Oakley DJ, Qazi A, Regnart J, Retha A, Santos LA, Sneddon DJ, Warren J, Westerbergh H, Wilson RJ, Melvin DG, Smedley D, Brown SD, Flicek P, Skarnes WC, Mallon AM, Parkinson H. The International mouse phenotyping consortium web portal, a unified point of access for knockout mice and related phenotyping data. *Nucleic Acids Res* 2014;42:D802–D809.
182. Arany Z, Novikov M, Chin S, Ma Y, Rosenzweig A, Spiegelman BM. Transverse aortic constriction leads to accelerated heart failure in mice lacking PPAR-gamma coactivator 1alpha. *Proc Natl Acad Sci U S A* 2006;103:10086–10091.
183. Lai L, Leone TC, Zechner C, Schaeffer PJ, Kelly SM, Flanagan DP, Medeiros DM, Kovacs A, Kelly DP. Transcriptional coactivators PGC-1alpha and PGC-1beta control overlapping programs required for perinatal maturation of the heart. *Genes Dev* 2008;22:1948–1961.
184. Sanna B, Brandt EB, Kaiser RA, Pfluger P, Witt SA, Kimball TR, van Rooij E, De Windt LJ, Rothenberg ME, Tschop MH, Benoit SC, Molkentin JD. Modulatory calcineurin-interacting proteins 1 and 2 function as calcineurin facilitators *in vivo*. *Proc Natl Acad Sci U S A* 2006;103:7327.
185. Ding JH, Xu X, Yang D, Chu PH, Dalton ND, Ye Z, Yeakley JM, Cheng H, Xiao RP, Ross J, Chen J, Fu XD. Dilated cardiomyopathy caused by tissue-specific ablation of SC35 in the heart. *Embo J* 2004;23:885–896.
186. Lelliott CJ, Medina-Gomez G, Petrovic N, Kis A, Feldmann HM, Bjursell M, Parker N, Curtis K, Campbell M, Hu P, Zhang D, Litwin SE, Zaha VG, Fountain KT, Boudina S, Jimenez-Linan M, Blount M, Lopez M, Meirhaeghe A, Bohlooly YM, Storlien L, Stromstedt M, Snaith M, Oresic M, Abel ED, Cannon B, Vidal-Puig A. Ablation of PGC-1beta results in defective mitochondrial activity, thermogenesis, hepatic function, and cardiac performance. *PLoS Biol* 2006;4:e369.
187. Yu YE, Morishima M, Pao A, Wang DY, Wen XY, Baldini A, Bradley A. A deficiency in the region homologous to human 17q21.33-q23.2 causes heart defects in mice. *Genetics* 2006;173:297–307.
188. Kuroda K, Han H, Tani S, Tanigaki K, Tun T, Furukawa T, Taniguchi Y, Kurooka H, Hamada Y, Toyokuni S, Honjo T. Regulation of marginal zone B cell development by MINT, a suppressor of Notch/RBP-J signaling pathway. *Immunity* 2003;18:301–312.



# CHAPTER

# 6

Quaking, an RNA-Binding Protein, is a  
Critical Regulator of vascular Smooth  
Muscle Cell Phenotype

*Circulation Research 2013*

### Collaborative effort by:

Eric P. van der Veer, Ruben G. de Bruin, Adriaan O. Kraaijeveld, Margreet R. de Vries, Ilze Bot, Tonio Pera, Filip M. Segers, Stella Trompet, Janine M. van Gils, Marko K. Roeten, Cora M. Beckers, Peter J. van Santbrink, Anique Janssen, Coen van Solingen, Jim Swildens, Hetty C. de Boer, Erna A. Peters, Roel Bijkerk, Mat Rousch, Merijn Doop, Johan Kuiper, Martin Jan Schali, Allard C. van der Wal, Stéphane Richard, Theo J.C. van Berkel, J. Geoffrey Pickering, Pieter S. Hiemstra, Marie Jose Goumans, Ton J. Rabelink, Antoine A.F. de Vries, Paul H.A. Quax, J. Wouter Jukema, Erik A.L. Biessen, Anton Jan van Zonneveld

### Abstract

**Rationale:** RNA-binding proteins are critical post-transcriptional regulators of RNA and can influence pre-mRNA splicing, RNA localization, and stability. The RNA-binding protein Quaking (QKI) is essential for embryonic blood vessel development. However, the role of QKI in the adult vasculature, and in particular in vascular smooth muscle cells (VSMCs), is currently unknown.

**Methods and Results:** We identified that QKI is highly expressed by neointimal VSMCs of human coronary restenotic lesions, but not in healthy vessels. In a mouse model of vascular injury, we observed reduced neointima hyperplasia in Quaking viable mice, which have decreased QKI expression. Concordantly, abrogation of QKI attenuated fibroproliferative properties of VSMCs, while potentially inducing contractile apparatus protein expression, rendering noncontractile VSMCs with the capacity to contract. We identified that QKI localizes to the spliceosome, where it interacts with the myocardin pre-mRNA and regulates the splicing of alternative exon 2a. This post-transcriptional event impacts the Myocd\_v3/Myocd\_v1 mRNA balance and can be modulated by mutating the quaking response element in exon 2a of myocardin. Furthermore, we identified that arterial damage triggers myocardin alternative splicing and is tightly coupled with changes in the expression levels of distinct QKI isoforms.

**Conclusions:** We propose that QKI is a central regulator of VSMC phenotypic plasticity and that intervention in QKI activity can ameliorate pathogenic, fibroproliferative responses to vascular injury.

## Introduction

RNA-binding proteins are central regulators of gene expression in both health and disease.<sup>1,2</sup> The RNA-binding protein Quaking (QKI) is a member of the highly conserved signal transduction and activator of RNA (STAR) family of RNA-binding proteins.<sup>3</sup> Alternative splicing of the mammalian qkl transcript yields 3 protein isoforms, notably QKI-5, QKI-6, and QKI-7,<sup>2</sup> with dimerization of QKI isoforms being required for the regulation of pre-mRNA splicing, mRNA export, and stability.<sup>2,4</sup> QKI drives central and peripheral nervous system myelination by regulating oligodendrocyte and Schwann cell differentiation, respectively.<sup>2,4,5</sup> However, a role for QKI outside the neural network is poorly understood.

QKI has been proposed to regulate processes outside the nervous system because of its ubiquitous expression profile<sup>2</sup> and capacity to impact the processing of many RNA species by binding to quaking response elements (qre's).<sup>5,6</sup> Importantly, Qkl null mice are embryonic-lethal because of an inability of immature mural cells to migrate and differentiate into vascular smooth muscle cells (VSMCs) effectively, resulting in perturbed investment and stabilization of nascent vessels in the yolk sac vasculature.<sup>7–9</sup> In adults, VSMCs of the artery wall contract and provide vascular tone.<sup>10</sup> However, in response to vascular injury, VSMCs can dedifferentiate from a contractile to a synthetic state.<sup>10,11</sup> The unabated expansion of VSMCs can lead to pathophysiologic complications, such as clinical restenosis after percutaneous coronary intervention,<sup>12,13</sup> arteriovenous shunt failure,<sup>14,15</sup> and transplant vasculopathy.<sup>16</sup> Generally, VSMCs are programmed to avoid this excessive reparative response, because they possess the capacity to sense and respond to extracellular and intracellular cues that trigger the reversion to the contractile phenotype. The transcriptional coactivator Myocardin (Myocd) is a primary driver of this redifferentiation process,<sup>17</sup> because interaction with serum response factor (SRF) at CArGbox–containing promoters<sup>18–20</sup> activates contractile apparatus protein expression that is required for physiological VSMC functioning.<sup>21,22</sup> Given that QKI is a regulator of embryonic vascular development, we sought to determine the role of QKI in the adult vasculature. Here, we show that the RNA-binding protein QKI is a critical regulator of VSMC phenotype by binding to and regulating Myocd expression and alternative splicing, implicating a critical role for QKI in the regulation of physiological VSMC function and vascular repair.

## Methods

### Human Studies

Coronary atherectomy specimens were obtained from a cohort of patients that underwent elective directional coronary atherectomy of the target vessel 3 to 6 months after percutaneous transluminal coronary angioplasty<sup>23</sup> and immunohistochemically stained for QKI using a mouse monoclonal antihuman pan-QKI antibody (clone N147/6; UC Davis/NIH NeuroMab Facility) and smooth muscle  $\alpha$ -actin (ACTA2; clone 1A4; Sigma-Aldrich, Zwijndrecht, the Netherlands). Antibody binding was visualized with NovaRED and Vector Blue substrates

(Vector Laboratories, Burlingame, CA). Human cortex cryosections were used as an isotype and reference control. Methylene green was used as counterstain.

### **Animal Studies**

Female Quaking viable (Qk<sup>v</sup>) mice on a C57/Bl6-J background together with age- and sex-matched C57Bl6-J wild-type (WT) mice (Jackson Laboratories, Bar Harbor, ME) were sheathed with a nonconstrictive cuff as previously described.<sup>24</sup> Immunohistochemical analysis and quantitation of femoral arteries was performed as described previously.<sup>25</sup> Incorporation of 5-bromo-2-deoxyuridine (BrdU) into DNA as a marker of DNA synthesis was studied by intraperitoneal BrdU injection (100 mg/kg) 72, 48, and 24 hours before euthanasia. QKI was detected using a rabbit polyclonal antihuman QKI antibody (N20; Santa Cruz Biotechnology, CA). Transluminal wire injury of the left common carotid artery was performed in female apoE<sup>-/-</sup> fed a Western-type diet as previously described.<sup>26</sup> Uninjured arteries (day 0) and wire-injured arteries were harvested at days 1, 3, 7, 14, 21, and 28. All animal work was approved by the regulatory authorities of the Leiden University and was in compliance with the Dutch government guidelines.

### **VSMC Isolation and Culture**

Aortic explants harvested from WT and Qk<sup>v</sup> mice were cultured in DMEM containing 10% FCS and 0.01 µg/mL glutamine at 37°C and 5% CO<sub>2</sub>. The human internal thoracic (HITC6 and HITA2) clonal cell lines were generated and cultured as previously described.<sup>21,27</sup> The Material and Methods section in the Online Data Supplement details cloning strategies and construction of vectors used for luciferase (pMIR-REPORT), splicing, and lentiviral overexpression of Myocd. Primary mouse and human VSMCs were stably transduced using lentiviral shRNA that specifically target qki or using a scrambled control shRNA (MISSION library; Sigma-Aldrich). Stable transductants were selected with 3 µg/mL puromycin for 72 hours. Clonal HITA2 subpopulations were scored microscopically and expanded for experiments.

### **Collagen Production Assay**

Primary WT and Qkv mouse VSMCs and HITC6 VSMCs were seeded at a density of 1.5×10<sup>4</sup> cells/cm<sup>2</sup>, extensively washed with PBS and fixed for 30 minutes using Formafix (Thermo Scientific, Waltham, MA). Cellular collagen production was assessed by staining with Sirius Red F3B dye and concentrations determined spectrometrically at 550 nm.

### **DNA Synthesis and Cellular Migration Assays**

DNA synthesis and cellular migration of VSMCs derived from WT and Qkv aortas and HITC6 VSMCs were performed as previously described.<sup>28</sup>

### **Western Blot Analysis**

Proteins were resolved by polyacrylamide electrophoresis. Primary antibodies used to detect QKI-5, QKI-6, and QKI-7 were either rabbit polyclonal (EMD Millipore, Amsterdam, the Netherlands) or mouse monoclonal antibodies that

specifically target QKI-5 (N195A/16), QKI-6 (N182/17), or QKI-7 (N183/15.1; UC Davis/NIH NeuroMab Facility). Mouse monoclonal antibodies were used to detect ACTA2 (clone 1A4; R&D Systems, Leiden, the Netherlands), calponin (CNN1; hCP; Sigma-Aldrich), caldesmon (CALD1; clone hHCD; Sigma-Aldrich), and smoothelin (SMTN; kindly provided by Dr G. van Eys, Maastricht University Medical Center). Hemagglutinin-tagged Myocd protein was detected using a monoclonal antimouse HA.11 antibody (clone 16B12). As a reference, a mouse monoclonal antibody was used to detect  $\alpha$ -tubulin (clone DM1A; Sigma-Aldrich), whereas a rabbit polyclonal antibody was used to detect  $\beta$ -actin (Abcam, Cambridge, United Kingdom).

### Functional Assessment of VSMC Contractility

To identify single contractile cells, stably transduced sh-cont and sh-qki HITA2 VSMCs or VSMCs overexpressing enhanced green fluorescent protein (EGFP), MYOCD-v1a, MYOCD-v1b, MYOCD-v3a, or MYOCD-v3b were seeded on deformable silicone substrates (stiffness 5 kPa; Excellness Biotech, Lausanne, Switzerland)<sup>29</sup> in M199 culture medium containing 1% FCS. Cells were seeded onto substrates coated with 10  $\mu$ g/mL fibronectin isolated from human plasma. Twenty-four hours after seeding, 10 random fields were photographed using phase contrast microscopy (Olympus CX41 and CellSens Entry software) and the percentage of cells inducing wrinkles was determined using ImageJ software.

### RNA Immunoprecipitation

RNA was isolated from HITA2 VSMCs as per manufacturer instructions using the Magna-RIP kit (EMD Millipore) using either goat antirabbit IgG antibody (control) or the IP-validated goat antirabbit QKI-5 antibody (EMD Millipore).

### Quantitation of mRNA and Alternative Transcript Generation

Generally, mouse and human cDNA was made using Oligo-dT primers (Invitrogen). For immunoprecipitation and alternative transcript studies, cDNA was generated using random primers (Invitrogen). qRT-PCR analysis for designated mRNA products was performed using SYBR Green master mix (Bio-Rad) in combination with primer combinations described in Online Table I.

### Statistics

For all experiments, N defines the number of biological replicates. All image quantitation was performed using Image J software, and results of Western blot and PCR quantitation are provided beneath the images. All in vitro and in vivo results were analyzed using either Student t test or ANOVA (with Tukey, Bonferonni, or Kruskal–Wallis post-test being used when appropriate). Results are expressed as mean $\pm$ SE or mean  $\pm$  SE, as indicated. Differences in probability values  $<0.05$  were considered significant, where degree of significance is indicated as follows: \* $P<0.05$ , \*\* $P<0.01$ , \*\*\* $P<0.001$ , # $P<0.0001$ . Quantitation of semiquantitative PCR and Western blots are provided in Online Table II.

## Results

### **QKI Is Highly Expressed in VSMCs of Human Restenotic Lesions**

Despite the developmental defects observed in the vasculature of QKI-deficient embryos,<sup>7-9</sup> no studies to date have investigated a role for this RNA-binding protein in VSMCs of the adult vasculature. Therefore, we assessed the levels of QKI expression in human healthy and restenotic atherectomy specimens immunohistochemically. In healthy tissue, QKI was virtually undetectable and confined to the endothelium (Figure 1A and 1C; n=4 subjects). In contrast, the VSMCs in the neointimal portion of restenotic tissue revealed a profound increase in QKI expression, with a few inflammatory foci also staining positive for QKI (Figure 1B and 1D; n=5 subjects). Restenotic lesions displayed overt fibrosclerotic morphology with incidental foci of stellate VSMC and myxoid matrix, characteristic of young, restenotic tissue. Costaining of coronary artery lesions for QKI and ACTA2 confirmed that VSMCs are the major QKI-expressing cell type in restenotic lesions (Figure 1E and 1F). Of note, the pan-QKI antibody exhibited its characteristic punctate intracellular staining pattern in human brain tissue (Figure 1G and 1H). These studies indicate that QKI is differentially expressed between contractile and proliferative VSMCs and suggest that QKI protein levels could regulate the hyperplastic response to vascular injury.

### **Qkv Mice Display Reduced Neointima Formation After Femoral Cuff Placement**

To determine if QKI is indeed a regulator of vascular remodeling, we first assessed the mRNA and protein expression profile of QKI using an arterial hyperplastic model that induces a VSMC-mediated fibroproliferative response in femoral arteries of C57BL6 (WT) mice. Qkl mRNA expression levels decreased immediately after nonconstrictive cuff placement, followed by a significant increase after 3 days and peak Qkl mRNA expression 7 days postinjury (Figure 2A; n=6 mice per time point; \*P<0.05, \*\*\*P<0.001), coinciding with the proliferative peak of VSMCs in vascular injury models.<sup>30</sup> Furthermore, we also assessed the temporal expression profile of Qkl-5, Qkl-6, and Qkl-7 mRNA after cuff placement in apoE<sup>-/-</sup> mice (n=4 mice per time point). These studies revealed that Qkl-5 and Qkl-6 mRNA are markedly increased at day 7 (Qkl-6; P<0.05), whereas Qkl-7 mRNA levels were consistently decreased in expression (Online Figure 1A). Similar to the mRNA profile, medial layer VSMCs displayed maximally increased QKI protein expression 7 days after femoral cuff placement (Figure 2B and



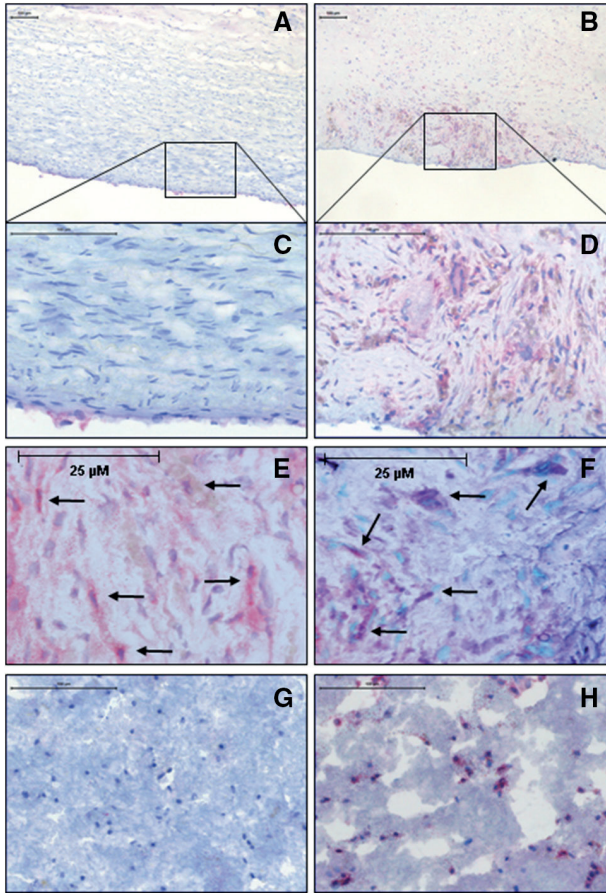


**Figure 1. Quaking (QKI) is abundantly expressed in vascular smooth muscle cells (VSMCs) in human restenotic lesions.** A and B, Low magnification images of pan-QKI expression in healthy coronary artery (n=4 subjects) and restenotic atherectomy specimens (n=5 subjects), with positive cells indicated by red immunostaining and nuclei staining deep blue. Scale bar, 100  $\mu$ m. C and D, High-magnification image of box provided in (A) and (B). E, High-magnification image of Pan-QKI expression in restenotic lesion. Arrows denote QKI-positive VSMCs. F, Double immunostain of restenotic lesion with Pan-Qki (red) and smooth muscle  $\alpha$ -actin (ACTA2; blue), with double-positive VSMCs (purple cells indicated with arrows). G, Isotype control of human cortex specimens were used as control tissue (IT). H, Pan-QKI expression in human cortex. Scale bars, 100  $\mu$ m.

Online Figure 1B). Interestingly, Qkl mRNA levels are significantly downregulated 14 days after cuff placement (Figure 2A). Next, we sought to determine if a reduction in QKI expression could impact neointima formation after femoral cuff placement, using WT and Qkv mice. Qkv mice possess a megabase deletion in the proximal region of chromosome 17. Quantitative analyses of Qkl mRNA levels from flash-frozen aortas (n=6; Online Figure 1C) and protein expression levels in VSMCs derived from WT and Qkv aortas revealed a significant decrease in expression of all 3 QKI isoforms (Figure 2C, with quantitation from 3 explant cultures provided beneath each Western blot along with statistical significance). As shown in Figure 2D, immunohistochemical analysis of WT and Qkv neointimal lesions for elastin and ACTA2 revealed significant reductions in neointimal area (Figure 2E; n=6 mice;  $P<0.05$ ), intimal/medial ratio (Figure 2F; WT  $0.34\pm0.06\%$  versus Qkv  $0.20\pm0.04\%$ ; n=6 mice;  $P<0.05$ ), luminal stenosis (Figure 2G; WT  $35\pm5\%$  versus Qkv  $20\pm4\%$ ; n=6 mice;  $P<0.05$ ), ACTA2-positive cells (Figure 2H; WT  $62.5\pm4.7\%$  versus Qkv  $46.5\pm4.1\%$ ; n=6 mice;  $P<0.05$ ), and neointimal BrdU incorporation (Figure 2I; n=8 mice;  $P<0.05$ ) 2 weeks after cuff placement. Total

vessel area (Figure 2J;  $n=6$  mice;  $P=0.42$ ) of cuffed portions of WT and Qkv femoral arteries was similar. We did not observe differences in lesional apoptosis (TUNEL staining), collagen, and CD45<sup>+</sup> leukocyte content (data not shown). Collectively, these studies demonstrate that a reduction in QKI expression *in vivo* decreases neointima formation after vascular injury.

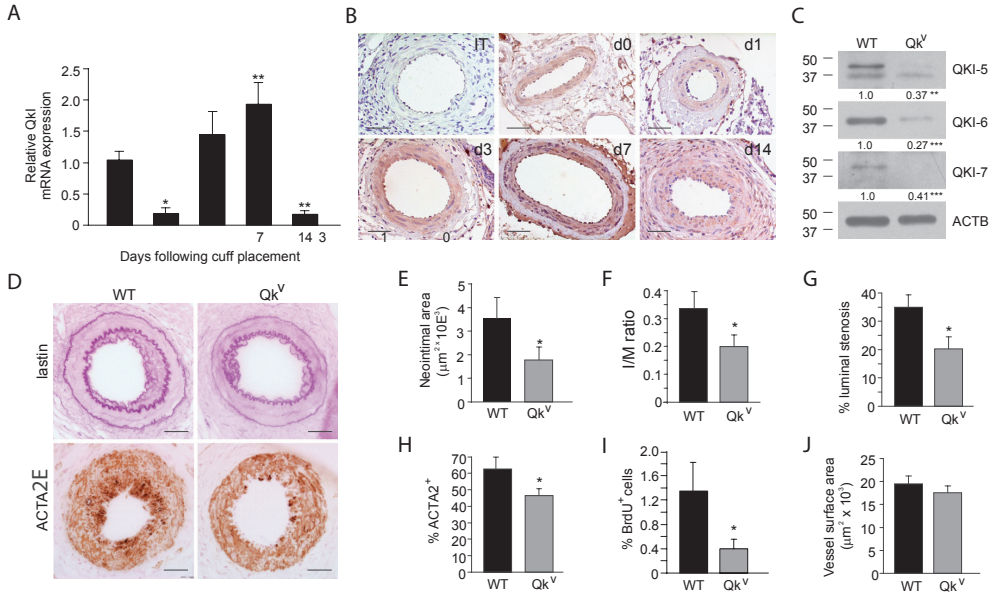


**Figure 2 | Quaking (QKI) expression levels influence neointima formation after vascular wall injury.** A, Temporal mRNA expression profile of *qki* after perivascular placement of cuffs around the femoral artery of 6 wild-type (WT) mice. Values shown are relative to uninjured controls and are normalized to GAPDH ( $n=6$  mice). B, Photomicrograph images displaying the spatiotemporal expression profile of QKI in femoral arteries after cuff placement in WT mice ( $n=6$ ; scale bars, 25  $\mu$ m; IT, isotype control). C, Western blot analysis of QKI isoform expression in WT and Quaking viable (Qkv) vascular smooth muscle cells (VSMCs) derived from arterial outgrowths. Quantitation of protein expression in Qkv mice relative to WT mice normalized to  $\beta$ -actin (ACTB) is provided below each blot ( $n=4$ –5 mice). D, Photomicrographs of WT and Qkv femoral arteries 14 days after femoral cuff placement. Elastin staining defines arterial layers (top), whereas smooth muscle  $\alpha$ -actin (ACTA2) defines VSMC content and localization (bottom;  $n=6$  mice; scale bars, 25  $\mu$ m). E–J, Quantitation of neointimal area (E), intimal/medial ratio (F), % luminal stenosis (G), % ACTA2-positive cells (H), % 5-bromo-2-deoxyuridine-positive cells (I), and vessel surface area (J) in WT and Qkv mice in femoral arteries 14 days after femoral cuff placement ( $n=6$  mice). Data are mean  $\pm$  SD. \* $P<0.05$ , \*\* $P<0.01$ , \*\*\* $P<0.001$ .

### VSMCs Derived From Qkv Mice Display Decreased Proliferation, Migration, and ECM Production

To further assess the functional consequences of abrogated QKI in adult VSMCs, we isolated primary VSMCs from WT and Qkv aortas. After 7 days, VSMC outgrowth was 1.8-fold reduced for Qkv versus WT (Figure 3A [left] and 3B;  $n=6$  mice with 6–7 pieces of tissue per aorta;  $P<0.001$ ). Additionally, Qkv VSMCs displayed a 3.5-fold decrease in cellular proliferation (Figure 3C;  $n=6$

mice;  $P < 0.01$ ), a 2.0-fold decrease in collagen production (Figure 3D;  $n = 4$  mice;  $P < 0.05$ ), and a 3.0-fold decrease in transwell migration (Figure 3E;  $n = 4$  mice;  $P < 0.01$ ) as compared with WT VSMCs. These findings were validated in human VSMCs derived from the human internal thoracic artery (designated HITC6) after lentiviral shRNA-mediated reduction of QKI (sh-cont and sh-qkl), resulting in a 5.7-fold decrease in proliferation (Figure 3F;  $n = 3$  transductions;  $P < 0.05$ ), a 3.6-fold decrease in collagen production (Figure 3G;  $n = 3$  transductions;  $P < 0.01$ ), and a 3.1-fold decrease in migration (Figure 3H;  $n = 3$  transductions;  $P < 0.01$ ). These findings show that the reductions in VSMC proliferation, migration, and collagen production observed in *Qkv* mice can be attributed to decreased QKI expression. Altogether, these data point to a significant role for QKI in regulating functions associated with dedifferentiated VSMCs.

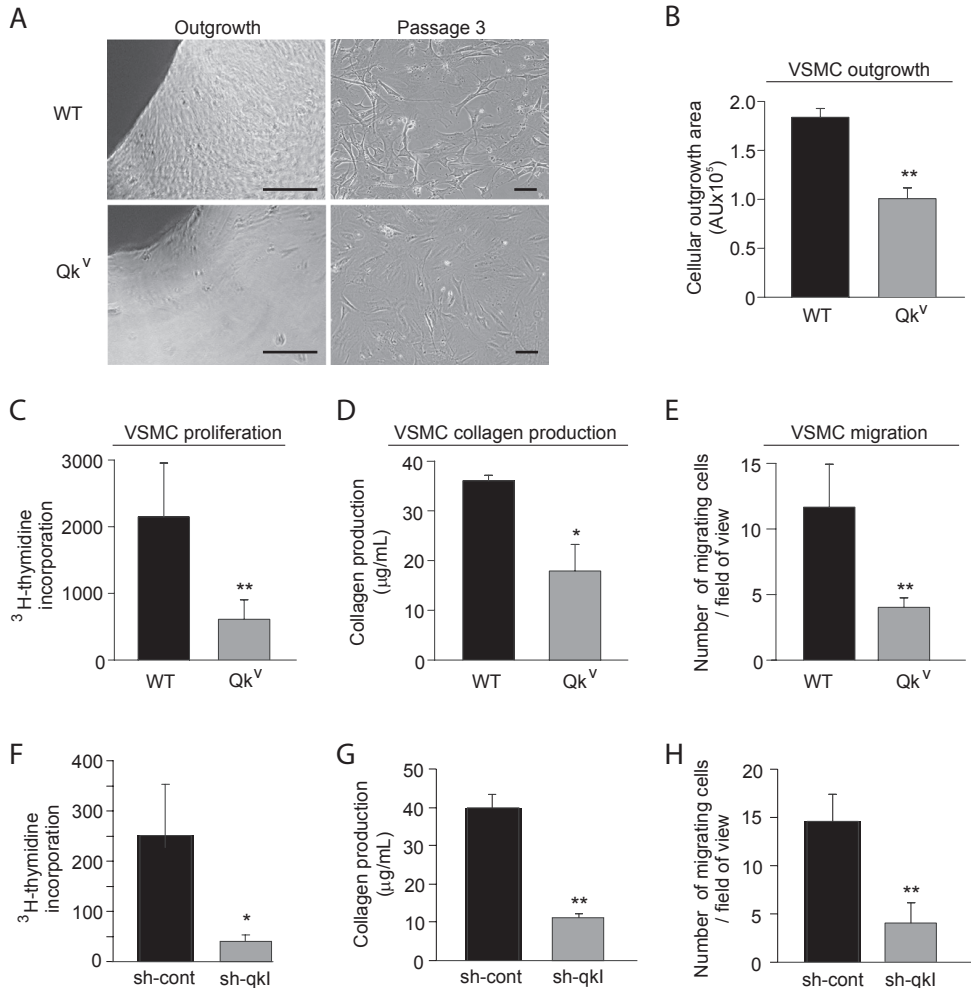


**Figure 3. Abrogation of Quaking (QKI) attenuates vascular smooth muscle cell (VSMC) fibroproliferation.**

A, Phasecontrast images of aortic explants derived from wild-type (WT) and Quaking viable (Qkv) mice (left) and VSMC cellular outgrowth after 3 passages (right; scale bar, 50  $\mu$ m). B, Quantitation of VSMC outgrowth area from WT and Qkv aortic explants (arbitrary units; n=6 with 6–7 pieces of tissue per aorta). C, VSMC proliferation assessed by quantification of [3H]-thymidine incorporation in WT and Qkv VSMCs (disintegrations per minute [dpm]; n=6). D, VSMC extracellular matrix production by WT and Qkv VSMCs (n=4). E, Transwell migration in the presence of a formyl methionyl leucyl phenylalanine (fMLP) gradient for WT and Qkv VSMCs. The average number of migrated cells was determined by counting 10 fields of view per well (n=4). F, VSMC proliferation as assessed by quantification of [3H]-thymidine incorporation in H1TC6 VSMCs stably transduced with sh-cont or sh-qkl lentiviral particles (dpm; n=3). G, VSMC collagen production by sh-cont and sh-qkl H1TC6 VSMCs (n=3). H, Transwell migration in the presence of an fMLP gradient for sh-cont- and sh-qkl-transduced H1TC6 VSMCs. The average number of migrated cells was determined by counting 10 fields of view per well (n=3). For all experiments, n is indicative of biological replicates. Data are mean $\pm$ SD. \*P<0.05, \*\*P<0.01.

### QKI Expression Levels Impact VSMC Phenotype

Our identification that QKI expression levels impact fibroproliferative properties of VSMCs suggests that QKI could play a role in regulating VSMC phenotype. Therefore, we investigated if the abrogation of QKI could drive synthetic VSMCs to the contractile state. For this, we assessed the mRNA expression profile of contractile apparatus proteins in serially passaged, aorta-derived VSMCs from WT and Qkv mice. As shown in Figure 4A, significantly higher levels of Acta2, smooth muscle myosin heavy chain (Myh11), and Cnn1 mRNAs were expressed in VSMCs derived from Qkv as compared with WT mice (n=6 mice; \*P<0.05, \*\*P<0.01). In contrast, the mRNA levels of smoothelin A (SmtnA) and SmtnB were unaltered (Figure 4B; n=6 mice; SmtnA, P=0.42; SmtnB, P=0.45). Western blot analyses of cellular lysates harvested from WT and Qkv aortic VSMCs revealed that a decrease in QKI expression yields increased ACTA2 levels (Figure 4B; n=5 mice; P<0.05). Interestingly, we did not observe any changes in the mRNA levels of contractile apparatus proteins harvested from snap-frozen aortas of WT and Qkv mice (data not shown). Next, we verified that decreased QKI expression is coupled with a global increase in contractile apparatus protein expression using H1TC6 VSMCs. Western blot analysis of lysates harvested from sh-qkl H1TC6 VSMCs showed a potent stimulation of ACTA2, CNN1, and the heavy isoform of CALD1 protein expression as compared with shcont H1TC6 VSMCs (Figure 4C; n=3 biological replicates; quantitation provided beneath respective Western blots), whereas the levels of SMTN were unchanged (Figure 4C; n=3 biological replicates). Further proof that QKI expression levels play a role in regulating VSMC phenotype was derived from the fact that H1TA2 VSMCs, a constitutively proliferative clonal cell population that poorly expresses contractile apparatus proteins,<sup>27</sup> expressed significantly higher levels of all 3 QKI isoforms as compared with H1TC6 VSMCs (Figure 4D). Interestingly, the forced reduction of QKI shifted H1TA2 VSMCs from a rhomboid to an elongated state (Figure 4E) and was associated with increased expression of contractile apparatus

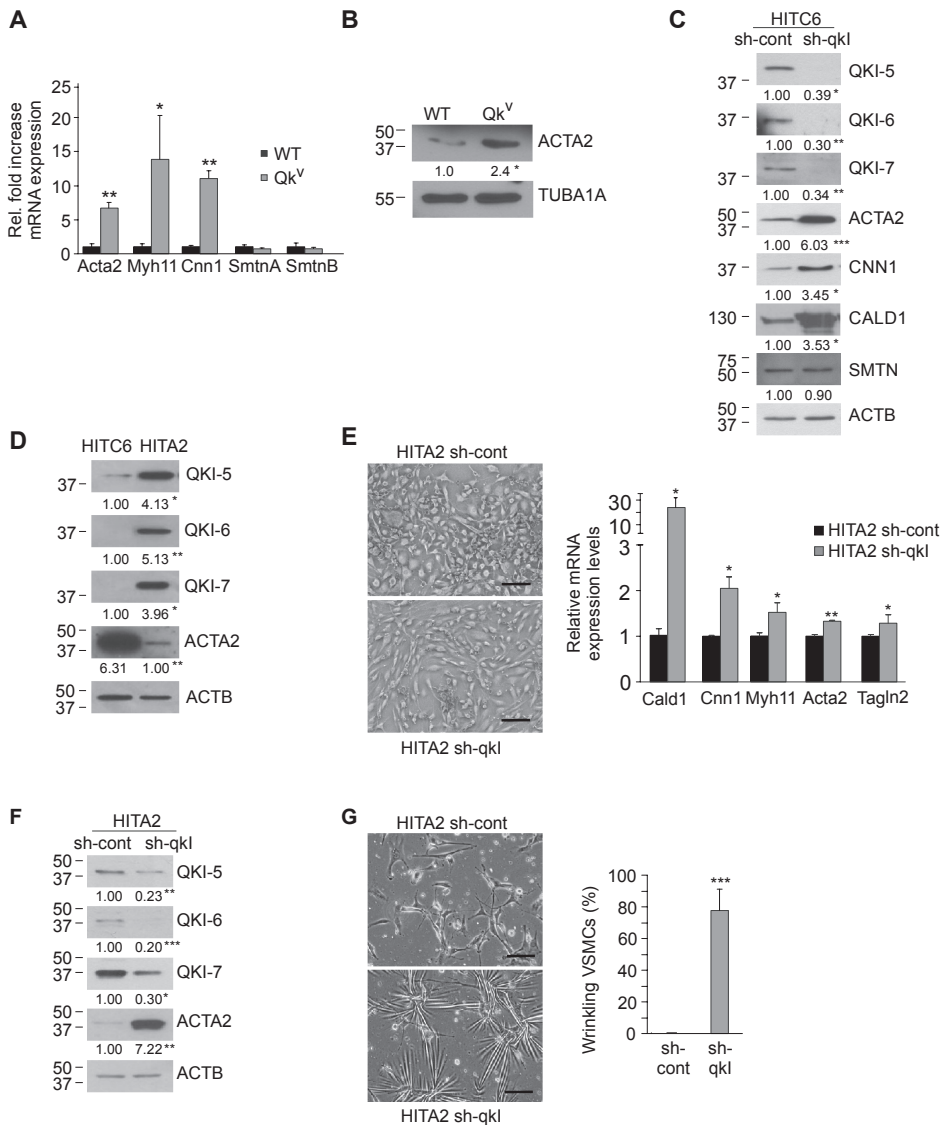


**Figure 4. Quaking (QKI) expression levels impact vascular smooth muscle cell (VSMC) phenotype.** A, mRNA transcript abundance for contractile apparatus proteins in wild-type (WT) and Quaking viable (Qkv) VSMCs relative to GAPDH mRNA abundance (n=6 mice). B, Western blot analysis of smooth muscle  $\alpha$ -actin in cellular lysates harvested from 5 separate WT and Qkv aortic explant cultures normalized to  $\alpha$ -tubulin (TUBA1A) (n=5). Quantitation of protein expression was normalized to  $\beta$ -actin and is shown beneath each blot along with statistical significance. C, Western blot analysis of contractile protein expression in sh-cont and sh-qkl HITC6 VSMCs (n=3 separate transductions). D, Western blot analysis of QKI expression in HITC6 and HITA2 VSMCs (n=3 separate cultures). E, Phasecontrast images of sh-cont- and sh-qkl- transduced HITA2 VSMCs (scale bar, 50  $\mu$ m), with corresponding relative mRNA transcript abundance detailing contractile apparatus expression (n=3 biological replicates). F, Western blots detailing protein expression levels in HITA2 sh-cont and HITA2 sh-qkl VSMCs. Blots are representative of 4 separate transductions. G, Phase-contrast images of sh-cont and sh-qkl HITA2 VSMCs seeded on fibronectin-coated, deformable elastomere substrate (5 kPa; left). Quantitation of contractioncompetent sh-cont- and sh-qkl- transduced HITA2 VSMCs (right; scale bar, 100  $\mu$ m; n=3). Data are mean $\pm$ SE. \*P<0.05, \*\*P<0.01, \*\*\*P<0.001.



mRNAs and protein (Figure 4E and 4F, respectively). We also observed an association between QKI expression levels and VSMC morphology, because clonally expanded cuboidal VSMCs expressed significantly higher levels of QKI than spindle-shaped VSMCs (Online Figure IIA). Moreover, we also tested if QKI levels could impact contractile function by seeding sh-cont and sh-qki HITA2 VSMCs on a silicone elastomere substrate, where cell contractile forces induce deformations that are visible as wrinkles under a phase contrast microscope. As shown in Figure 4G, sh-cont HITA2 VSMCs were incapable of contracting the elastomere substrate, whereas 77% of sh-qki HITA2 VSMCs acquired the capacity to contract the elastomere substrate functionally (Figure 4G;  $n=3$  biological replicates;  $***P<0.001$ ). Collectively, these findings strongly suggest that a reduction in QKI protein levels shifts VSMCs to the contractile phenotype.

### **QKI Modulates Myocd Expression and Alternative Splicing**

VSMC maturation is largely dependent on the interaction of SRF with the transcriptional coactivator Myocd at CArGboxes in the promoters of contractile apparatus proteins.<sup>18,19</sup> Because attenuation of QKI was associated with increased contractile apparatus protein expression, we investigated whether QKI levels could impact Myocd expression. We found that Myocd mRNA expression was significantly increased in both Qkv and sh-qki HITC6 VSMCs (Figure 5A) as compared with WT and sh-cont VSMCs (WT  $1.0\pm0.35$  versus Qkv  $3.0\pm0.25$  fold;  $n=4$  mice;  $P<0.01$ ; sh-cont  $1.0\pm0.39$  versus sh-qki  $2.64\pm0.24$  fold;  $n=3$  transductions;  $P<0.05$ ). Next, we tested whether overexpression of QKI in human VSMCs could impact Myocd mRNA expression levels. For this, we stably transduced HITA2 VSMCs with QKI-5, QKI-6, or QKI-7. These studies revealed positive and negative feedback loops among the distinct QKI isoforms (Figure 5B; left), and that QKI-6 overexpression significantly attenuates the expression of Myocd mRNA (Figure 5B; right;  $n=3$  transductions;  $P<0.05$ ). Although previous *in silico* analyses identified a qre in the 3'-UTR of the Myocd mRNA,<sup>6</sup> our assessment of the Myocd pre-mRNA uncovered 3 qre's that are conserved between mice and human, namely a coding sequence qre (qre-1), as well as 2 3'-UTR qre's (qre-2 and qre-3; Figure 5C). This led us to investigate whether QKI could bind to the Myocd (pre)-mRNA transcript. Therefore, we performed RNA immunoprecipitation of QKI isoforms in HITA2 using anti-QKI-5 antibody. Indeed, QKI was found to bind to the Myocd (pre)-mRNA 5.1-fold more effectively than an anti-IgG control (Figure 5D and 5E;  $n=3$  separate IPs;  $P<0.05$ ). However, luciferase reporter experiments revealed no regulation of QKI at the qre's in the Myocd 3'-UTR (Online Figure IIIA and IIIB). Therefore, we focused our attention on qre-1 in the Myocd coding region. Importantly, this qre is located at a critical junction of the Myocd pre-mRNA, namely the 3'-splice site of an alternative exon termed exon 2a (Figure 5C). Moreover, QKI has recently been shown to regulate alternative splicing events globally in myotubes by binding proximally to exon-intron boundaries.<sup>36</sup> Interestingly, the inclusion of exon 2a introduces a premature stop codon into the mature Myocd transcript (termed Myocd\_v3). The subsequent use of a downstream ATG leads to the generation of an 856-amino acid MYOCD\_v3 isoform that is greatly enriched in VSMCs as compared with cardiac or skeletal

muscle.<sup>20,31</sup> Surprisingly, HITA2 VSMCs immunostained for QKI-5, QKI-6, and QKI-7 revealed that QKI-6 colocalized with spliceosomal proteins in the cellular nucleus (Figure 5F). Next, we tested if the abrogation of QKI protein could influence *Myocd\_v3* expression levels. For this, we assessed the mRNA levels of *Myocd\_v3* in explanted aortic VSMCs derived from WT and *Qkv* mice (Figure 5G and Online Figure IIB). WT aortic VSMCs exclusively expressed *Myocd\_v1* after serial passaging (Figure 5G; quantitation shown below PCR), whereas *Qkv* VSMCs retained 30.9% exon 2a inclusion (*Myocd\_v3*; *n*=4 biological replicates; *P*<0.05). This association between a reduction in QKI expression and enriched exon 2a inclusion was validated in sh-qkl HITA2 VSMCs (6.8-fold versus sh-cont; *n*=3 transductions; *P*<0.05) and spindle HITA2 VSMC (3.8-fold versus cuboidal; *n*=3; *P*<0.01; Online Figure IIC and IID). To confirm that QKI expression levels impact the *Myocd\_v3/Myocd\_v1* mRNA balance, we harvested RNA from HITA6 VSMCs cultured in the presence of serum and 3 days after serum withdrawal, which drives these cells toward a contractile phenotype. As a control, we also tested if QKI impacts the *Myocd\_v4/Myocd\_v2* balance; however, we did not observe alternative splicing of *Myocd* exon 10a, which in the absence of *qre* proximal to this alternative exon is unlikely (Figure 5H; bottom).<sup>31</sup> As shown in Figure 5H and Online Figure IIIC, proliferative sh-cont HITA6 VSMCs primarily express *Myocd\_v1* (lane 1; 27% *Myocd\_v3*). In contrast, *Myocd\_v3* is the primary mRNA transcript expressed in shqkl HITA6 VSMCs (lane 2; 51% *Myocd\_v3*). Interestingly, serum withdrawal-induced ablation of QKI enhanced exon 2a inclusion in sh-cont VSMCs (lane 3; 40% *Myocd\_v3*), while triggering the virtually exclusive inclusion of exon 2a in shqkl VSMCs (lane 4; 78% *Myocd\_v3*). Given that *Myocd\_v1* is the primary splice variant expressed in the heart, we sought to determine if QKI-5, QKI-6, and QKI-7 expression levels were increased in the heart as compared with the aorta. As shown in Online Figure IVA, QKI mRNA expression levels are significantly higher in the heart than in the aorta, providing the interesting possibility that QKI protein levels are also involved in regulating *Myocd\_v3/Myocd\_v1* balance in the healthy and diseased heart (*n*=6 mice). Finally, to test the role of QKI directly in regulating exon 2a alternative splicing, we generated a splicing reporter construct by replacing exon 2 of the encoded  $\beta$ -hemoglobin (*hbb*) gene by the genomic sequence encoding *myocd* exon 2a along with flanking intronic regions (2a-wt-qre). Next, we mutated the *qre* from ACTAA→ACTGA (2a-mut-qre; Figure 5I). This mutation was chosen because it maintains the presence of a stop codon in exon 2a, while concomitantly abolishing the capacity of QKI to bind there. Mutation of the *qre* in exon 2a led to a striking enhancement of exon 2a inclusion (Figure 5I and 5J). Our findings strongly suggest that QKI regulates the expression and alternative splicing of *Myocd*.

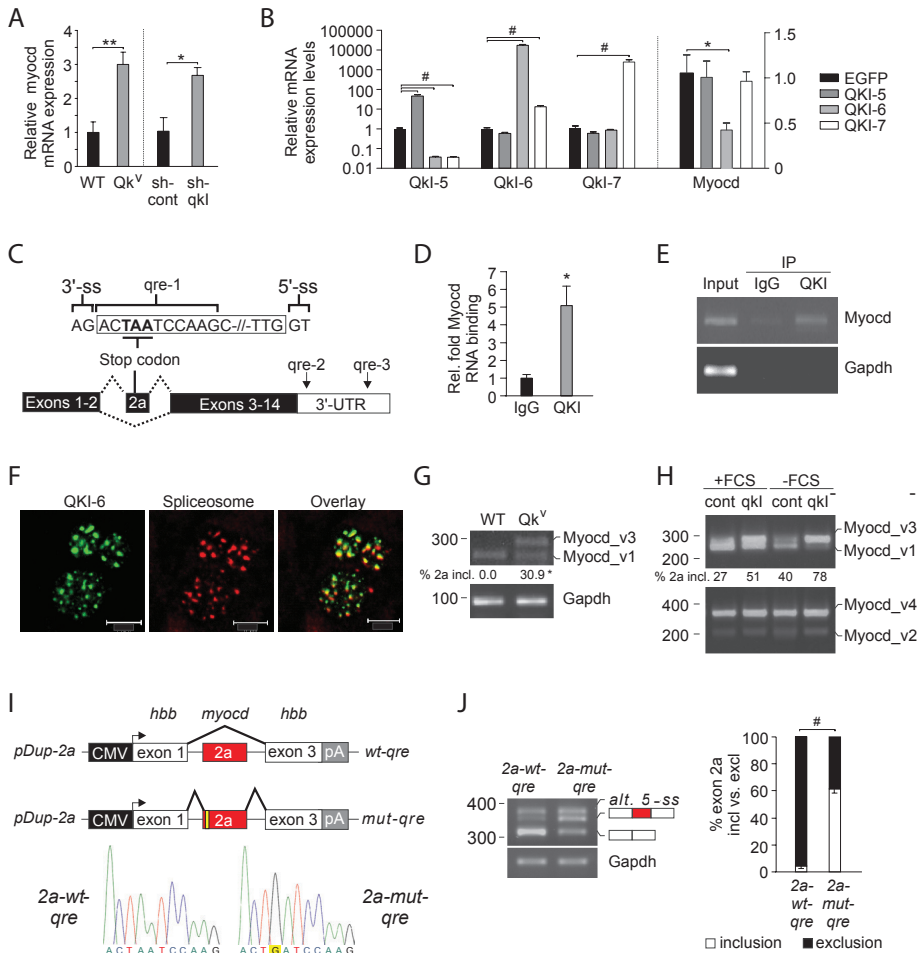


**Figure 5 | Quaking (QKI) regulates the expression and alternative splicing of the myocardin (Myocd) pre-mRNA.**

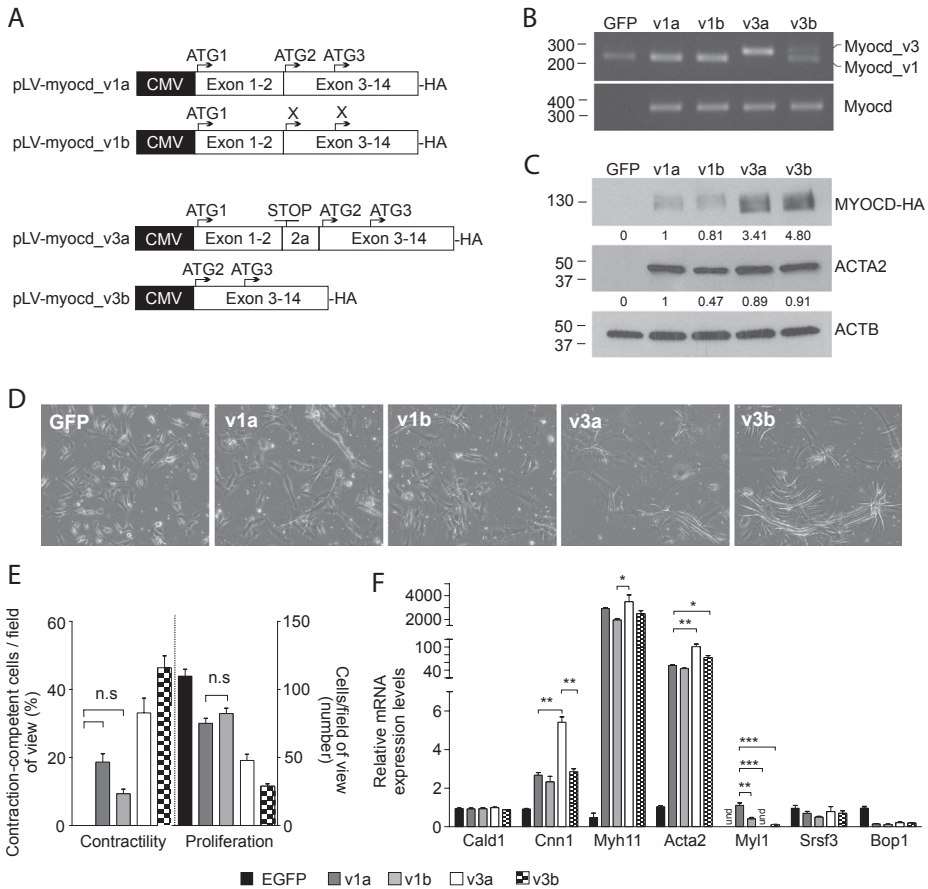
**A**, Relative mRNA abundance of Myocd in vascular smooth muscle cells (VSMCs) derived from Quaking viable (Qkv) mice as compared with wild-type (WT) VSMCs (n=5 mice; \*P<0.05) and sh-cont versus sh-qkl human VSMCs (n=3). **B**, Relative expression levels of distinct QKI transcripts in VSMCs overexpressing EGFP, QKI-5, QKI-6, or QKI-7 (left) and consequences of QKI isoform overexpression on Myocd transcript levels (right; n= 3 biological replicates with 1-way ANOVA and Dunnett post hoc test). **C**, Schematic depicting the coding and 3'-UTR of the myocd pre-mRNA, with coding qre-1 (exon 2a with surrounding 5'- and 3'-splice sites) and noncoding qre-2 and qre-3 (in 3'-UTR). **D**, Relative Myocd mRNA transcript immunoprecipitated using goat antirabbit IgG or goat antirabbit QKI-5 (from 3 separate IPs). **E**, qRT-PCR for Myocd and Gapdh mRNA as described in (D). **F**, Confocal fluorescent images of HITA2 VSMCs immunostained for QKI-6 (green; left), antisliceosome (red; middle), and an overlay of the 2 images (yellow; right; n=5; scale bar, 10  $\mu$ m). **G**, PCR analysis for Myocd\_v3 and Myocd\_v1 expression levels in primary aortic VSMCs derived from WT and Qkv mice (image is representative of 4 biological replicates).



Figure 5 legend continued. H, PCR analysis of sh-cont- and sh-qkl-transduced (qkl-) HITC6 VSMCs cultured in the presence of serum (+FCS) and 3 days after serum withdrawal (-FCS; n=3) for Myocd\_v3 and Myocd\_v1 (top) and Myocd\_v4 and Myocd\_v2 expression levels (bottom). I, Schematic of pDup-2a splicing reporters based on Myocd exon 2a. Sequence encoding myocd exon 2a (red box) was inserted into pDup51, which contains sequence encoding exons 1 and 3 from  $\beta$ -globin. The qre in the WTsequence was mutated within exon 2a (yellow box; ACTAA→ACTGA). HEK293s were transfected with depicted constructs and RNA harvested after 24 hours. J, PCR analysis of spliced variants in 2a-wt-qre- and 2a-mut-qre-transfected HEK293s (middle; n=6 for each condition) with quantification of splicing provided to the right. Data are mean±SE. \*P<0.05, \*\*P<0.01, \*\*\*P<0.001, #P<0.0001.

### Myocd\_v3 Expression Levels Impact VSMC Contractile Function

To gain insight into the consequences of Myocd pre-mRNA alternative splicing events, we transduced HITA2 VSMCs with lentivirus encoding EGFP, 2 variants of MYOCD\_v1 (v1a lacks exon 2a, whereas v1b lacks ATG2 and ATG3 and, therefore, exclusively produces MYOCD\_v1), or 2 MYOCD\_v3 variants (v3a includes exon 2a, whereas in v3b the first 2 exons are deleted from the encoded cDNA leading exclusively to the production of MYOCD\_v3; Figure 6A and see Material and Methods section in the Online Data Supplement). As a vector expression control, total Myocd mRNA levels were significantly increased in all cases as compared with EGFP (primers in common sequence; Online Figure VA; n=3; P<0.001), whereas exon 2 to 5 expression levels in EGFP- and v3boverexpressing VSMCs were comparable because of the fact that v3b lacks the 5'-primer site (Figure 6A and Online Figure VB). Gel electrophoresis of these mRNA species confirmed that EGFP-, v1a-, and v1b-transduced VSMCs exclusively express Myocd\_v1 (Figure 6B; lanes 1–3), whereas v3a-overexpression exclusively yields Myocd\_v3 (Figure 6B; lane 4). Interestingly, transduction of VSMCs with v3b was found to induce expression of endogenous Myocd\_v3 (Figure 6B; lane 5, upper band). Subsequent Western blot analysis for HA-tagged MYOCD revealed that overexpression of v3a and v3b in VSMCs increased MYOCD protein expression as compared with v1aand v1b-overexpressing VSMCs (Figure 6C). In keeping with literature, both MYOCD\_v1 and MYOCD\_v3 overexpression potently induced ACTA2 protein expression<sup>32</sup> (Figure 6C). To determine if augmentation of MYOCD\_v3 could indeed impact VSMC contractility, we seeded EGFP-, v1a-, v1b-, v3a-, and v3b-transduced HITA2 VSMCs on the aforementioned silicone elastomere substrate. Similar to sh-cont- transduced HITA2 VSMCs (Figure 4G), EGFP-transduced VSMCs did not contract the substrate and remained proliferative (Figure 6D and 6E; n=3 biological replicates). In contrast, MYOCD\_v1a and v1b overexpression induced a low level of contraction and modest proliferation, whereas MYOCD\_v3a- and v3b-overexpressing VSMCs displayed both significantly greater cellular contractility and decreased cellular proliferation (Figure 6D and 6E). In keeping with literature, we observed modest, yet significant increases in the mRNA levels of contractile apparatus protein as a result of MYOCD\_v3 overexpression as compared with MYOCD\_v1 overexpression (Figure 6F; n=3 biological replicates).<sup>31</sup> Collectively, these studies suggest that the expression levels of the distinct MYOCD isoforms can indeed influence VSMC contractile function.



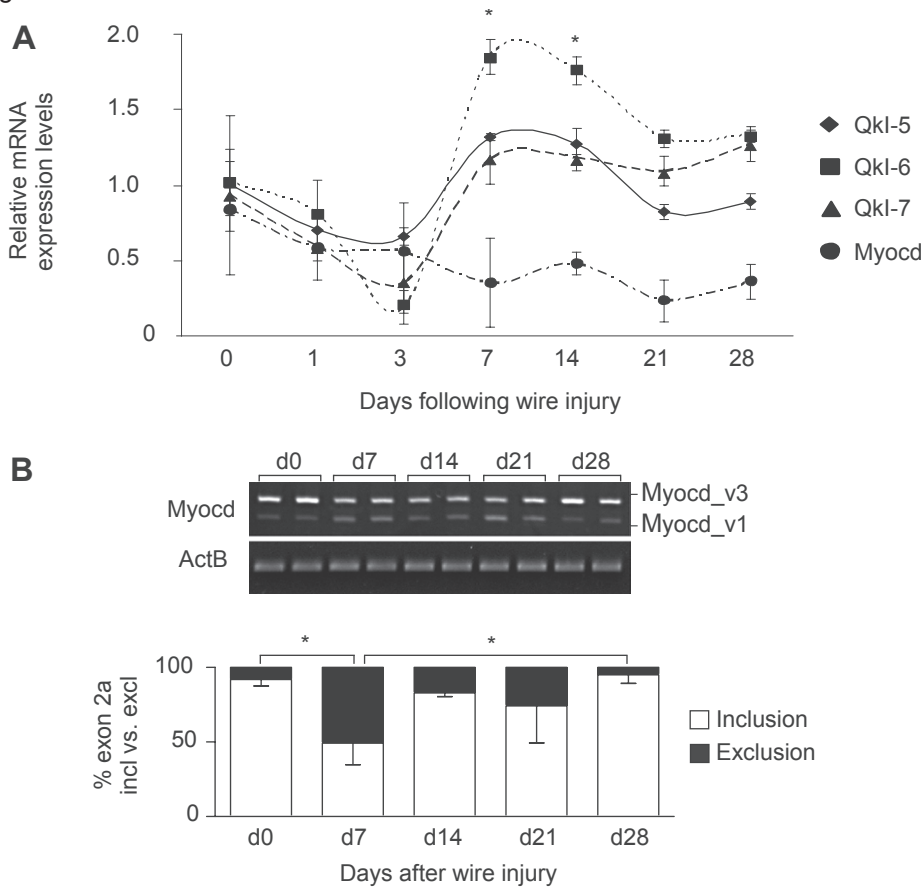
**Figure 6 | Expression levels of Myocardin (Myocd) isoforms impact vascular smooth muscle cell (VSMC) contraction competency.** A, Schematic representation of overexpressed Myocd isoforms, with primary translational start site (ATG1), alternative translational start sites (ATG2+ATG3), and premature stop site within exon 2a. B and C, mRNA and Western blot analysis (HA tag) for Myocd expression after transduction with constructs described in A (n=3 separate transductions). Densitometry of Western blots is depicted underneath (normalized to  $\beta$ -actin; pooled protein lysates from 3 separate transductions). Expression levels assessed by qRT-PCR are shown in Online Figure V. D, Phase-contrast images of VSMCs transduced with myocd constructs described in (A), seeded onto deformable silicone substrate. E, Quantitation of contraction competence and cellular proliferation in transduced VSMCs (n=3;  $P<0.0001$ ; ANOVA with Bonferroni multiple comparison test; n.s. denotes nonsignificant). F, Relative mRNA expression levels of CARg (Cald1, Cnn1, Myh11, Acta2) and MEF (Myl1, Srsf3, Bop1)-induced genes (n=3 biological replicates; und denotes undetectable). Data are mean $\pm$ SE. \* $P<0.05$ , \*\* $P<0.01$ , \*\*\* $P<0.001$ .

### Vascular Injury Triggers Myocd Alternative Splicing

It is well established that arterial injury induces VSMC dedifferentiation.<sup>30</sup> To test if this response to arterial injury is associated with a change in the expression levels of Myocd splice variants, apoE<sup>-/-</sup> mice on a Western-type diet underwent wire injury of the left carotid artery. At days 0 (uninjured), 1, 3, 7, 14, 21, and

28, the injured carotid arteries were harvested and mRNA transcript levels of Qkl-5, Qkl-6, Qkl-7, total Myocd, and Myocd\_v3/Myocd\_v1 mRNA balance were determined (n=4 mice per time point). In keeping with the Qkl mRNA expression profile observed after femoral cuff placement in WT and apoE<sup>-/-</sup> mice (Figure 2A and Online Figure 1A), wire injury of the carotid artery resulted in an initial decrease in Qkl mRNA expression levels, followed by an increase in qkl mRNA expression levels, with, in particular, a 1.85-fold increase in Qkl-6 mRNA levels after 7 days (Figure 7A; \*P<0.05). Concordantly, Myocd expression was 2.7-fold reduced 7 days after arterial injury and was coupled with a striking shift in expression of Myocd\_v3 to Myocd\_v1 expression (n=4 mice per time point; 2 mice per time point shown on gel; P<0.05; Figure 7B). This coexpression of both Myocd\_v3 and Myocd\_v1 persisted until 21 days post-wire injury, whereas by 28 days the expression of Myocd in carotid arteries had once again reverted to the almost exclusive expression of Myocd\_v3 (Figure 7B). These findings strongly suggest that QKI-induced alternative splicing of the Myocd pre-mRNA is functionally relevant and generates MYOCD isoforms that are required for both physiological and pathophysiological situations in the artery wall.

Figure 7



C

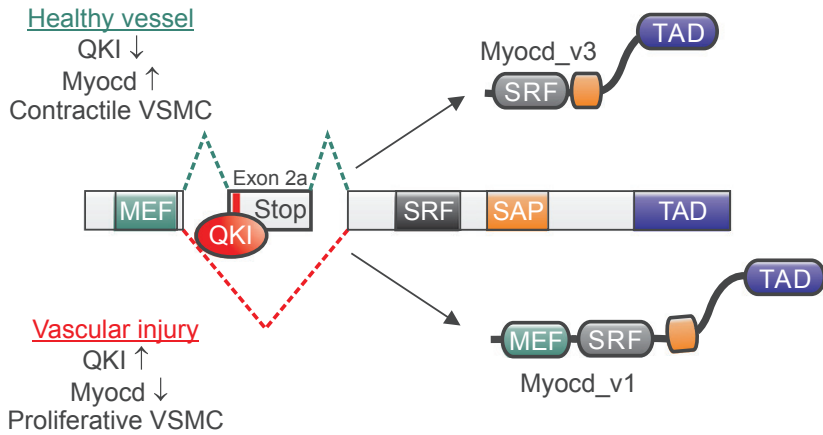
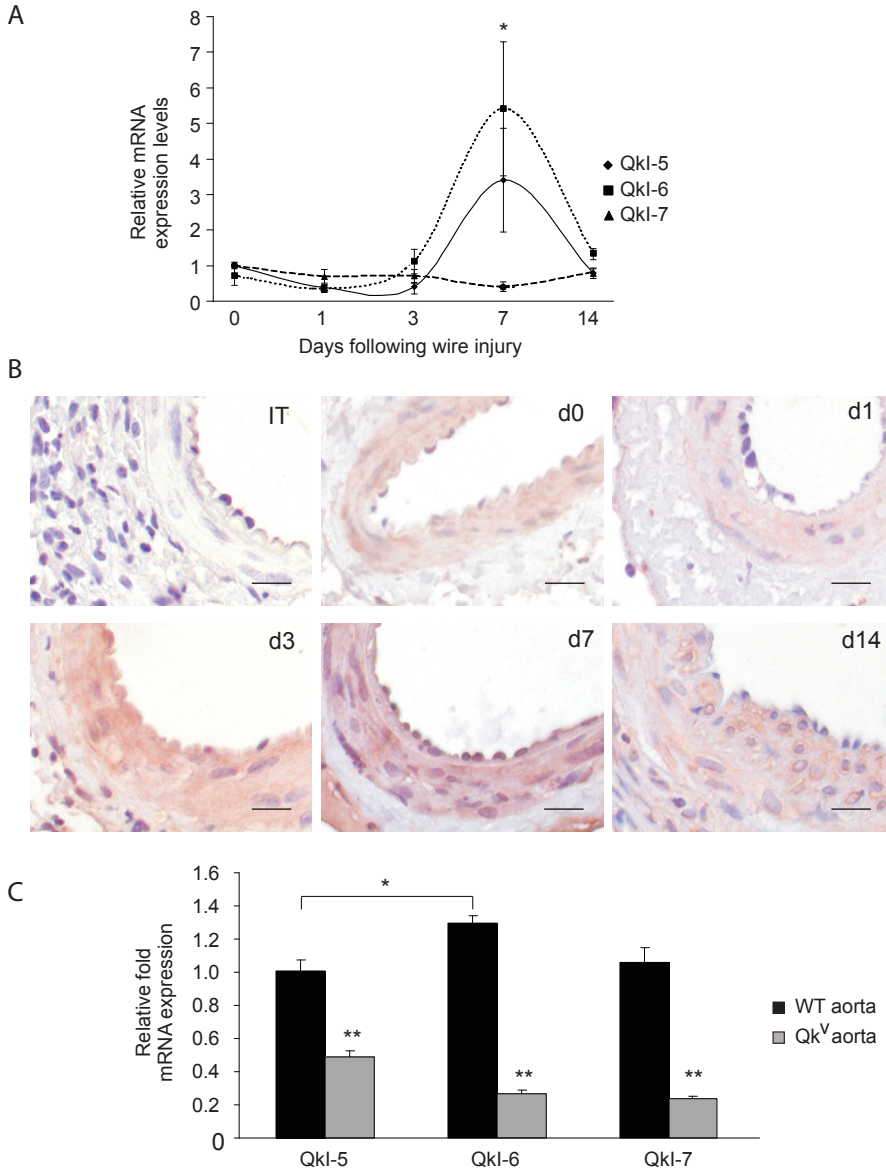


**Figure 7 | Vascular injury triggers induction of Quaking (qkl) and alternative splicing of myocardin (Myocd).** A, Temporal expression profile for Qkl-5, Qkl-6, and Qkl-7 and myocd mRNA abundance at various time points after wire injury to the carotid artery of 4 apoE<sup>-/-</sup> per time point (n=4; Kruskal–Wallis ANOVA). B, PCR analysis of Myocd\_v3 and Myocd\_v1 expression at various time points after wire injury to the mouse carotid artery (top) and quantitation of relative expression levels at designated time points (bottom; n=4; Kruskal–Wallis ANOVA for exon 2a inclusion). Data are mean±SE. \*P<0.05. C, In the healthy artery, QKI is poorly expressed, enhancing inclusion of Myocd exon 2a. This Myocd splice variant, Myocd\_v3, encodes the 856-amino acid MYOCD isoform (MYOCD\_v3) because of the presence of a premature stop codon in the mature mRNA. MYOCD\_v3 is the primary isoform expressed in contractile vascular smooth muscle cells (VSMCs). In the diseased artery, QKI is highly expressed and binds to the quaking response element in exon 2a, resulting in exon 2a exclusion from the mature Myocd mRNA (myocd\_v1). This Myocd splice variant encodes the 935-amino acid MYOCD isoform (MYOCD\_v1) and is enriched in proliferative VSMCs.

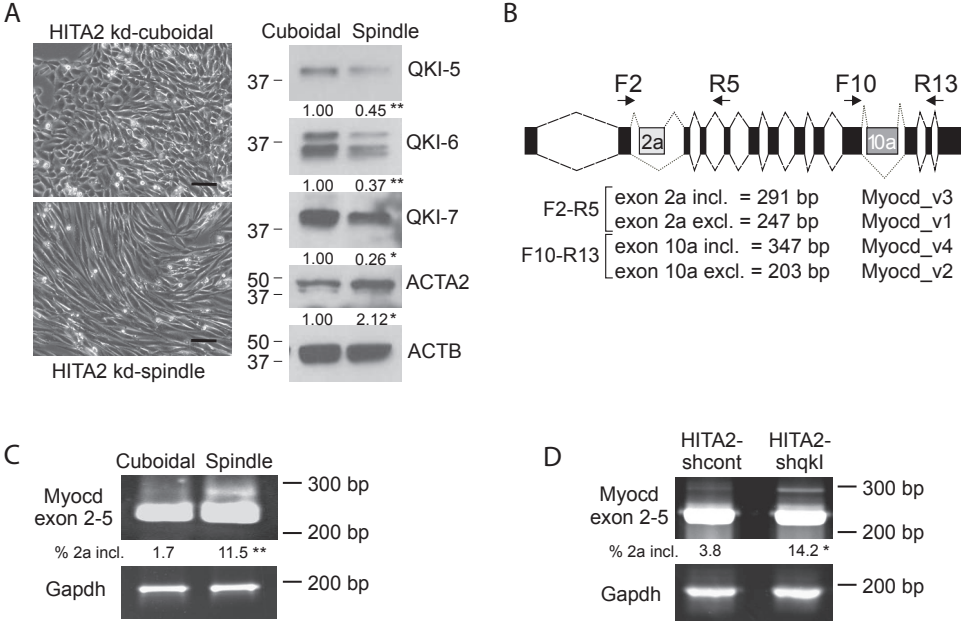
## Discussion

The current study demonstrates that QKI expression levels play a central role in the determination of VSMC phenotype. We have identified that QKI is poorly expressed in VSMCs of healthy coronary artery specimens, suggesting that the RNA-binding properties of QKI are repressed in contractile VSMCs. In contrast, our in vivo studies indicate that QKI expression is strongly induced in VSMCs in response to vascular injury, indicating a potential role for QKI in guiding VSMC dedifferentiation, enabling the VSMC to aid in the repair of the damaged portion of the artery wall. Importantly, the unabated proliferation of synthetic VSMCs can lead to rapid luminal narrowing.<sup>12,15,32</sup> To this end, gene expression profiles that VSMCs require to proliferate, migrate, and produce ECM production. At present, little is known regarding a role for RNA-binding proteins in regulating VSMC biology in either healthy or diseased situations. HuR, a RNA-binding protein that targets AU-rich regions in 3'-UTRs, has been found to be highly expressed

in VSMCs of neointimal lesions where it stabilizes mRNAs encoding cell cycle proteins.<sup>33</sup> In contrast to HuR, recent studies have identified that the majority of *qre*'s in (pre-)mRNAs are localized to intronic regions,<sup>34,35</sup> whereas recent studies by Hall et al<sup>36</sup> identified that the depletion of QKI in C2C12 myoblasts critically regulates alternative splicing events in these cells. In keeping with this the observed decrease in neointima formation in *Qkv* mice after femoral cuff placement could be the direct result of a decreased capacity to activate *notion*, we identified that QKI is a critical post-transcriptional regulator of the *Myocd* pre-mRNA (Figure 7C). This event profoundly impacts MYOCD isoform production,<sup>20,31,37</sup> as exon 2a exclusion (*Myocd\_v1*) leads to the generation of a 935-amino acid MYOCD\_v1 isoform, whereas exon 2a inclusion (*Myocd\_v3*) leads to the production of a 856-amino acid MYOCD\_v3 isoform. Although both isoforms serve as cotranscriptional activators of SRF,<sup>20,38</sup> the N-terminal portion of MYOCD\_v1 confers the protein with the capacity to interact with the myocyte enhancing factor 2 (MEF2) family of transcription factors and encodes a RPEL domain responsible for the interaction with G-actin.<sup>20</sup> Evidence that the QKI-mediated alternative splicing of the *Myocd* pre-mRNA is physiologically relevant can be derived from the fact that QKI is virtually absent in VSMCs of the healthy artery wall, where *Myocd* is highly expressed and almost exclusively present as *Myocd\_v3* splice variant (Figure 7C). It is well established that injury to the artery wall triggers VSMC dedifferentiation.<sup>10,22,30,32</sup> We identified that this event is tightly coupled with the dynamic modulation of QKI expression, and that the differential expression of the distinct QKI isoforms induces the enrichment of the *Myocd\_v1* splice variant in proliferative VSMCs. Here, we hypothesize that alterations in the *Myocd* splice variant balance are part of the VSMC-mediated response to vascular injury, possibly enhancing the expression of MEF2 target genes (Figure 7C). Importantly, Firulli et al<sup>39</sup> have previously identified that MEF2A, MEF2B, and MEF2D are abundantly expressed in neointimal VSMCs of rat restenotic tissue, whereas Creemers et al<sup>20</sup> identified that MEF2 dose-dependently titrates MYOCD\_v1 protein from interaction with SRF. As such, a reduction in *Myocd* expression coupled with a decreased interaction with SRF could be required to activate gene expression profiles that drive arterial repair. Importantly, our data also suggest that VSMCs preferentially express MYOCD\_v3 protein, because VSMCs expressing equivalent levels of the *Myocd\_v1* and *Myocd\_v3* splice variants expressed markedly more MYOCD\_v3 protein, indicating that QKI-mediated alternative splicing of *Myocd* exon 2a plays a role in regulating MYOCD protein abundance. SMCs also serve critical roles in the physiological functioning of the intestines, testis, uterus, and urinary bladder. Interestingly, QKI is abundantly expressed in these tissues,<sup>40</sup> providing the interesting possibility that, similar to the artery wall, alterations in QKI expression levels could play a regulatory role in pathological complications in these tissues, such as uterine leiomyoma formation,<sup>41</sup> epididymal hyperplasia,<sup>42</sup> and bladder dysfunction.<sup>43,44</sup> In conclusion, our findings imply that QKI is not exclusively associated with neural development and disease, but that QKI is in fact a critical regulator of the functional plasticity that is required for VSMC function under both physiological and pathophysiological conditions.



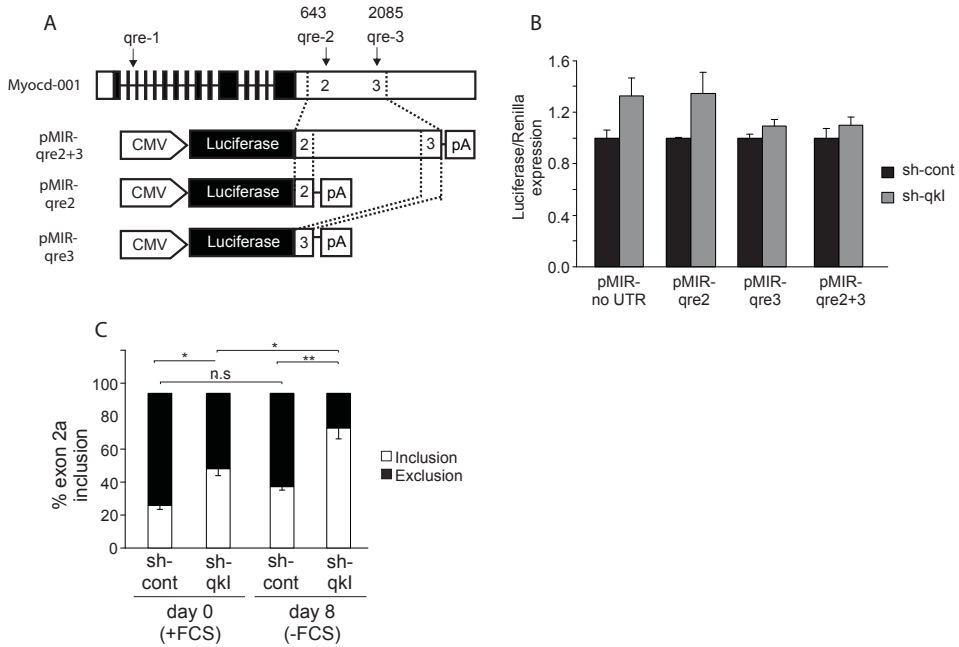
**Online Figure 1 | Expression levels of qkl transcripts are affected by injury to the vessel wall.** (A) Temporal mRNA expression profile of Qkl-5, Qkl-6, Qkl-7 in response to femoral artery placement of a perivascular cuff in 3 apoE<sup>-/-</sup> mice per timepoint. Values shown are relative to uninjured control and are normalized to Gapdh (n=3). (B) High magnification images of femoral arteries displayed in Figure 2 illustrating the spatiotemporal expression profile of Qkl protein after perivascular cuff placement in WT mice (n=6 mice; scale bars, 10  $\mu$ m; IT, isotype control). (C) Relative change in Qkl-5, -6 and -7 mRNA expression levels in flash-frozen aortas of WT and Qk<sup>V</sup> mice (n=6). Data are normalized to Gapdh and are relative to Qkl-5 mRNA expression levels. Data are mean  $\pm$  s.e. \*p<0.05, \*\*p<0.01.



**Online figure 2 | QKI gene dosage determines VSMC morphology and phenotype.** (A) isolated and clonally subcultured cuboidal and spindle sh-qkl HITA2 VSMCs. Western blot analysis of QKI and contractile apparatus protein expression in whole cell lysates harvested from cuboidal and spindle sh-qkl HITA2 VSMCs (n=3). Quantitation of protein expression in contractile VSMCs is relative to cuboidal VSMCs and is normalized to ACTB (n=3). (B) Schematic depicting primer sets used to assess Myocd splice variants. Light grey boxes indicate alternative exons of Myocd. (C-D) PCR analysis of Myocd exon 2-5 in HITA2 kd-cuboidal and HITA2 kd-spindle VSMCs (C) and HITA2 sh-cont and HITA2 sh-qkl VSMCs (D). Top panel: The approximately 300 bp fragment illustrates inclusion of exon 2a. Quantitation provided is indicative of percent exon 2a inclusion and is normalized to Gapdh. Cuboidal vs. contractile, n=3; sh-cont vs. sh-qkl, n=4. \*p<0.05, \*\*p<0.01.

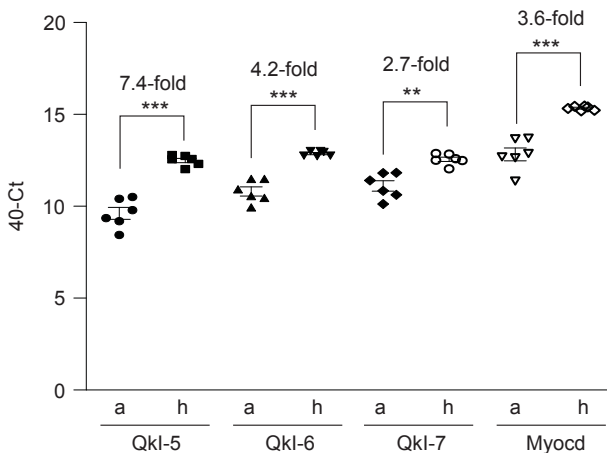


## Online Figure 3



**Online Figure 3 | Mechanisms of modulation of myocd pre-mRNA by qkl.** (A) Schematic depicting the coding region of the myocardin locus, including the 5- and 3-UTR regions (white boxes), exonic regions (black boxes), and intronic regions (lines between exons). The qre in the myocd 3'-UTR are defined as qre-2 and qre-3 (which are 643 and 2085 base pairs downstream of the translational stop codon in exon 14), which are also found in the luciferase constructs (bottom right). qre-1 is found in the intronic region between exon 2 and exon 3, and is located on the 3' -splice site of exon 2a (top left). (B) Luciferase/Renilla relative expression levels of pMIR-REPORT-qre2, qre3 and qre-2+3 constructs as depicted in (A) 24h after transient transfection into three separate sh-cont and sh-qkl transduced HEK293 cultures (n=3 separate transfection with aforementioned luciferase constructs). (C) Quantitation of percent exon 2a inclusion in sh-cont and sh-qkl HITC6 VSMCs cultured in the presence (day 0) and absence (day 8) of serum. Data are mean  $\pm$  s.e. n.s indicates non-significant, \*p<0.05, \*\*p<0.01.

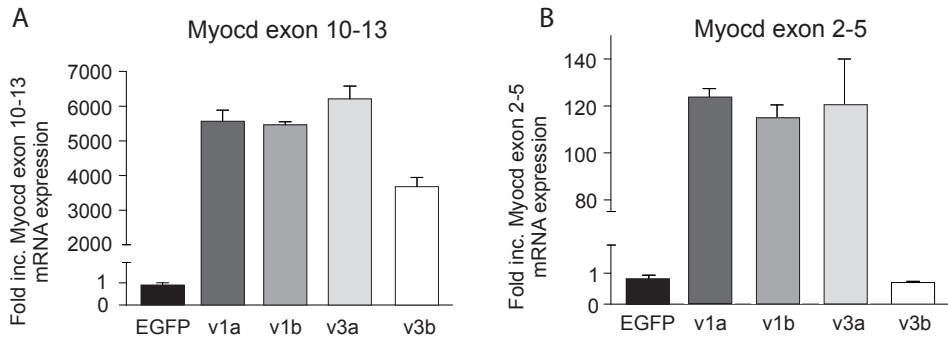
## Online figure 4



**Online Figure 4 | qkl is abundantly expressed in the heart.** (A) Qkl and Myocd mRNA expression levels were assessed quantitatively in the aorta (designated a) and heart (designated h) of 6 WT mice. 40-Ct values are depicted due to large differences in Gapdh expression levels in aorta versus heart (n=6 mice, \*\*p<0.01, \*\*\*p<0.001).



## Online figure 5



**Online Figure 5 | Quantitative assessment of myocd mRNA expression in VSMCs overexpressing distinct Myocd isoforms.** (A-C) Relative mRNA abundance of myocd exon 10-13 (A) and myocd exon 2-5 (B) in human VSMCs overexpressing EGFP, v1a, v1b, v3a or v3b (C). N=3. Data are mean  $\pm$  S.E.

### Sources of Funding

This work was supported by the Netherlands Heart Foundation (grant M93.001 to A.O. Kraaijeveld and E.A.L. Biessen). J.W. Jukema and E.A.L. Biessen are (Clinical) Established Investigators of the Netherlands Heart Foundation (grants 2001-D0-32 and 2003T201, respectively). R.G. de Bruin and J.M. van Gils were supported by research grants from the Netherlands Institute of Regenerative Medicine and the Dutch Kidney Foundation (NSN C 09.2329), respectively. T.J.C. van Berkel and E.A.L. Biessen belong to the European Vascular Genomics Network (<http://www.evgn.org>), a Network of Excellence supported by the European Community's Sixth Framework Program for Research Priority 1 (Life Sciences, Genomics, and Biotechnology for Health; contract LSHM-CT-2003-503254).

## References

1. Apponi LH, Corbett AH, Pavlath GK. RNA-binding proteins and gene regulation in myogenesis. *Trends Pharmacol Sci.* 2011;32:652–658.
2. Chénard CA, Richard S. New implications for the QUAKING RNA binding protein in human disease. *J Neurosci Res.* 2008;86:233–242.
3. Vernet C, Artzt K. STAR, a gene family involved in signal transduction and activation of RNA. *Trends Genet.* 1997;13:479–484.
4. Bockbrader K, Feng Y. Essential function, sophisticated regulation and pathological impact of the selective RNA-binding protein QKI in CNS myelin development. *Future Neurol.* 2008;3:655–668.
5. Ryder SP, Williamson JR. Specificity of the STAR/GSG domain protein Qk1: implications for the regulation of myelination. *RNA.* 2004;10:1449–1458.
6. Galarneau A, Richard S. Target RNA motif and target mRNAs of the Quaking STAR protein. *Nat Struct Mol Biol.* 2005;12:691–698.
7. Bohnsack BL, Lai L, Northrop JL, Justice MJ, Hirschi KK. Visceral endoderm function is regulated by quaking and required for vascular development. *Genesis.* 2006;44:93–104.
8. Li Z, Takakura N, Oike Y, Imanaka T, Araki K, Suda T, Kaname T, Kondo T, Abe K, Yamamura K. Defective smooth muscle development in qk1-deficient mice. *Dev Growth Differ.* 2003;45:449–462.
9. Noveroske JK, Lai L, Gaussin V, Northrop JL, Nakamura H, Hirschi KK, Justice. Quaking is essential for blood vessel development. *Genesis.* 2002;32:218–230.
10. Owens GK, Kumar MS, Wamhoff BR. Molecular regulation of vascular smooth muscle cell differentiation in development and disease. *Physiol Rev.* 2004;84:767–801.
11. Ross R. The pathogenesis of atherosclerosis: a perspective for the 1990s. *Nature.* 1993;362:801–809.
12. Agema WR, Jukema JW, Pimstone SN, Kastelein JJ. Genetic aspects of restenosis after percutaneous coronary interventions: towards more tailored therapy. *Eur Heart J.* 2001;22:2058–2074.
13. Ross R. Atherosclerosis—an inflammatory disease. *N Engl J Med.* 1999;340:115–126.
14. Lee T, Roy-Chaudhury P. Advances and new frontiers in the pathophysiology of venous neointimal hyperplasia and dialysis access stenosis. *Adv Chronic Kidney Dis.* 2009;16:329–338.
15. Roy-Chaudhury P, Arend L, Zhang J, Krishnamoorthy M, Wang Y, Banerjee R, Samaha A, Munda R. Neointimal hyperplasia in early arteriovenous fistula failure. *Am J Kidney Dis.* 2007;50:782–790.
16. Mitchell RN, Libby P. Vascular remodeling in transplant vasculopathy. *Circ Res.* 2007;100:967–978.
17. Chen J, Kitchen CM, Streb JW, Miano JM. Myocardin: a component of a molecular switch for smooth muscle differentiation. *J Mol Cell Cardiol.* 2002;34:1345–1356.
18. Du KL, Ip HS, Li J, Chen M, Dandre F, Yu W, Lu MM, Owens GK, Parmacek MS. Myocardin is a critical serum response factor cofactor in the transcriptional program regulating smooth muscle cell differentiation. *Mol Cell Biol.* 2003;23:2425–2437.
19. Miano JM. Serum response factor: toggling between disparate programs of gene expression. *J Mol Cell Cardiol.* 2003;35:577–593.
20. Creemers EE, Sutherland LB, Oh J, Barbosa AC, Olson EN. Coactivation of MEF2 by the

- SAP domain proteins myocardin and MASTR. *Mol Cell*. 2006;23:83–96.
21. Li S, Sims S, Jiao Y, Chow LH, Pickering JG. Evidence from a novel human cell clone that adult vascular smooth muscle cells can convert reversibly between noncontractile and contractile phenotypes. *Circ Res*. 1999;85:338–348.
22. Owens GK. Regulation of differentiation of vascular smooth muscle cells. *Physiol Rev*. 1995;75:487–517.
23. Rittersma SZ, Meuwissen M, van der Loos CM, Koch KT, de Winter RJ, Piek JJ, van der Wal AC. Eosinophilic infiltration in restenotic tissue following coronary stent implantation. *Atherosclerosis*. 2006; 184:157– 162.
24. Pires NM, Pols TW, de Vries MR, van Tiel CM, Bonta PI, Vos M, Arkenbout EK, Pannekoek H, Jukema JW, Quax PH, de Vries CJ. Activation of nuclear receptor Nur77 by 6-mercaptopurine protects against neointima formation. *Circulation*. 2007;115:493–500.
25. Lardenoye JH, de Vries MR, Löwik CW, Xu Q, Dhore CR, Cleutjens JP, van Hinsbergh VW, van Bockel JH, Quax PH. Accelerated atherosclerosis and calcification in vein grafts: a study in APOE\*3 Leiden transgenic mice. *Circ Res*. 2002;91:577–584.
26. Krohn R, Raffetseder U, Bot I, Zerneck A, Shagdarsuren E, Liehn EA, van Santbrink PJ, Nelson PJ, Biessen EA, Mertens PR, Weber C. Y-box binding protein-1 controls CC chemokine ligand-5 (CCL5) expression in smooth muscle cells and contributes to neointima formation in atherosclerosis- prone mice. *Circulation*. 2007;116:1812–1820.
27. Li S, Fan YS, Chow LH, Van Den Diepstraten C, van Der Veer E, Sims SM, Pickering JG. Innate diversity of adult human arterial smooth muscle cells: cloning of distinct subtypes from the internal thoracic artery. *Circ Res*. 2001;89:517–525.
28. Bot I, von der Thüsen JH, Donners MM, Lucas A, Fekkes ML, de Jager SC, Kuiper J, Daemen MJ, van Berkel TJ, Heeneman S, Biessen EA. Serine protease inhibitor Serp-1 strongly impairs atherosclerotic lesion formation and induces a stable plaque phenotype in ApoE<sup>-/-</sup> mice. *Circ Res*. 2003;93:464–471.
29. Hinz B, Celetta G, Tomasek JJ, Gabbiani G, Chaponnier C. Alpha- smooth muscle actin expression upregulates fibroblast contractile activity. *Mol Biol Cell*. 2001;12:2730–2741.
30. Clowes AW, Reidy MA, Clowes MM. Kinetics of cellular proliferation after arterial injury. I. Smooth muscle growth in the absence of endothelium. *Lab Invest*. 1983;49:327–333.
31. Imamura M, Long X, Nanda V, Miano JM. Expression and functional activity of four myocardin isoforms. *Gene*. 2010;464:1–10.
32. Lusis AJ. Atherosclerosis. *Nature*. 2000;407:233–241.
33. Pullmann R Jr, Juhaszova M, López de Silanes I, Kawai T, Mazan- Mamczarz Halushka MK, Gorospe M. Enhanced proliferation of cultured human vascular smooth muscle cells linked to increased function of RNA-binding protein HuR. *J Biol Chem*. 2005;280:22819–22826.
34. Hafner M, Landthaler M, Burger L, Khorshid M, Hausser J, Berninger P, Rothballer A, Ascano M Jr, Jungkamp AC, Munschauer M, Ulrich A, Wardle GS, Dewell S, Zavolan M, Tuschl T. Transcriptome-wide identification of RNA-binding protein and microRNA target sites by PAR-CLIP. *Cell*. 2010;141:129–141.
35. Scheibe M, Butter F, Hafner M, Tuschl T, Mann M. Quantitative mass spectrometry and PAR-CLIP to identify RNA-protein interactions. *Nucleic Acids Res*. 2012;40:9897–9902.
36. Hall MP, Nagel RJ, Fagg WS, Shiue L, Cline MS, Perriman RJ, Donohue JP, Ares M Jr. Quaking and PTB control overlapping splicing regulatory networks during muscle cell

- differentiation. *RNA*. 2013;19: 627–638.
37. Ilagan RM, Genheimer CW, Quinlan SF, Guthrie KI, Sangha N, Ramachandran S, Kelley RW, Presnell SC, Basu J, Ludlow JW. Smooth muscle phenotypic diversity is mediated through alterations in myocardin gene splicing. *J Cell Physiol*. 2011;226:2702–2711.
  38. Wang Z, Wang DZ, Pipes GC, Olson EN. Myocardin is a master regulator of smooth muscle gene expression. *Proc Natl Acad Sci U S A*. 2003;100:7129–7134.
  39. Firulli AB, Miano JM, Bi W, Johnson AD, Casscells W, Olson EN, Schwarz JJ. Myocyte enhancer binding factor-2 expression and activity in vascular smooth muscle cells. Association with the activated phenotype. *Circ Res*. 1996;78:196–204.
  40. Kondo T, Furuta T, Mitsunaga K, Ebersole TA, Shichiri M, Wu J, Artzt K, Yamamura K, Abe K. Genomic organization and expression analysis of the mouse *qkl* locus. *Mamm Genome*. 1999;10:662–669.
  41. Mesquita FS, Dyer SN, Heinrich DA, Bulun SE, Marsh EE, Nowak RA. Reactive oxygen species mediate mitogenic growth factor signaling pathways in human leiomyoma smooth muscle cells. *Biol Reprod*. 2010;82:341–351.
  42. Blach O, Pollack AMA, Douglas D. Smooth muscle hyperplasia of the epididymis. *J Surg Case Reports* 2011;1–4.
  43. Estrada CR, Adam RM, Eaton SH, Bägli DJ, Freeman MR. Inhibition of EGFR signaling abrogates smooth muscle proliferation resulting from sustained distension of the urinary bladder. *Lab Invest*. 2006;86: 1293–1302.
  44. Wang J, Niu W, Nikiforov Y, Naito S, Chernausk S, Witte D, LeRoith D, Strauch A, Fagin JA. Targeted overexpression of IGF-I evokes distinct patterns of organ remodeling in smooth muscle cell tissue beds of transgenic mice. *J Clin Invest*. 1997;100:1425–1439.





# CHAPTER

# 7

Quaking promotes monocyte  
differentiation into pro-atherogenic  
macrophages by controlling  
pre-mRNA splicing and gene expression

*Nature Communications 2016*

**Collaborative effort by:**

Ruben G. de Bruin, Lily Shiue, Jurriën Prins, Hetty C. de Boer, Anjana Singh, W. Samuel Fagg, Janine M. van Gils, Jacques M.G.J. Duijs, Sol Katzman, Adriaan O. Kraaijeveld, Stefan Böhringer, Wai Y. Leung, Szymon M. Kielbasa, John P. Donahue, Patrick H.J. van der Zande, Rick Sijbom, Carla M.A. van Alem, Ilze Bot, Cees van Kooten, J. Wouter Jukema, Hilde Van Esch, Ton J. Rabelink, Hilal Kazan, Erik A.L. Biessen, Manuel Ares Jr., Anton Jan van Zonneveld, Eric P. van der Veer

**Abstract**

A hallmark of inflammatory diseases is the excessive recruitment and influx of monocytes to sites of tissue damage and their ensuing differentiation into macrophages. Numerous stimuli are known to induce transcriptional changes associated with macrophage phenotype, but posttranscriptional control of human macrophage differentiation is less well understood. Here we show that expression levels of the RNA-binding protein Quaking (QKI) are low in monocytes and early human atherosclerotic lesions, but are abundant in macrophages of advanced plaques. Depletion of QKI protein impairs monocyte adhesion, migration, differentiation into macrophages and foam cell formation in vitro and in vivo. RNA-seq and microarray analysis of human monocyte and macrophage transcriptomes, including those of a unique QKI haploinsufficient patient, reveal striking changes in QKI-dependent messenger RNA levels and splicing of RNA transcripts. The biological importance of these transcripts and requirement for QKI during differentiation illustrates a central role for QKI in posttranscriptionally guiding macrophage identity and function.



## Introduction

Monocytes serve as danger sensors within the circulation. The activation of blood-borne monocytes by inflammatory stimuli triggers their adhesion and homing to sites of tissue injury, where they differentiate into macrophages and collectively aid in the resolution of damage<sup>1,2</sup>. However, the chronic accumulation of macrophages at these sites of injury is a hallmark of inflammatory diseases such as rheumatoid arthritis<sup>3</sup>, Crohn's disease<sup>4</sup> and atherosclerosis<sup>5-7</sup>. Dynamic changes in gene expression are associated with monocyte to macrophage differentiation, where PU.1<sup>8</sup>, Signal Transducer and Activator of Transcription (STATs)<sup>9</sup> and CCAAT/Enhancer Binding Protein (C/EBP)<sup>10</sup> are key transcription factors that drive this alteration in cellular phenotype and function<sup>11,12</sup>. Importantly, numerous studies have identified critical roles for both microRNAs (miRNAs) and RNA-binding proteins (RBPs) in posttranscriptionally regulating monocyte<sup>13</sup> and macrophage<sup>14</sup> biology. However, the posttranscriptional regulation of monocyte to macrophage differentiation has generally been limited to studies detailing miRNA-based targeting of individual transcription factors or effector molecules that either stimulate or delay this phenotypic conversion<sup>15-17</sup>. In contrast to miRNAs, RBPs mediate both quantitative and qualitative changes to the transcriptome, interacting with pre-mRNAs to influence (alternative) splicing, transcript stability, editing, subcellular localization and translational activation or repression<sup>18-20</sup>. This broad arsenal of RNA-based control points enables RBPs to modulate the proteome in response to immunogenic stimuli<sup>17</sup>, shifting inflammatory cells from an immature or naive state to a mature or activated state, as has previously been established in lymphoid cells<sup>21,22</sup>. In recent times, we discovered that expression of the RBP Quaking (QKI) is induced in human restenotic lesion-resident vascular smooth muscle cells (VSMCs), where it directly mediates a splicing event in the Myocardin pre-mRNA that governs VSMC function<sup>23</sup>. This finding prompted us to investigate whether QKI could similarly serve as an inflammation-sensitive posttranscriptional guide during monocyte to macrophage differentiation. Alternative splicing of the QKI pre-mRNA yields mature transcripts of 5, 6 or 7 kb that encode distinct protein isoforms, namely QKI-5, -6 and -7<sup>24,25</sup>. QKI-5 possesses a nuclear localization signal in the carboxy-terminal region and is found in the nucleus of cells. In contrast, QKI-6 and QKI-7 are found in the cytoplasm. However, QKI-6 and QKI-7 can also translocate to the nucleus<sup>23,26</sup>. The presence of a KH-family homology domain confers QKI with the capacity to bind RNA<sup>27</sup>, albeit dimerization is required<sup>26,28</sup> to bind with high affinity to the QKI response element (QRE) sequence (NACUAAY N1-20 UAAY) on target RNAs<sup>29-33</sup>. Importantly, aberrant QKI expression is associated with inflammatory diseases such as schizophrenia<sup>34,35</sup>, cancer<sup>36</sup> and restenosis<sup>23</sup>. Here we show that the RBP QKI plays a critical role in regulating the conversion of monocytes into macrophages in, for example, atherosclerotic lesions. Our studies pinpoint QKI as a dynamic regulator of pre-mRNA splicing and expression profiles that drive monocyte activation, adhesion and differentiation into macrophages, and facilitates their conversion into foam cells.

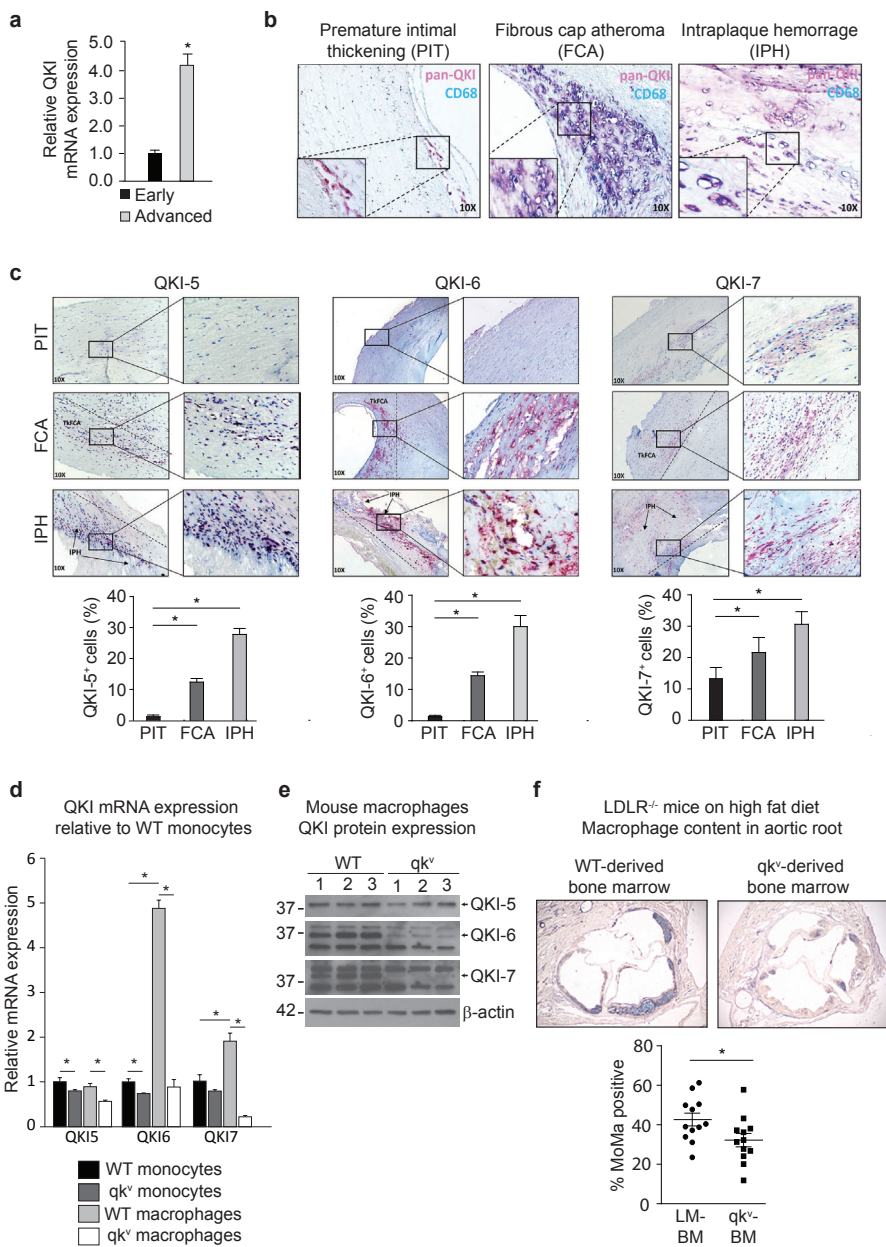


FIGURE 1

**Figure 1 | Quaking is expressed in macrophages within atherosclerotic lesions.** (a) Pan-QKI mRNA expression levels in CD68<sup>+</sup> macrophages of early and advanced atherosclerotic lesions isolated by laser-capture microdissection (n/4). Data expressed as mean±s.e.m.; Student's t-test, \*P<0.05. Scale bar, 50 mm. (b) Immunohistochemical analysis of co-localization of pan-QKI and CD68 expression in preliminary intimal thickening (PIT), FCA and intraplaque haemorrhage (IPH). Dashed line denotes intimal/adventitial border. Scale bar, 50 mm.

Figure 1 legend continued | (c) Immunohistochemical analysis of QKI-5, -6 and -7 expression in PIT, FCA and IPH (top), and quantification of QKI-positive cells mm<sup>2</sup> per tissue sample (n=5). Data expressed as mean±s.e.m.; one-way analysis of variance (ANOVA), Bonferroni's post-hoc test; \*P<0.05, \*\*P<0.01. (d) Quantitative RT-PCR (qRT-PCR) analysis of QKI mRNA expression in naive BM-derived CD115<sup>+</sup> mouse monocytes and 7 days M-CSF stimulated macrophages of either wt-littermates (LM) or quaking viable (qkv) mice (n = at least 3 mice per condition). Data expressed as mean±s.e.m.; one-way ANOVA, Bonferroni's post-hoc test; \*P<0.05 and \*\*P<0.01. (e) Western blot analysis of QKI-5, -6 and -7 expression levels in 7 days M-CSF stimulated macrophages derived from BM of wt and qkv mice. Each lane represents an individual mouse lysate (biological n=3). (f) Immunohistochemical analysis for atherosclerotic plaque-resident macrophages (% MoMa-positive area) in aortic root sections of g-irradiated (8 Gy) LDLR<sup>-/-</sup> mice that subsequently were transplanted with BM from either qkv mice (qkv-BM) or littermates (LM-BM) and fed a high-fat diet for 8 weeks to develop atherosclerotic lesions (n=12 per group). Scale bar, 200 µm. Data expressed as mean±s.e.m.; Student's t-test, with \*P<0.05.

## Results

### Human atherosclerotic lesion macrophages express QKI.

We previously observed QKI expression in VSMCs<sup>23</sup> and in leukocyte foci within human coronary restenotic lesions. Based on this observation, we used laser-capture microdissection to harvest CD68<sup>+</sup> macrophages from early and advanced atherosclerotic lesions of human carotid arteries. QKI mRNA was 4.2-fold enriched in macrophages derived from advanced as compared with early atherosclerotic lesions (Fig. 1a). Next, using immunohistochemistry, we assessed QKI protein expression in human tissue sections at various stages of atherosclerotic lesion development, namely early pathological intimal thickening (PIT), fibrous cap atheroma (FCA) and intraplaque haemorrhaging (IPH). Although QKI was detectable in CD68<sup>+</sup> myeloid cells of PIT, it was abundantly expressed in macrophage-rich FCA and IPH lesions (Fig. 1b). Furthermore, QKI-5, -6 and -7 were detectable in the nuclear, perinuclear and cytoplasmic regions of intimal macrophages in both FCA and IPH, respectively (Fig. 1c). We conclude that the accumulation of macrophages in human atherosclerotic lesions is associated with increased mRNA and protein expression of all three QKI isoforms within the macrophage.

### A reduction in QKI decreases lesional macrophage burden.

To investigate whether decreased QKI expression in monocytes and macrophages could influence atherosclerotic lesion formation, we transplanted bone marrow (BM) from QKI viable (qkv) mice<sup>37</sup>, which express reduced levels of QKI protein, or their wild-type (wt) littermate controls (LM) into atherogenic LDLR<sup>-/-</sup> mice. Although qk knockout mice die as embryos, the qkv mouse harbours a spontaneous 1Mb deletion in the QK promoter region that leads to reduced levels of QKI mRNA and protein<sup>37</sup>. Indeed, macrophage colony-stimulating factor (M-CSF)- mediated conversion of LM and qkv BM-derived monocytes to macrophages showed subtly reduced QKI-5 mRNA and protein levels, and almost a complete ablation of QKI-6 and -7 protein (Fig. 1d,e). Following BM transplantation, the LDLR<sup>-/-</sup>/qkv and LDLR<sup>-/-</sup>/LM mice were fed a high-fat diet for 8 weeks, to induce atherosclerotic lesion formation.

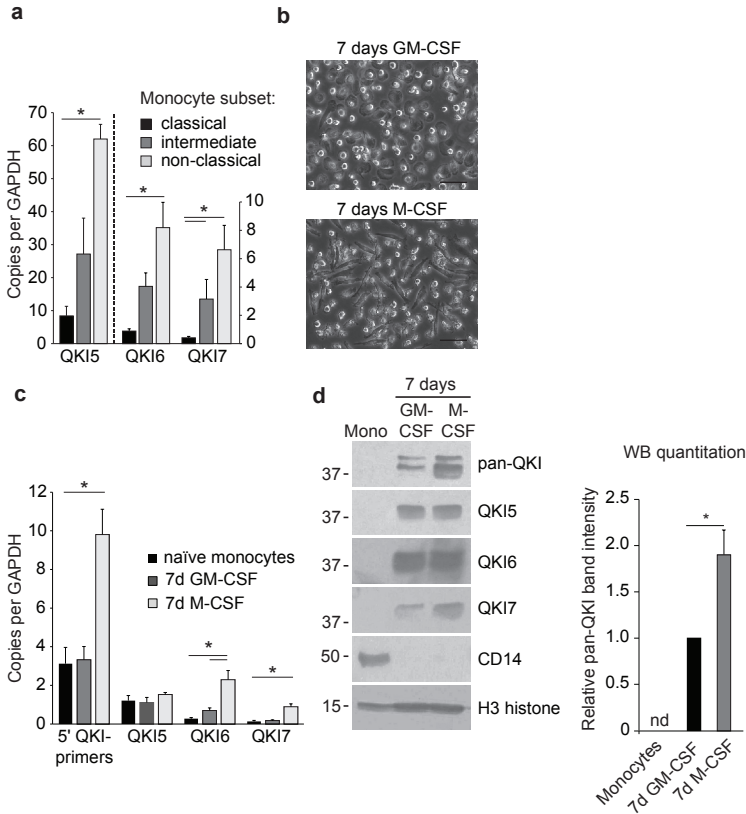


**Figure 2 | QKI is highly expressed in macrophages derived from PB monocytes.** (a) mRNA expression levels of distinct QKI isoforms following negative selection and FACS sorting for blood-derived human monocyte subsets, namely classical (CD14<sup>++</sup>, CD16<sup>-</sup>), intermediate (CD14<sup>++</sup>, CD16<sup>+</sup>) and non-classical (CD14<sup>+</sup>, CD16<sup>+</sup>). Expression is depicted relative to copies per glyceraldehyde 3-phosphate dehydrogenase (GAPDH). Data expressed as mean $\pm$ s.e.m.; one-way analysis of variance (ANOVA), Bonferroni's post-hoc test; \* $P$ <0.05 and \*\* $P$ <0.01. (b) Phase-contrast photomicrographs of human PB monocytes cultured for 7 days in the presence of either GM-CSF or M-CSF. Scale bar, 50  $\mu$ m. (c) Quantitative RT-PCR (qRT-PCR) analysis for QKI mRNA isoforms in naïve PB monocytes isolated using CD14 $\mu$  microbeads, 7 days GM-CSF and 7 days M-CSF differentiated macrophages ( $n$ =3). Expression is depicted relative to copies per GAPDH. Data expressed as mean $\pm$ s.e.m.; one-way ANOVA, Bonferroni's post-hoc test; \* $P$ <0.05 and \*\* $P$ <0.01. (d) Western blot analysis of QKI protein isoforms in naïve monocytes, 7 days GM-CSF and 7 days M-CSF differentiated macrophages (pan-QKI and CD14:  $n$ =5, QKI-5, 6 and 7:  $n$ =1) with quantification of pan-QKI ( $n$ =5). Data expressed as mean $\pm$ s.e.m.; Student's  $t$ -test, with \*\* $P$ <0.01. Equivalent concentrations of whole-cell lysates were loaded per lane as determined using a BCA protein assay.

Interestingly, the longterm reduction of QKI expression during haematopoietic reconstitution limited neutrophil and monocytic repopulation (Supplementary Data 1). In keeping with this finding, immunohistochemical analysis of the aortic root revealed significantly decreased monocyte/macrophage content within atherosclerotic lesions of LDLR-/-/qkv mice (Fig. 1f), a finding that immunohistochemical analysis revealed was independent of plaque size or collagen content. These findings suggested that changes in haematopoietic and monocytic QKI expression could influence the macrophage content of atherosclerotic lesions.

### **QKI is induced on monocyte to macrophage differentiation.**

Having identified high QKI expression in macrophages in atherosclerotic lesions, we first explored whether QKI mRNA expression levels differ in macrophage precursors, namely classical (CD14<sup>++</sup>/CD16<sup>-</sup>), intermediate (CD14<sup>++</sup>/CD16<sup>+</sup>) and non-classical (CD14<sup>+</sup>/CD16<sup>-</sup>) monocytes derived from human peripheral blood (PB)<sup>2</sup>. All three monocyte subpopulations abundantly expressed QKI-5, -6 and -7 mRNAs as compared with glyceraldehyde 3-phosphate dehydrogenase (Fig. 2a). Moreover, QKI-5, -6 and -7 mRNA levels increased as classical monocytes progressed towards intermediate or non-classical monocytes. Interestingly, QKI-5 mRNA was the most abundantly expressed transcript in all three subpopulations. (Fig. 2a). Next, we assessed QKI mRNA and protein levels in human PB monocytes treated with granulocyte–macrophage CSF (GM-CSF) and M-CSF, to stimulate their conversion to pro-inflammatory and anti-inflammatory macrophages, respectively (Fig. 2b). We observed remarkable increases in the expression of all QKI mRNA transcripts in mature macrophages (Fig. 2c). However, despite abundant QKI mRNA, the distinct QKI isoforms were poorly expressed in freshly isolated PB monocytes as compared with mature macrophages (Fig. 2d). The GM-CSF or M-CSF-induced conversion of monocytes into macrophages was associated with striking increases in QKI-5, -6 and -7 protein levels, with a more pronounced increase in all three isoforms observed with M-CSF treatment (Fig. 2d).

### **QKI haploinsufficiency perturbs macrophage differentiation.**

To further assess the role of QKI in monocyte and macrophage biology, we undertook an in-depth analysis of a unique, QKI haploinsufficient individual (Pat-QKI+/-) and her sister control (Sib-QKI+/+)38. This patient is the only known carrier of a balanced reciprocal translocation (t(5;6)(q23.1;q26)), where a breakpoint in one of her QKI alleles specifically reduces QKI expression by 50% in both QKI mRNA38 and QKI protein levels as compared with her sibling (Sib-QKI+/+; Fig. 3a,b). RNA sequencing (RNA-seq) analysis (see below) confirmed altered QKI expression and furthermore revealed the precise location of the translocation breakpoint in intron 4 of QKI (Fig. 3b and Supplementary Fig. 1a). We next compared the circulating monocytes of these two individuals for the expression of well-established monocyte cell surface markers such as CD14, CD16, CX3CR1, CCR2, SELPLG and CSF1R by fluorescence-activated cell sorting (FACS) analysis. Although monocyte subset ratios were not different (Supplementary Fig. 2a), the expression of CSF1R, the receptor that drives

macrophage commitment, was elevated in Pat-QKI+/- non-classical monocytes as compared with Sib-QKI+/+ (Supplementary Fig. 2b). As CSF1R is normally reduced when monocytes differentiate into macrophages, this observation points towards a potential defect in monocyte maturation in the patient. Next, we investigated the consequences of decreased QKI expression on monocyte to macrophage differentiation. For this, we obtained freshly isolated Pat-QKI+/- and Sib-QKI+/+ monocytes from venous blood and treated the cells for 7 days in the presence of either GM-CSF or M-CSF. Similar to the results in Fig. 2b, Sib-QKI+/+ monocytes possessed the capacity to adopt the characteristic pro-inflammatory macrophage morphology, whereas monocytes from Pat-QKI+/- generally retained a monocytic morphology (Fig. 3c top panels). We harvested RNA and protein from these macrophages and found that both QKI mRNA and protein levels were decreased (Fig. 3d,e). Surprisingly, this reduction in QKI did not appear to have an impact on the conversion of monocytes into anti-inflammatory macrophages (Fig. 3c bottom panels), a finding that prompted us to focus on the role of QKI in monocyte to macrophage differentiation in a pro-inflammatory setting.

### **QKI impacts transcript abundance in monocytes and macrophages.**

The observed increase in QKI expression during macrophage differentiation and well-established function as a splicing and translational regulator<sup>23,31,39,40</sup> suggested that QKI is necessary for posttranscriptional control of events that lead to macrophage identity. To identify potential regulatory targets of QKI at a genome-wide level, we characterized the transcriptomes of Sib-QKI+/+ and Pat-QKI+/- monocytes and GM-CSF-stimulated macrophages by RNA-seq (Supplementary Data 2). First, we assessed the expression levels of established immune-regulated genes<sup>11,12</sup>. As shown in Fig. 3f, the mRNA levels of many monocyte to macrophage differentiation markers<sup>11,12</sup> were similarly regulated in Sib-QKI+/+ and Pat-QKI+/- (CD68↑, ApoE↑, ITGAM↑, CD14↓, CX3CR1↓ and CD163↓). In contrast, the expression levels of several key pro- and anti-inflammatory markers indicated an antiatherogenic shift in Pat-QKI+/- macrophages (Fig. 3f right; IL6↓, IL23a↓, CD16A↓, CD16B↓, ApoE↓ and IL10↑). At the genome-wide level, QKI haploinsufficiency altered the abundance of 2,433 and 1,306 mRNA species in monocytes and macrophages (Fig. 3g, Supplementary Data 2 and Supplementary Fig. 3 top), respectively. Subsequently, we computationally determined the subset of mature mRNA transcripts in the genome that contain a QKI-binding sequence motif (termed QRE)<sup>30</sup> (Supplementary Data 2). Our data suggested that QKI directly modulates the expression of 215 (128↑ and 87↓) and 154 (100↑ and 54↓) mRNAs in PB monocytes and macrophages, respectively (Fig. 3g, Venn sum of intersect). The five most differentially expressed genes in the patient relative to the sibling that harbour a QRE are shown in Fig. 3h. By selecting genes containing QREs, we identified a substantial number of putative QKI-mediated changes in transcript abundance (Fig. 3i). Previous genome-wide studies have reported contrasting roles for QKI as both a repressor and stabilizer of target mRNAs<sup>31,33</sup>. Intrigued by this ambiguity, we determined the consequences of QKI haploinsufficiency on mRNA transcript abundance in monocytes and macrophages. For this, we tested whether the presence of a



QRE within a target mRNA was associated with increased or decreased mRNA abundance in the patient relative to her sibling (Supplementary Fig. 3 top). For this, we plotted the cumulative distribution fraction (CDF: y axis, as a fraction of total genes) against the transcript Log2FC (x axis: Pat-QKI+/- / Sib-QKI+/+) and stratified for either putative QKI targets (with QRE) or non-targets (no QRE). In PB monocytes, a reduction in QKI was associated with significantly lowered target mRNA expression (Fig. 3j left panel, left shift of cyan line). In contrast, in PB macrophages the expression levels of mature mRNAs containing QREs was strikingly increased in the patient relative to her sibling, as compared with those without QREs (Fig. 3j right panel, right shift of cyan line). Collectively, these studies suggested that QKI potentially regulates gene expression during monocyte-to-macrophage differentiation.

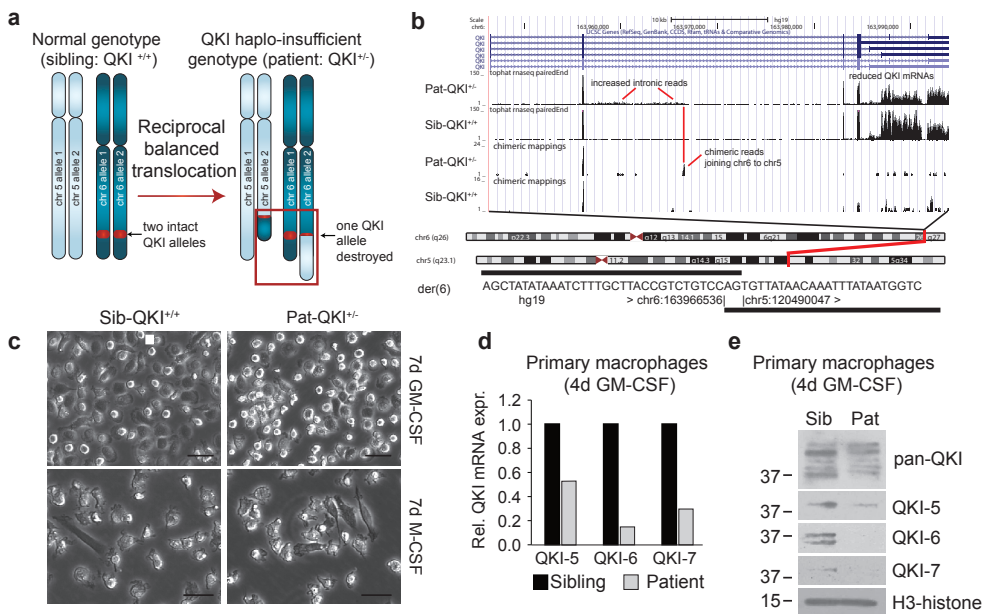


**Figure 3 | Characterization of monocyte and macrophage biology in a unique QKI haploinsufficient patient.** (a) Schematic of chromosomal translocation event in the *qki* haploinsufficient patient (Pat-QKI<sup>+/-</sup>), reducing QKI expression to 50% that of her sister control (Sib-QKI<sup>+/+</sup>). (b) Top: UCSC Genome Browser display of reference genome QKI locus with standard and chimeric reads for the patient and sibling. The reduced expression levels and altered 3'-untranslated region (UTR) composition in the patient RNA as compared with a sibling control is noteworthy. Patient shows increased intronic RNA extending to the point where chimeric reads map at the breakpoint to chr5. Middle: chromosome diagrams showing normal chromosomes 5 and 6 with the red line, indicating the location of the breakage fusion point. Bottom: sequence across the fusion point. The chromosomal origin of the AG dinucleotide is ambiguous. (c) Photomicrographs of sibling and patient macrophages, cultured in GM-CSF or M-CSF for 7 days, respectively.

**Figure 3 legend continued** | (d,e) Assessment of QKI isoform mRNA and protein expression in 4-day GM-CSF-stimulated macrophages in the sibling and patient. (f) Hierarchical clustering (Euclidean algorithm) of key monocyte differentiation genes depicting changes in RNA-seq-derived mRNA abundance where dark blue=low expression, whereas light blue=high expression (\* and/or # indicates >1.5-fold expression change in monocytes or macrophages, respectively). (g) Venn diagrams with numbers of differentially expressed genes (minimally  $\pm 1.5$ -fold; patient/sibling expression) for unstimulated (top) and GM-CSF stimulated macrophages (bottom). An expression cutoff (Pat+Sib expression >1 CPM) was applied. (h) The most differentially expressed genes, harbouring a QRE are depicted. (i) Genome-wide scatterplot of mRNA abundance (y axis: Log10 CPM) versus the log2FC (x axis: Patient/sibling CPM) after an expression cutoff (Pat+Sib expression >1 CPM) in monocytes (left) and GM-CSF-stimulated macrophages (right). Blue dots indicate QRE-containing transcripts minimally  $\pm 1.5$ -fold differentially expressed. Grey dots do not fulfill these criteria. (j) CDF (y axis) for QKI target (QRE containing: blue line) and non-target (non-QRE containing: cyan line) mRNAs (x axis: log2FC) in monocytes (left) and macrophages (right). Left shift indicates lower expression of QKI target genes, whereas a right shift indicates higher expression of QKI targets in the patient samples. Distributions were compared using a Wilcoxon rank-sum test

### QKI controls splicing in monocytes and macrophages.

Given previous reports that QKI is involved in splicing of pre-mRNAs<sup>23,39–42</sup>, we tested whether QKI acts similarly in monocytes and macrophages. First, we evaluated our RNA-seq analysis of Sib-QKI+/+ and Pat-QKI+/- PB monocytes and macrophages for splicing changes (Supplementary Data 3). This analysis uncovered 1,513 alternative splicing events between Pat-QKI+/- and Sib-QKI+/+ monocytes and macrophages, revealing events that were unique to either monocytes or macrophages, as well as common events (Supplementary Data 3). Previous observations for QKI and other RBPs suggested that when a splicing factor binds the intron downstream of an alternative exon, it promotes exon inclusion; however, when binding the intron upstream of the alternative exon, the RBP promotes exon skipping<sup>19,43</sup>. We analysed the RNA-seq data for such a trend using the set of splicing events that change between the Pat-QKI+/- and Sib-QKI+/+, to determine the frequency of the QKI-binding motif, ACUAA, around these regulated exons, relative to a background set of exons that is expressed, but inclusion is unchanged between the two data sets. The results of these analyses are shown in Fig. 4a and Supplementary Data 4, and demonstrate ACUAA motif enrichment upstream of exons with increasing inclusion in Pat-QKI+/- (QKI repressed exons) relative to background exons, as well as an increase in ACUAA motif frequency downstream of exons with increased skipping (QKI activated) relative to background. This suggested that similar to C2C12 myoblasts<sup>39</sup>, QKI promotes exon skipping by binding the upstream intron, while promoting inclusion of alternative exons by binding to the downstream intron, in monocytes and in macrophages. These data strongly support a direct, position-dependent role for QKI in regulating alternative splicing, while also providing additional protein diversity during monocyte-to-macrophage differentiation. As shown in Fig. 4b, QKI haploinsufficiency triggered alternative splicing events in PB monocytes (orange tracks) and macrophages (blue tracks). Interestingly, the presence of QKI-binding sites, as defined by either experimentally determined QKI PAR-CLIP sites<sup>39</sup> and/or ACUAA motifs clearly associated with changes in exon inclusion



(for example, *ADD3*), alternative 5'-splice sites (*PARP2*), alternative 3'-splice sites (*M6PR*) and intron retention (for example, *BICD2*), thereby expanding the detection of veritable QKI-regulated events beyond cassette exons (splice event 'se' location defined by brackets). Importantly, strong correlations were observed between QKI expression levels and the magnitude of the splicing event, be it between the patient and sibling control, or between monocytes and macrophages (Fig. 4b). Finally, we validated several alternatively spliced cassette exons, including events in *ADD3*, *LAIR1* and *UTRN* by reverse transcriptase-PCR (RT-PCR), using primers in flanking exons (Fig. 4c). Collectively, our RNA-seq data analysis of this unique QKI haploinsufficient individual strongly suggested a direct role for QKI in regulating alternative splicing events that could influence monocyte to macrophage differentiation. To extend results obtained with the QKI haploinsufficient patient, we abrogated QKI expression in naive primary human monocytes harvested from freshly drawn venous blood of healthy controls. We designed GapmeR antisense oligonucleotides that either targeted QKI for degradation (QKI-Gap), or are scrambled as a control (Scr-Gap), coupled with a 50-FAM label to track their cellular uptake. The QKI-Gap and Scr-Gap compounds were administered to the freshly isolated monocytes, concomitant with GM-CSF for 96 h, to drive the differentiation to pro-inflammatory macrophages. In contrast to our attempts to reduce QKI mRNA levels using other well-established approaches, we observed virtually no signs of cytotoxicity or apoptosis following GapmeR treatment. Furthermore, the treatment did not hamper the capacity of monocytes to differentiate into macrophages (Fig. 4d top), while uptake efficiency approached 100% (based on FAM+ cells; Fig. 4d bottom). After 96 h, we harvested RNA from the QKI-Gap- and Scr-Gap-treated macrophages, which yielded a minimal reduction in QKI-5 mRNA levels but remarkable reductions in QKI-6 and QKI-7 mRNAs (Fig. 4e). Albeit that the GapmeR-mediated reduction in QKI expression in primary human macrophages was not as striking as that observed in the QKI haploinsufficient patient, it nonetheless enabled us to visualize and validate significant changes in several of the aforementioned QKI-mediated alternative splicing events, such as *ADD3* and *FcγR-IIb* (*FCGR2B*) (Fig. 4f; n=3 donors). It should be noted that the inability to remarkably reduce the expression of the nuclear QKI isoform, namely QKI-5, could be responsible for the discrepancy between the striking shift in splicing observed in the QKI haploinsufficient patient as compared with the GapmeR-mediated abrogation of QKI expression. Taken together, these studies clearly pinpoint QKI as a regulator of pre-mRNA splicing during monocyte-to-macrophage differentiation and implicate QKI gene dosage as a determinant of splicing event magnitude.

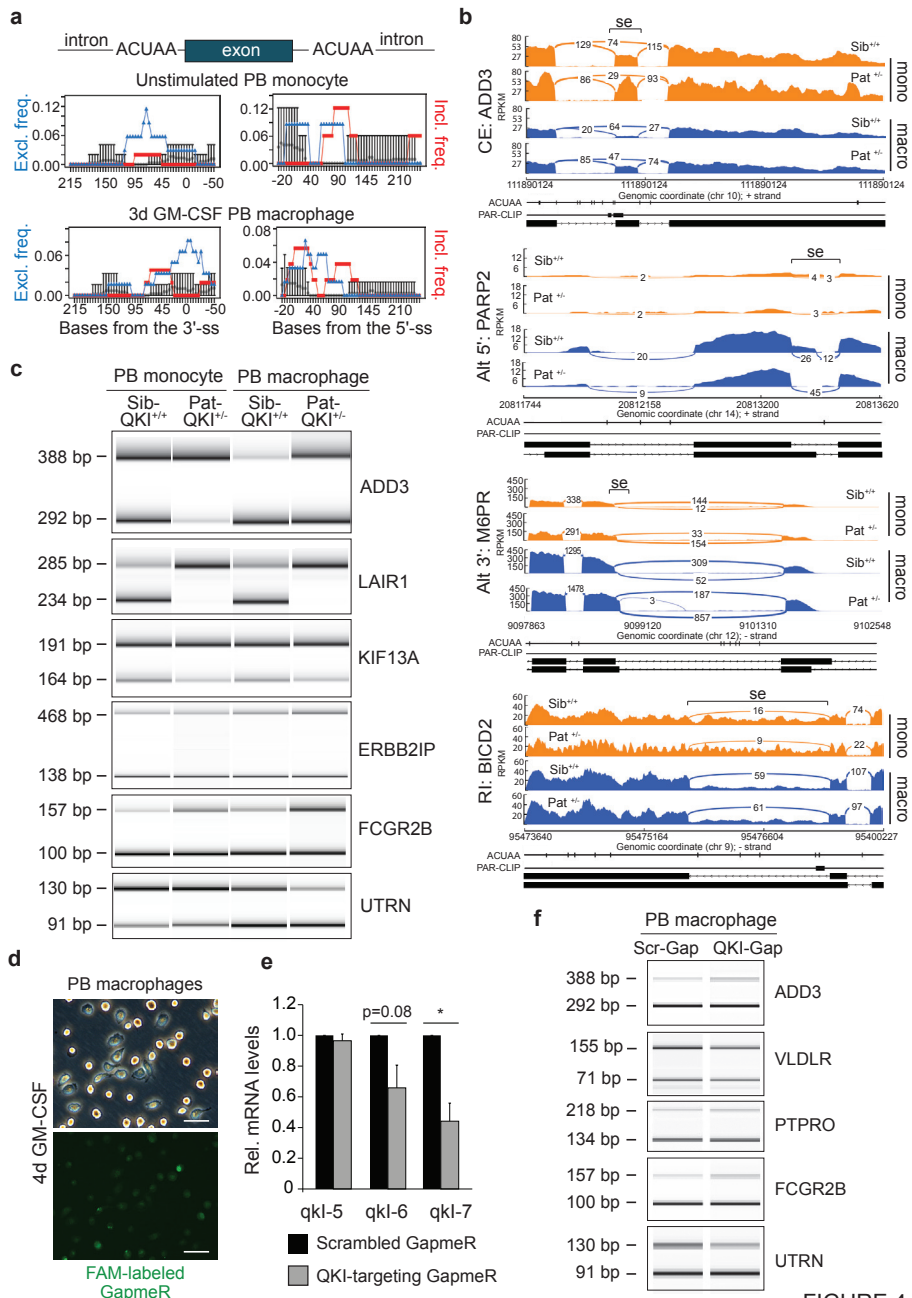


FIGURE 4

**Figure 4 | QKI influences pre-mRNA splicing in naive PB monocytes and macrophages.** (a) SpliceTrap assessment of the proximal ACUAA RNA motif enrichment in 50-bp windows upstream and downstream of alternatively spliced cassette exons (as compared with a background set of exons; grey circles). The relationship between the frequency of exon exclusion (blue triangles) or exon inclusion (red squares) and ACUAA RNA motif enrichment over the genomic locus are depicted.

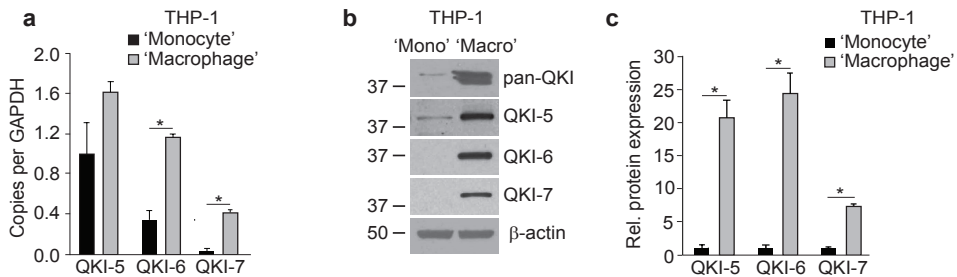
**Figure 4 legend continued** | (b) Sashimi plots illustrate RNA-seq read coverage for selected alternative splicing events in Pat-QKI<sup>+/-</sup> versus Sib-QKI<sup>+/+</sup> PB monocytes (orange) and macrophages (blue). Splicing events (se) are highlighted by inverted brackets. The location of ACUAA motifs and QKI PAR-CLIPs are provided below. Splicing events were defined based on the genomic organization of RefSeq transcripts (bottom tracks). Full event details are provided in Supplementary Data 3. (c) PCR validation of alternatively spliced cassette exons in Sib-QKI<sup>+/+</sup> and Pat-QKI<sup>+/-</sup> PB-derived monocytes and macrophages. Primers were designed to target constitutive flanking exons. PCR product size for exon inclusion (top) and exclusion (bottom) variants are provided (left). (d) Phase-contrast and fluorescence-microscopy photographs (scale bar, 50  $\mu$ m) of primary human, PB macrophages of healthy controls that have been treated with FAM-labelled GapmeRs, to reduce QKI expression. (e) Quantitative RT-PCR (qRT-PCR) of QKI mRNA isoform expression in GapmeR-treated macrophages (n=3). Data expressed as mean $\pm$ s.e.m.; Student's t-test, with \*\*P<0.01. (f) PCR validation of alternatively spliced cassette exons in GapmeR-treated PB-derived macrophages. Primers were designed to target constitutive flanking exons. PCR product size for exon inclusion (top) and exclusion (bottom) variants are provided (left). A representative illustration is shown of an n=3 donors. Data expressed as mean $\pm$ s.e.m.; Student's t-test, with \*\*P<0.01 and #P=0.08.

### QKI regulates transcript abundance in THP-1 cells.

To provide further support for a regulatory role for QKI during monocyte-to-macrophage differentiation, we tested whether QKI could similarly modulate transcript abundance and pre-mRNA splicing in a well-established monocyte cell line, namely THP-1 cells. Similar to GM-CSF-induced differentiation of PB monocytes into macrophages, the 12,13-phorbol myristyl acetate (PMA)-induced transition of THP-1 'monocytes' to 'macrophages' was associated with the following: (1) significantly increased expression of all QKI mRNA transcripts (Fig. 5a); (2) barely detectable levels of QKI protein in THP-1 'monocytes' (Fig. 5b and Supplementary Fig. 4a); and (3) significantly increased expression of QKI protein during THP-1 'monocyte' to 'macrophage' differentiation (Fig. 5b,c). Next, we stably transduced THP-1 'monocytes' with either short-hairpin RNA (shRNA) targeting QKI (sh-QKI) to specifically deplete QKI or with a non-targeting shRNA control (sh-Cont) (Supplementary Fig. 4b). Similar to GM-CSF-stimulated Pat-QKI<sup>+/-</sup> versus Sib-QKI<sup>+/+</sup> monocytes, sh-QKI THP-1 'monocytes' displayed an inability to adopt the 'macrophage' morphology following stimulation with PMA as compared with sh-Cont THP-1 'monocytes' (Supplementary Fig. 4c arrows). We subsequently determined mRNA levels using an exon junction microarray<sup>44</sup> analysing RNA isolated from unstimulated and 3 days PMA-stimulated THP-1 sh-Cont and sh-QKI 'monocytes' and 'macrophages' (Supplementary Data 5). Next, as shown in Fig. 5d, we assessed the expression profile of established monocyte differentiation genes (for example, CD14 $\uparrow$ , CXCL8 $\uparrow$ , CSF1R $\uparrow$ , ApoE $\uparrow$ , CX3CR1 $\downarrow$ , CCR2 $\downarrow$  and CCL22 $\downarrow$ ). Similar to QKI haploinsufficient macrophages, several markers in sh-QKI THP-1 'macrophages' displayed an anti-atherogenic phenotypic shift (IL6 $\downarrow$ , IL23a $\downarrow$ , CD16A $\downarrow$ , CD16B $\downarrow$ , ApoE $\downarrow$  and IL10 $\uparrow$ ) as compared with sh-Cont THP-1 'macrophages' (Fig. 5d). At the genome-wide level, the reduction of QKI significantly altered the abundance of 359 and 573 mRNAs in THP-1 'monocytes' and 'macrophages', respectively (Fig. 5e, Supplementary Data 5 and Supplementary Fig. 3 bottom). Of these differentially expressed mRNAs, 56 and 128 were computationally predicted QKI targets based on the presence of a QRE in the mature mRNA (Fig. 5e intersect). The most differentially

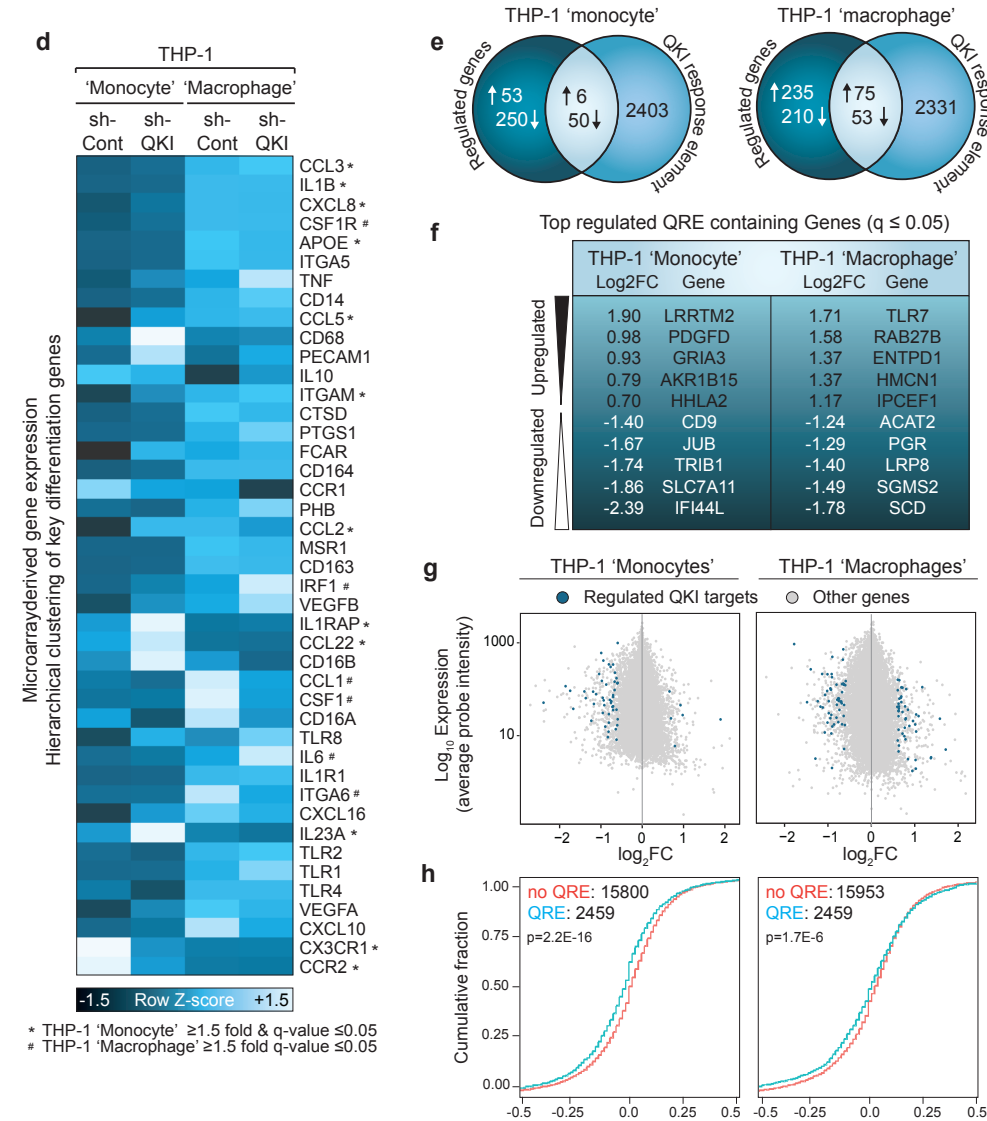
expressed transcripts harbouring a QRE are denoted in Fig. 5f. The expression levels of mRNAs targeted by QKI in THP-1 'monocytes' and 'macrophages' are depicted in Fig. 5g (blue dots) and Fig. 5h (blue lines), relative to those not directly affected by changes in QKI levels (Fig. 5g grey dots and Fig. 5h cyan lines). Consistent with our analyses in PB monocytes, putative direct QKI target mRNAs were mostly reduced on a targeted QKI reduction in THP-1 'monocytes' (Fig. 5h, left plot), although a shift towards increased target mRNA abundance in THP-1 'macrophages' was not observed (Fig. 5h, right plot).

Figure 5



**Figure 5 | QKI influences mRNA transcript abundance during differentiation of THP-1 monocyte-like cells to THP-1 macrophage-like cells.** (a) mRNA expression of the QKI isoforms as compared with glyceraldehyde 3-phosphate dehydrogenase (GAPDH) in THP-1 'monocytes' and 8 days differentiated THP-1 'macrophages' (biological n=3). Data expressed as mean±s.e.m.; Student's t-test; \*P<0.05 and \*\*P<0.01. (b) Western blot analysis of whole-cell lysates of THP-1 'monocytes' and THP-1 'macrophages'. (c) Western blot quantification of QKI protein isoforms, normalized to β-actin in THP-1 'monocytes' and THP-1 'macrophages' (n=3). Data expressed as mean±s.e.m.; Student's t-test; \*\*P<0.01. (d) Hierarchical clustering (Euclidean algorithm) of key monocyte differentiation genes depicting changes in microarray-derived mRNA abundance THP-1 'monocytes' (left two lanes) and THP-1 'macrophages' (right two lanes), where dark blue=low expression, whereas light blue=high expression (\* and/or # beside gene name is indicative of a significant >1.5- fold change in expression in monocytes or macrophages, respectively). (e) Venn diagrams depicting the number of microarray-derived differentially expressed genes (minimally ±1.5-fold; sh-QKI/sh-Cont expression, q-value <0.05) for unstimulated THP-1 'monocytes' (left Venn diagram) and THP-1 'macrophages' (right Venn diagram). (f) The most significantly differentially expressed genes harbouring a QRE are shown. (g) Genome-wide scatterplot of mRNA abundance in THP-1 'monocytes' (left scatterplot) and THP-1 'macrophages' (right scatterplot); y axis: Log10 probe intensity versus the x axis: log2FC: sh-QKI average probe intensity/sh-Cont average probe intensity. Blue dots indicate QRE-containing transcripts that are minimally ±1.5 fold differentially expressed (q<0.05). Grey dots do not fulfill these criteria. (h) CDF (y axis) for QKI target (QRE containing: blue line) and non-target (non- QRE containing: cyan line) mRNAs (x axis: log2FC) in THP-1 'monocytes' (left plot) and THP-1 'macrophages' (right plot). Left shift indicates lower expression of QKI target genes in the sh-QKI samples, whereas a right shift is indicative of higher expression of QKI targets in the sh-QKI samples. Distributions were compared using a Wilcoxon rank-sum test.

Figure 5 continued



### **QKI modifies pre-mRNA splicing patterns in THP-1 cells.**

Having identified that QKI haploinsufficiency generates pre-mRNA splicing events that probably have an impact on monocyte and macrophage biology, we also analysed RNA isolated from sh-Cont and sh-QKI THP-1 ‘monocytes’ and ‘macrophages’ for alternative splicing events using the exon junction microarray platform<sup>44</sup>. This highly sensitive technology uses probes that are designed specifically to detect both constitutive exon–exon junctions and alternative exon–exon junctions, enabling one to quantify inclusion ratios for alternative splicing events. These studies uncovered 571 and 629 differentially regulated alternative splicing events in THP-1 ‘monocytes’ and ‘macrophages’, respectively, including numerous cassette exons, alternative 50- and 30-splice sites, and retained introns (Fig. 6a and Supplementary Data 6; n=3). Detected splicing events are illustrated in Fig. 6b, where the skip and include intensities (y axis and x axis, respectively) of transcript-specific hybridization probes directed to either the constitutive or alternatively spliced exons are plotted. The separation score, obtained by determining slope differences, indicates the magnitude of the splicing event. Similar to the motif enrichment analyses performed for the RNA-seq of PB monocytes and macrophages, these studies confirmed that exon skipping frequency was significantly correlated with alternative exons that had an ACUAA motif in the upstream intron (Fig. 6c left panels and Supplementary Data 4). In contrast to the subtle enrichment of inclusion frequency observed in Pat-QKI+/- and Sib-QKI+/- monocytes and macrophages (Fig. 3a right panels), exon inclusion frequency in THP-1 ‘monocytes’ and ‘macrophages’ was clearly associated with the presence of ACUAA motifs in the downstream intron (Fig. 6c and Supplementary Data 4). Finally, alternative cassette exons in THP-1 ‘monocytes’ and ‘macrophages’ were PCR validated (Fig. 6d). Importantly, we also selected several top splicing events from THP-1 ‘monocytes’ and ‘macrophages’ (Supplementary Data 6), and validated these in RNA harvested from wt and qkv mice, including REPS1, PTPRO and FGFR10P2 (Fig. 6e).

### **QKI targets monocyte activation and differentiation pathways.**

We subsequently determined how QKI-induced changes in mRNA transcript abundance could have an impact on Gene Ontology (GO) enrichment of coordinately regulated pathways during monocyte-to-macrophage differentiation. As shown in Table 1 and Supplementary Data 7, these GO analyses point towards a central regulatory role for QKI in immune responses to injury, processes that play a critical role in the onset and development of atherosclerosis and other inflammation-based diseases. In both monocytes and macrophages, changes in QKI expression clearly had an impact on Liver X Receptor (LXR)/ Retinoid X Receptor (RXR) activation and Peroxisome Proliferator-Activated Receptor (PPAR) activation and signalling, implicating a key role for QKI in regulating cholesterol biosynthesis and metabolism. Furthermore, a reduction in QKI expression also appeared to influence T-cell and Toll-like receptor signalling, biological processes that play prominent roles in the rapid resolution of infection, while in chronic settings exacerbate inflammatory conditions. Finally, the gene enrichment analysis suggested that posttranscriptional processing of factors driving the recruitment, adhesion and diapedesis of immune cells were affected by changes in QKI expression.

Figure 6

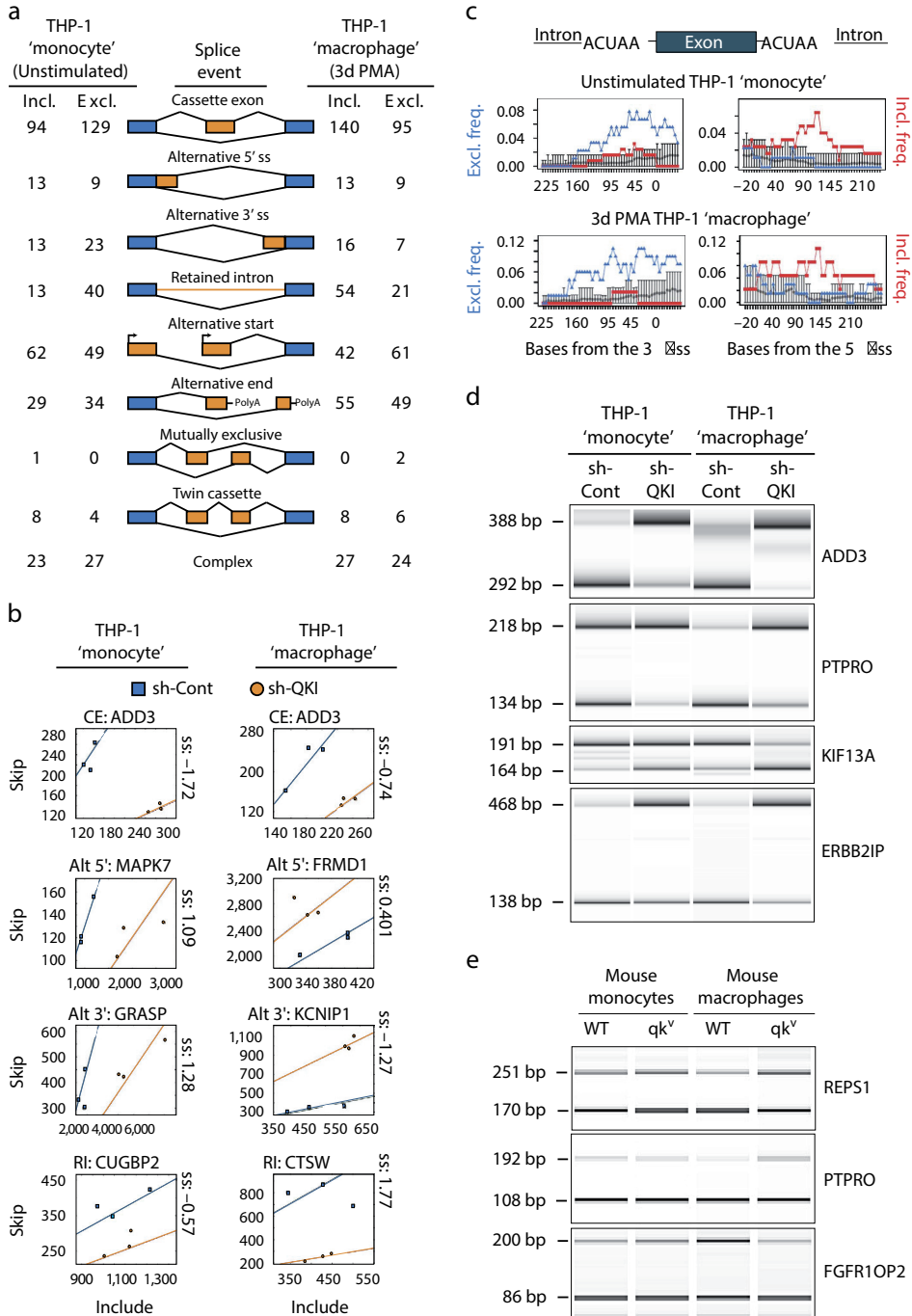




**Figure 6 | QKI expression levels influence pre-mRNA splicing during THP-1-based monocyte-like to macrophage-like cell differentiation.** (a) Schematic depicting detectable alternative splicing events with the splicing-sensitive microarray platform and number of inclusion (incl.; top lines) or exclusion (excl.; bottom lines) events observed in unstimulated THP-1 'monocytes' (left) and 3-day PMA-stimulated THP-1 'macrophages' (n=3, q<0.05). (b) Scatterplots of skip (y axis) and include (x axis) probe set intensity for selected alternative splicing events in sh-Cont (blue boxes) versus sh-QKI (orange circles) in unstimulated and 3 days PMA-stimulated THP-1 'monocytes' and 'macrophages', respectively. Regression coefficients (constrained to pass the origin) are depicted as solid lines. The log2 difference in the slopes (termed separation score; ss) are provided to the right of the plots for each event, with for example, an ss of 1.72, indicating a 3.3-fold more inclusion of ADD3 exon 13 in sh-QKI versus sh-Cont THP-1 'monocytes'. Full event details are provided in Supplementary Data 6. CE, cassette exon; Alt 50 or 30, alternative 50 or 30 splice site; RI, retained intron. (c) SpliceTrap assessment of average proximal ACUAA RNA motif enrichment in 50 bp windows upstream and downstream of alternatively spliced cassette exons as compared with a background set of exons (grey circles). The relationship between the frequency of exon exclusion (blue triangles) or exon inclusion (red squares) and ACUAA RNA motif enrichment are depicted. (d) PCR validation of alternatively spliced cassette exons in sh-Cont and sh-QKI THP-1 'monocytes' and 'macrophages'. Primers were designed to target constitutive flanking exons. PCR product size for exon inclusion (top) and exclusion (bottom) variants are provided (left). All experiments depict biological n=3. (e) PCR validation of three splicing events in wt and qkv mouse-derived primary monocytes and 7 days M-CSF-stimulated macrophages. PCR product size for exon inclusion (top) and exclusion (bottom) variants are provided (left). Depicted is a representative PCR for at least a biological n=3.

**Table 1 | IPA assessment of pre-defined canonical pathways affected by changes in QKI expression.**

Monocytes			Macrophages		
THP-1 sh-QKI versus sh-Cont			THP-1 sh-QKI versus sh-Cont		
Affected canonical pathway	- Log (P-value)	Affected genes	Affected canonical pathway	- Log (P-value)	Affected genes
Atherosclerosis signalling	9.2	CXCL8, APOE, ICAM1, PDGFA, PLA2, G4C, CCR2, F3, LY2, CCL2, ORM1, APOC1, IL1B, ORM2, PDGFD, TNF	Superpathway of cholesterol biosynthesis	10.6	FDPS, PDFT1, EBP, DHCR7, ACAT2, IDI1, HSD17B7, MSMO1, HMGCS1, CYP51A1
Superpathway of cholesterol biosynthesis	8.2	MYD, FDPS, CHCR7, ACAT2, HSD17B7, MSMO1, HMGCS1, CYP51A1	Cholesterol biosynthesis I, II, and III	8.1	FDFT1, EBP, DHCR7, DHCR24, HSD17B7, MSMO1, CYP51A1
LXR/RXR activation	7.4	SCD, APOE, LY2, ORM1, CCL2, APOC1, IL1B, ORM2, CD14, PTGS2, IL1RAP, TNF, CYP51A1	Superpathway of gernanylgeranylphosphate Biosynthesis I	4.4	FDPS, ACAT2, IDI1, FNTB, HMGCS1
Hepatic fibrosis/hepatic stellate cell activation	6.1	CXCL8, APOE, ICAM1, PDGFA, PLA2, G4C, CCR2, F3, LY2, CCL2, ORM1, APOC1, IL1B, ORM2, PDGFD, TNF	LXR/RXR activation	4.4	SCD, FDFT1, LY2, IL1A, LDLR, IL36RN, NR1H3, IL6, CLU, CYP51A1, IL36B, AGT
PPAR signalling	5.8	PPARG, JUN, PPARD, PDGFA, MRAS, IL1B, PTGS2, PDGFD, TNF, IL1RAP	Altered T-cell and B-cell signalling in rheumatoid arthritis	4.3	IL1A, CSF1, IL36RN, TLR6, TLR8, TLR7, IL6, CSF2, IL36B, IL17A
RNA-seq Pat-QKI versus Sib-QKI			RNA-seq Pat-QKI versus Sib-QKI		
Affected canonical pathway	- Log (P-value)	Affected genes	Affected canonical pathway	- Log (P-value)	Affected genes
T-cell receptor signalling	8.9	CD247, PTPN7, CAMK4, PRKCO, CD3E, PLCG1, CD8A, CD3D, CD8B, CD28, CD3G, LCK, TXK, ZAP70, ITK	Granulocyte adhesion and diapedesis	4.9	CXCL8, IL1A, HRH2, MMP7, SDC1, PPBP, ITGA6, RDX, CCL24, CCL17, MMP2, CCL22, C5, FPR1, CCL13, ICAM2, IL1RN, MMP19, ITGA4
CCR5 signalling in macrophages	7.8	CD247, CD3G, CCR5, CAMK4, PRKCO, CCL4, CD3E, PLCG2, PLCG1, CCL3, CD3D, GNG10	Agranulocyte adhesion and diapedesis	4	CXCL8, MMP7, IL1A, PPBP, ITGA6, RDX, CCL24, CCL17, MMP2, CCL22, C5, MYL9, CCL13, ICAM2, IL1RN, PODXL, MMP19, ITGA4
Role of NFAT in regulation of the immune response	7	CD247, CAMK4, PRKCO, CD3E, GCER1A, PLCG1, CD3D, GNG10, CD28, CD3G, LCK, GNAT1, PLCG2, ZAP70, FCGR3A/FCGR3B, FCGR1B, ITK	Toll-like receptor signalling	3	MAP2K6, IL1A, TICAM2, IL1RN, TLR7, MAPK13, TLR3, IRAK2, TRAF1
EIF2 signalling	5.8	RPL24, RPL36A, RPS3A, RPS27, RPL17, RPS18, RPS1Q, RPL39, RPL12, RPL7A, RPL7, RPL9, RPS28, RPL23A, RPL39L, RPSA	Cysteine biosynthesis/homocysteine degradation	2.9	CBS/CBSL, CTH
iCOS-iCOSL signalling in T-helper cells	5.7	CD247, CD3G, CD28, LCK, CAMK4, PRKCO, CD3E, ZAP70, PLCG1, CD3D, ICOSLG/LOC102723996, ITK	Axonal guidance signalling	2.9	SLIT3, ERAP2, MMP7, SLIT1, PDGFA, SEMA6A, BCAR1, TUBB2B, EPHB1, TUBA8, MYSM1, PRKAR1B, GNB1L, WNT5B, ITGA4, SEMA3G, PAK4, ADAM15, TUBA4A, MMP2, KEL, MYL9, FZD4, ADAM12, SEMA4G, SEMA7A, FZD7

IPA, Ingenuity Pathway Analysis; QKI, Quaking.  
The top five affected canonical pathways are shown, along with their respective -log(P-value) and the genes that are affected within the particular pathway. Full IPA output is provided in Supplementary Data 7.



### **QKI facilitates monocyte adhesion and migration.**

Our experimentally determined changes in (pre)-mRNA splicing and expression, as well as bioinformatically predicted changes in biological processes, prompted us to evaluate whether these QKI-induced posttranscriptional modifications could affect monocyte and macrophage function. To test this, we first assessed whether cell survival is affected by a reduction of QKI expression in THP-1 'monocytes'. Importantly, the cumulative population doublings and apoptotic rates were not affected by decreased QKI levels (Fig. 7a,b). Next, we assessed cell adhesion to glass coverslips treated with effector molecules (collagen and activated platelets) in the presence of fluid shear stress, an experimental design that mimics the response of monocytes to endothelial denudation in the vessel<sup>45</sup>. Live-cell imaging clearly showed that the shRNA-mediated depletion of QKI in THP-1 'monocytes' reduced cellular adhesion under flow conditions, as evidenced by their continued rolling along the substrate and inability to firmly attach (Fig. 7c and Supplementary Movies 1 and 2). This firm adhesion of monocytes is aided by the activation of b1-integrins on the cell surface that mediate high-affinity interactions with the extracellular matrix at sites of injury<sup>36</sup>. We tested whether QKI depletion had an impact on b1-integrin function by incubating sh-Cont and sh-QKI THP-1 'monocytes' with an antibody (TS2/16) that forces b1-integrins into the activated, adhesive conformation<sup>37</sup>. Interestingly, the abrogation of QKI did not affect monocyte adhesion properties in this setting (Fig. 7d), indicating that proper integrin expression and functionality is not dependent on QKI. We subsequently tested whether QKI expression levels could have an impact on monocyte migration in vitro by seeding sh-QKI or sh-Cont THP-1 'monocytes' into transwell migration chambers and assessed their ability to migrate towards the chemoattractant formyl-methionyl-leucyl-phenylalanine (fMLP). Indeed, depletion of QKI in monocytes inhibited migration (Fig. 7e). This finding prompted us to similarly assess the capacity of Pat-QKI+/- and Sib-QKI+/+ monocytes freshly isolated from venous blood to migrate to macrophage chemoattractant protein 1, a physiologic recruiter of monocytes at sites of vascular injury. These studies revealed a significant reduction in transwell migration for Pat-QKI+/- monocytes (Fig. 7e), validating our findings in THP-1 'monocytes', and provided evidence that QKI influences monocyte adhesion and migration in inflammatory settings.

### **QKI drives foam cell formation.**

As QKI expression remarkably increased during monocyte-to-macrophage differentiation (Fig. 2c–f) and our aforementioned GO analysis revealed a strong association for changes in QKI expression and lipid metabolism (Fig. 7a), we tested whether a reduction in QKI expression influences the handling of lipids. For this, we first assessed the mRNA expression levels of a subset of established lipid-related genes in monocytes and macrophages derived from WT and qkv mice. As shown in Fig. 8a, monocytes from qkv mice are characterized by significant reductions in NR1H3 (known as LXRa) and PPARG (PPARg) expression, as well as cholesterol uptake (CD36 and LDLR) and efflux (ABCG1) receptors, as compared with WT monocytes. These effects were diminished on conversion to macrophages (Fig. 8a). We subsequently assessed the expression levels of

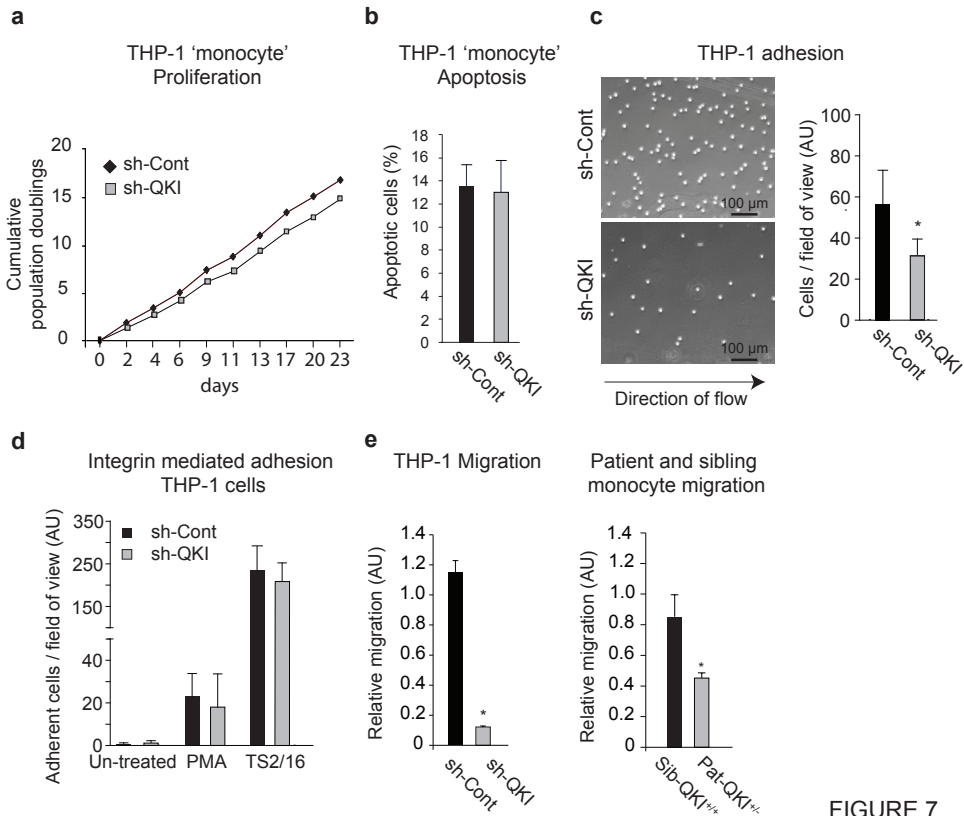


FIGURE 7

**Figure 7 | QKI expression levels have an impact on monocyte adhesion as well as migration and differentiation.** (a) Cumulative population doublings (y axis: CPDs) were counted to assess the effect of QKI reduction on cellular proliferation over time (x axis: days). Population growth curves were compared using linear regression analysis. (b) Quantification of cellular apoptosis, where annexin V+ and propidium iodide+ cells were categorized as apoptotic, as determined by FACS analysis. (c) Quantification of sh-Cont and sh-QKI THP-1 'monocyte' adhesion to collagen matrix pretreated with platelet-rich plasma under flow, mimicking in-vivo endothelial denudation. Direction of flow is indicated below the photomicrographs (n=3). Data expressed as mean $\pm$ s.e.m.; Student's t-test; \*P<0.05. Scale bar, 100  $\mu$ m. (Also see Supplementary Movies 1 and 2). (d) Assessment of integrin-mediated adhesion. Quantification of adhesion to collagen for untreated, PMA- or TS2/16-treated sh-Cont and sh-QKI THP-1 'monocytes' are plotted. TS2/16 is an antibody that turns all  $\beta$ 1-integrins in the high-affinity conformation, inducing cellular adhesion. (e) Quantification of cellular transwell migration towards either fMLP (for THP-1 'monocytes') or macrophage chemoattractant protein 1 (MCP-1; for PB monocytes from either sibling or patient (n4 technical replicates). Data expressed as mean $\pm$ s.e.m.; Student's t-test; \*P<0.05 and \*\*P<0.01.

these lipid metabolism/homeostasis genes in human PB-derived monocytes and macrophages (Fig. 8b and Supplementary Fig. 5). Similar to qkv monocytes, Pat-QKI<sup>+/-</sup> monocytes were characterized by decreased NR1H3 and PPARG expression, as well as LDLR and SCARB1 (Fig. 8b). In contrast to qkv monocytes, ABCG1 expression was potentially increased. Similar to qkv macrophages,

this differential gene expression profile appeared to normalize in Pat-QKI+/- macrophages as compared with Sib-QKI+/+ macrophages (Fig. 8b). Moreover, in primary human macrophages where GapmeR-mediated knockdown of QKI was realized, we observed significant increases in MYLIP/IDOL and ABCG1 expression, whereas CD36 displayed a trend towards decreased expression (Supplementary Fig. 5). Having identified that changes in QKI expression levels had an impact on lipid-associated gene expression, we investigated whether lipid loading affected QKI expression levels. Indeed, treatment with either acetylated low-density lipoprotein (acLDL) or b-very low-density lipoprotein (b-VLDL) led to significant increases in QKI-5 mRNA levels, while QKI-6 and QKI-7 levels also increased, albeit not significantly (Fig. 8c). In contrast to primary monocytes and macrophages, THP-1 'monocytes' did not display significant changes in lipid metabolism gene expression. However, as shown in Fig. 8d, treatment with modified LDL increased expression of cholesterol uptake genes (CD36 and VLDLR), along with significant increases in cholesterol efflux genes (ABCA1 and ABCG1). Taken together, these studies suggested that changes in QKI expression could have an impact on the net balance of genes that control lipid metabolism and homeostasis. Finally, we tested whether these QKI-mediated changes in lipid-associated gene expression could translate into consequences for lipid uptake and foam cell formation, a phenomenon tightly associated with pro-inflammatory macrophage function<sup>7</sup>. As shown in Fig. 8e, the impact of decreased QKI expression on foam cell formation on loading with b-VLDL was clear, as sh-QKI THP-1 'macrophages' displayed less extensive lipid staining as compared with sh-Cont THP-1 'macrophages' (Fig. 8e). Similarly, in Pat-QKI+/- macrophages we observed significantly less lipid staining after b-VLDL treatment (Fig. 8f). Even more striking was the potent decrease in oxidized LDL (oxLDL) loading, an atherosclerosis-relevant antigen, in Pat-QKI+/- macrophages (Fig. 8f). Collectively, these studies strongly suggested that the posttranscriptional processing of (pre-) mRNA transcripts by QKI is essential for the physiologic functioning of monocytes and macrophages in disease settings such as atherosclerosis.

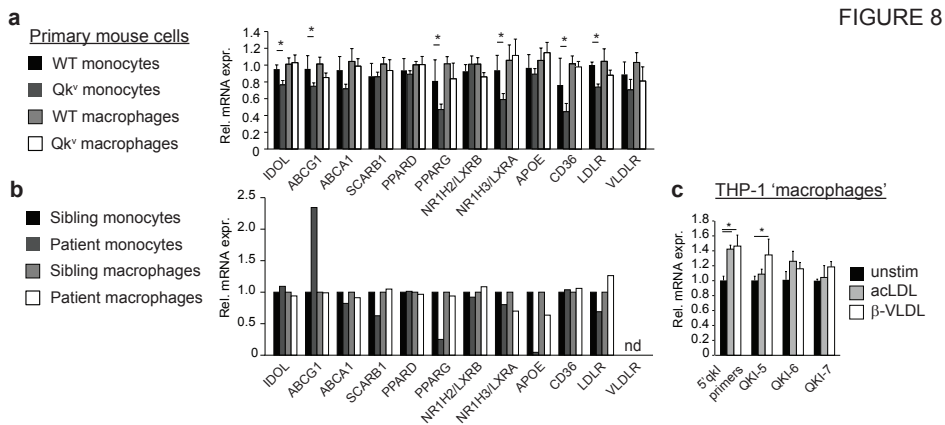
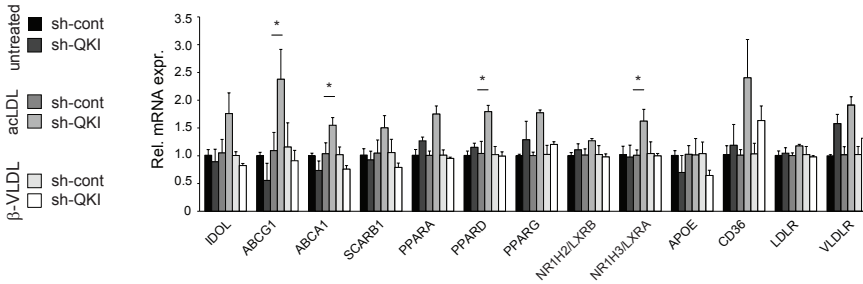
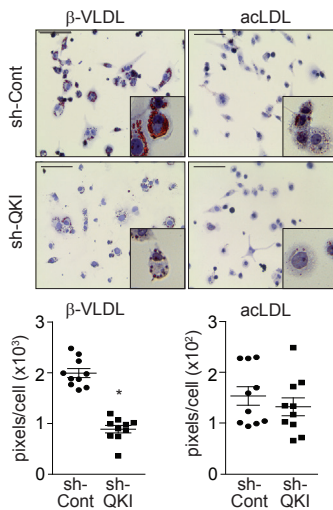


FIGURE 8

**d** THP-1 'macrophages' Figure 8 continued



**e** THP-1 'Macrophages'



**f** Patient and sibling macrophages

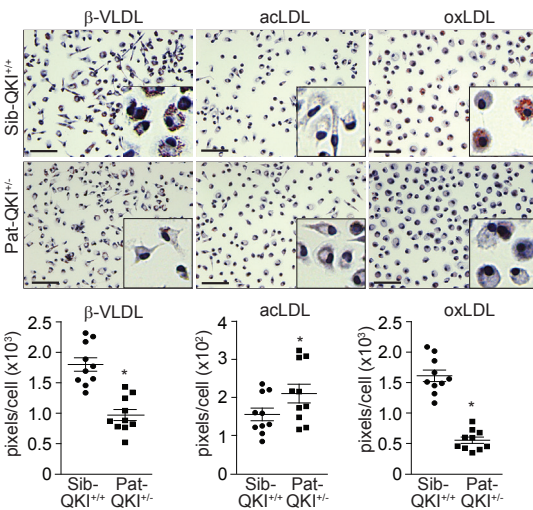


### Figure 8 | QKI regulates the expression of atherosclerosis-related mRNAs and impairs foam cell formation.

(a) Quantitative RT-PCR (qRT-PCR) analysis of established atherosclerosis-related genes in wt of qkv-derived monocytes and macrophages. Gene expression in qkv samples are relative to either WT monocytes or WT macrophages (n=3). Data expressed as mean±s.e.m.; Student's t-test; \*P<0.05, \*\*P<0.01. (b) RNA-seq-derived expression values to illustrate the expression of established atherosclerosis-related genes in sibling or patient monocytes and macrophages. (c) qRT-PCR analysis of QKI isoform mRNA expression in unstimulated THP-1 'macrophages', or treated with β-VLDL or acLDL for 24 h. Data expressed as mean±s.e.m.; one-way analysis of variance (ANOVA), Bonferroni's post-hoc test; \*P<0.05. (d) qRT-PCR analysis of well-known atherosclerosis-related genes in sh-cont or sh-QKI THP-1 'macrophages' that were either left untreated or treated with acLDL or β-VLDL to induce foam cell formation (n/3). Data expressed as mean±s.e.m.; Student's t-test; \*P<0.05 and \*\*P<0.01. (e) Photomicrographs of an Oil-red-O staining to assess β-VLDL, acLDL uptake in either sh-Cont or sh-QKI THP-1 'macrophages'. Scale bar, 100 μm. Inset is a high-magnification image of lipid-droplet accumulation. Data expressed as mean±s.e.m.; Student's t-test; \*\*P<0.01. (f) Photomicrographs of an Oil-red-O staining to assess β-VLDL, acLDL or oxidized LDL (oxLDL) uptake in either Sib-QKI<sup>+/+</sup> (upper panels) or Pat-QKI<sup>+/-</sup> (lower panels) macrophages that were first differentiated for 7 days with GM-CSF. Scale bar, 100 μm. Inset is a high-magnification image of lipid-droplet accumulation. Data expressed as mean±s.e.m.; Student's t-test; \*P<0.05 and \*\*P<0.01.

## Discussion

Genes involved in regulating the transition of monocytes into pro-inflammatory macrophages serve as excellent therapeutic targets for limiting the progression of inflammation-driven diseases such as rheumatoid arthritis and atherosclerosis<sup>3,6</sup>. Our data indicate that alongside wide-ranging changes in gene expression, the differentiation of monocytes to macrophages requires extensive alternative splicing of pre-mRNA species and pinpoint QKI as a novel posttranscriptional regulator of both of these processes (Fig. 9). Expression of the transcription factor PU.1 is associated with the activation of gene expression profiles that drive the differentiation of CD34+ haematopoietic progenitor cells towards a myeloid fate, including monocytes and macrophages<sup>46,47</sup>. Recent work by Pham et al.<sup>48</sup> identified that the binding of PU.1 appears to be enhanced by cooperativity with neighbouring transcription factor binding sites, such as KLF4. Importantly, PU.1 induces the expression of critical monocyte transcription factors, including KLF4<sup>49</sup>. Of note, KLF4 has been demonstrated to bind to the QKI promoter region of VSMCs, which is GC rich<sup>50</sup>. Furthermore, chromatin immunoprecipitation sequencing data derived from HL-60 cells embedded in the UCSC Encode browser revealed two experimentally determined PU.1-binding sites in the QKI promoter<sup>51</sup> (Supplementary Fig. 6). Collectively, these findings suggest that PU.1, potentially in concert with KLF4, could be responsible for driving QKI expression during monocyte-to macrophage differentiation. Our findings also suggest that the abundant expression of QKI mRNAs in naive monocytes could serve to prime these cells with the capacity to rapidly respond to pro-inflammatory triggers at sites of injury. Although we did not assess the translational kinetics of QKI mRNA into protein, our investigation of monocyte activation, adhesion and differentiation strongly suggests that the determination of pre-mRNA fate by QKI critically has an impact on the capacity of the monocyte to aid in response to vascular injury. To date, the genome-wide (alternative) splicing patterns during monocyte-to-macrophage differentiation had not been described. However, the consequences of many splicing events herein described, such as  $\gamma$ -adducin (ADD3), FCGR2B and VLDLR are unknown. However, given that phosphorylation of the g-adducin C terminus triggers dissociation from spectrin and cortical actin loss<sup>52</sup>, it is plausible that the QKI-mediated exclusion of a 13 amino acid coding exon proximal to this region could have an impact on cytoskeletal dynamics in monocytes and macrophages. Furthermore, alternative splicing of exon 6 in FCGR2B could potentially have an impact on the inhibitory role of this protein in monocyte- and macrophage-mediated phagocytosis at sites of vascular injury<sup>53</sup>. Therapeutic strategies tailored to target such splicing events in monocytes could potentially deter their conversion to disease-accelerating macrophages. The expanding repertoire of RNA species have led to the emergence of RNA-based therapeutics as a novel means of treating both rare and common diseases, such as muscular dystrophy and cancer, respectively<sup>54,55</sup>. This is based on extensive efforts geared towards identifying how changes in coding (alternative splicing) and non-coding RNAs (miRNA and longnon- coding RNA) have an impact on cellular pathophysiology<sup>56</sup>. Importantly, the fate of these coding and non-coding

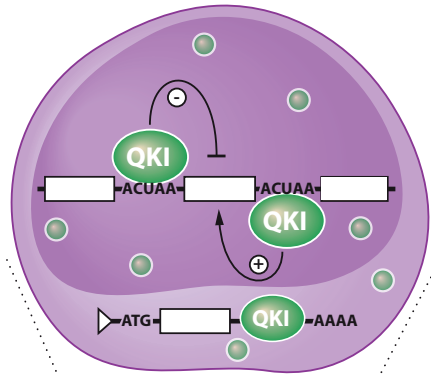
RNAs at the cellular level are determined primarily by the more than 500 RBPs that regulate eukaryotic cell biology<sup>32</sup>. Recently, the RNA motifs to which a significant portion of these RBPs bind has been characterized<sup>32</sup>, enabling the systematic identification of RNA targets for a given RBP within cells, including QKI<sup>29–32</sup>. Our genome-wide evaluation of posttranscriptional events mediated by QKI implicate both direct and indirect posttranscriptional roles for this protein, where the absence of ACUAA motifs or QREs could nonetheless involve QKI, potentially by tethering to other RBPs, or through QKI-mediated changes in the expression of other RBPs<sup>57</sup>. Moreover, in spite of the presence of QREs within target mRNAs, monocytes and macrophages probably express a large variety of RBPs that compete with QKI for access to either identical or similar motifs with varying affinities within a short stretch of RNA nucleotides<sup>19</sup>, which could preclude the observation of a posttranscriptional event. In conclusion, we have identified QKI as a critical posttranscriptional regulator of pre-mRNA splicing and transcript abundance in monocytes and macrophages. We propose that the RBP-induced reprogramming of the posttranscriptional landscape could generate novel targets for the effective attenuation of inflammatory diseases. Note added in proof: After the acceptance of our paper, we were informed by Dehghan et al.<sup>58</sup> of the CHARGE Consortium's identification that single nucleotide polymorphisms proximal to QKI significantly associated with myocardial infarction and coronary heart disease risk.

---

**Figure 9 | Schematic depicting how QKI posttranscriptionally regulates monocyte to macrophage differentiation and atherosclerosis development.** QKI mRNA expression increases in intermediate monocytes, reaching a peak in the non-classical monocyte (middle). Monocytes adhere to the endothelium at sites of tissue injury, leading to their activation and migration into the subendothelial space. This process requires QKI, as the targeted ablation of QKI impaired monocyte adhesion and migration, and the evident transition in cellular phenotype requires extensive reprogramming of the post-transcriptional landscape. On tissue entrance, the monocyte differentiates into a macrophage, a conversion that was associated with a potent increase in QKI protein. This increase potentiates the interaction of QKI with (pre-)mRNA targets, enhancing splicing and target mRNA repression. The loss of QKI in macrophages results in an inability to adopt the macrophage phenotype and a perturbation of lipid uptake and foam cell formation.



### Monocyte Low QKI



### QKI mediated post-transcriptional events:

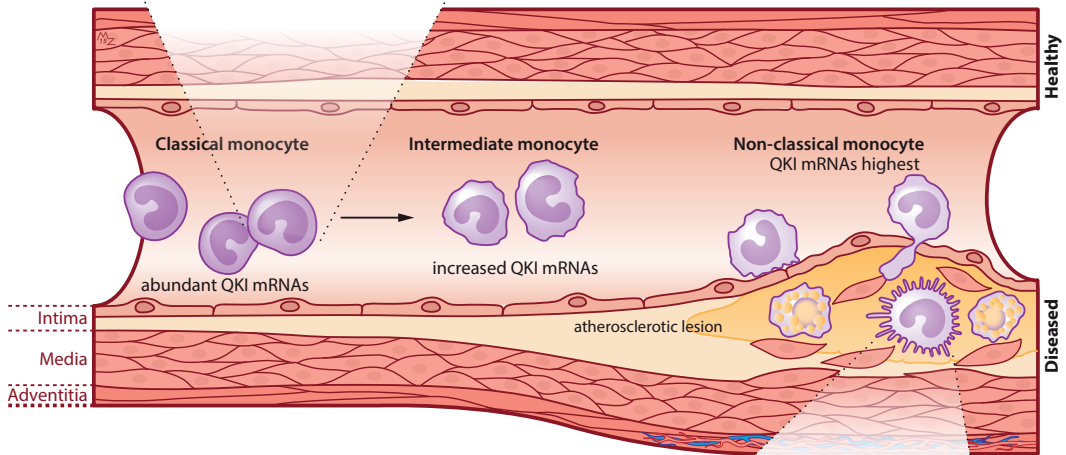
1. Pre-mRNA splicing
2. mRNA stabilization

### Biological processes regulated by QKI:

1. Atherosclerosis signalling
2. Lipid metabolism, (LXR/PPAR) activation
3. Immune response
4. EIF2 signalling, regulation of translation
5. iCOS-iCOSL signalling

### Cellular functions regulated by QKI:

1. Adhesion
2. Migration



### QKI-mediated post-transcriptional events:

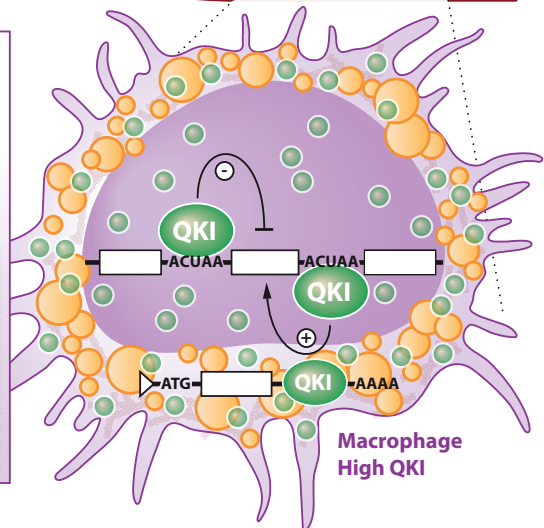
1. pre-mRNA splicing
2. mRNA repression

### Biological processes regulated by QKI:

1. Lipid metabolism (LXR/RXR activation)
2. Leukocyte activation, adhesion, migration
3. Toll-like receptor signalling
4. (Homo-)cysteine biosynthesis and degradation
5. Axonal guidance signalling

### Cellular functions regulated by QKI:

1. Cytoskeletal induced morphology
2. Lipid uptake and foam cell formation



### Supplementary video 1 Control-sh THP-1 adhesion



<http://www.nature.com/article-assets/npg/ncomms/2016/160331/ncomms10846/extref/ncomms10846-s2.avi>

### Supplementary video 2 sh-QKI THP-1 adhesion

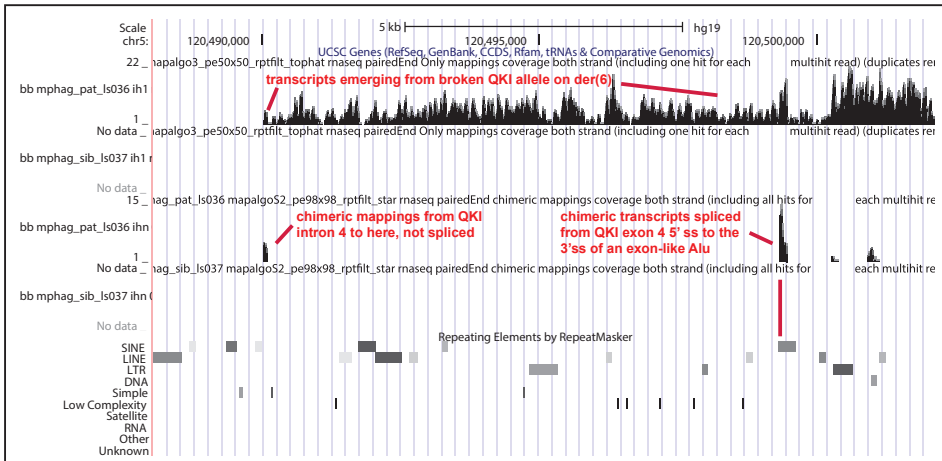


<http://www.nature.com/article-assets/npg/ncomms/2016/160331/ncomms10846/extref/ncomms10846-s3.avi>

**Supplementary videos 1 & 2** | Initial adhesion of sh-Cont or sh-QKI THP-1 'monocytes' in an in vitro cell perfusion system. Glass coverslips were coated with type I collagen, after which the system was perfused with platelet-rich plasma for 10 minutes, leading to the deposition of effector molecules to which the monocyte can adhere. These movies display the perfusion of sh-Cont or sh-QKI THP-1 'monocytes' over this bio-active substrate, leading to their attachment to the surface. Total cellular perfusion time was 5 minutes with a flow rate of 1 dyne cm<sup>-2</sup>. The movie is representative of at least three perfusions.

### Supplementary figure 1

Chimeric reads in chromosome 5

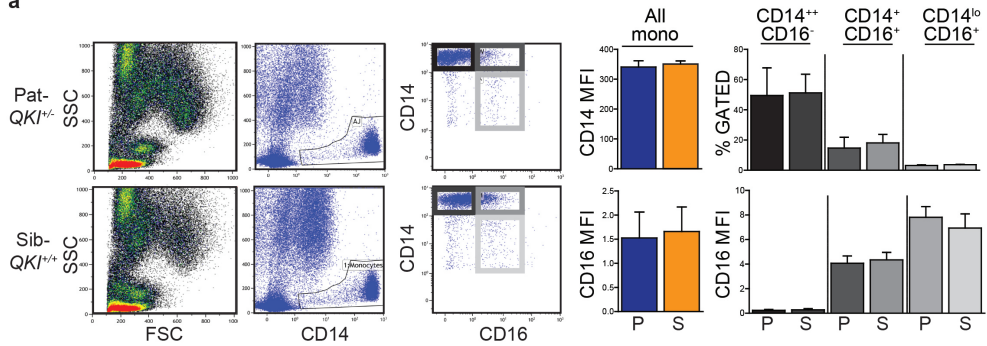


**RNA-seq shows chr6-derived read coverage on chr5.** Genomic location according to UCSC genome browser on chromosome 5. Read coverage is only seen in patient tracks.

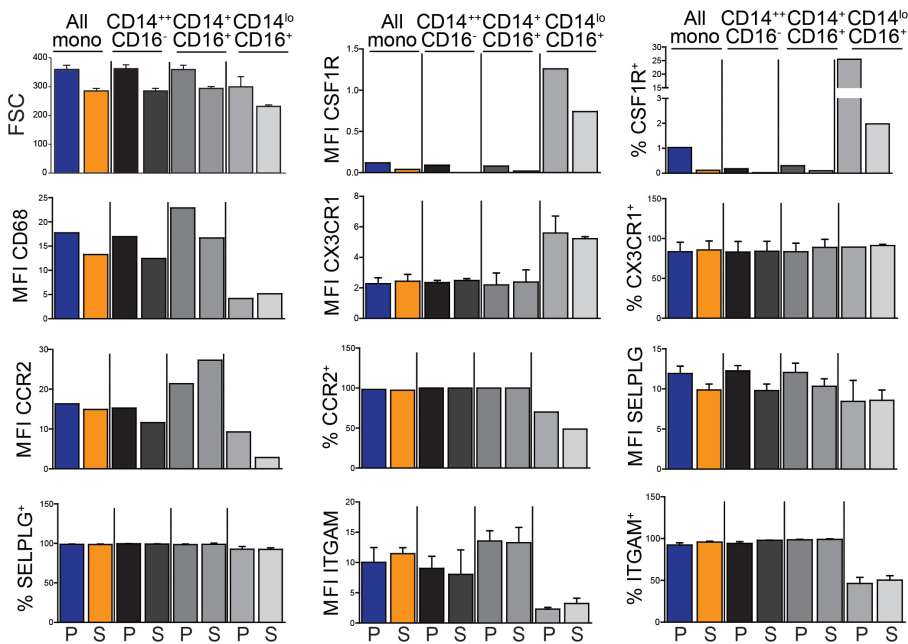


## Supplementary figure 2

a

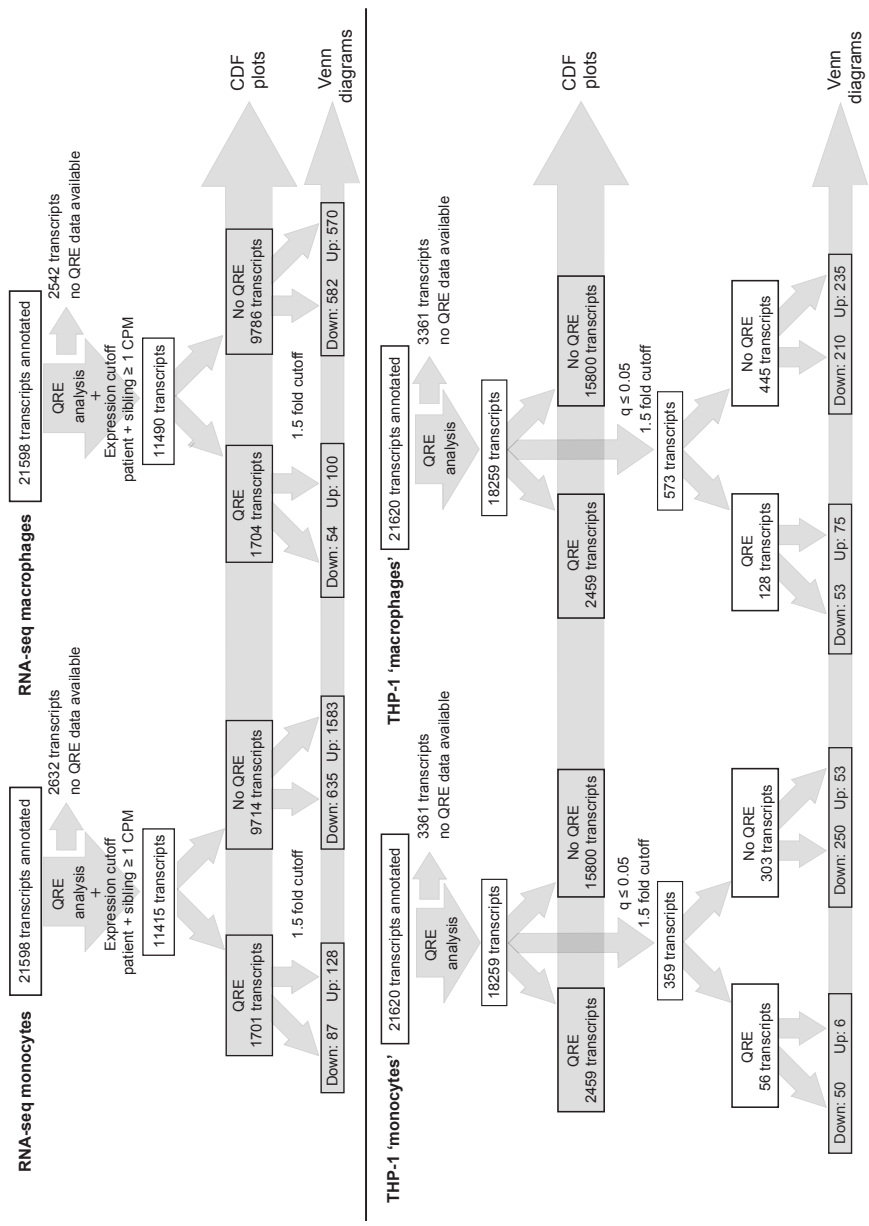


b



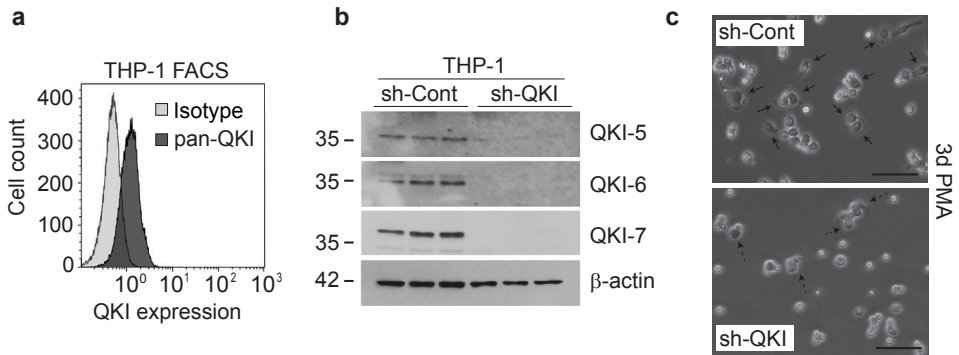
**Supplementary Figure 2: FACS analysis of surface marker expression levels in monocyte subsets in the QKI haploinsufficient patient and her sibling.** **a.** FACS analysis of PB harvested from the QKI haploinsufficient patient (P denotes Pat-QKI<sup>+/-</sup>) as compared with an age- and sex-matched sibling control (S denotes Sib-QKI<sup>+/+</sup>). Live cells were first gated in the FSC/SSC gate, after which monocytes were selected based in CD14/SSC expression. Monocyte subpopulations were defined as CD14<sup>++</sup>/CD16<sup>-</sup>, CD14<sup>+</sup>/CD16<sup>+</sup>, and CD14<sup>lo</sup>/CD16<sup>+</sup>. MFI denotes mean fluorescent index. (n=1 biological replicate; n=7 technical replicates). **b.** Quantitation of average monocyte size in Pat-QKI<sup>+/-</sup> and Sib-QKI<sup>+/+</sup> monocytes based on FSC parameter. All other panels represent quantification of either MFI or percentage of gated monocytes (defined as % gene name<sup>+</sup>) that express the designated surface markers at levels higher than background signal, such as CSF1R. Data are based on biological n=1, while error bars indicate technical replicates for surface markers included in more than one sample in the phenotype characterization panel (minimal n=2).

Supplementary figure 3 - data analysis flow diagram



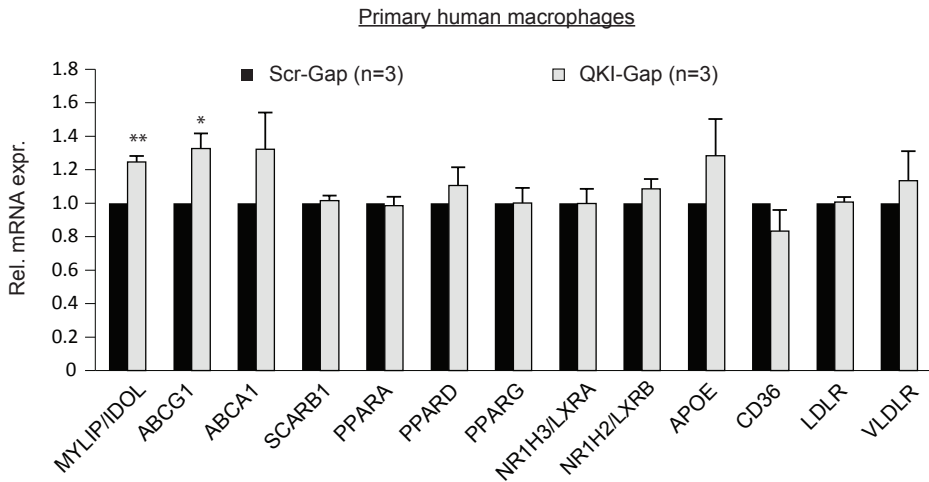
**Supplementary Figure 3 | Schematic representation of transcript stratification.** Flow-diagram illustrating the bioinformatic approach utilized for analysis of RNA-seq data (top) and microarray-based data (bottom). Vertical arrows depict stratification based on the presence or absence of QRE's intrascripts and those achieving expression and/or significance cut-offs. Horizontal arrows indicate transcripts used to generate Venn diagrams (Fig.3g,5e), tables of most up and downregulated genes (Fig. 3h, 5f), scatterplots (Fig. 3i, 5g) and Cumulative Distribution Fraction plots (Fig. 3j, 5h).

## Supplementary figure 4



**Supplementary Figure 4 | QKI protein is differentially expressed during THP-1 monocyte- like to macrophage-like differentiation.** a. Intracellular FACS analysis of THP-1 'monocytes' for total QKI expression. b. Western blot analysis of QKI-5, -6 and -7 expression in cellular lysates harvested from sh-Cont and sh-QKI transduced THP-1 'macrophages' following stimulation with PMA for 3d. c. Phase-contrast photomicrographs of 3 days stimulated THP-1 'macrophages'. Scale bar = 50  $\mu$ m.

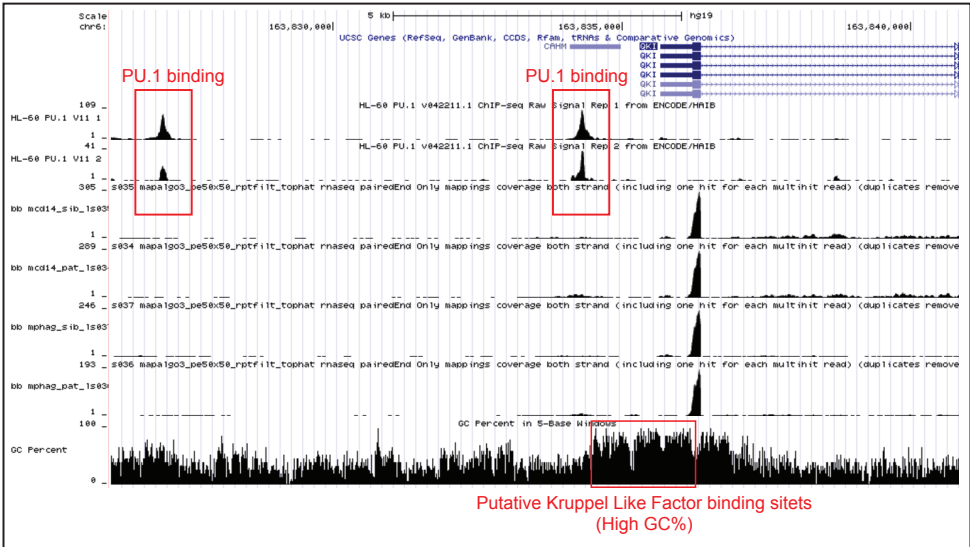
## Supplementary figure 5



**Supplementary Figure 5 | GapmeR-mediated reduction of QKI expression regulates the expression of atherosclerosis-related mRNAs.** qRT-PCR analysis of established atherosclerosis-related genes in QKI-Gap as compared to Scr-Gap treated macrophages. Gene expression in QKI-Gap macrophages are relative to Scr-Gap macrophages (n=3). Data expressed as mean  $\pm$  s.e.m; Student's t-test; \*p<0.05, \*\* p<0.01.

Supplementary figure 6

Transcription factors that bind to the QKI promoter region



**Supplementary Figure 6 | Experimentally determined and putative transcription factor binding sites in the QKI promoter region.** Top tracks: Genomic location and organization according to UCSC genome browser on chromosome 6 mapping to the QKI locus. Tracks 2 and 3 represent the read coverage for two independent chromatin-immunoprecipitations in HL60 cells for PU.1 1, a well-known myeloid transcription factor. Tracks 4,5,6,7 represent read coverage for sibling and patient monocyte and macrophages. Track 8 represents percentage GC in 5 bp windows, indicative of putative Kruppel-Like Factor binding sites.



**Supplementary excel files |** Data on gene expression and splicing events derived from RNA-seq data in monocytes and macrophages and the splicing-microarray in THP-1 'monocytes' and 'macrophages'.

<http://www.nature.com/articles/ncomms10846#supplementary-information>

## Methods

### Human immunohistochemistry studies.

Early lesions are defined as fatty streaks or PIT, whereas advanced plaques consist of both FCA and IPH (fibroatheroma with early-stage or late-stage necrotic core). Scoring of plaque stage, based on characteristics such as thin cap fibroatheroma (vulnerable or ruptured plaques), vascularization, IPH and/or thrombi/fibrin deposits, were scored by a trained pathologist. Paraffin tissue sections from human carotid arteries were deparaffinized and rehydrated. After pre-treatment with TE buffer (pH 9 for QKI-5 and QKI-7) or citrate buffer (pH 6 for QKI 6) for antigen retrieval, sections were incubated overnight at 4°C with primary mouse-anti-human pan-QKI (10 mg ml<sup>-1</sup>, clone N147/6; UC Davis/NIH NeuroMab Facility, Davis, CA, USA), mouse anti-human QKI-5 (10 mg ml<sup>-1</sup>, clone N195A/16; NeuroMab/Antibodies, Inc.); mouse anti-human QKI-6 (10 mg ml<sup>-1</sup> clone N182/17; NeuroMab/Antibodies Inc.) or mouse anti-human QKI-7 (10 mg ml<sup>-1</sup>, clone N183/15; NeuroMab/Antibodies Inc.) diluted in Tris-buffered saline containing 1% BSA and 0.1% Tween 20. Subsequently, sections were washed in Tris-buffered saline and incubated with a secondary biotinylated sheep-anti-mouse antibody (GE Healthcare, Eindhoven, The Netherlands). Next, the sections were incubated with streptavidin ABC-alkaline phosphatase (Vector Laboratories, Peterborough, UK) and colour was developed using the Vector Red staining kit (Vector Laboratories), followed by haematoxylin counterstaining. No primary antibody was used for the negative control. QKI/CD68 co-localization immunostaining was achieved using CD68 (Dako-KP1, DakoCytomation) and pan-QKI antibodies, with CD68 and QKI being counterstained with Vector Blue and Vector Red, respectively. For quantification, slides were analysed in a blinded manner using a Leica DM3000 light microscope (Leica Microsystems) coupled to computerized morphometry (Leica Qwin 3.5.1).

### BM transplantation.

Male LDLR<sup>-/-</sup> mice were housed in sterile filter-top cages and fed a chow diet (Special Diet Services, Witham, Essex, UK). Drinking water was infused with antibiotics (83 mg l<sup>-1</sup> ciprofloxacin and 67 mg l<sup>-1</sup> polymyxin B sulfate) and 6.5 g l<sup>-1</sup> sugar and was provided ad libitum. BM transplantation studies were performed as previously described with minor modifications<sup>59</sup>. Briefly, to induce BM aplasia, 10- to 12-week-old recipient mice were exposed to a single dose of 9 Gy (0.19 Gy min<sup>-1</sup>, 200 kV, 4 mA) total body irradiation, using an Andrex Smart 225 Ro<sup>+</sup>ntgen source (YXLON International, Copenhagen, Denmark) with a 6-mm aluminium filter, 1 day before transplantation. After 24 h, BM cell suspensions were prepared by flushing the femurs of 12-week-old qkv mice or age-matched LM controls (C57/BL6-J background; Jackson Laboratories, Bar Harbor, USA) with PBS, after which 5 × 10<sup>6</sup> cells were injected into the tail vein of recipient mice. After 8 weeks of recovery, the mice were placed on a Western-type diet, containing 0.25% cholesterol and 15% cacao butter (Special Diet Services) for 8 weeks (n=12 per group). Immunohistochemical analysis and quantification of the aortic root using anti-Monocyte and Macrophage-2 (MOMA2) antibody (Sigma-Aldrich)

for MOMA2-positive cell area (expressed as a percentage of total plaque area), VSMC content (smooth muscle  $\alpha$ -actin-positive cells) and collagen (picrosirius red staining) was performed in a blinded manner. Haematologic chimerism of the transplanted LDLR<sup>-/-</sup> mice was validated using the following primers: qk forward primer 5'-TGTGACTTGGGGACTGTCAA-3' ; qk reverse primer 5'-AAAGGGAAAATTTAGCAACAA-3' . BM-derived WT and qkv monocytes were isolated using CD115+ antibody coupled to magnetic beads (Miltenyi Biotech, Leiden, The Netherlands) and differentiated for 7 days to macrophages using mouse recombinant M-CSF (PeproTech, Hamburg, Germany) in RPMI 1640 medium (Gibco, Bleiswijk, The Netherlands) containing 10% FCS (Bodinco, Alkmaar, The Netherlands) and 0.01 mgml<sup>-1</sup> glutamine, 50 units per ml penicillin and 50 mgml<sup>-1</sup> streptomycin.

### **Lentiviral transduction of monocytes.**

Human THP-1 'monocytes' (ATCC, Manassas, VA, USA) were transduced with lentiviral particles encoding either sh-QKI or sh-Cont (catalogue number: SHC202; MISSION library, Sigma-Aldrich). Stable transductants were selected using 3 mgml<sup>-1</sup> puromycin (Sigma-Aldrich) for 72 h.

### **GapmeR design.**

A single-stranded RNA–DNA hybrid antisense oligonucleotide (GapmeR) was designed to target exon 2 of QKI (Eurogentec, Maastricht, The Netherlands), along with a scrambled GapmeR control. Both the GapmeR and scrambled control were 22 nucleotides in length and consisted of RNA (A,C,G,U) and DNA (dA, dC, dG, dT) in a 6-10-6 manner, with a phosphorothioate backbone (\*) and a 6-FAM label on the 50-end. GapmeR sequences were as follows: 50-A\*C\* A\*U\*G\*U\*dC\*dT\*dT\*dT\*dC\*dC\*dG\*dT\* dA\*dC\*U\*C\*U\*G\*C\*U-30 for the QKI-targeting GapmeR and 50-U\*G\*C\*C\*U\*C\* dT\*dC\*dT\*dC\*dG\*dT\*dA\*dC\*dC\*dG\*U\*A\*U\*U\*U\*A-30 for the scrambled control.

### **Monocyte subpopulation analysis.**

Human monocytes were derived from healthy donor buffy coats (Ethical Approval Number BTL 10.090) following Ficoll density gradient centrifugation and isolated from the PB mononuclear cell fraction using a negative selection cocktail to isolate unlabelled monocytes (StemCell Technologies, Grenoble, France). Purified monocytes were subsequently incubated with 1 mgml<sup>-1</sup> CD14-FITC and 1 mgml<sup>-1</sup> CD16-Pc5 (Beckman Coulter, Woerden, The Netherlands) for 30 min at 4°C and FACS sorted using a FACSCalibur (BD Biosciences, Breda, The Netherlands). RNA was isolated from the subpopulations using Trizol reagent (Thermo Fisher Scientific, Bleiswijk, The Netherlands).

### **Monocyte and macrophage culture.**

Human monocytes were isolated from buffy coats of healthy donors with an antibody to CD14, conjugated to magnetic beads to allow for MACS sorting (Miltenyi Biotech). Cells were cultured in RPMI media supplemented with 10% FCS and 0.01 mgml<sup>-1</sup> glutamine at 37°C and 5% CO<sub>2</sub>. Differentiation of primary

CD14<sup>+</sup> monocytes to pro-inflammatory macrophages was achieved by stimulating with 5 ngml<sup>-1</sup> GM-CSF (Thermo Fisher Scientific) or 5ngml<sup>-1</sup> M-CSF (Milenyi Biotech). Human THP-1 'monocytes' were cultured in RPMI media supplemented with 10% FCS and 0.01 mgml<sup>-1</sup> glutamine at 37C and 5% CO<sub>2</sub>, with differentiation into macrophages being induced by treating with 100nM PMA<sup>60</sup>. TS/216 for integrin activation experiments was kindly provided by Dr Arnoud Sonneberg, Netherlands Cancer Institute, Amsterdam, The Netherlands. Foam-cell formation was assessed by treating sh-Cont and sh-QKI THP-1 'macrophages' or Sib-QKI<sup>+/+</sup> and Pat-QKI<sup>+/-</sup> macrophages for 24 h with either 25 mgml<sup>-1</sup> b-VLDL or 50 mgml<sup>-1</sup> acLDL, or 10 mgml<sup>-1</sup> oxLDL, after which the cells were fixed with 10% Formafix, and Oil-Red-O stained and haematoxylin counterstained. Oil-Red-O area per field of view was divided by the number of cells using ImageJ software.

### **In vitro perfusion assay.**

Glass coverslips were coated with type I collagen, after which the system was perfused with platelet-rich plasma for 10 min. Next, the system was flushed with flow buffer (20 mmol l<sup>-1</sup> HEPES, 132 mmol l<sup>-1</sup> NaCl, 6 mmol l<sup>-1</sup> KCl, 1 mmol l<sup>-1</sup> MgSO<sub>4</sub>, 1.2 mmol l<sup>-1</sup> KH<sub>2</sub>PO<sub>4</sub>, 5 mmol l<sup>-1</sup> glucose, 1.0 mmol l<sup>-1</sup> CaCl<sub>2</sub> and 0.5% BSA) for 2min. Sh-Cont and sh-QKI THP-1 were resuspended in flow buffer at a concentration of 4x10<sup>6</sup> ml<sup>-1</sup>, after which the cells were perfused over the substrate for 5min at 1 dyne cm<sup>-2</sup>. Cellular adhesion was tracked visually using a Leica DMI5000 microscope. The flow rate was subsequently increased to 2 dynes cm<sup>2</sup> for 2min, followed by the visual assessment of firm adhesion of perfused monocytes for a duration of 3 min, after which photomicrographs of ten random fields of view in the fluidic chamber were taken and quantified.

### **Cellular migration assays.**

Transwell cellular migration studies of sh-Cont and sh-QKI THP-1 'monocytes' towards 1 nM N-formyl-methionyl-leucyl-phenylalanine (fMLP, Sigma-Aldrich) or 10 ng ml<sup>-1</sup> macrophage chemoattractant protein 1 (R&D Systems, Abingdon, UK) for human primary monocytes were performed as previously described<sup>61</sup>. Briefly, cell migration was assessed using Corning Transwell polycarbonate membrane cell culture inserts (6.5mm transwell with 5.0 mm pore size, Sigma). The lower chamber was loaded with RPMI containing 0.25% BSA and desired chemoattractant. Wells containing no chemoattractant were used as negative controls. Cells were loaded in the upper chamber of the transwell inserts (105 cells) and incubated overnight at 37C. The following day, cell migration (adherent cells) was quantified by manual counting or ImageJ.

### **Gene expression microarrays.**

RNA was isolated from unstimulated sh-Cont and sh-QKI THP-1 'monocytes' (day 0), and from sh-Cont and sh-QKI THP-1 cells stimulated with 100nM PMA for 3 days using Trizol (Thermo Fisher Scientific) and the RNeasy Mini Kit (Qiagen, Heidelberg, Germany) according to the manufacturer's instructions. RNA quantity and quality was measured using a NanoDrop spectrophotometer (Nanodrop Technologies, Wesington, USA) and an Agilent 2100 bioanalyser



(Agilent Technologies, Santa Clara, USA). Samples meeting a RNA integrity number criteria of >8 were used for further analysis.

### Splicing microarrays.

Microarray data is deposited in GEO under the accession number GSE74887. Targets were prepared from three replicate cultures for each sample. Complementary DNA synthesis and amplification was performed using the WT Expression Kit (Ambion, Bleiswijk, The Netherlands). Samples were enzymatically fragmented and biotinylated using the WT Terminal Labeling Kit (Affymetrix, Santa Clara, California, USA). Labelled target was hybridized to the HJAY Chip (Affymetrix 540091). Chips were washed and scanned using the Fluidics Station 450 and Affymetrix Gene ChIP Scanner 3000 7G (Affymetrix). Data were analysed as previously described<sup>62</sup>. Briefly, in the absence of mismatch probes on these microarrays, probe intensities were first used to construct an empirical CDF, which was subsequently used to calculate an empirical P-value that a particular probe's intensity arose from the background of all probes. Probes were stratified for GC content (thermodynamically favourable GC base pairing). For each probe set, the median P-value of the set of individual probes in the probe set was used as the P-value for that probe set. Before assessing for alternatively spliced transcripts from a particular locus, we first determined whether the gene was expressed. Next, if the expression criteria was met, we determined whether RNA containing two or more alternative splice junctions was detectable using the isoform-specific probes. In situations where the probe sets for two or more alternative isoforms were 'present' in any sample of the data, an alternative splicing event was scored. For these events, the junction probe sets that hybridized to individual isoforms were identified and the probes they contained were used for the Kruskal–Wallis test. Next, we normalized individual probe intensities and grouped the replicate values. Subsequently, using R software, the `kruskal.test` function was used to test the hypothesis that the probe intensities come from identical populations. If the resulting P-value was small enough, the null hypothesis was rejected and the alternative hypothesis that the probes were differentially expressed was accepted. To determine an appropriate value for the 0.01 significance level, 12,740 Kruskal–Wallis tests on randomly selected probe sets were performed, yielding an a-value that associated with the 1% quantile of randomly selected probes ( $1.975486 \times 10^3$ ). To account for multiple testing, a Bonferroni-corrected a-value of  $1.975486 \times 10^3 / 1.2740 \times 10^4 = 1.550617 \times 10^7$  was used as a P-value cutoff for significance. The Sepscore is  $\log_2$  (Include/Skip ratio) of the experimental sample over the reference sample. Exon inclusion generates a positive Sepscore, whereas exon exclusion generates a negative Sepscore.

### Word (5-mer) enrichment and positional mapping.

Counts of all 5-mers (ACUAA) in the selected region of an exon set are compared with their counts from a background set of sequences using Fisher's exact test, with multiple testing correction. For motif mapping, we plotted the frequency of specific motifs in 50- nucleotide windows slid along the intron sequences upstream



and downstream of each selected exon set with 5-nucleotide sampling intervals. At each interval, we computed the average number of motifs in exons activated or repressed in shRNA-treated cells, and background exons in the same experiment with no splicing change. For the background set, we empirically estimated the 95% confidence interval of motif frequency (error bars). For peaks of consecutive points outside the 95% interval, we applied the Mann–Whitney–Wilcoxon test to estimate a P-value that the motif frequency at each point within the peak is greater than background. As the points were not independent, we estimated a q-value for each peak by finding the most significant P-value for any point in the peak and applying Bonferroni correction for the number of points within the peak. A second Bonferroni correction controlled for the number of possible positions at which a peak might occur, yielding the final q-values. To explain further; the effect of QKI depletion on every assessed exon was calculated from the RNA-seq or the splicing-sensitive microarray: that is, whether a reduction in QKI causes inclusion or exclusion from the final mature mRNA transcript. Next, the intronic regions around differentially spliced exons were analysed for the presence of ACUAA motifs (5-mers). By doing this for every alternatively spliced exon, we could detect an enrichment of ACUAA motifs in the upstream introns of the exons that were included in a ‘QKI-deficient’ cell: QKI is not binding upstream; thus, the exon is included, as measured by RNA-seq or splicing-sensitive microarray. In contrast, we could detect an enrichment of ACUAA motifs in the downstream introns of the exons that are included on QKI reduction. QKI binding in the downstream intron would normally give inclusion, but now QKI cannot bind downstream; thus, exclusion is now favoured as assessed by the RNA-seq or splicing-sensitive microarray.

### **RNA-seq library preparation.**

RNA-seq data are deposited in GEO under the accession number GSE74979. For each sample, the non-ribosomal fraction of 3 mg of total RNA was isolated using a Ribo-Zero rRNA removal Kit (Epicentre, Madison, Wisconsin, USA). Ribo-Zero-treated RNAs were used to generate barcoded cDNA libraries using the TruSeq RNA Sample Preparation kit (Illumina), with the following additions. Size selections were performed before and after cDNA amplification on an E-gel Safe Imager (Invitrogen) using 2% E-gel SizeSelect gels (Invitrogen). The cDNA fraction of 300 bp in size (including adapters) was isolated and purified. Indexed libraries were pooled and sequenced (paired-end 50 or 100 bp reads) on the Illumina HiSEQ platform to a depth of 41–70 million reads per sample (QB3 Vincent J. Coates Genomics Sequencing Laboratory). After removal of PCR duplicates and repeats, there were 21–26 million uniquely mapping paired-end reads (37–61%).

### **Mapping and analysis of RNA-seq data.**

All samples were mapped using Tophat2<sup>63,64</sup> with Bowtie2<sup>64</sup> as the underlying alignment tool. The input Illumina fastq files consisted of paired-end reads with each end containing 100 bp (except for 2 samples with 50 bp of paired-end reads). For equivalency, 100-bp reads were trimmed to 50 bp before mapping.

The target genome assembly for the human samples was GRCh37/UCSC-hg19 and Tophat was additionally supplied with a gene model (using its '-GTF' parameter) with data from the hg19 UCSC KnownGenes track<sup>65</sup>. For multiple-mapped fragments, only the highest scoring mapping determined by Bowtie2 was kept. Only mappings with both read ends aligned were kept. Potential PCR duplicates (mappings of more than one fragment with identical positions for both read ends) were removed with the samtools 'rmdup'<sup>66</sup> function, keeping only one of any potential duplicates. The final set of mapped paired-end reads for a sample were converted to position-by-position coverage of the relevant genome assembly using the bedtools 'genomeCoverageBed' function<sup>67</sup>. To determine the count of fragments mapping to a gene, the position-by-position coverage was summed over the exonic positions of the gene. This gene total coverage was divided by a factor of 100, to account for the 100-bp of coverage induced by each mapped paired-end fragment (50 bp from each end) and rounded to an integer. This was calculated for each gene in the UCSC Known Gene set. For input to DESeq<sup>68</sup>, all genes with non-zero counts in any sample were considered. Two replicates of each sample were combined per the DESeq methodology. SpliceTrap<sup>69</sup> was used to analyse splicing changes with the parameters j15, ch0.1, ir0.1 and IRMyes. For mapping of reads that are chimeric to the reference genome<sup>70</sup>, to identify the translocation breakpoint on chr6 we used STAR-Fusion <https://github.com/STAR-Fusion/>. Non-splice junction reads from the macrophage samples that mapped from the QKI gene on chr6 to any location on chr5 were inspected and several were found, which mapped from QKI intron 4 to a site that is strongly transcribed from chr5 in the patient but not at all in her sibling.

### Genome-wide computational analysis for RNA motifs.

Human mature mRNA sequences were downloaded from UCSC RefSeq database (hg19). Computational screening was performed for the QRE motif, UACUAAY N1-20 UAAY, and counts calculated for the longest annotated transcript. After cross-referencing these transcripts with either the transcripts annotated on the microarray or the RNA-seq, we annotated the number of QREs in the Supplementary Data. Transcripts of which we were unable to assess whether they contain one or more QREs, we annotated as NA and these were excluded from analysis to generate the CDF plots in Figs 3j and 5h. To generate the Venn diagrams and scatterplots for the RNA-seq of monocytes and macrophages (Fig. 3g,i), a  $\pm 1.5$ -fold change cutoff was applied together with a minimal expression cutoff of patient+sibling Z1 CPM, to avoid artificially large fold changes due to very low expression values. To generate the Venn diagrams and scatterplots for the THP-1-derived expression data (Fig. 5e, g), we applied a  $\pm 1.5$ -fold change cutoff and applied a DESeq-derived q-value cutoff of  $q < 0.05$ .

### MISO analysis.

Mixture of isoforms (MISO) analysis was used to assess, quantify and visualize alternative transcripts based on RNA-seq data. Sequences obtained from RNA-seq were aligned using TopHat2 to the human genome v19 transcriptome (annotation-set kindly provided by Dr Christopher Burge, MIT, Cambridge,

USA). Using the alignment files (BAM files), MISO analyses was performed on our RNA-seq paired-end sequencing data to identify alternative splicing events, as previously described<sup>71</sup>. Second, an annotation set containing only exons surrounding the splicing event were included in the analysis to generate a more in-depth analysis of select splicing events. A pairwise comparison was performed using the sibling and patient monocyte and macrophage on both the full and selected annotation sets. Additional visualization was performed using the sashimi plot subpackage from MISO, while modifications in the plotting procedure were made to allow visualization of supplementary annotation tracks including ACTAA and QKI PAR-CLIP sites, along with RefSeq transcripts that define the event at (<https://github.com/wyleung/rnaveer>).

### **Western blot analysis.**

Polyacrylamide gel electrophoresis was used to resolve proteins from cellular lysates harvested in RIPA buffer. Protein determinations (BCA) were performed to ensure equal loading of protein on a per-sample basis. QKI-5, -6 and -7 were detected using primary mouse monoclonal antibodies that target pan-QKI (1:1,000, N73/168; UC Davis/NIH NeuroMab Facility), QKI-5 (1:1,000, N195A/16; UC Davis/NIH NeuroMab Facility), QKI-6 (1:1,000, N182/17; UC Davis/NIH NeuroMab Facility) or QKI-7 (1:1,000, N183/15.1; UC Davis/NIH NeuroMab Facility), or polyclonal antibodies targeting QKI-5 (1:1,000, AB9904; Millipore, Amsterdam, The Netherlands), QKI-6 (1:2,000, AB9906; Millipore) and QKI-7 (1:2,000, AB9908; Millipore). For loading references, rabbit polyclonal antibodies were used to detect b-actin or Histone H3 (both 1:4,000; Abcam, Cambridge, UK). All gels were run and blotted with Bio-Rad TGX pre-cast gels and blotted on nitrocellulose 0.2 mm using the Bio-Rad TurboBlot system (Bio-Rad Laboratories). Full blots are shown in Supplementary Fig. 7.

### **Quantification of pre-mRNA expression levels by PCR.**

RNA was harvested from monocytes and macrophages using Trizol reagent (Thermo Fisher Scientific). Standard mouse and human cDNA was made using oligo-dT primers (Invitrogen), whereas cDNA for alternative splicing studies was synthesized using random primers (Invitrogen). Primer sets designed for specific pre-mRNA amplification by quantitative RT-PCR analysis are provided in Supplementary Table 1. Quantitative RT-PCR analysis for designated mRNA products was performed using SYBR Green master mix (Bio-Rad, Veenendaal, The Netherlands). For optimal resolution of pre-mRNA splicing patterns, samples were run on an Agilent 2100 bioanalyser (Agilent), with full images provided in Supplementary Figs 8–10.

### **Statistics.**

For all experiments, N defined the number of biological replicates. All in vitro and in vivo results were analysed using GraphPad software with either a Student's t-test or analysis of variance (with a Bonferonni post-test being used). All results are expressed as mean±s.e.m. Differences in P-values <0.05 or <0.01 were considered significant and indicated as follows: \*P<0.05 or \*\*P<0.01, respectively.

## **Ethics.**

Informed consent was obtained for all patient-derived samples. Approval for these studies was provided by the relevant medical ethics committees, namely Maastricht University Medical Center, The Netherlands (Professor Dr E.A.L. Biessen), for immunohistochemical studies, and Leuven University Hospital, Belgium (Professor Dr H. Van Esch), for the QKI haploinsufficient and control materials. All mouse experiments were approved by the regulatory authorities of the Leiden University and were in compliance with the Dutch Government Guidelines.

## **Acknowledgements**

For the studies described in this manuscript, we greatly appreciate the participation and cooperation of the QKI haploinsufficient patient and her family members. R.G.d.B. and E.P.v.d.V. were supported by Netherlands Institute for Regenerative Medicine research grants (Grant No. FES0908). This research was also made possible by a private research endowment to E.P.v.d.V. L.S., S.K., J.P.D. and M.A.J. were supported by US National Institutes of Health grant GM040478 and W.S.F. was supported by training grants CIRM TG2-01157 and NIH T32 GM008646. H.K. was supported by European Union Marie Curie CIG grant (PTRCODE) and TUBITAK grant (113E159). We also gratefully acknowledge Dr Christopher Burge and his laboratory at the Massachusetts Institute of Technology, for assistance with the generation of sashimi plots from our RNA-seq data. In addition, we acknowledge Dr Arnoud Sonneberg at the Netherlands Cancer Institute for the in-depth discussions and integrin antibodies.

## **Author contributions**

R.G.d.B., M.A.J., A.J.v.Z. and E.P.v.d.V. conceived the ideas and experiments within the study. R.G.d.B. and E.P.v.d.V. performed the majority of the experiments detailed in the study. L.S., S.K. and J.P.D. performed the RNA-Seq and splicing-sensitive microarray studies, and analysed the data. J.P., H.C.d.B., A.S., J.M.v.G., J.M.G.J.D., A.O.K., P.H.J.v.d.Z., R.S., C.M.A.v.A, and I.B. assisted with experiments and analyses. R.G.d.B., L.S., S.B., W.Y.L., S.M.K., J.P.D. and H.K. provided bioinformatics and statistical assistance. H.V.E. provided access to the QKI haploinsufficient patient and sibling. R.G.d.B., A.J.v.Z. and E.P.v.d.V. wrote and edited the manuscript, and prepared the figures. J.M.v.G., W.S.F., C.v.K., J.W.J., H.V.E., T.J.R., E.A.L.B., M.A.J. and A.J.v.Z. provided critical experimental commentary, discussion and assistance with manuscript preparation and editing. T.J.R., E.A.L.B., M.A.J., A.J.v.Z. and E.P.v.d.V. provided funding for the studies.

**Additional information Accession code:**

RNA sequencing and microarray data were deposited in NCBI's Gene Expression Omnibus (GEO) under accession codes GSE74979 (for RNA-seq data) and GSE74887 (for the splicing-sensitive microarray data). Supplementary Information accompanies this paper at <http://www.nature.com/naturecommunications>  
Competing financial interests: The authors declare no competing financial interests. Reprints and permission information is available online at <http://npg.nature.com/reprintsandpermissions>

## References

1. Auffray, C., Sieweke, M. H. & Geissmann, F. Blood monocytes: development, heterogeneity, and relationship with dendritic cells. *Annu. Rev. Immunol.* 27, 669–692 (2009).
2. Ziegler-Heitbrock, L. et al. Nomenclature of monocytes and dendritic cells in blood. *Blood* 116, e74–e80 (2010).
3. van Zonneveld, A. J., de Boer, H. C., van der Veer, E. P. & Rabelink, T. J. Inflammation, vascular injury and repair in rheumatoid arthritis. *Ann. Rheum. Dis.* 69(Suppl 1): i57–i60 (2010).
4. Schwarzmaier, D., Foell, D., Weinhage, T., Varga, G. & Dabritz, J. Peripheral monocyte functions and activation in patients with quiescent Crohn's disease. *PLoS ONE.* 8, e62761 (2013).
5. Libby, P., Nahrendorf, M., Pittet, M. J. & Swirski, F. K. Diversity of denizens of the atherosclerotic plaque: not all monocytes are created equal. *Circulation* 117, 3168–3170 (2008).
6. Ross, R. Atherosclerosis—an inflammatory disease. *N. Engl. J. Med.* 340, 115–126 (1999).
7. Hilgendorf, I., Swirski, F. K. & Robbins, C. S. Monocyte fate in atherosclerosis. *Arterioscler. Thromb. Vasc. Biol.* 35, 272–279 (2015).
8. Zhang, D. E., Hetherington, C. J., Chen, H. M. & Tenen, D. G. The macrophage transcription factor PU.1 directs tissue-specific expression of the macrophage colony-stimulating factor receptor. *Mol. Cell Biol.* 14, 373–381 (1994).
9. Coccia, E. M. et al. STAT1 activation during monocyte to macrophage maturation: role of adhesion molecules. *Int. Immunol.* 11, 1075–1083 δ1999b:
10. Williams, S. C. et al. C/EBPε is a myeloid-specific activator of cytokine, chemokine, and macrophage-colony-stimulating factor receptor genes. *J. Biol. Chem.* 273, 13493–13501 (1998).
11. Martinez, F. O., Gordon, S., Locati, M. & Mantovani, A. Transcriptional profiling of the human monocyte-to-macrophage differentiation and polarization: new molecules and patterns of gene expression. *J. Immunol.* 177, 7303–7311 (2006).
12. Martinez, F. O. The transcriptome of human monocyte subsets begins to emerge. *J. Biol.* 8, 99 (2009).
13. Lu, J. Y., Sadri, N. & Schneider, R. J. Endotoxic shock in AUF1 knockout mice mediated by failure to degrade proinflammatory cytokine mRNAs. *Genes Dev.* 20, 3174–3184 (2006).
14. Lu, Y. C. et al. ELAVL1 modulates transcriptome-wide miRNA binding in murine macrophages. *Cell Rep.* 9, 2330–2343 (2014).
15. Eigsti, R. L., Sudan, B., Wilson, M. E. & Graff, J. W. Regulation of activation-associated microRNA accumulation rates during monocyte-to-macrophage differentiation. *J. Biol. Chem.* 289, 28433–28447 (2014).
16. Lin, H. S. et al. miR-199a-5p inhibits monocyte/macrophage differentiation by targeting the activin A type 1B receptor gene and finally reducing C/EBPα expression. *J. Leukoc. Biol.* 96, 1023–1035 (2014).
17. Kafasla, P., Karakasiliotis, I. & Kontoyiannis, D. L. Decoding the functions of post-transcriptional regulators in the determination of inflammatory states: focus on macrophage activation. *Wiley. Interdiscip. Rev. Syst. Biol. Med.* 4, 509–523 (2012).
18. Chenard, C. A. & Richard, S. New implications for the QUAKING RNA binding protein in

- human disease. *J. Neurosci. Res.* 86, 233–242 (2008).
19. Fu, X. D. & Ares, Jr. M. Context-dependent control of alternative splicing by RNA-binding proteins. *Nat. Rev. Genet.* 15, 689–701 (2014). ARTICLE NATURE COMMUNICATIONS | DOI: 10.1038/ncomms10846 18 NATURE COMMUNICATIONS | 7:10846 | DOI: 10.1038/ncomms10846 | www.nature.com/naturecommunications
  20. Kafasla, P., Skliris, A. & Kontoyiannis, D. L. Post-transcriptional coordination of immunological responses by RNA-binding proteins. *Nat. Immunol.* 15, 492–502 (2014).
  21. Mukherjee, N., Lager, P. J., Friedersdorf, M. B., Thompson, M. A. & Keene, J. D. Coordinated posttranscriptional mRNA population dynamics during T-cell activation. *Mol. Syst. Biol.* 5, 288 (2009).
  22. Turner, M. & Hodson, D. J. An emerging role of RNA-binding proteins as multifunctional regulators of lymphocyte development and function. *Adv. Immunol.* 115, 161–185 (2012).
  23. van der Veer, E. P. et al. Quaking, an RNA-binding protein, is a critical regulator of vascular smooth muscle cell phenotype. *Circ. Res.* 113, 1065–1075 (2013).
  24. Hardy, R. J. et al. Neural cell type-specific expression of QKI proteins is altered in quaking viable mutant mice. *J. Neurosci.* 16, 7941–7949 (1996).
  25. Kondo, T. et al. Genomic organization and expression analysis of the mouse qki locus. *Mamm. Genome* 10, 662–669 (1999).
  26. Pilotte, J., Larocque, D. & Richard, S. Nuclear translocation controlled by alternatively spliced isoforms inactivates the QUAKING apoptotic inducer. *Genes Dev.* 15, 845–858 (2001).
  27. Zorn, A. M. et al. Remarkable sequence conservation of transcripts encoding amphibian and mammalian homologues of quaking, a KH domain RNA-binding protein. *Gene* 188, 199–206 (1997).
  28. Chen, T., Damaj, B. B., Herrera, C., Lasko, P. & Richard, S. Self-association of the single-KH-domain family members Sam68, GRP33, GLD-1, and Qk1: role of the KH domain. *Mol. Cell Biol.* 17, 5707–5718 (1997).
  29. Corcoran, D. L. et al. PARalyzer: definition of RNA binding sites from PAR-CLIP short-read sequence data. *Genome Biol.* 12, R79 (2011).
  30. Galanteau, A. & Richard, S. Target RNA motif and target mRNAs of the Quaking STAR protein. *Nat. Struct. Mol. Biol.* 12, 691–698 (2005).
  31. Hafner, M. et al. Transcriptome-wide identification of RNA-binding protein and microRNA target sites by PAR-CLIP. *Cell* 141, 129–141 (2010).
  32. Ray, D. et al. A compendium of RNA-binding motifs for decoding gene regulation. *Nature* 499, 172–177 (2013).
  33. Teplova, M. et al. Structure-function studies of STAR family Quaking proteins bound to their in vivo RNA target sites. *Genes Dev.* 27, 928–940 (2013).
  34. Jiang, L., Saetre, P., Jazin, E. & Carlstrom, E. L. Haloperidol changes mRNA expression of a QKI splice variant in human astrocytoma cells. *BMC Pharmacol.* 9, 6 (2009).
  35. Saetre, P. et al. Inflammation-related genes up-regulated in schizophrenia brains. *BMC Psychiatry* 7, 46 (2007).
  36. Brosseau, J. P. et al. Tumor microenvironment-associated modifications of alternative splicing. *RNA* 20, 189–201 (2014).
  37. Sidman, R. L., Dickie, M. M. & Appel, S. H. Mutant mice (Quaking and Jimpy) with deficient myelination in the central nervous system. *Science* 144, 309–311 (1964).
  38. Backx, L. et al. Haploinsufficiency of the gene Quaking (QKI) is associated with the 6q



- terminal deletion syndrome. *Am. J. Med. Genet. A* 152A, 319–326 (2010).
39. Hall, M. P. et al. Quaking and PTB control overlapping splicing regulatory networks during muscle cell differentiation. *RNA* 19, 627–638 (2013).
  40. Wu, J. I., Reed, R. B., Grabowski, P. J. & Artzt, K. Function of quaking in myelination: regulation of alternative splicing. *Proc. Natl Acad. Sci. USA* 99, 4233–4238 (2002).
  41. Zong, F. Y. et al. The RNA-binding protein QKI suppresses cancer-associated aberrant splicing. *PLoS Genet.* 10, e1004289 (2014).
  42. Pastuszak, A. W. et al. An SF1 affinity model to identify branch point sequences in human introns. *Nucleic Acids Res.* 39, 2344–2356 (2011).
  43. Licatalosi, D. D. et al. HITS-CLIP yields genome-wide insights into brain alternative RNA processing. *Nature* 456, 464–469 (2008).
  44. Srinivasan, K. et al. Detection and measurement of alternative splicing using splicing-sensitive microarrays. *Methods* 37, 345–359 (2005).
  45. An, G. et al. P-selectin glycoprotein ligand-1 is highly expressed on Ly-6Chi monocytes and a major determinant for Ly-6Chi monocyte recruitment to sites of atherosclerosis in mice. *Circulation* 117, 3227–3237 (2008).
  46. Pacis, A., Nedelec, Y. & Barreiro, L. B. When genetics meets epigenetics: deciphering the mechanisms controlling inter-individual variation in immune responses to infection. *Curr. Opin. Immunol.* 29, 119–126 (2014).
  47. Pham, T. H. et al. Dynamic epigenetic enhancer signatures reveal key transcription factors associated with monocytic differentiation states. *Blood* 119, e161–e171 (2012).
  48. Pham, T. H. et al. Mechanisms of in vivo binding site selection of the hematopoietic master transcription factor PU.1. *Nucleic Acids Res.* 41, 6391–6402 (2013).
  49. Feinberg, M. W. et al. The Kruppel-like factor KLF4 is a critical regulator of monocyte differentiation. *EMBO J.* 26, 4138–4148 (2007).
  50. Shankman, L. S. et al. KLF4-dependent phenotypic modulation of smooth muscle cells has a key role in atherosclerotic plaque pathogenesis. *Nat. Med.* 21, 628–637 (2015).
  51. Gertz, J. et al. Distinct properties of cell-type-specific and shared transcription factor binding sites. *Mol. Cell* 52, 25–36 (2013).
  52. Kuhlman, P. A., Hughes, C. A., Bennett, V. & Fowler, V. M. A new function for adducin. Calcium/calmodulin-regulated capping of the barbed ends of actin filaments. *J. Biol. Chem.* 271, 7986–7991 (1996).
  53. Chan, K. R. et al. Ligation of Fc gamma receptor IIB inhibits antibodydependent enhancement of dengue virus infection. *Proc. Natl Acad. Sci. USA* 108, 12479–12484 (2011).
  54. Jirka, S. & Aartsma-Rus, A. An update on RNA-targeting therapies for neuromuscular disorders. *Curr. Opin. Neurol.* 28, 515–521 (2015).
  55. Yin, H. et al. Non-viral vectors for gene-based therapy. *Nat. Rev. Genet.* 15, 541–555 (2014).
  56. Esteller, M. Non-coding RNAs in human disease. *Nat. Rev. Genet.* 12, 861–874 (2011).
  57. Lim, J. et al. A protein-protein interaction network for human inherited ataxias and disorders of Purkinje cell degeneration. *Cell* 125, 801–814 (2006).
  58. Dehghan, A. et al. Genome-wide association study for incident myocardial infarction and coronary heart disease in prospective cohort studies: the CHARGE consortium. *PLoS ONE* 11, e0144997 (2016).
  59. van Eck, M. et al. Bone marrow transplantation in apolipoprotein E-deficient mice.



- Effect of ApoE gene dosage on serum lipid concentrations, (beta)VLDL catabolism, and atherosclerosis. *Arterioscler. Thromb. Vasc. Biol.* 17, 3117–3126 (1997).
60. Daigneault, M., Preston, J. A., Marriott, H. M., Whyte, M. K. & Dockrell, D. H. The identification of markers of macrophage differentiation in PMA-stimulated THP-1 cells and monocyte-derived macrophages. *PLoS ONE* 5, e8668 (2010).
  61. Bot, I. et al. Serine protease inhibitor Serp-1 strongly impairs atherosclerotic lesion formation and induces a stable plaque phenotype in ApoE<sup>-/-</sup> mice. *Circ. Res.* 93, 464–471 (2003).
  62. Sugnet, C. W. et al. Unusual intron conservation near tissue-regulated exons found by splicing microarrays. *PLoS. Comput. Biol.* 2, e4 (2006).
  63. Kim, D. & Salzberg, S. L. TopHat-Fusion: an algorithm for discovery of novel fusion transcripts. *Genome Biol.* 12, R72 (2011).
  64. Langmead, B. & Salzberg, S. L. Fast gapped-read alignment with Bowtie 2. *Nat. Methods* 9, 357–359 (2012).
  65. Hsu, F. et al. The UCSC known genes. *Bioinformatics* 22, 1036–1046 (2006).
  66. Li, H. et al. The Sequence Alignment/Map format and SAMtools. *Bioinformatics* 25, 2078–2079 (2009).
  67. Quinlan, A. R. & Hall, I. M. BEDTools: a flexible suite of utilities for comparing genomic features. *Bioinformatics* 26, 841–842 (2010).
  68. Anders, S. & Huber, W. Differential expression analysis for sequence count data. *Genome Biol.* 11, R106 (2010).
  69. Wu, J. et al. SpliceTrap: a method to quantify alternative splicing under single cellular conditions. *Bioinformatics* 27, 3010–3016 (2011).
  70. Stransky, N., Cerami, E., Schalm, S., Kim, J. L. & Lengauer, C. The landscape of kinase fusions in cancer. *Nat. Commun.* 5, 4846 (2014).
  71. Katz, Y., Wang, E. T., Airoidi, E. M. & Burge, C. B. Analysis and design of RNA sequencing experiments for identifying isoform regulation. *Nat. Methods* 7, 1009–1015 (2010).



# CHAPTER

# 8

The RNA-binding Protein Quaking  
Maintains Endothelial Barrier Function  
and Affects VE-cadherin and  
 $\beta$ -catenin Protein Expression

*Scientific Reports 2016*

**Collaborative effort by:**

Ruben G. de Bruin, Eric P. van der Veer, Jurriën Prins, Dae Hyun Lee, Martijn J. C. Dane, Huayu Zhang, Marko K. Roeten, Roel Bijkerk, Hetty C. de Boer, Ton J. Rabelink, Anton Jan van Zonneveld, Janine M. van Gils

**Abstract**

Proper regulation of endothelial cell-cell contacts is essential for physiological functioning of the endothelium. Interendothelial junctions are actively involved in the control of vascular leakage, leukocyte diapedesis, and the initiation and progression of angiogenesis. We found that the RNA-binding protein quaking is highly expressed by endothelial cells, and that its expression was augmented by prolonged culture under laminar flow and the transcription factor KLF2 binding to the promoter. Moreover, we demonstrated that quaking directly binds to the mRNA of VE-cadherin and  $\beta$ -catenin and can induce mRNA translation mediated by the 3'UTR of these genes. Reduced quaking levels attenuated VE-cadherin and  $\beta$ -catenin expression and endothelial barrier function in vitro and resulted in increased bradykinin-induced vascular leakage in vivo. Taken together, we report that quaking is essential in maintaining endothelial barrier function. Our results provide novel insight into the importance of post-transcriptional regulation in controlling vascular integrity.

## Introduction

All blood vessels are lined with a single layer of endothelial cells (ECs), which form a vital barrier between the blood and underlying tissue. The control of the EC barrier is critical to maintain vascular stability and retain circulating fluids, solutes, proteins and cells within the vasculature. Excessive vascular permeability plays a key role in many pathophysiological conditions such as septic shock, vascular leakage, hypertension, edema and atherosclerosis<sup>1,2</sup>. Inter-endothelial contacts within the monolayer must therefore be maintained for proper barrier function, while on the other hand, the cellular junctions must be sufficiently plastic to allow the growth and development of blood vessels, as well as the passage of leukocytes to the underlying tissue in case of an inflammatory reaction<sup>3</sup>. These specialized endothelial cell-cell adhesions are mediated by adherens, tight- and gap junctions<sup>2</sup>. In ECs, cell-cell interactions at adherens junctions are facilitated by the transmembrane protein VE-cadherin, of which the extracellular domain forms a zipper-like structure between the cells<sup>4</sup>. The intracellular domain of VE-cadherin is linked to the actin cytoskeleton via a complex array of structural and signaling proteins, including  $\beta$  -,  $\gamma$  -,  $\alpha$  - and p120-catenins<sup>2</sup>. In recent years, the importance of post-transcriptional control of gene expression in EC biology has become increasingly evident. For instance, microRNAs, such as the EC-enriched microRNA-126, were shown to play a critical role in vascular integrity and EC homeostasis<sup>5-7</sup>. Next to microRNAs, non-coding RNAs such as tie-1AS, MIAT and TUG1, are also novel players in endothelial function<sup>8-11</sup>. So far, RNA-binding proteins (RBP) have attracted less attention as essential post-transcriptional regulators of RNA fate. The human genome encodes an estimated 424 RBPs many of which function in post-transcriptional regulation driving alternative splicing of pre-mRNAs, nuclear export or retention, RNA stability and degradation, sequestration in granules and, ultimately, the translation into protein<sup>11</sup>. RBPs can mediate RNA and protein expression by binding to the 3' UTR of target mRNAs<sup>12</sup>. RBPs are classified by their capacity to directly interact with RNA through RNA-binding domains such as the RNA-Recognition-Motif or the K-Homology Domain. Similar to transcription factors binding to DNA motifs, RBPs can recognize and bind to their targets by recognizing specific RNA sequence motifs<sup>13</sup>. Given the large repertoire of RBPs present in any given cells, little is known about the role of RBPs in endothelial cell biology. The double-stranded RBP 76/NF70 was shown to facilitate vascular endothelial growth factor expression under hypoxic conditions by promoting vascular endothelial growth factor mRNA loading onto polysomes<sup>14</sup>. Also, splicing factor 2 regulates alternative splicing of the endothelial endoglin gene<sup>15</sup> and stabilization of the Sirtuin 1 mRNA by the RBP HuR was shown to repress the endothelial inflammatory response<sup>16</sup>. The RNA-binding protein Quaking (QKI) may also be highly relevant for endothelial function as it was shown to be essential for embryonic blood vessel development and visceral endoderm function<sup>17,18</sup>, and has also been implicated in angiogenesis<sup>19</sup>. While, QKI was originally identified for its role in myelination of the central and peripheral nervous system, later studies revealed that the RBP QKI is more ubiquitously expressed<sup>20</sup>. There are three major QKI protein isoforms; QKI-5, QKI-6, and

QKI-7 that require to either homo- or hetero-dimerize in order to bind RNA<sup>21</sup>. The post-transcriptional events published to be orchestrated by QKI include pre-mRNA splicing, mRNA export, mRNA stability and translation<sup>22–26</sup>. Consequently, QKI is involved in multiple cellular processes such as cellular differentiation, apoptosis, proliferation and migration<sup>20</sup>. Upon vascular injury, we have previously demonstrated that QKI plays a critical role in the proliferation and contractility of vascular smooth muscle cells by mediating the alternative splicing of the transcription factor myocardin<sup>27</sup>. During these studies, we noted that QKI is highly enriched in the endothelium of healthy control arteries. Therefore we assessed whether QKI contributes to endothelial function in vitro and in vivo. Here we identify QKI as a novel post-transcriptional regulator of expression of both VE-cadherin and  $\beta$ -catenin and as an essential regulator of EC barrier function.

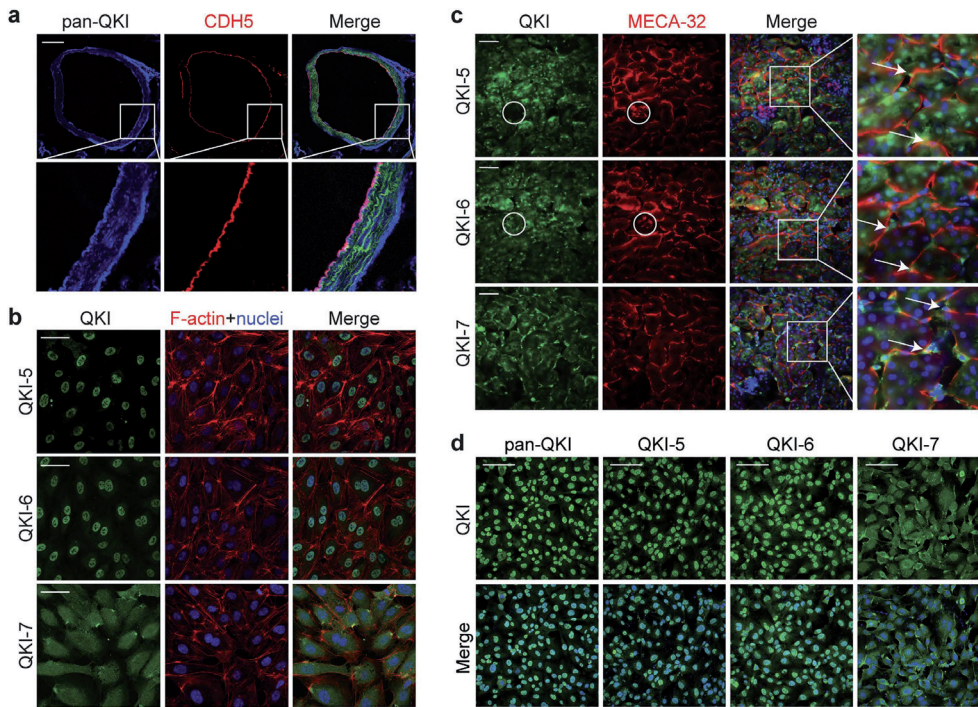


**Figure 1 | Quaking is highly expressed in macro- and micro-vascular endothelial cells.** (a) Immunofluorescent staining of pan-QKI (blue) and endothelium marker (red, VE-cadherin-CreER/RosatdTomato) in mouse aorta sections. Scale bar 200  $\mu$  m. (b) Immunofluorescent staining of QKI-5, QKI-6 or QKI-7 (green), F-actin (red) and DAPI (blue) in HUVECs. Scale bars 50  $\mu$  m. (c) Immunofluorescent staining of QKI-5, QKI-6 or QKI-7 (green), endothelium marker (red, MECA-32) and DAPI (blue) in mouse kidney sections. Arrows indicate peritubular capillaries, circles indicate glomeruli. Scale bars 50  $\mu$  m. (d) Immunofluorescent staining of pan-QKI, QKI-5, QKI-6 or QKI-7 (green), and DAPI (blue) in MVECs. Scale bars 100  $\mu$  m.

## Results

### **Quaking is expressed in macro- and micro-vascular endothelial cells.**

Given our previous observation that QKI is expressed in the endothelium of healthy human arteries<sup>27</sup>, we first assessed QKI expression in ECs of the native macrovascular vessels *in vivo*. For this we performed immunostaining of QKI on aortic sections of VE-cadherin-CreER/RosatdTomato reporter mice. QKI protein was highly enriched in ECs as compared to medial smooth muscle cells in the healthy artery as evidenced by its co-localization with the endothelial specific marker VE-cadherin (Fig. 1a). In the deeper layers of the adventitia, perivascular fibroblasts were also found to stain positive for QKI. To confirm whether QKI was also expressed in cultured human macrovascular ECs we assessed mRNA and protein levels of the three major isoforms of QKI in cultured human umbilical vein endothelial cells (HUVECs). The mRNAs of all three isoforms, QKI-5, QKI-6 and QKI-7 were abundantly expressed with the most abundant isoform Qki5 expressed at a similar level as the endothelial *Nos3* gene under static culture conditions (Supplementary Fig. 1a). Also, western blot readily confirmed the presence of the corresponding QKI protein isoforms in the lysates of the cells (Supplementary Fig. 1b). As earlier reports showed distinct cellular localization of the QKI protein isoforms in glial cells<sup>28</sup> and Hela cells<sup>29</sup> we performed immunostaining for the QKI isoforms in the cultured ECs. Indeed, confirming these previous reports, QKI-5 and QKI-6 expression was highly enriched in the nuclei while QKI-7 displayed a cytoplasmic localization (Fig. 1b). We next assessed QKI expression in ECs of the microvasculature by immunostaining of the QKI protein isoforms in mouse kidney sections and cultured human pulmonary microvascular endothelial cells (MVECs). Co-staining for the mouse endothelial antigen-23 (MECA32) clearly demonstrated QKI expression in the microvascular beds including the peritubular capillaries (Fig. 1c, arrows) and to a lesser extent the glomerular endothelium (Fig. 1c, circles). Evident staining was also observed in the kidney epithelium. Moreover, similar to HUVECs, distinct sub-cellular localization of the QKI-protein isoforms was observed in MVECs (Fig. 1d). Interestingly, particularly at higher magnification, in both HUVECs and MVECs, QKI-7 appeared to be focally enriched at the plasma membrane. Staining with an antibody that recognizes all three protein isoforms (pan-QKI) showed that the vast majority of QKI protein is localized in the nucleus (Fig. 1d). Taken together, these results demonstrate that QKI is highly expressed in the endothelium of both the macrovascular as well as in the microvascular beds.

### Laminar shear stress induces QKI expression.

Depending on their location in the vascular tree, ECs are exposed to varying magnitudes and types of shear stress caused by the flowing blood. It has been well established that the type of shear stress, either by laminar or disturbed flow, drives distinct cellular signaling pathways resulting in either quiescent or inflammatory EC phenotype, respectively<sup>30</sup>. Given the marked expression of QKI in ECs in healthy vessels, we postulated that vascular protective hemodynamic conditions may drive the expression of QKI. To test this, we cultured ECs under laminar shear for 7 days (10 dyne/cm<sup>2</sup>). Compared to statically cultured control cells, ECs exposed to laminar flow showed higher expression of the shear-responsive genes *Nos3* and Krüppel-Like Factor 2 (*Klf2*)<sup>31,32</sup> (Fig. 2a,b). Consistent with this quiescent EC phenotype, laminar flow exposed ECs showed well organized VE-cadherin at the cell-cell junctions, as well as short dense shear-fiber formation and alignment to the direction of the flow (Fig. 2b). Using this culture system, we determined whether prolonged laminar flow could also induce QKI expression. Quantitative RT-PCR revealed that the mRNA of all three Qki isoforms is indeed augmented by a shear dependent mechanism (Fig. 2c). Moreover, immunoblot analysis and fluorescent immunostaining of control (static) and 7 days sheared ECs revealed an evident increase in QKI protein expression (Fig. 2d,e). Interestingly, the mRNA and protein levels of the cytoplasmic isoform QKI-7 showed the most prominent increase upon prolonged laminar flow. To assess the molecular pathway by which QKI expression is augmented under laminar flow conditions we examined the promoter region of QKI. This revealed a prominent GC-rich DNA stretch, encompassing 78.1% GC content in the 1000 base pairs upstream of the QKI ATG start site with many CpG sites present (Fig. 3a, upper illustration). The shear induced transcription factor KLF2 binds to GC-rich DNA sequences<sup>33</sup> and has been described to drive a laminar shear dependent anti-inflammatory gene expression profile in EC<sup>34,35</sup>. We utilized a QKI promoter-luciferase reporter gene to test whether QKI expression could be directly induced by binding of KLF2 to the promoter region. Co-transfection of this reporter gene with the KLF2 cDNA in HEK293T cells resulted in an induction of the activity of the QKI promoter region (Fig. 3a, bar graph). Next, we tested whether lentiviral overexpression of KLF2 in HUVECs could also induce QKI expression. Overexpression of KLF2 resulted in increased expression of *Nos3* mRNA, but did not result in altered Qki mRNA levels (Fig. 3b). In contrast, overexpression of KLF2 did result in a marked increase in QKI protein levels, as evidenced by immunostaining and immunoblot analysis (Fig. 3c,d). NOS3 protein detection was taken along for validation that a functional KLF2 was overexpressed (Fig. 3b–d). These experiments support the hypothesis that QKI protein expression can be mediated by the transcription factor KLF2, either through direct interaction with the QKI promoter region and/or through additional post-transcriptional mechanisms. Taken together, we show that QKI expression is particularly expressed in quiescent, healthy ECs.



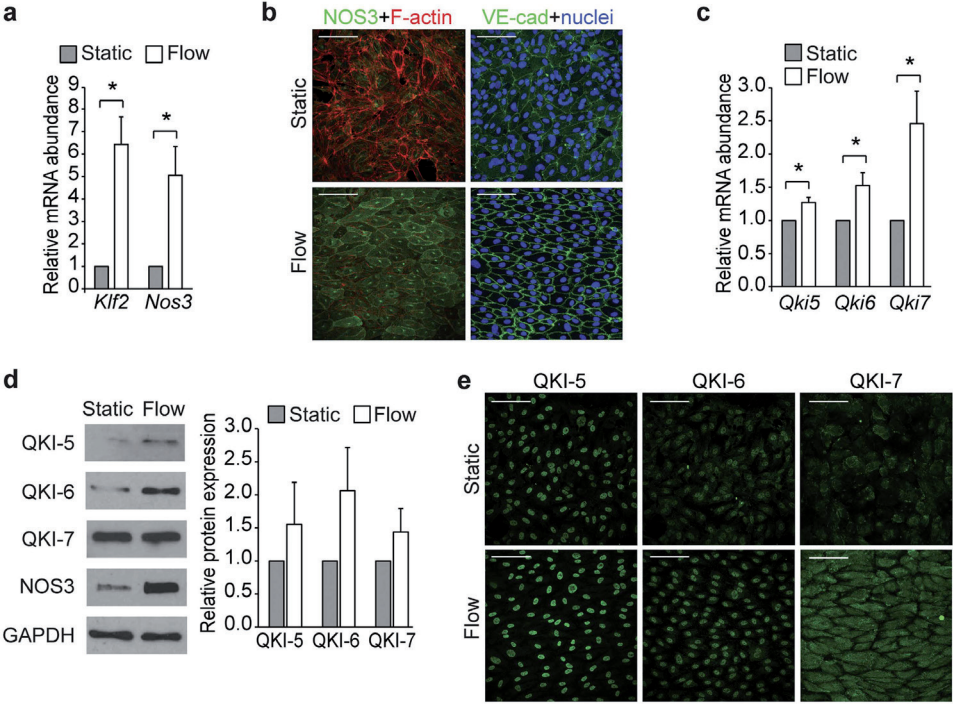


**Figure 2 | Endothelial cells cultured under laminar flow show increased QKI expression.** (a) Quantitative RT-PCR analysis of *Klf2* and *Nos3* mRNA isolated from HUVECs cultured under static or laminar flow conditions. Results are presented relative to static cultured cells, set as 1. Mean  $\pm$  s.e.m of  $n = 3-6$ . \* $P < 0.05$ . (b) Immunofluorescent staining of NOS3 (green, left panels) or VE-cadherin (green, right panels) and nuclei (blue) or F-actin (red) in HUVECs cultured under static or laminar flow conditions. Scale bars 100  $\mu$  m. (c) Quantitative RT-PCR analysis of *Qki5*, *Qki6* and *Qki7* mRNA isolated from HUVECs cultured under static or laminar flow conditions. Results are presented relative to static cultured cells, set as 1. Mean  $\pm$  s.e.m of  $n = 6-7$ . \* $P < 0.05$ . (d) Immunoblot analysis of QKI-5, QKI- 6, QKI-7, NOS3 or GAPDH (loading control) in protein lysates of HUVECs cultured under static or laminar flow conditions. Bar graph shows quantification of 3 independent experiments, mean  $\pm$  s.e.m. Results are relative to static cultured cells, set as 1. (e) Immunofluorescent staining of QKI-5, QKI- 6 or QKI-7 (green) in HUVECs cultured under static or laminar flow conditions. Scale bars 100  $\mu$  m.

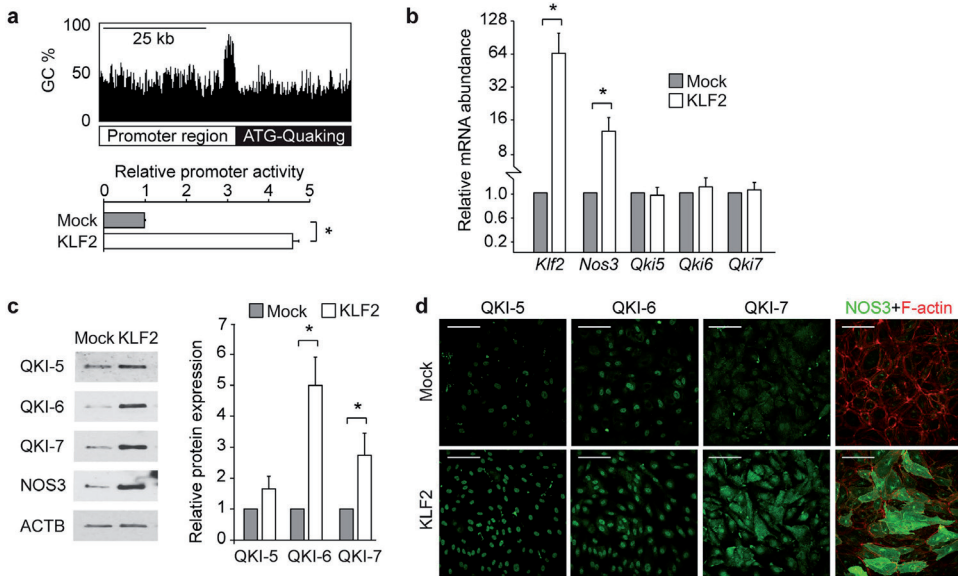


**Figure 3 | Quaking is induced by KLF2.** (a) Schematic representation of the promoter of QKI gene, demonstrating a high GC content (upper panel). Bar graph shows QKI promoter-luciferase reporter activity in HEK293T cells after transduction with lenti-KLF2 virus or lenti-mock virus. Results are presented relative to reporter activity in mock transduced cells, set as 1. Mean  $\pm$  s.d. from one experiment representative of three independent experiments. \* $P < 0.05$ . (b) Quantitative RT-PCR analysis of *Klf2*, *Nos3*, *Qki5*, *Qki6* and *Qki7* mRNA isolated from HUVECs transduced with mock or KLF2 overexpressing lenti-virus. Results are presented relative to cells transduced with mock virus, set as 1. Mean  $\pm$  s.e.m. of  $n = 4$ . \* $P < 0.05$ . (c) Immunoblot analysis of QKI-5, QKI-6, QKI-7, NOS3 or ACTB (loading control) in protein lysates of HUVECs transduced with mock or KLF2 overexpressing lenti-virus. Bar graph shows quantification of 3 independent experiments, mean  $\pm$  s.e.m. Results are relative to static cultured cells, set as 1. \* $P < 0.05$ . (d) Immunofluorescent staining of QKI-5, QKI-6, QKI-7 or NOS3 (green) and F-actin (red, right panels) in HUVECs cultured transduced with mock or KLF2 overexpressing lenti-virus. Scale bars 100  $\mu$ m.

### QKI affects endothelial barrier function and binds the VE-cadherin and $\beta$ -catenin mRNAs to promote translation.

To gain insight into the function of QKI in ECs we silenced QKI expression in ECs using lentiviral shRNA vectors targeting the QKI mRNA (shQKI) and a non-QKI targeting control shRNA (shCtrl). Repression of QKI expression was validated using qRT-PCR, immunoblot analysis and immunofluorescent staining (Fig. 4a–c). Next, shCtrl- and shQKI-treated ECs were seeded on gelatin-coated culture chambers that have electrodes present in the growth area to facilitate the measuring of electrical resistance by Electric Cell-substrate Impedance Sensing (ECIS)<sup>36</sup>. Targeted reduction of QKI in ECs did not affect the capacity of the cells

Figure 4

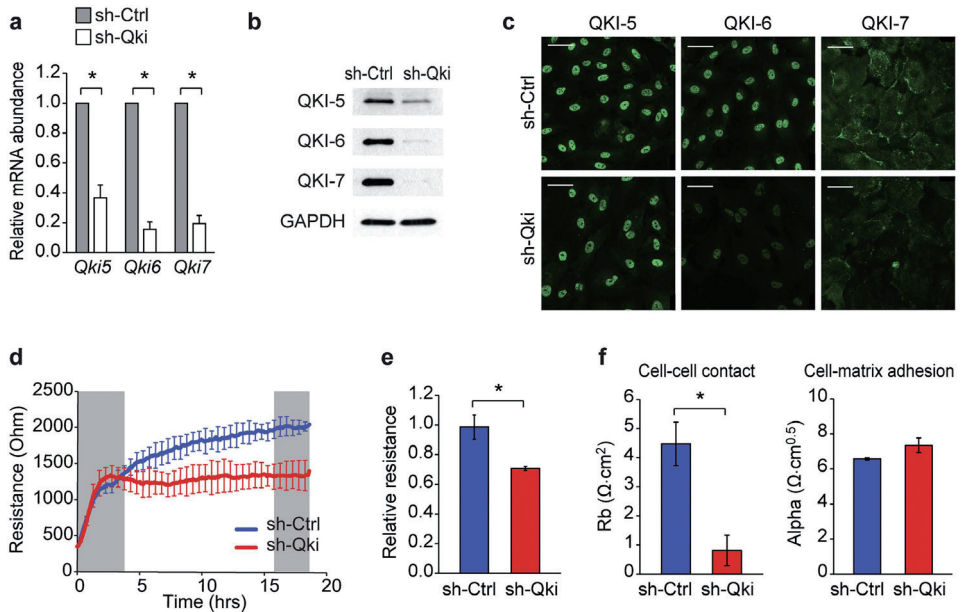


**Figure 4 | Targeting QKI perturbs endothelial barrier function in vitro.** (a) Quantitative RT-PCR analysis of *Qki5*, *Qki6* and *Qki7* mRNA isolated from HUVECs transduced with anti-Qki shRNA (shQKI) or control shRNA (shCtrl). Results are presented relative to shCtrl, set as 1. Mean  $\pm$  s.e.m. of  $n = 5$ . \* $P < 0.05$ . (b) Immunoblot analysis of QKI-5, QKI-6, QKI-7 or GAPDH (loading control) in protein lysates of shCtrl or shQKI HUVECs. (c) Immunofluorescent staining of QKI-5, QKI-6 or QKI-7 (green) in shCtrl or shQKI HUVECs. Scale bars 50  $\mu$ m. (d) Transendothelial electrical resistance of shCtrl or shQKI transduced HUVECs seeded on ECIS electrodes. Left grey box indicates time frame of adhesion and spreading, right grey box indicates time frame of stable monolayer. (e) Relative transendothelial electrical resistance of shCtrl or shQKI HUVEC stable monolayer, time frame indicated by right grey box in d, shCtrl set so 1. Mean  $\pm$  s.e.m. of  $n = 3$ . \* $P < 0.05$ . (f) Absolute endothelial electric resistance attributable to cell-cell contact ( $R_b$ , left bar graph) and cellmatrix interaction ( $\alpha$ , right bar graph) of shCtrl or shQki HUVECs. Mean  $\pm$  s.d. of  $n = 2$ . \* $P < 0.05$ .

to adhere and spread (Fig. 4d), but did result in the inability to form a proper high resistance monolayer as compared to control cells (Fig. 4d,e). Applying further mathematical modeling using the provided ECIS software, this modeling uses the impedance data to calculate the cell morphological parameters cell-cell contact and cell-matrix interaction<sup>37,38</sup>, it was confirmed that QKI reduction potently and specifically attenuated the endothelial cell-cell interactions (Fig. 4f). Given the RNA-binding properties of QKI, we postulated that the effects on barrier function could be explained by the post-transcriptional regulation of the mRNAs of genes involved in cell-cell interactions. To identify potential binding partners of QKI that are involved in barrier function, we examined the previously published gene list of 1430 potential target genes that have been computationally determined to contain a Quaking Response Element (QRE) (NACUAAY-N1-20-UAAY)<sup>39</sup>. Interestingly, VE-cadherin and  $\beta$ -catenin, essential for endothelial adherent junctions, both were shown to harbor high-affinity QREs in the 3' UTRs of their

mRNA (Supplementary Fig. 2). Next to this we as well examined the published QKI PAR-CLIP in HEK293 cells<sup>40</sup>, as well as the pre-mRNA sequence of VE-cadherin, since VE-cadherin is not expressed in HEK293T cells (Supplementary Fig. 2). In intronic regions several QREs are present, however no alternative splicing events of the flanking exons have been annotated (UCSC or Refseq). Using RNA immuno-precipitation, we first assessed whether QKI could bind to the mRNA of VE-cadherin and  $\beta$ -catenin. Indeed qRT-PCR analysis confirmed that mRNAs of both VE-cadherin and  $\beta$ -catenin were highly enriched in the QKI-antibody precipitated RNA fraction both in HUVECs (Fig. 5a,b) as well as in MVECs (Supplementary Fig. 3a,b). Since the QREs in the VE-cadherin and  $\beta$ -catenin mRNAs were localized in their 3' UTRs, we next sought to determine whether, next to binding, QKI as well has an effect on protein translation. For this we utilized luciferase-reporter genes fused to the 3' UTRs of both genes. Indeed, the presence of a QRE in the 3' UTRs from both genes showed a clear increase in luciferase activity, while these effects were blunted when QKI was repressed (Fig. 5c,d). These data indicate that QKI does not only bind to the mRNA of VE-cadherin and  $\beta$ -catenin, but also increases the translation by binding to the 3' UTRs of these mRNAs.

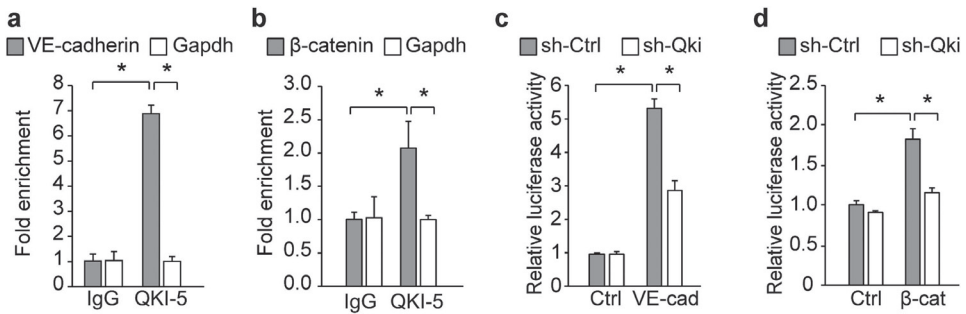


**Figure 5 | Quaking protein binds to VE-cadherin and  $\beta$ -catenin mRNA and affects translation**  
(a,b) RNAimmunoprecipitation in HUVECs using an IgG control or QKI-5 antibody. VE-cadherin (a),  $\beta$ -catenin (b) or Gapdh mRNA abundance in immune-precipitated fraction was determined by qRT-PCR. Results are presented relative to IgG immunoprecipitation, set as 1. Mean  $\pm$  s.d. from one experiment representative of three independent experiments. \*P < 0.05. (c,d) VE-cadherin (c),  $\beta$ -catenin (d) or Control (Ctrl) 3' UTR luciferasereporter constructs were co-transfected with shCtrl or shQKI in HEK293T cells and luciferase activity levels measured. Results are presented relative to Ctrl 3' UTR in shCtrl cells, set as 1. Mean  $\pm$  s.d. from one experiment representative of three independent experiments. \*P < 0.05.

### Reducing QKI predisposes to vascular leakage

We next used ECs to validate that a reduction of QKI indeed decreases the abundance of VE-cadherin and  $\beta$ -catenin expression. While shRNA-mediated QKI knockdown in the EC did not reveal a pronounced reduction of either VE-cadherin or  $\beta$ -catenin mRNA (Fig. 6a), immunoblot analysis did show reduced VE-cadherin and  $\beta$ -catenin protein levels in ECs (Fig. 6b). In addition, immunofluorescence staining of VE-cadherin and  $\beta$ -catenin in shCtrl or shQKI

ECs revealed that the expression of both VE-cadherin and  $\beta$ -catenin were diminished at the adherent junctions of shQKI treated cells (Fig. 6c). These data confirm that in ECs, QKI does not regulate mRNA transcript abundance, but instead mediates translation and thereby protein expression of VE-cadherin and  $\beta$ -catenin. Finally, we postulated that decreased QKI expression would also result in impaired EC barrier function in vivo. To that end, we used the Quakingviable (Qkv) mouse strain that has been widely used as a model to study the effects of decreased QKI levels. Vascular leakage and EC barrier function was assessed in vivo by Evans blue extravasation upon stimulation with bradykinin. Bradykinin is a well described potent permeability-increasing inflammatory mediator by signaling through the bradykinin receptors (BDKRB1 and BDKRB2)<sup>41</sup> and Orsenigo et al. have shown VE-cadherin mediated vascular leakage in response to bradykinin<sup>42</sup>. Moreover, it has been reported that the mouse intestine microvasculature shows a strong susceptibility to bradykinin<sup>43</sup>. Therefore, we used a similar approach to robustly quantify extravasated Evans blue 5 minutes after intravenous injection of bradykinin. In concordance with our in vitro studies, a reduction of QKI expression in vivo indeed resulted in a significant 40% increase of Evans blue leakage upon bradykinin stimulation (Fig. 6d). These results further confirm that QKI expression is required for maintaining the integrity of EC barrier function in vivo.

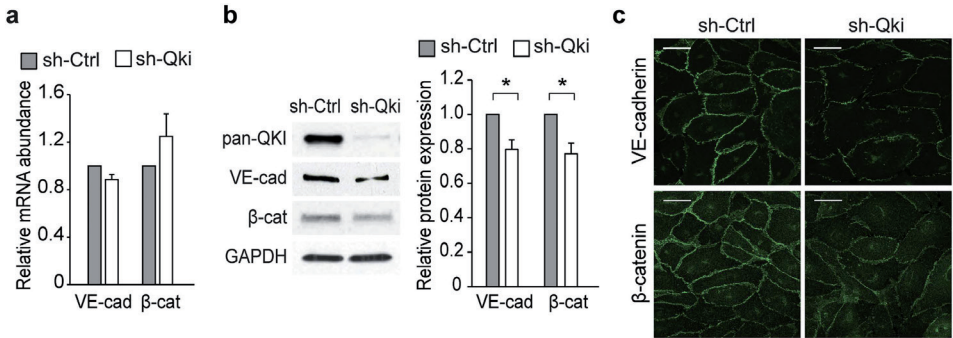


**Figure 6 | Abridged QKI results in reduced VE-cadherin and  $\beta$ -catenin and enhanced vascular leakage.** (a) Quantitative RT-PCR analysis of VE-cadherin and  $\beta$ -catenin mRNA isolated from shCtrl or shQKI HUVECs. Results are presented relative to shCtrl, set as 1. Mean  $\pm$  s.e.m. of  $n = 5$ . \* $P < 0.05$ . (b) Immunoblot analysis of pan-QKI, VE-cadherin,  $\beta$ -catenin or GAPDH (loading control) in protein lysates of shCtrl or shQKI HUVECs. Bar graph shows quantification of 3 independent experiments, mean  $\pm$  s.e.m. Results are relative to static cultured cells, set as 1. \* $P < 0.05$ . (c) Immunofluorescent staining of VE-cadherin or  $\beta$ -catenin in shCtrl or shQKI HUVECs. Scale bars 50  $\mu$ m.



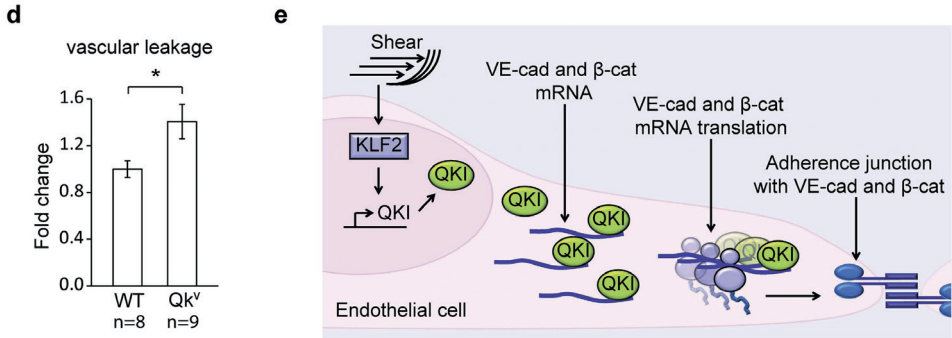


**Figure 6 legend continued** | (d) Vascular leakage upon Bradykinin (8 mg/kg) stimulation was measured in the gut microvasculature of WT and Qkv mice, by spectrophotometric quantification of extravasated albumin that was labeled using Evans Blue. Results are presented relative to those of WT mice, set as 1. Mean  $\pm$  s.e.m. of  $n = 8-9$ . \* $P < 0.05$ . (e) A schematic diagram of endothelial QKI, induced by laminar flow and KLF2, in maintaining endothelial adherence junctions by binding to and inducing translation of VE-cadherin and  $\beta$ -catenin mRNA.

## Discussion

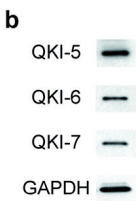
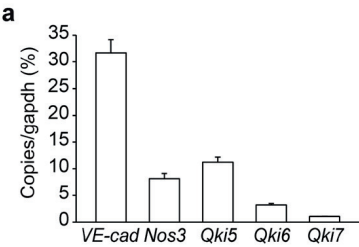
In this study we provide evidence that the RBP QKI is highly expressed in quiescent ECs and is required for the maintenance of endothelial barrier function by increasing the expression of VE-cadherin and  $\beta$ -catenin in the intra-cellular junctions of the endothelium. Following the notion that the 3' UTRs of both the  $\beta$ -catenin and VE-cadherin mRNA contained QKI-binding sites, we investigated the role of QKI in the expression of these genes and demonstrated that the interaction of QKI with the 3' UTR region of VE-cadherin and  $\beta$ -catenin mRNA resulted in increased translation of these genes (Fig. 6e). Previous reports demonstrated that the binding of QKI to the 3' UTR region of target mRNAs can affect mRNA stability and translation in a transcript and cell-specific fashion. For instance, in oligodendrocytes, QKI binding to the mRNAs of myelin basic protein (MBP)<sup>44</sup> and its regulator Hnrnpa1<sup>45</sup> was demonstrated to stabilize these mRNA levels by counteracting their rate of degradation. In contrast, QKI binding to the UTR of the Forkhead Box O1 mRNAs in cancer cells results in lower levels of this mRNA<sup>46,47</sup>. In contrast, our data in this study have indicated that in endothelial cells, binding of QKI to VE-cadherin and  $\beta$ -catenin 3' UTRs does not impact the mRNA levels, yet does enhance protein expression of VE-cadherin and  $\beta$ -catenin. Two previous reports have also implicated post-transcriptional regulation of  $\beta$ -catenin by QKI. In those studies adenovirus-mediated overexpression of QKI resulted in a decrease of protein expression, similarly without a change in mRNA abundance<sup>47,48</sup>. Together these results point to complex regulatory mechanisms, for example the direct competition of QKI and other RBPs binding to the 3' UTR, such as the RBPs Tristeraprolin<sup>49</sup> or HuR<sup>50,51</sup>. Increased expression of VE-cadherin and  $\beta$ -catenin following the binding of QKI to their 3' UTRs could also be explained by a direct competition for binding with microRNAs that would

cause translational arrest without mRNA degradation. However, *in silico* analyses revealed no known microRNA binding sites at the QRE site in the 3' UTRs of VE-cadherin and  $\beta$ -catenin. Alternatively, increased expression of the QKI-bound mRNAs could be related to affect QKI-dependent localization and shuttling of these mRNAs. The homo- or hetero-dimerization dependent binding of RNA<sup>52,53</sup>, the distinct subcellular localization of the QKI isoforms<sup>29</sup> and the presence of QKI in specific RNA containing granules<sup>26</sup> are consistent with a role for QKI in the intracellular distribution of mRNA between the nucleus and various cytoplasmic compartments. For instance, nuclear retention was demonstrated for the MBP-1 mRNA in Qkv mice<sup>54</sup>. Given the above, it is tempting to speculate that, in EC, QKI-7 containing heterodimers serve to shuttle bound mRNA to the cellular periphery and facilitate the local translation at for example adherens junctions. Endothelial barrier function and the prevention of vascular leakage is tightly coupled to signaling pathways that are induced by laminar shear stress<sup>55</sup>. Our observation that ECs cultured for prolonged time under laminar flow, induced QKI mRNA and protein expression and most likely, influenced its junction-stabilizing functions, is consistent with this concept. Notably, lentiviral overexpression of the flow induced transcription factor KLF2 did reveal an increased QKI protein expression as assessed by immunostaining and immunoblot. Therefore, our promoter activity experiments indicate that KLF2 mediates the promoter activity of QKI. This hypothesis was supported by the work of Redmond and co-workers who reported that, compared to control cells, QKI was one of the most repressed genes in the embryonic yolk sack erythroid cells of KLF2 knockout mice<sup>56</sup>.

Together this points towards a regulation of QKI by KLF2, however it cannot be excluded that other parallel pathways are involved. For instance, several microRNA-mediated feedback loops have been described in literature, such as KLF2 driven microRNA-143 and microRNA-148 expression<sup>57</sup> which, based on *in silico* analyses, are also predicted to bind to the 3' UTRs of the QKI mRNAs. Based on *in silico* analysis these microRNAs could target the QKI 3' UTRs, but not VE-cadherin and  $\beta$ -catenin, and induce mRNA degradation in HUVECs. Strikingly, genome wide *in silico* analyses suggested that the QKI 3' UTRs are probably extremely susceptible to microRNA regulation, ranking number 11 genome wide in the number of potential microRNA seed sequences present in its 3' UTR<sup>58</sup>. Combined with the induced QKI promoter activity by KLF2, microRNAs could result in an induction of QKI protein expression without an evident increase in QKI mRNA levels, as observed upon lentiviral KLF2 overexpression in HUVEC cells. The difference seen in QKI mRNA levels upon laminar flow and induced KLF2 expression, could be explained by other changes. Laminar flow induces not only KLF2, but also other signalling pathways that might contribute to the regulation of QKI mRNA and protein expression. Next to the change in microRNAs and QKI by KLF2 and/or laminar flow we do not exclude that the expression of other RNA-binding proteins might also be changed and capable of influencing QKI mRNA and protein levels. Taken together, while previous studies demonstrated a critical role for QKI in embryonic blood vessel development by mediating intra-cellular interactions between ECs and the cells of the visceral endoderm, we now

show that the RNA-binding protein QKI also serves a postnatal role in the proper formation of endothelial cell-cell contacts and barrier function (Fig. 6e). Our data underscore the importance of post-transcriptional regulation in endothelial homeostasis and might have implications for future therapeutic strategies aimed to preserve vascular integrity in health and disease.

Supplementary data

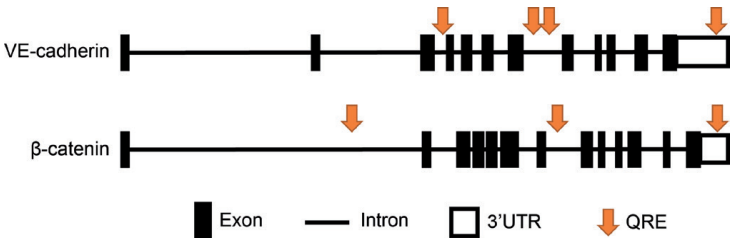


Supplementary figure 1 | Quaking is highly expressed in HUVECs (a)

Quantitative RT-PCR analysis of VE-cadherin, Nos3, Qki5, Qki6 and Qki7 mRNA isolated from HUVECs. Results are presented as percentage of GAPDH. Mean  $\pm$  s.e.m. of n=15. (b) Immunoblot analysis of QKI-5, QKI-6, QKI-7 or GAPDH (loading control) in protein lysates of HUVECs.

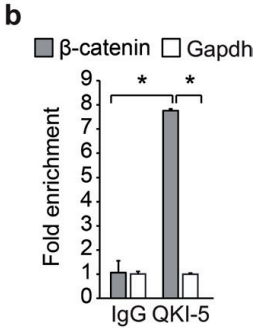
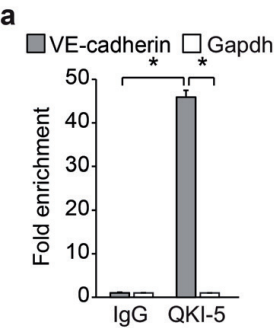
Supplementary figure 2 | Quaking Response elements in VE-cadherin and  $\beta$ -catenin.

A schematic diagram of VE-cadherin and  $\beta$ -catenin pre-mRNA with QKI response elements (QREs).



Supplementary figure 3 | Quaking protein binds to VE-cadherin and  $\beta$ -catenin mRNA (a-b)

RNA-immunoprecipitation in MVECs using an IgG control or QKI-5 antibody. VE-cadherin (a),  $\beta$ -catenin (b) or Gapdh mRNA abundance in immune-precipitated fraction was determined by qRT-PCR. Results are presented relative to IgG immunoprecipitation, set as 1. Mean  $\pm$  s.d. from one experiment representative of four independent experiments. \*P<0.05.





## Methods

### Mice

C57BL/6 J mice were obtained from the Jackson Laboratory. Inducible Tg(Cdh5-cre/ERT2)1Rha (Jackson Laboratory) mice were crossed to B6.Cg-Gt(ROSA)26Sortm14(CAG-tdTomato)Hze/J (Jackson Laboratory) to obtain VE-cadherin-CreER/RosatdTomato reporter mice. Tamoxifen (Sigma-Aldrich) was dissolved in a sunflower oil/ethanol (10:1) mixture at 10 mg/ml. Tamoxifen 2 mg was injected daily intraperitoneal into 8-week-old VE-cadherin-CreER/RosatdTomato mice for 5 consecutive days. Quakingviable (Qkv) mice were generously provided by dr. S. Richard, McGill University, Montreal, Canada. Quakingviable mice have an autosomal recessive 1 Mb deletion in the promoter region of the Qki gene<sup>59,60</sup>. This results in decreased expression of QKI-6 and QKI-7 isoforms and serves as a well-recognized model to study QKI dependent effects in vivo. All animal use and experimental procedures were approved by the regulatory authorities of the Leiden University Medical Center and within the guidelines set by the Dutch government. All experiments were performed in accordance with relevant guidelines and regulations.

### Cell culture

HUVECs were isolated from human umbilical cords. The umbilical cords were collected and kept at 4 °C in PBS for a maximum of 3 days. To harvest the ECs, the vein was cannulated and flushed with sterile PBS. Thereafter, pre-heated (37 °C) trypsin-EDTA (Gibco) was incubated for 15 minutes in 37 °C PBS after which the vein was flushed with PBS again. The resulting cell suspension was spun down (1500 rpm, RT, 10 minutes), resuspended in Endothelial growth medium-2 (Lonza), and plated on 1% gelatin coated T75 flasks, cultured at 37 °C, 5% CO<sub>2</sub>. Experiments were performed with cell passage 1–3. MVEC were a kind gift from Prof. M.J.T.H. Goumans, Leiden University Medical Center, Leiden, the Netherlands. MVECs are human pulmonary microvascular endothelial cells and were culture in microvascular endothelial cell medium-2 (EGM-2-MV, Lonza). Human embryonic kidney cells (HEK293T) were cultured in DMEM (Gibco) supplemented with 100 U/ml penicillin, 100 U/ml streptomycin, 300 µg/ml glutamin (all from Gibco) and 10% fetal calf serum (Cambrex).

### Primary antibodies

Antibodies used to detect QKI-5, QKI-6 or QKI-7 were obtained from Millipore (rabbit polyclonals) or Neuromab (mouse monoclonals). MECA-32, VE-cadherin and NOS3 from BD Biosciences, GAPDH and  $\beta$ -catenin from Cell Signaling and  $\beta$ -actin from Abcam.

### Immunofluorescent staining

Cells cultured on glass coverslips or Ibidi 8-well  $\mu$ -slides, cross-sections of aorta from VE-cadherin-CreER/RosatdTomato mice, or cross-sections of kidney from C57BL/6 J mice were washed twice with Hanks' Balanced Salt Solution containing Ca<sup>2+</sup> and Mg<sup>2+</sup> (HBSS, Gibco), fixed with 3.7% formalin (Millipore)

for 10 minutes and permeabilized with 0.5% Triton X-100 for 2 minutes (Sigma-Aldrich) in HBSS. Indicated antibodies were incubated in HBSS containing 1% bovine serum albumin and 1% fetal calf serum for 1 hour. Appropriate secondary antibodies labeled with Alexa fluorophores were obtained from Invitrogen and phalloidin-rhodamine was obtained from Sigma-Aldrich. Cells or sections were mounted with Prolong® gold antifade mountant with DAPI (Life technologies) and imaging was performed on an inverted Leica SP5 confocal imaging system.

### **Quantitative RT-PCR**

RNA isolation was performed using TRIZOL reagent (Invitrogen) and isolated using Qiagen's RNAeasy kit according to manufactures instructions. 500–2000 ng of total RNA was used for reverse transcription mediated cDNA synthesis using random primers (Invitrogen) according to the manufactures protocols. SYBR Select (Invitrogen) and a Biorad CFX384 were used for qRT-PCR analysis (primers, Table 1). The change in mRNA expression was calculated by the comparative change-in-cycle-method ( $\Delta\Delta CT$ ).

### **Immunoblot analysis**

Protein lysates were generated using radioimmunoprecipitation buffer supplemented with protease inhibitors cocktail (Complete, Roche), total protein content was determined using BCA Protein Assay Kit (Pierce), and 5–20  $\mu$ g of total protein was resolved using Any-kD Mini-PROTEAN TGX Precast SDS page gels (Biorad). Gels were blotted onto nitrocellulose membranes using the Trans-Blot Turbo Transfer System (Biorad) and blocked with 5% non-fat milk powder in PBS with 0.01% of Tween (PBST). Membranes were incubated with primary antibodies overnight at 4 °C, thereafter appropriate HRP-labeled secondary antibodies were incubated for 1 hour at room temperature and thoroughly washed with PBST. Next, membranes were incubated with SuperSignal West Dura Chemiluminescent Substrate (Pierce) and exposed on BioMax XAR Film (Kodak) or Ultracruz autoradiography film (Santa Cruz).

### **Laminar shear stress experiments**

Laminar shear stress experiments were performed using an Ibidi flow system. HUVECs were seeded onto closed perfusion chambers (IbidiTreat 0.4  $\mu$ -Slide I or VI, Luer) at a concentration of  $1.5 \times 10^6$  cells per ml. Cells were allowed to adhere for 3 hours and the chamber was connected to a computer-controlled air pressure pump and a fluidic unit with a two-way switching valve. The pump setup allowed pumping of 16 ml cell culture medium from two reservoirs in a unidirectional way through the flow channel over the monolayer of ECs at a constant shear stress of 10 dyne/cm<sup>2</sup>. The chamber and reservoirs containing the medium were kept in an incubator at 37 °C and 5% CO<sub>2</sub>. Medium was refreshed after 1 and 4 days of culture. RNA was isolated from cells not subjected to flow or subjected to shear stress for 7 days in a 0.4  $\mu$ -Slide I Luer flow chamber, while the 6 lanes of a 0.4  $\mu$ -Slide VI Luer were used for immunofluorescent stainings.

### **Lentiviral vectors, lentiviral particle production and transduction**

Four different shRNA constructs targeting human QKI were obtained from the Mission Library (Sigma Aldrich) and tested for their efficiency to knock down QKI. The best shRNA was selected to perform all experiments. As a control, a non-targeting shRNA was used. The human KLF2 overexpression construct was kindly provided by Prof. A. Horrevoets, VU University Medical Center, Amsterdam, the Netherlands. Lentiviral particles were produced as described by the Sigma Library protocol using HEK293T cells. Lentiviral transductions of HUVECs were done with cell passage 1 or 2. Lentiviral particles were incubated overnight and puromycin selection (0.5  $\mu$ g/ml) for 24 hours was started 24 hours after lentiviral transduction.

### Endothelial barrier measurements

Endothelial barrier was measured by Electric-cell impedance sensing. HUVEC cultures were grown to confluency, where after the cells were detached using trypsin-EDTA solution, counted using trypan blue and seeded in the electrode arrays (Ibidi, 8 wells, 10 electrodes per well) coated with gelatin (1% in 0.9% NaCl) at a density of 50.000 cells/well. Measurements of trans-endothelial electrical resistance were performed in real time by means of an ECIS-Z $\theta$  instrument (Applied Biophysics) at 37 °C, 5% CO<sub>2</sub>. Cell spreading and monolayer formation were subsequently monitored by measuring the resistance at 4000 Hz. For the mathematical modelling to calculate resistance attributable to the functions cell-cell adhesion and cell-matrix interaction, the resistance and capacitance were measured at 11 different AC frequencies ranging from 62.5 Hz up to 64000 Hz.

### RNA immunoprecipitation

RNA-immunoprecipitation was performed using Millipore's validated RIPAb + QKI-5 kit according to manufacture instructions.

### Luciferase assays

HEK293T cells were transfected with a human QKI promoter-luciferase reporter construct (SwitchGear Genomics), human  $\beta$ -catenin 3' UTR luciferase-reporter plasmid (SwitchGear Genomics), human VE-cadherin 3' UTR luciferase-reporter plasmid (last 545 bp of 3' UTR of human VE-cadherin cloned into pMIR-REPORT™ miRNA Expression Reporter Vector System; Applied Biosystems), control 3' UTR luciferase-reporter plasmid (60 bp of murine SDF-1 3' UTR cloned into pMIR-REPORT™ miRNA Expression Reporter Vector System; Applied Biosystems) or empty 3' UTR luciferase-reporter construct (SwitchGear Genomics) through the use of polyethylenimine (3  $\mu$ g/1  $\mu$ g DNA; Polysciences Inc). When indicated shRNA against QKI or non-targeting shRNA were co-transfected. Twenty-four hours after transfection luciferase activity was assessed with the Dual Luciferase Reporter reagents (Promega) and a GloMax® 96 microplate luminometer (Promega) and was normalized to a constitutively expressed renilla reporter.

### In vivo vascular leakage

Female Quaking viable (Qkv) mice or wild type littermates aged 16–20 weeks old were anesthetized by intraperitoneal injection with 10 ml/kg of fentanyl (50

$\mu$  g/ml), dexmedetomidine (Dexdomitor, 0.5 mg/ml), and midazolam (Dormicum, 5 mg/ml). Next, the mice were injected intravenous with 100  $\mu$  l of 1% Evans Blue (Sigma-Aldrich) in PBS. After 15 minutes 8 mg/kg bradykinin was injected intravenous and mice were exsanguinated by cardiac puncture after 5 minutes. Plasma was collected, mice were perfused with 20 ml of PBS. The gut was taken out from stomach until the rectum, weighed, cut into small pieces and incubated overnight at 55 °C in 2 ml of Formamide (Sigma-Aldrich). Next, tubes were spun down, and supernatants were collected to determine light absorbance at 450 nm (reference) and 620 nm (Evans blue) wavelengths using a 96-wells plate in a spectrophotometer (SpectraMax, Molecular Devices). The Evans Blue OD/reference OD ratio per gram of wet tissue is given.

### Statistical analysis

The difference between two groups was analyzed by Student's t-test. P values of less than 0.05 were considered significant.

### Acknowledgements

We thank Iris Schmidt and Steven van Woerkens for their technical support. Supported by the Dutch Kidney Foundation (NSN C 09.2329 to A.J.Z.), the Netherlands Institute of Regenerative Medicine (R.G.B, E.P.V) and the Netherlands Heart Foundation (2013T127 to H.Z. and J.M.G.).

### Author Contributions

Conceptualization, R.G.B. and J.M.G. Investigation, R.G.B., E.P.V., J.P., D.H.L., M.J.C.D., H.Z., M.K.R., R.B. and J.M.G.; Writing – original draft, R.G.B. and J.M.G.; Writing – review & editing, R.B., H.C.B. and A.J.Z. Supervision, E.P.V., T.J.R., A.J.Z. and J.M.G. Funding acquisition, T.J.R., A.J.Z. and J.M.G.

### Additional Information

Supplementary information accompanies this paper at <http://www.nature.com/srep>

### Competing financial interests

The authors declare no competing financial interests.

**How to cite this article:** de Bruin, Ruben G. et al. The RNA-binding protein quaking maintains endothelial barrier function and affects VE-cadherin and  $\beta$ -catenin protein expression. *Sci. Rep.* 6, 21643; doi: 10.1038/srep21643 (2016).

## References

1. Deanfield, J. E., Halcox, J. P. & Rabelink, T. J. Endothelial function and dysfunction testing and clinical relevance. *Circulation* 115, 1285–1295 (2007).
2. Dejana, E., Tournier-Lasserre, E. & Weinstein, B. M. The control of vascular integrity by endothelial cell junctions: molecular basis and pathological implications. *Dev. Cell* 16, 209–221 (2009).
3. Wallez, Y. & Huber, P. Endothelial adherens and tight junctions in vascular homeostasis, inflammation and angiogenesis. *Biochim Biophys Acta* 1778, 794–809 (2008).
4. Vestweber, D., Winderlich, M., Cagna, G. & Nottebaum, A. F. Cell adhesion dynamics at endothelial junctions: VE-cadherin as a major player. *Trends Cell Biol* 19, 8–15 (2009).
5. Chamorro-Jorganes, A., Araldi, E. & Suarez, Y. MicroRNAs as pharmacological targets in endothelial cell function and dysfunction. *Pharmacol Res* 75, 15–27 (2013).
6. Reijerkerk, A. et al. MicroRNAs regulate human brain endothelial cell-barrier function in inflammation: implications for multiple sclerosis. *J Neurosci* 33, 6857–6863 (2013).
7. Pepini, T., Gorbunova, E. E., Gavrilovskaya, I. N., Mackow, J. E. & Mackow, E. R. Andes virus regulation of cellular microRNAs contributes to hantavirus-induced endothelial cell permeability. *J Virol* 84, 11929–11936 (2010).
8. Uchida, S. & Dimmeler, S. Long noncoding RNAs in cardiovascular diseases. *Circ Res* 116, 737–750 (2015).
9. Li, K. et al. A noncoding antisense RNA in tie-1 locus regulates tie-1 function in vivo. *Blood* 115, 133–139 (2010).
10. Yan, B. et al. lncRNA-MIAT regulates microvascular dysfunction by functioning as a competing endogenous RNA. *Circ Res* 116, 1143–1156 (2015).
11. Keene, J. D. RNA regulons: coordination of post-transcriptional events. *Nat Rev Genet* 8, 533–543 (2007).
12. Eom, T., Antar, L. N., Singer, R. H. & Bassell, G. J. Localization of a beta-actin messenger ribonucleoprotein complex with zipcodebinding protein modulates the density of dendritic filopodia and filopodial synapses. *J Neurosci* 23, 10433–10444 (2003).
13. Ray, D. et al. A compendium of RNA-binding motifs for decoding gene regulation. *Nature* 499, 172–177 (2013).
14. Vumbaca, F., Phoenix, K. N., Rodriguez-Pinto, D., Han, D. K. & Claffey, K. P. Double-stranded RNA-binding protein regulates vascular endothelial growth factor mRNA stability, translation, and breast cancer angiogenesis. *Mol Cell Biol* 28, 772–783 (2008).
15. Blanco, F. J. & Bernabeu, C. Alternative splicing factor or splicing factor-2 plays a key role in intron retention of the endoglin gene during endothelial senescence. *Aging Cell* 10, 896–907 (2011).
16. Ceolotto, G. et al. Sirtuin 1 stabilization by HuR represses TNF-alpha- and glucose-induced E-selectin release and endothelial cell adhesiveness in vitro: relevance to human metabolic syndrome. *Clin Sci (Lond)* 127, 449–461 (2014).
17. Bohnsack, B. L., Lai, L., Northrop, J. L., Justice, M. J. & Hirschi, K. K. Visceral endoderm function is regulated by quaking and required for vascular development. *Genesis* 44, 93–104 (2006).
18. Noveroske, J. K. et al. Quaking is essential for blood vessel development. *Genesis* 32, 218–230 (2002).
19. van Mil, A. et al. MicroRNA-214 inhibits angiogenesis by targeting Quaking and reducing

- angiogenic growth factor release. *Cardiovasc Res* 93, 655–665 (2012).
20. Chenard, C. A. & Richard, S. New implications for the QUAKING RNA binding protein in human disease. *J.Neurosci.Res.* 86, 233–242 (2008).
21. Kondo, T. et al. Genomic organization and expression analysis of the mouse qkl locus. *Mamm.Genome* 10, 662–669 (1999).
22. Conn, S. J. et al. The RNA binding protein quaking regulates formation of circRNAs. *Cell* 160, 1125–1134 (2015).
23. Hall, M. P. et al. Quaking and PTB control overlapping splicing regulatory networks during muscle cell differentiation. *RNA* 19, 627–638 (2013).
24. Larocque, D. et al. Protection of p27(Kip1) mRNA by quaking RNA binding proteins promotes oligodendrocyte differentiation. *Nat Neurosci* 8, 27–33 (2005).
25. Saccomanno, L. et al. The STAR protein QKI-6 is a translational repressor. *Proc Natl Acad Sci USA* 96, 12605–12610 (1999).
26. Wang, Y. et al. The QKI-RNA binding protein localizes with the MBP mRNAs in stress granules of glial cells. *PLoS One* 5, e12824 (2010).
27. van der Veer, E. P. et al. Quaking, an RNA-binding protein, is a critical regulator of vascular smooth muscle cell phenotype. *Circ.Res.* 113, 1065–1075 (2013).
28. Wang, Y., Vogel, G., Yu, Z. & Richard, S. The QKI-5 and QKI-6 RNA binding proteins regulate the expression of microRNA 7 in glial cells. *Mol.Cell Biol.* 33, 1233–1243 (2013).
29. Wu, J., Zhou, L., Tonissen, K., Tee, R. & Artzt, K. The quaking I-5 protein (QKI-5) has a novel nuclear localization signal and shuttles between the nucleus and the cytoplasm. *J Biol Chem* 274, 29202–29210 (1999).
30. Frueh, J. et al. Systems biology of the functional and dysfunctional endothelium. *Cardiovasc Res* 99, 334–341 (2013).
31. Dekker, R. J. et al. Prolonged fluid shear stress induces a distinct set of endothelial cell genes, most specifically lung Kruppel-like factor (KLF2). *Blood* 100, 1689–1698 (2002).
32. Uematsu, M. et al. Regulation of endothelial cell nitric oxide synthase mRNA expression by shear stress. *Am J Physiol* 269, C1371–1378 (1995).
33. Anderson, K. P., Kern, C. B., Crable, S. C. & Lingrel, J. B. Isolation of a gene encoding a functional zinc finger protein homologous to erythroid Kruppel-like factor: identification of a new multigene family. *Mol.Cell Biol.* 15, 5957–5965 (1995).
34. Dekker, R. J. et al. KLF2 provokes a gene expression pattern that establishes functional quiescent differentiation of the endothelium. *Blood* 107, 4354–4363 (2006).
35. SenBanerjee, S. et al. KLF2 Is a novel transcriptional regulator of endothelial proinflammatory activation. *J Exp Med* 199, 1305–1315 (2004).
36. Tiruppathi, C., Malik, A. B., Del Vecchio, P. J., Keese, C. R. & Giaever, I. Electrical method for detection of endothelial cell shape change in real time: assessment of endothelial barrier function. *Proc. Natl. Acad. Sci. USA* 89, 7919–7923 (1992).
37. Giaever, I. & Keese, C. R. Micromotion of mammalian cells measured electrically. *Proc. Natl. Acad. Sci. USA* 88, 7896–7900 (1991).
38. Szulcek, R., Bogaard, H. J. & van Nieuw Amerongen, G. P. Electric cell-substrate impedance sensing for the quantification of endothelial proliferation, barrier function, and motility. *J Vis Exp* 85, e51300 (2014).
39. Galarneau, A. & Richard, S. Target RNA motif and target mRNAs of the Quaking STAR protein. *Nat. Struct. Mol. Biol.* 12, 691–698 (2005).
40. Hafner, M. et al. Transcriptome-wide identification of RNA-binding protein and microRNA

- target sites by PAR-CLIP. *Cell* 141, 129–141 (2010).
41. Kaplan, A. P. & Ghebrehiwet, B. The plasma bradykinin-forming pathways and its interrelationships with complement. *Mol Immunol* 47, 2161–2169 (2010).
  42. Orsenigo, F. et al. Phosphorylation of VE-cadherin is modulated by haemodynamic forces and contributes to the regulation of vascular permeability in vivo. *Nat Commun* 3, 1208 (2012).
  43. Figini, M. et al. Substance P and bradykinin stimulate plasma extravasation in the mouse gastrointestinal tract and pancreas. *Am J Physiol* 272, G785–793 (1997).
  44. Li, Z., Zhang, Y., Li, D. & Feng, Y. Destabilization and mislocalization of myelin basic protein mRNAs in quaking dysmyelination lacking the QKI RNA-binding proteins. *J Neurosci* 20, 4944–4953 (2000).
  45. Zearfoss, N. R., Clingman, C. C., Farley, B. M., McCoig, L. M. & Ryder, S. P. Quaking regulates *Hnrnpa1* expression through its 3' UTR in oligodendrocyte precursor cells. *PLoS Genet* 7, e1001269 (2011).
  46. Yu, F. et al. Post-transcriptional repression of FOXO1 by QKI results in low levels of FOXO1 expression in breast cancer cells. *Oncol Rep* 31, 1459–1465 (2014).
  47. Yang, G. et al. RNA-binding protein quaking, a critical regulator of colon epithelial differentiation and a suppressor of colon cancer. *Gastroenterology* 138, 231–240 e231-235 (2010).
  48. Ji, S. et al. miR-574-5p negatively regulates Qki6/7 to impact beta-catenin/Wnt signalling and the development of colorectal cancer. *Gut* 62, 716–726 (2013).
  49. Ciais, D., Cherradi, N. & Feige, J. J. Multiple functions of tristetraprolin/TIS11 RNA-binding proteins in the regulation of mRNA biogenesis and degradation. *Cell Mol Life Sci* 70, 2031–2044 (2013).
  50. Berkovits, B. D. & Mayr, C. Alternative 3' UTRs act as scaffolds to regulate membrane protein localization. *Nature* 522, 363–367 (2015).
  51. Pullmann, R., Jr. & Rabb, H. HuR and other turnover- and translation-regulatory RNA-binding proteins: implications for the kidney. *Am J Physiol Renal Physiol* 306, F569–576 (2014).
  52. Beuck, C., Qu, S., Fagg, W. S., Ares, M., Jr. & Williamson, J. R. Structural analysis of the quaking homodimerization interface. *J Mol Biol* 423, 766–781 (2012).
  53. Ali, M. & Broadhurst, R. W. Solution Structure of the QUA1 Dimerization Domain of pXqua, the *Xenopus* Ortholog of Quaking. *PloS one* 8, e57345 (2013).
  54. Larocque, D. et al. Nuclear retention of MBP mRNAs in the quaking viable mice. *Neuron* 36, 815–829 (2002).
  55. Seebach, J. et al. Endothelial barrier function under laminar fluid shear stress. *Laboratory investigation* 80, 1819–1831 (2000).
  56. Redmond, L. C. et al. Kruppel-like factor 2 regulated gene expression in mouse embryonic yolk sac erythroid cells. *Blood Cells Mol. Dis.* 47, 1–11 (2011).
  57. Hergenreider, E. et al. Atheroprotective communication between endothelial cells and smooth muscle cells through miRNAs. *Nat Cell Biol* 14, 249–256 (2012).
  58. Artzt, K. & Wu, J. I. STAR trek: An introduction to STAR family proteins and review of quaking (QKI). *Advances in experimental medicine and biology* 693, 1–24 (2010).
  59. Ebersole, T. A., Chen, Q., Justice, M. J. & Artzt, K. The quaking gene product necessary in embryogenesis and myelination combines features of RNA binding and signal transduction proteins. *Nat. Genet.* 12, 260–265 (1996).
  60. Sidman, R. L., Dickie, M. M. & Appel, S. H. Mutant Mice (Quaking and Jimpy) with Deficient Myelination in the Central Nervous System. *Science* 144, 309–311 (1964).





# CHAPTER

# 9

Targeting Quaking ameliorates  
macrophage-induced renal interstitial  
fibrosis and induces alternative splicing  
of pre-mRNA transcripts in  
differentiated macrophages

*Manuscript in preparation*

**Collaborative effort by:**

Ruben G. de Bruin, Gillian Vogel, Jacques M. J. G. Duijs, Jurrien Prins, Roel Bijkerk, Lama Darbelli, Hendrik J.P. van der Zande, Janine M. van Gils, Hetty C. de Boer, Ton J. Rabelink, Anton Jan van Zonneveld, Stéphane Richard #  
Eric P. van der Veer<sup>#</sup>

# Authors share senior authorship

**Abstract**

In the pathophysiologic setting of acute and chronic kidney injury, the excessive activation and recruitment of blood-borne monocytes prompts their differentiation into pro-inflammatory macrophages, a process that leads to progressive glomerulosclerosis and interstitial fibrosis. Importantly, this differentiation of monocytes into macrophages requires the meticulous coordination of gene expression at both the transcriptional and post-transcriptional level. The transcriptomes of these cells are ultimately determined by RNA-binding proteins such as Quaking, that define their pre-mRNA splicing and mRNA transcript patterns. Here, we demonstrate that the specific abrogation of Quaking expression in monocytes, using a recently developed conditional null allele of quaking in mice, is associated with changes in splicing that ameliorates the activation of pro-inflammatory processes due to an inability to fully adopt the pro-inflammatory macrophage phenotype. This led to a reduction of macrophage infiltration and significantly diminished interstitial collagen deposition upon unilateral urethral obstruction. Collectively, diminished Quaking expression in monocytes and macrophages limits renal interstitial fibrosis and is associated with Quaking-mediated alternative splicing of pre-mRNA transcripts in differentiated macrophages. Modulation of the cellular transcriptome by interfering with RBP expression or activity deserves attention as a novel means of limiting disease progression by skewing monocytes towards an anti-inflammatory and anti-fibrotic phenotype.

## Introduction

In the pathophysiologic setting of acute and chronic kidney injury, the recruitment of circulating monocytes has been extensively described to play a central role in driving glomerulosclerosis and interstitial fibrosis<sup>1-3</sup>. The chronic and progressive sclerosis of the kidney, commonly known as chronic kidney disease (CKD) can lead to end-stage renal disease (ESRD) caused by e.g. diabetes, hypertension, ischemia reperfusion injury following kidney transplantation and acute or chronic allograft rejection<sup>4,5</sup> and has a life-time prevalence of approximately 10%<sup>6</sup>. Strikingly, this fibrotic process is directly associated with decreased renal function, necessitating renal-replacement therapies such as dialysis or organ transplantation<sup>7,8</sup>. Furthermore, CKD is associated with a high mortality rate due to an increased risk of cardiovascular events<sup>6,9</sup>. As such, gaining a better understanding of macrophage-induced kidney injury, and their role in the initiation, maintenance and progression of CKD into ESRD represents an unmet clinical need to develop new therapeutic strategies to prevent loss of renal function.

Circulating monocytes serve as potent mediators of inflammation and organ damage by their homing, extravasation and differentiation into tissue macrophages at sites of injury<sup>10,11</sup>. Depending on the local milieu, monocytes differentiate into macrophages that are characterized by distinct capacities to generate pro- and/or anti-inflammatory cytokines, phagocytose dead cells and debris, and instruct adaptive immune responses by presenting antigens. A subset of these circulating monocytes, namely non-classical monocytes, has been implicated in directing processes that are geared towards resolving detrimental organ dysfunction by promoting angiogenesis, tissue remodelling and scar-tissue formation<sup>12</sup>. This well-orchestrated reparative response ideally restores tissue architecture and organ function.

The inflammatory response to tissue injury has been proposed to be primarily coordinated at the post-transcriptional level within immune cells<sup>13,14,15</sup>. In particular microRNAs and RNA-binding proteins (RBPs) are being allocated defining roles in this process due to their capacity to impact RNA stability, localization, (alternative) splicing, and translation<sup>14,16-19</sup>. One such RBP is the signal transduction and activation of RNA (STAR) family member Quaking (QKI), which comprises three main isoforms, termed QKI-5, QKI-6 and QKI-7 based on the length of their respective mRNA. Of note, the differential expression of QKI, which binds to RNA species through a conserved binding motif<sup>20-22</sup> has been demonstrated to dynamically alter the post-transcriptional landscape in microglia, oligodendrocytes, endothelial cells, (smooth) muscle cells, monocytes and macrophages<sup>23-35</sup>, linking changes in QKI expression levels with angiocentric gliomas, schizophrenia, cancer, atherosclerosis, and vascular stenosis respectively.

Recently, we demonstrated that the RBP QKI serves an essential role in orchestrating the transcriptome of monocytes and macrophages by governing pre-mRNA splicing and gene expression in atherosclerosis<sup>36</sup>. Given that

monocyte recruitment and infiltration into the damaged kidney, and subsequent generation of pro-inflammatory cytokines by macrophages is associated with kidney injury and the subsequent fibrotic response, we sought to determine if the specific abrogation of QKI in monocytes could attenuate interstitial fibrosis. Here, we detail our discovery that the attenuation of QKI in monocytes *in vivo*, using a recently generated conditional null allele of *qki* in mice, ameliorates their capacity to drive pro-inflammatory processes, thereby reducing renal interstitial fibrosis upon unilateral urethral obstruction (UUO). We postulate that the modulation of the cellular transcriptome by interfering with RBP expression or activity represents a novel and potent means of shifting cells from a pro-inflammatory and disease-advancing, to an anti-inflammatory and tissue regenerative phenotype.

## Results

### Quaking is abundantly expressed in the kidney

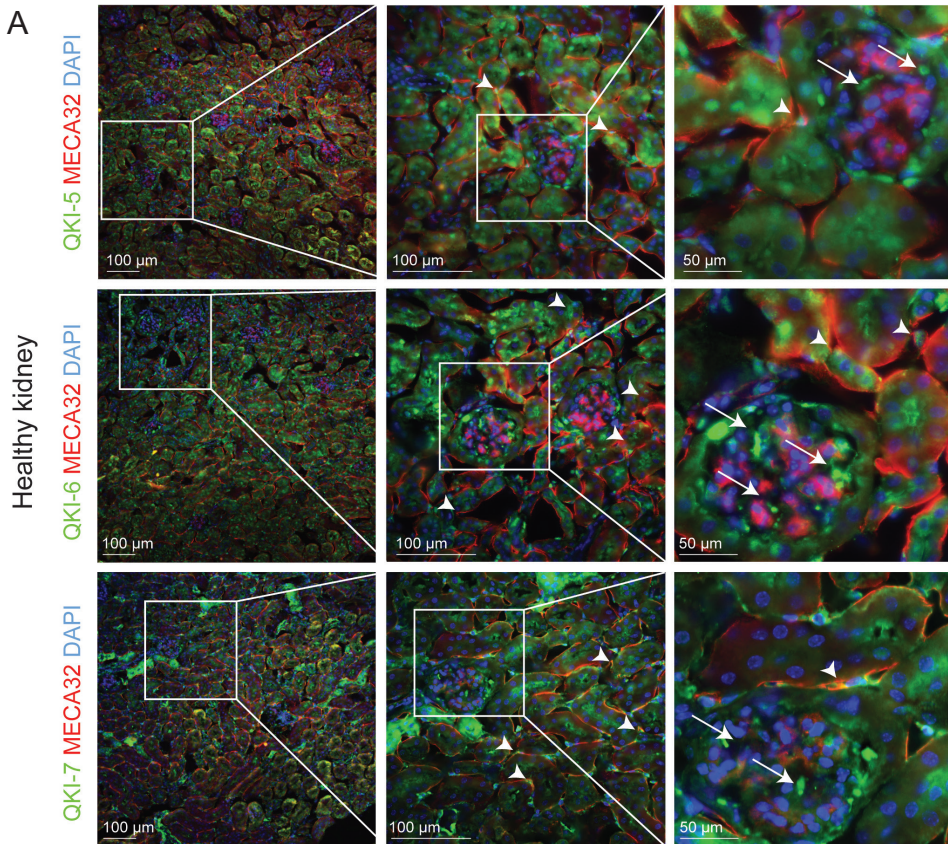
To determine the expression of the QKI protein isoforms within the kidney, we performed immunohistochemistry on cryo-sections of healthy mouse kidneys using antibodies that specifically detect the individual QKI-5, QKI-6 and QKI-7 isoforms, together with the endothelial cell marker MECA-32. As illustrated in Figure 1A, all three QKI isoforms are expressed in tubular epithelial cells, although some tubuli appear void of QKI-7. Also endothelial cells (arrowheads) and a few striking intraglomerular cells (arrows) that are MECA-32 negative, do express QKI. Strikingly, the latter are too few in number to represent either mesangial cells or podocytes. As previously described<sup>25,30,32,34</sup>, QKI-5 and QKI-6 display nuclear enrichment within renal cells, but are also abundantly detected in the cytoplasm of the tubular epithelium. In contrast, QKI-7 is located primarily peri-nuclear and thus cytoplasmic (Figure 1A; arrows lower panels). Given that QKI is regarded as a global regulator of the cellular transcriptome, the expression of QKI in individual cell-types within the kidney could impact their transcriptome and thereby cellular function in a disease setting.

### Macrophages expressing QKI home to the kidney upon injury

Previously we have established that QKI modulates the transcriptome in monocytes and macrophages in atherosclerosis<sup>36</sup>. Following this notion, we next examined if QKI is also involved in the inflammatory response to renal injury. To test this, we performed unilateral urethral obstruction (UUO) in wild-type C57BL6 mice, a kidney injury model that is associated with tubular cell injury, inflammation and elaborate interstitial fibrosis<sup>37</sup>. After 10 days, we harvested RNA and tissue from the damaged (UUO) and contralateral (CLK) kidneys. As expected, we detected increased production of the extracellular matrix protein collagen 1a1 (COL1A1), as well as enhanced intracellular expression of the fibroblast-marker smooth-muscle alpha actin ( $\alpha$ -SMA) in UUO kidneys (Figure 1B), confirming the induction of a vast fibrotic response. While *qki-5* mRNA was most abundant in kidney lysates, and *qki-6* and *qki-7* mRNA's were relatively less expressed (Figure 1C, white bars) and mRNA expression levels of all three QKI variants were significantly increased in fibrotic kidneys as compared to healthy

contra-lateral kidneys (Figure 1C, grey bars), possibly through the influx of inflammatory cells such as bone marrow-derived monocytes and macrophages. It should be mentioned however that other kidney-resident cell types, such as activated fibroblasts that undergo a striking proliferative response<sup>38,39</sup>, could thereby also impact the observed enrichment in QKI mRNA expression levels in UUO kidney lysates. Nevertheless, immunohistochemical analysis revealed high expression of QKI in infiltrating macrophages upon UUO, as evidenced by Pan-QKI (staining all three QKI-isoforms) and F4/80 co-localization in UUO kidneys (Figure 1D, arrowheads). Moreover, M-CSF stimulated bone marrow-derived mouse macrophages were found to abundantly express QKI *in vitro* (Figure 2a, open bars). Next, we determined whether the expression of macrophage-specific markers such as CD115 and F4/80 were augmented in the fibrotic kidneys, profiles that would be indicative of monocyte/macrophage influx (Figure 1B, set of bars at the right). Collectively, these findings suggest that QKI mRNA levels are enriched in the fibrotic kidney due to, at least in part, infiltrating monocytes/macrophages.

**Figure 1**



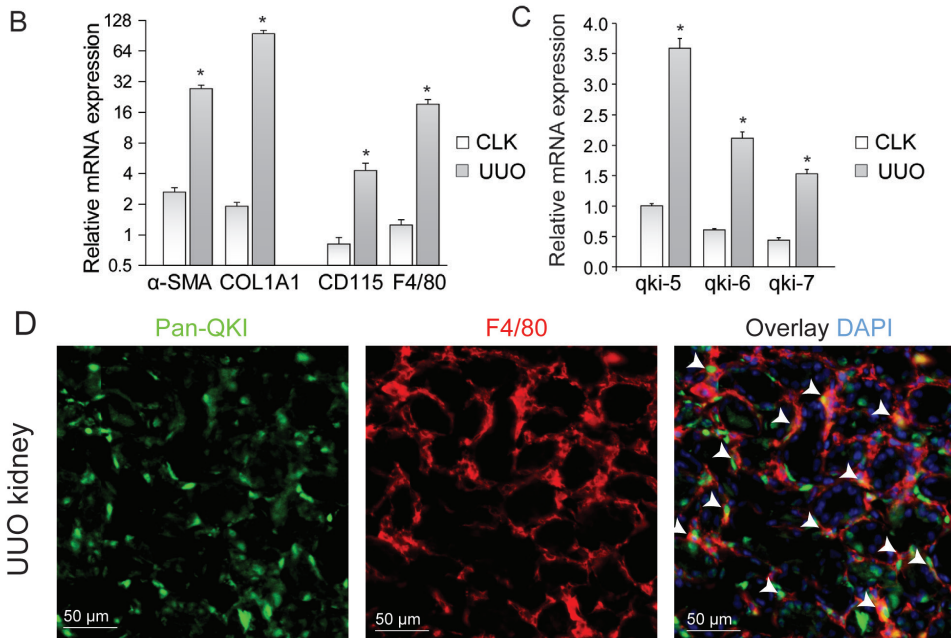


**Figure 1 | QKI is expressed in infiltrating macrophages upon unilateral urethral obstruction.** (A) Immunostaining of mouse kidney cryosections for QKI-5 (green, upper panels), QKI-6 (green, middle panels) and QKI-7 (green, lower panels). Endothelial cells are stained using the MECA-32 antibody in red. Nuclei are stained blue using DAPI. (B) Whole kidney lysates of either CLK or UUO kidneys were assessed for mRNA levels of fibrosis markers (α-SMA, COL1A1) and macrophage markers (CD115, F4/80). (C) Whole kidney lysates are assessed for QKI mRNA levels using qRT-PCR in healthy contralateral kidneys (CLK) as compared to fibrotic kidneys 10 days after UUO. (D) Immunostaining for Pan-QKI (green) and F4/80 (macrophage marker in red) on cryosections of fibrotic kidneys 10 days after UUO. \*  $p \leq 0.05$  by Students' t-test, error bars represent SEM.

### QKI viable mice show decreased interstitial fibrosis upon UUO

Next, we assessed whether a reduction in QKI expression levels could ameliorate the inflammatory response upon kidney injury. For this, we employed the Quaking viable (qkv) mouse, which has previously been described to express reduced levels of QKI throughout its' tissues<sup>40,41</sup> and assessed whether these mice are protected from renal interstitial fibrosis. In vitro, we could validate that QKI mRNA levels were significantly reduced in qkv bone marrow-derived macrophages derived from qkv mice, as compared to WT littermate controls (Figure 2A). Importantly, while fibrotic kidneys harvested from WT littermate controls displayed abundant expression of the macrophage specific markers F4/80 and CD115 10 days after UUO, qkv mouse fibrotic kidneys were characterized by significantly reduced mRNA levels of macrophage specific markers F4/80 and CD115 at day 5 and day 10 (Figure 2B). These results are indicative of reduced monocyte influx and differentiation into macrophages when QKI levels are decreased. The reduction in macrophage content was validated by Western blot analysis of whole-kidney lysates for the macrophage marker CD206, in which decreased expression was



observed in *qkv* kidneys (Figure 2C, quantitation of  $n=7$  mice is presented below). Given the attributing role of infiltrating macrophages in inducing renal fibrosis, we assessed whether the fibrosis markers  $\alpha$ -SMA and COL1A1 mRNA levels were similarly reduced in *qkv* UUO kidneys. Indeed, these markers were substantially less abundant in *qkv* UUO kidneys on the mRNA (Figure 2D) and protein level as assessed by western blot (Figure 2C, upper blot, quantitation of  $n=7$  mice is presented below). To further substantiate these anti-fibrotic effect observed in *qkv* UUO kidneys, we performed Sirius Red staining of paraffin embedded kidney sections to visualise and quantitate all interstitially deposited collagens. These studies clearly showed decreased interstitial fibrosis as evidenced by less collagen staining in *qkv* UUO kidneys as compared to WT-littermate control UUO kidneys (representative photomicrographs are presented in Figure 2E and colorimetric quantitation in Figure 2F). Moreover, a strong correlation between F4/80 and COL1A1 mRNA expression existed (Pearson  $R=0.68$ ,  $p<0.0001$ , Figure 2G). Taken together, these data suggest that ubiquitous reduction of QKI expression leads to reduced macrophage influx and subsequently reduced interstitial fibrosis of the kidney.

Figure 2

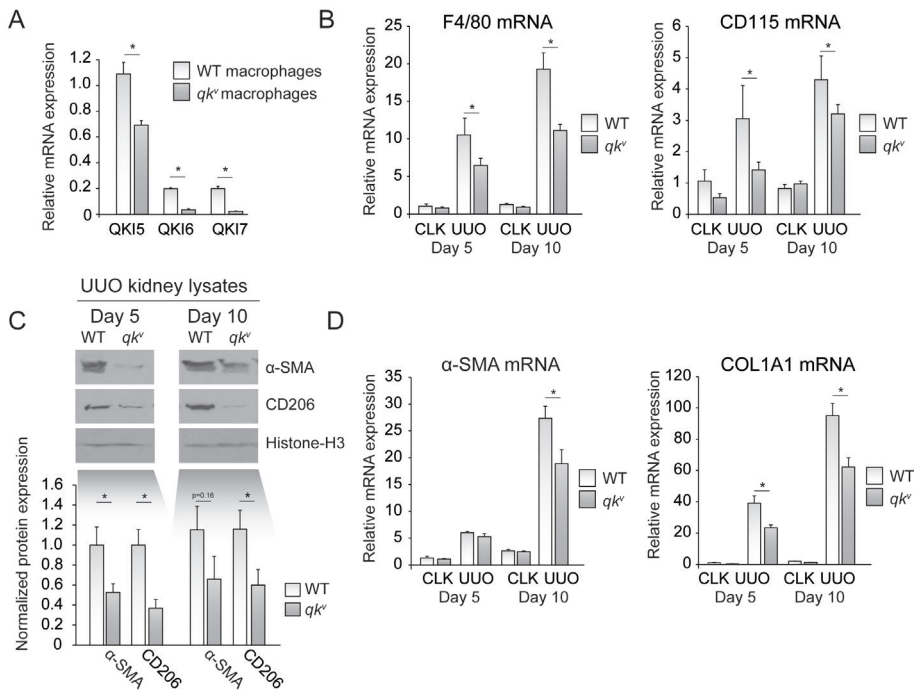
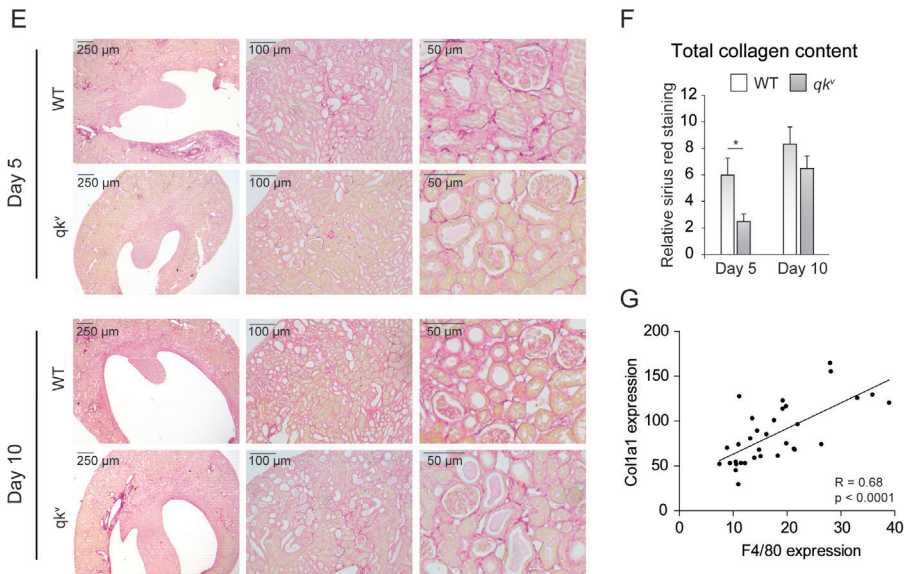


Figure 2 continued



**Figure 2 | Quaking viable mice display decreased macrophage influx and decreased interstitial fibrosis upon unilateral urethral obstruction.** (A) mRNA expression of QKI mRNA levels in cultured macrophages of either Quaking viable (*qkv*) or wild-type (WT) littermate controls. (B) mRNA levels of macrophage markers (F4/80, CD115) in whole kidney lysates derived from either *qkv* mice (grey bars) or WT littermate controls on day 5 and day 10 after UUO. (C) Western blot analysis of whole UUO kidney lysates for  $\alpha$ -SMA, CD206 and Histone-H3. Quantitation using ImageJ software is provided below. (D) mRNA levels of fibrosis markers ( $\alpha$ -SMA and COL1A1) in whole kidney lysates derived from either *qkv* mice (grey bars) or WT littermate controls (open bars) on day 5 and day 10 after UUO. (E) Representative photomicrographs of Sirius Red staining for collagen on 4 micron sections of 5 or 10 day UUO kidneys from either *qkv* or WT littermate controls. (F) Quantitation of Sirius red staining is provided. (G) Pearson R correlation is plotted for COL1A1 and F4/80 expression. \*  $p \leq 0.05$  by Students' t-test, error bars represent SEM.

### Monocyte-specific knockout of QKI ameliorates renal interstitial fibrosis

To test whether the observed effects were cell autonomous to monocytes and macrophages and not the result of a reduction of QKI in e.g. interstitial fibroblasts or renal epithelial cells, we generated *qkl<sup>FL/FL</sup>;LysM-cre* mice, yielding a monocyte/macrophage specific reduction of QKI (Figure 3A). These genetically modified *qkl<sup>FL/FL</sup>;LysM-cre* mice constitutively express a Cre-recombinase driven by the LysM promoter (also described as *Lyz2*), yielding monocyte/macrophage-specific Cre-recombinase expression<sup>42</sup>. The presence of loxP sites flanking the genomic DNA sequence encoding exon 2 of the *qkl* gene induces an exonic frame-shift that generates a premature stop codon in exon 3, leading to the monocyte-specific abrogation of all QKI protein isoforms that are generated by extensive



Figure 3

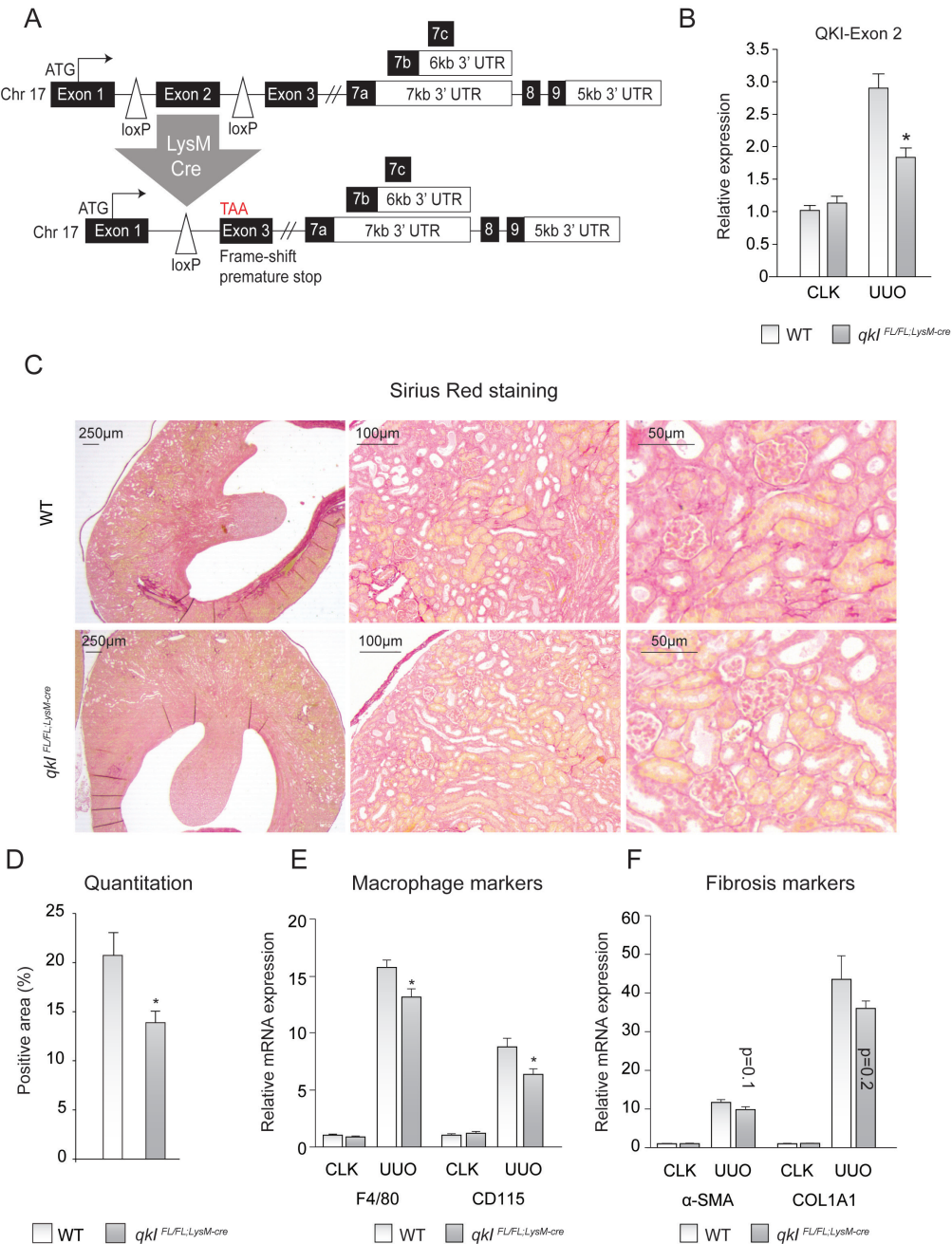


**Figure 3 | Monocyte specific knockout of QKI ameliorates interstitial fibrosis upon unilateral urethral obstruction.** (A) Schematic representing the genomic architecture of the conditional QKI knockout mouse (not to scale). (B) mRNA levels of the floxed exon 2 of the QKI mRNA in 10 day CLK and UUO kidneys. (C) Sirius red staining for collagen in 4 micron sections of 10 day UUO kidneys derived from *qkl*<sup>FL/FL;LysM-cre</sup> or WT littermate controls. (D) Colorimetric quantitation of Sirius Red staining using ImageJ software. (E) mRNA levels of macrophage markers (CD115,

F4/80) in whole kidney lysates derived from either  $qkl^{FL/FL;LysM-cre}$  fl mice (grey bars) or WT littermate controls (open bars) on day 10 after UUO. (F) mRNA levels of fibrosis markers ( $\alpha$ -SMA, COL1A1) in whole kidney lysates derived from either  $qkl^{FL/FL;LysM-cre}$  fl mice (grey bars) or WT littermate controls (open bars) on day 10 after UUO. \*  $p \leq 0.05$  by Students' t-test, error bars represent SEM.

alternative splicing of their 3' end (as illustrated in figure 3A). Although the LysM-driven LoxP-recombination event doesn't terminate transcription of the  $qkl$  locus in the non-myeloid cells of the kidney, mRNA levels of the floxed exon 2 were significantly reduced in whole kidney lysates of  $qkl^{FL/FL;LysM-cre}$  UUO kidneys (Figure 3B). Moreover, this demonstrates that the recombination event is specifically induced in infiltrating cells in UUO kidneys and not in contralateral kidneys that are void of infiltrating cells. We subsequently assessed whether these mice are protected from UUO-induced kidney fibrosis, similar to the  $qkv$  mice. Indeed,  $qkl^{FL/FL;LysM-cre}$  mice also showed reduced interstitial fibrosis as evidenced by decreased sirius red staining (representative photomicrographs are shown in Figure 3C and quantitation is provided in Figure 3D). Furthermore, mRNA levels of the macrophage markers F4/80 and CD115 were significantly reduced in  $qkl^{FL/FL;LysM-cre}$  fibrotic kidneys (Figure 3E), whereas the fibrosis genes  $\alpha$ -SMA and COL1A1 only showed a trend towards reduced expression levels in  $qkl^{FL/FL;LysM-cre}$  UUO kidneys (Figure 3F). These data further support our hypothesis that it is the expression of QKI in monocytes and macrophages that contributes to the formation of interstitial fibrosis upon UUO.

### QKI mediates alternative splicing of genes involved in macrophage function

Given that extensive literature exists regarding a role for QKI in guiding alternative splicing of pre-mRNA transcripts<sup>21,23,24,29,32,33,35</sup>, we assessed whether these effects could similarly be affected macrophages from  $qkl^{FL/FL;LysM-cre}$  mice. To this end we cultured bone marrow-derived macrophages using M-CSF stimulation (Figure 4A). Indeed, using an N-terminal antibody that detects all three QKI isoforms, QKI was almost completely abrogated in these cultured macrophages (Figure 3C). Surprisingly, an aspecific band is visible in  $qkl^{FL/FL;LysM-cre}$  lysates, either resembling cross-reactivity of the antibody to other KH-domain containing RBPs when used for western blot analysis or subtotal recombination in this culture.

Using PCR and primers in the exons flanking the exon of interest, we could show several striking alternative splicing events regulated by QKI, including  $\gamma$ -adducin (ADD3), protein tyrosine phosphatase receptor type O (PTPRO), Fibroblast Growth Factor Receptor 1 Oncogene Partner 2 (FGFR1OP2) and RalBP1-associated Eps domain-containing protein 1 (REPS1) (Figure 4C, quantitation in Figure 4E). Moreover, in silico analysis of the splicing events clearly demonstrated that the presence of a quaking binding site (QBS), defined as an ACUAA/AUUAA nucleotide motif, exerted position-dependent effects as evidenced by the alternative splicing of cassette exons upon QKI depletion. As illustrated in Figure 4D, a QBS located upstream of the ADD3 and PTPRO cassette exons indicate that in the presence of QKI, binding of QKI to this motif induces exon skipping. In contrast, diminished expression of QKI in  $qkl^{FL/FL;LysM-cre}$  macrophages limits the interaction of QKI at these QBSs, thereby decreasing exon skipping and favouring exon inclusion. This effect is reversed when a QBS is located downstream of

the cassette exon, such as within the *FGFR1OP2* gene. In this setting, exon skipping is favoured in the *qkl*<sup>FL/FL;LysM-cre</sup> macrophages. Finally, the *REPS1* gene illustrates that the presence of a QBS both upstream and downstream of the cassette exon appears to promote exon skipping in WT macrophages. These findings show that the removal of QKI causes a drastic switch in mRNA isoforms encoding *ADD3*, *PTPRO*, *FGFR1OP2* and *REPS1*, that may be responsible for the observed anti-fibrotic phenotype.

Figure 4

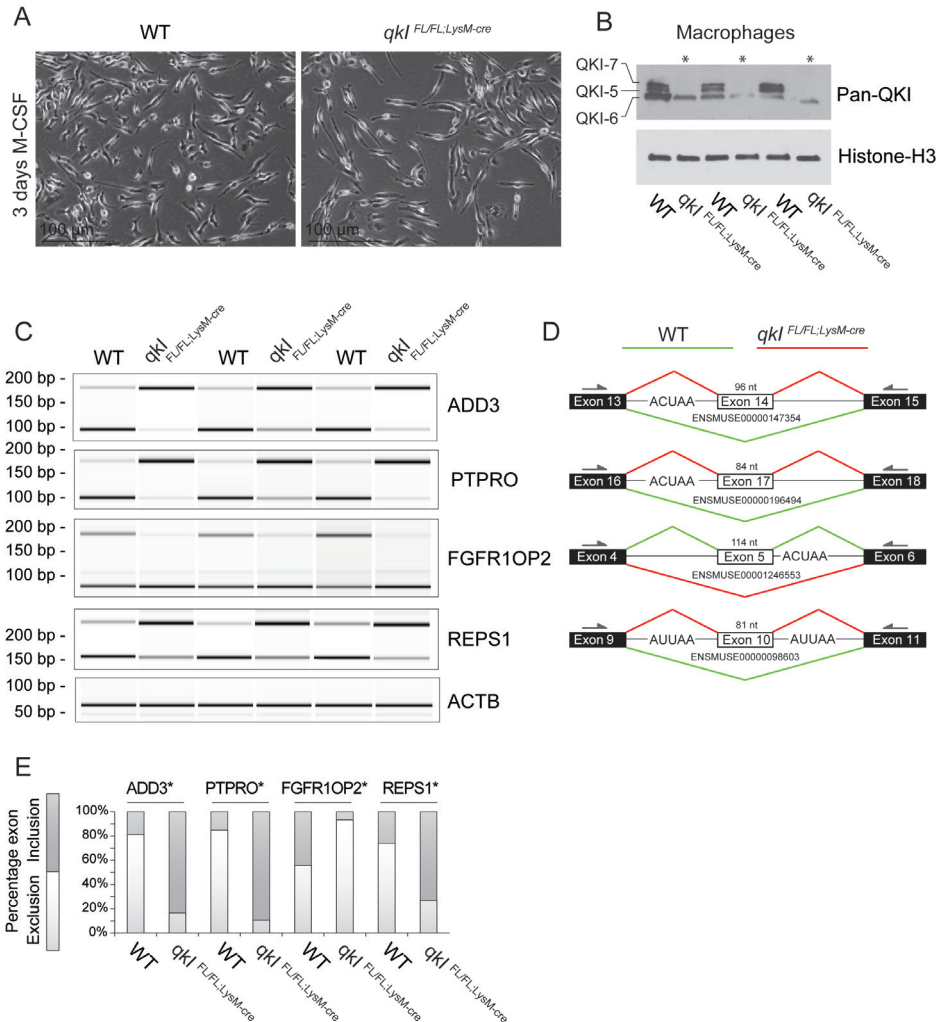


**Figure 4 | QKI mediates alternative splicing in macrophages** (A) Photomicrographs of cultured bone marrow-derived macrophages 3 days after M-CSF stimulation. (B) Western blot analysis of cultured mouse macrophages from *qkl*<sup>FL/FL;LysM-cre</sup> or WT littermate controls using a pan-qki (N-terminal) antibody and HistoneH3 loading control. (C) PCR analysis of cassette exon alternative splicing in 5 days M-CSF stimulated cultured macrophages derived from either WT or *qkl*<sup>FL/FL</sup>

FL<sup>LysM-cre</sup> mouse bone marrow. Gel electrophoresis of PCR products generated using primers in flanking exons are shown, illustrating the abundance of alternative mRNA isoforms expressed. (E) Densometric quantitation using ImageJ software and statistical testing is provided for the assessed splicing events. (D) In silico analysis of the particular exon assessed illustrates the predicted alternative splicing event based on QBS position (defined as an ACUAA/AUUAA motif) and denotes the predominant splicing event in WT (green line) or qkl<sup>FL<sup>LysM-cre</sup></sup> (red line) macrophages. \* p≤0.05 by Students' t-test.

## Discussion

The well-coordinated recruitment of monocytes to sites of tissue injury represents a critical aspect of damage resolution, while their excessive recruitment and conversion into macrophages is disease-advancing. Within the kidney, the monocyte plays a central role following acute kidney injury, while the macrophage drives inflammatory pathways that enhance fibrotic responses that are a hallmark of chronic kidney disease<sup>1,5,7,43</sup>. Here, we identified that the targeted reduction of the RNA-binding protein QKI, in two distinct mouse models skews these myeloid cells into an anti-inflammatory and anti-fibrotic phenotype. Moreover, a cell autonomous reduction of QKI decreased monocyte influx upon kidney damage. Previously, a pivotal role of QKI in mediating alternative splicing and gene expression has been demonstrated, thereby determining cellular phenotype and function<sup>23,24,29,32,33,35</sup>. In this study we were able to identify several key splicing events in this recently developed conditional QKI knockout mouse, further substantiating the role of QKI in pre-mRNA splicing. Interestingly, the presence of a QBS upstream and downstream of the cassette exon in the REPS1 pre-mRNA, illustrates that it cannot be excluded that competition with other splicing factors or e.g. the secondary structure of the pre-mRNA influences effect that QKI exerts on a particular alternative splicing event. Moreover, the recent discovery that QKI also mediates the generation of circular RNAs through a splicing-dependent mechanism when a QBS is present upstream and downstream of an exon, such as in the REPS-1 mRNA, opens another interesting avenue of investigation<sup>29</sup>. Our identification that QKI expression levels potently mediate alternative splicing in the ADD3 locus, a structural cytoskeletal protein that influences the cortical actin layer<sup>44</sup>, could very well influence the homing of monocytes to the injured kidney. Moreover, PTPRO, a tyrosine phosphatase, has been shown to localise to the cellular “integrin adhesome”<sup>45</sup>, which is essential in monocyte adhesion and migration<sup>46</sup>. PTPRO has furthermore been implicated in ischemia reperfusion injury of the liver by activating Nuclear factor-κB (NF-κB)<sup>47</sup> and thereby the classical or non-classical activation of monocytes/macrophages<sup>48,49</sup>. Interestingly, FGFR1OP2 is extensively investigated in the context of hematopoietic malignancies including acute myeloid leukemia and myelomonocytic leukemia where it is involved in monocyte precursor differentiation in the bone marrow<sup>50-52</sup>. The conclusion that the described alternative splicing events and their resulting protein isoforms contribute to proper physiological monocyte/macrophage function is likely, but remains to be fully elucidated.

It is tempting to speculate that a reduction of QKI expression levels not only affects the phenotype of monocytes and infiltrating macrophages, but could also skew these cells towards a tissue-regenerative and fibrosis-ameliorating function. Although some controversy still exists about the exact role of monocytes and macrophages in organ fibrosis, it has been suggested that macrophages can also contribute to the resolution of fibrosis by affecting myofibroblast function and enhancing matrix metalloproteinase (MMP) and collagenase expression, while concomitantly decreasing the expression of tissue inhibitors of MMPs (TIMPs)<sup>53-55</sup>. While numerous studies have provided evidence that organ fibrosis can be reversed<sup>56-62</sup>, a limited number of studies have actually shown regression or resolution of fibrotic lesions in the renal compartment<sup>63-65</sup>. Recently, Sugimoto and colleagues provided evidence of effective renal fibrosis resolution following the administration of an activator of Activin-like kinase 3 (ALK3/BMPRI1A), namely THR-123<sup>66</sup>. Similar to our observation that a reduction of QKI in a monocyte-specific fashion reduces monocyte infiltration, inflammation and kidney fibrosis, the THR-123 treatment regimen employed, lead to a decrease in monocyte influx and a reversal of kidney fibrosis *in vivo*. Similarly, our lab previously identified that modifying the transcriptome bone marrow cells by hematopoietic overexpression of microRNA-126, exerts anti-inflammatory and anti-fibrotic effects *in vivo*. We therefore propose that monocytes and macrophages are the ideal cell type of which the cellular phenotype can be tailored to ameliorate or even direct reversal of kidney fibrosis.

At present, abrogating the expression or activity of RNA-binding proteins does not yet belong to the list of therapeutic modalities utilized for limiting disease progression in general. This could potentially be due to their upstream hierarchical position in guiding cellular transcriptomes in health and disease. Nonetheless, our data suggest that targeting QKI in the monocyte could be an effective means of limiting their adhesion, extravasation and differentiation at sites of kidney injury. To achieve this goal, several technologies could be implemented, namely: 1) naked or lipid-encapsulated siRNAs to target RBPs (reviewed in <sup>67</sup>); 2) pRNAs and RNAaptamer-based approaches <sup>68-70</sup>; and 3) RNA-based antisense oligonucleotides.

In conclusion, we have identified that the RNA-binding protein QKI impacts the phenotype of infiltrating macrophages and their capacity to drive inflammatory processes in the setting of kidney injury. As opposed to triggering pro-inflammatory cascades, limiting QKI expression in monocytes and macrophages could serve as an effective means of limiting renal fibrosis in the damaged kidney.

## Material and Methods

### Cell culture

Mouse macrophages were derived from whole bonemarrow samples of mouse femurs. Cells were plated in 6 well plates at a density of  $2 \times 10^6$  cells per well in RPMI medium containing 100 U/ml penicillin, 100 U/ml streptomycin, 300 µg/ml glutamin (Gibco) and 10% fetal calf serum (Cambrex). Additionally, 10ng/ml recombinant mouse M-CSF (Peprotech) was added to differentiate the cells into macrophages in 7 days. Medium was changed once after 3 days. Monocytes were isolated using MACS-technology using the CD115 positive selection kit for mouse monocytes (Myltenyi).

9

Antibody	Manufacturer	Cat nr	Application
Rabbit α-QKI-5	Millipore	AB9904	WB + IF
Rabbit α-QKI-6	Millipore	AB9906	IF
Rabbit α-QKI-7	Millipore	AB9908	IF
Rat α-Meca-32	BD Pharmingen	550563	IF
Rat α-F4/80	Abcam	ab6640	IF
Mouse α-Pan-QKI	Neuromab	75-168	WB
Mouse α-QKI-5	Neuromab	73-232	WB
Mouse α-QKI-6	Neuromab	73-190	WB
Mouse α-QKI-7	Neuromab	73-200	WB
Rabbit α-CD206	Abcam	ab64693	WB
Mouse α-αSMA	Abcam	ab7817	WB
Rabbit α-HistoneH3	Abcam	ab1791	WB

### Western blot analysis

A quarter of a kidney was homogenised using a IKA® tissue homogeniser in 500ul RIPA buffer (Sigma Aldrich) containing Complete® protease inhibitors (Roche). Subsequently, a Pierce BCA protein assay (Thermo Scientific) was performed to assess the absolute quantity of protein in each sample. Next 10-40 micrograms of total protein lysate was loaded per lane on precast Any-kD acrylamide gels (Bio-rad) for gel-electrophoresis. Using the Trans-Blot® Turbo™ Transfer system (Bio-rad), protein was transferred to Nitrocellulose (Bio-rad) membranes for further analysis. Membranes were blocked and antibodies incubated o/n at 4°C in 5% skim milk powder (Nutricia) in PBS. The appropriate HRP-labeled secondary antibodies (Dako) were incubated for 1 hour at room temperature, followed by extensive washing with PBS. Band-visualisation was achieved using SuperSignal West-Dura® Extended Duration Substrate (Thermo Scientific) for HRP. Next, exposure on UltraCruz® Autoradiography Film or KODAK-XAR film and development by a Konica developer followed. Finally, band-intensities were quantified using ImageJ software.

### RNA isolation, cDNA synthesis and qRT-PCR analysis

A quarter of a kidney was lysed in Trizol Reagent (Invitrogen) using an electrical tissue homogeniser (IKA®). Subsequently, chloroform and ethanol were used to phase-separate the RNA and subsequently RNeasy mini-columns (Qiagen)



were used to further purify the RNA according to manufacturers' guidelines. A on-column DNase step was also performed to eliminate any contaminating genomic DNA. cDNA synthesis was performed using 1ug RNA, random primers, FS-buffer, DNTs, M-MLV-RT in the presence of RNAsin according to the manufacturers' guidelines (all Promega products). qRT-PCR was performed using SYBR-select (Invitrogen) and PCR was run on a Biorad CFX-384. Relative mRNA expression was calculated using the  $\Delta\Delta CT$  method, and was normalised to GAPDH mRNA levels. PCR products generated by the splicing primers were run on an Agilent Bioanalyzer for quantitative analysis. Primer pairs used are listed below.

### mRNA expression & splicing primers 5' - 3'

FW-QKI5	GTGTATTAGGTGCGGTGGCT
REV-QKI5	ATAGGTTAGTTGCCGGTGGC
FW-QKI6	ACCTAGTGGTGTATTAGGTATGGCT
REV-QKI6	CCGGAGGCTGCTGAGACTA
FW-QKI7	ACATTGGCACCAGCTACATCA
REV-QKI7	CAGCAAGTCAATGGGCTGAAAT
FW-EMR1	CCTGGACGAATCCTGTGAAG
REV-EMR1	GGTGGGACCACAGAGAGTTG
FW-CD115	AGAGTGATGTGTGGTCTAC
REV-CD115	GTTAGCATAGTCCTGGTCTC
FW-COL1A1	TGACTGGAAGAGCGGAGAGT
REV-COL1A1	GTTCCGGGCTGATGTACCACT
FW-aSMA	CTGACAGAGGCACCACTGAA
REV-aSMA	CATCTCCAGAGTCCAGCACA
FW-exon2-QKI	GGTGGGACCCATTGTTTCAGT
REV-exon5-QKI	AGGCTGTCTTCACCTTCAGC
FW-GAPDH	ACTCCCACTCTTCACCTTC
REV-GAPDH	CACCACCCTGTTGCTGTAG
FW-ACTB	AGGTCATCACTATTGGCAACGA
REV-ACTB	CCAAGAAGGAAGGCTGGAAAA
FW-ADD3-splicing	CCACCTCCTGGAAGGAGAAC
REV-ADD3-splicing	CATGGAGGTGAAGCTCTTGGA
FW-PTPRO-splicing	ATGTGGAGCTGGCACGTTTG
REV-PTPRO-splicing	ACGGGGTTTGTAGTTTCCTCT
FW-FGFR1OP2-splicing	CATGGCCAGCAAGAAAGATGAC
REV-FGFR1OP2-splicing	TTTGGTCAACATGTGCTTGC
FW-REPS1-splicing	AGCCAGGTGAGGTAGGTTACT
REV-REPS1-splicing	CTGCATGTGGATTTTGCTTGGA

## Conditional mouse design and genotyping

The mouse *qki* conditional null allele was constructed using a previously described targeting vector<sup>71,72</sup>. The final genomic organisation is depicted in Figure 3A with two loxP sequences flanking exon 2 of the *qki* gene. Ear biopsies were used to isolate gDNA using the AccuStart II PCR Genotyping Kit (Quanta-Bio) for genotyping using primers listed in the table below. The appropriate genotype, as well as successful recombination was always verified by PCR in every mouse. The conditional mouse model is further validated in previous studies within our labs<sup>23</sup>.

### Genotyping primers 5' - 3'

FW-QKI-flox	ACAGAGGCTTTTCCTGACCA
REV-QKI-flox	TTCAGAACCCCCACATTACC
FW-QKI-recombination	CCTGGAATGGTGCTTTCCTA
REV-QKI-recombination	TTCAGAACCCCCACATTACC
FW-quaking viable genotyping	TCTAAAGAGCATTTCGAAGT
REV-quaking viable genotyping	TTGCTAACTGAATATTACT

### Immunohistochemistry

Fluorescent stainings were all performed on mouse kidney cryosections that were obtained by freezing tissue samples embedded in O.C.T. (TissueTek®) in a mold and placing the mold in an Isopentane solution cooled by Liquid nitrogen. Next, 4 micron sections were cut using a cryostat (Leica), slides were air-dried for 30 minutes, then fixed in actone for 10 minutes at room temperature, air-dried again for 30 minutes and stored at -20°C. Before staining, slides were washed three times in PBS at room temperature. Thereafter put in blocking buffer (PBS+1%BSA + 1% FCS) for at least 1 hour at room temperature. Slides were incubated with primary antibodies in blocking buffer for at least 3 hours at room temperature or at 4°C o/n, whereafter extensive washing in PBS followed and subsequently incubated with the appropriate Alexa® (Invitrogen) labelled secondary antibodies in blocking buffer. Embedding the slides was done in Pro-Long gold (Invitrogen) containing DAPI. Imaging was performed on a Leica DM5500 or a Leica SP5 confocal imaging system.

Histochemistry analysis for collagen content was done using Picosirius red staining on formalin fixed, paraffin embedded tissues. CLK and UUO kidneys were fixed in 3,7% formalin in PBS for 2 hours then put on 70% ethanol and subsequently dehydrated o/n followed by paraffin embedding according to standard hospital protocols. For analyses 4 micron sections were cut. Prior to staining, slides were brought to water by first deparaffinising in Xylene, then taken through a series of solutions decreasing in ethanol percentage (100% to 50%) in 10% steps taking 5 minutes at a time, finally incubation in H<sub>2</sub>O for half an hour. Slides were submerged in Sirius Red F3B solution (0.1% Direct Red 80, Sigma Aldrich) in a saturated aqueous solution of picric acid for 1 hour at room temperature. Slides were washed in 3 stages of acidified water consisting of 5 ml glacial acetic acid (Millipore) in 1 liter of H<sub>2</sub>O (Braun). After this, slides were dehydrated to 100%



ethanol and thereafter Xylene, then embedded in Entellan. Images were taken using a Leica DMI4400B microscope and collagen deposition was quantified using ImageJ software. Outliers were removed using an statistical outlier test.

### **Statistical analysis**

All data was statistically tested using a two-tailed Students' t-test. Error bars in all figures represent SEM.

### **Mouse studies**

All mouse studies were approved and performed according to the guidelines of the relevant authorities of the Leiden University Medical Center/Leiden University in The Netherlands or the Lady Davis Institute/McGill University, Montreal, Canada. Unilateral Urethral Obstruction was performed as described earlier<sup>37</sup>.

### **Acknowledgements**

We gratefully acknowledge funding by the Netherlands Institute for Regenerative Medicine to (Grant no: FES0908). We also acknowledge a private research endowment to EV. Also, we thank Dr. Koren K. Mann for in depth discussions, materials and practical help culturing mouse macrophages. Lastly, we acknowledge the staff of the small animal research facilities of both the Lady Davis Institute and the Leiden University Medical Center.

### **Author contributions**

RB, GV, JD, JP, RB, LD, EV, JG and HZ performed experiments included in the manuscript. RB, GV, AZ, SR, EV designed the experiments and edited the manuscript. RB composed all the figures. JG, HB and TR contributed through in depth discussions, experimental advice and revision of the manuscript. AJ, SR and EV provided funding.

### **Author disclosures**

All authors have no competing financial interest related to this research

## References

- 1 Anders, H.-J. & Ryu, M. Renal microenvironments and macrophage phenotypes determine progression or resolution of renal inflammation and fibrosis. *Kidney international* 80, 915-925 (2011).
- 2 Lin, S. L., Castaño, A. P., Nowlin, B. T., Lupher, M. L. & Duffield, J. S. Bone marrow Ly6Chigh monocytes are selectively recruited to injured kidney and differentiate into functionally distinct populations. *The Journal of Immunology* 183, 6733-6743 (2009).
- 3 Wada, T. et al. Involvement of bone-marrow-derived cells in kidney fibrosis. *Clinical and experimental nephrology* 15, 8-13 (2011).
- 4 Rogers, N. M., Ferenbach, D. A., Isenberg, J. S., Thomson, A. W. & Hughes, J. Dendritic cells and macrophages in the kidney: a spectrum of good and evil. *Nature reviews. Nephrology* 10, 625-643, doi:10.1038/nrneph.2014.170 (2014).
- 5 Meng, X. M., Nikolic-Paterson, D. J. & Lan, H. Y. Inflammatory processes in renal fibrosis. *Nature reviews. Nephrology* 10, 493-503, doi:10.1038/nrneph.2014.114 (2014).
- 6 Coresh, J. et al. Prevalence of chronic kidney disease in the United States. *Jama* 298, 2038-2047, doi:10.1001/jama.298.17.2038 (2007).
- 7 Zeisberg, M. & Neilson, E. G. Mechanisms of tubulointerstitial fibrosis. *J Am Soc Nephrol* 21, 1819-1834, doi:10.1681/ASN.2010080793 (2010).
- 8 Levey, A. S. & Coresh, J. Chronic kidney disease. *The Lancet* 379, 165-180 (2012).
- 9 Foley, R. N., Parfrey, P. S. & Sarnak, M. J. Epidemiology of cardiovascular disease in chronic renal disease. *J Am Soc Nephrol* 9, S16-23 (1998).
- 10 Shi, C. & Pamer, E. G. Monocyte recruitment during infection and inflammation. *Nature reviews. Immunology* 11, 762-774, doi:10.1038/nri3070 (2011).
- 11 Geissmann, F. et al. Development of monocytes, macrophages, and dendritic cells. *Science* 327, 656-661 (2010).
- 12 Murray, P. J. & Wynn, T. A. Protective and pathogenic functions of macrophage subsets. *Nature reviews. Immunology* 11, 723-737, doi:10.1038/nri3073 (2011).
- 13 Kafasla, P., Karakasiliotis, I. & Kontoyiannis, D. L. Decoding the functions of post-transcriptional regulators in the determination of inflammatory states: focus on macrophage activation. *Wiley Interdiscip Rev Syst Biol Med* 4, 509-523, doi:10.1002/wsbm.1179 (2012).
- 14 Kafasla, P., Skliris, A. & Kontoyiannis, D. L. Post-transcriptional coordination of immunological responses by RNA-binding proteins. *Nature immunology* 15, 492-502, doi:10.1038/ni.2884 (2014).
- 15 de Klerk, E. & t Hoen, P. A. Alternative mRNA transcription, processing, and translation: insights from RNA sequencing. *Trends Genet* 31, 128-139, doi:10.1016/j.tig.2015.01.001 (2015).
- 16 Anderson, P. Post-transcriptional control of cytokine production. *Nature immunology* 9, 353-359, doi:10.1038/ni1584 (2008).
- 17 Leppek, K. et al. Roquin promotes constitutive mRNA decay via a conserved class of stem-loop recognition motifs. *Cell* 153, 869-881, doi:10.1016/j.cell.2013.04.016 (2013).
- 18 Contreras, J. & Rao, D. MicroRNAs in inflammation and immune responses. *Leukemia* 26, 404-413 (2012).
- 19 Nilsen, T. W. & Graveley, B. R. Expansion of the eukaryotic proteome by alternative splicing. *Nature* 463, 457-463, doi:10.1038/nature08909 (2010).

- 20 Galarneau, A. & Richard, S. Target RNA motif and target mRNAs of the Quaking STAR protein. *Nature structural & molecular biology* 12, 691-698, doi:10.1038/nsmb963 (2005).
- 21 Hafner, M. et al. Transcriptome-wide identification of RNA-binding protein and microRNA target sites by PAR-CLIP. *Cell* 141, 129-141, doi:10.1016/j.cell.2010.03.009 (2010).
- 22 Ray, D. et al. A compendium of RNA-binding motifs for decoding gene regulation. *Nature* 499, 172-177, doi:10.1038/nature12311 (2013).
- 23 Darbelli, L., Vogel, G., Almazan, G. & Richard, S. Quaking Regulates Neurofascin 155 Expression for Myelin and Axoglial Junction Maintenance. *The Journal of neuroscience : the official journal of the Society for Neuroscience* 36, 4106-4120, doi:10.1523/JNEUROSCI.3529-15.2016 (2016).
- 24 Darbelli, L. & Richard, S. Emerging functions of the Quaking RNA-binding proteins and link to human diseases. *Wiley interdisciplinary reviews. RNA* 7, 399-412, doi:10.1002/wrna.1344 (2016).
- 25 Larocque, D. et al. The QKI-6 and QKI-7 RNA binding proteins block proliferation and promote Schwann cell myelination. *PloS one* 4, e5867 (2009).
- 26 Aberg, K., Saetre, P., Jareborg, N. & Jazin, E. Human QKI, a potential regulator of mRNA expression of human oligodendrocyte-related genes involved in schizophrenia. *Proceedings of the National Academy of Sciences of the United States of America* 103, 7482-7487, doi:10.1073/pnas.0601213103 (2006).
- 27 Bandopadhyay, P. et al. MYB-QKI rearrangements in angiocentric glioma drive tumorigenicity through a tripartite mechanism. *Nature genetics* 48, 273-282, doi:10.1038/ng.3500 (2016).
- 28 Chen, A.-J. et al. STAR RNA-binding protein Quaking suppresses cancer via stabilization of specific miRNA. *Genes & development* 26, 1459-1472 (2012).
- 29 Conn, S. J. et al. The RNA binding protein quaking regulates formation of circRNAs. *Cell* 160, 1125-1134 (2015).
- 30 Larocque, D. et al. Nuclear retention of MBP mRNAs in the quaking viable mice. *Neuron* 36, 815-829 (2002).
- 31 de Bruin, R. G. et al. The RNA-binding protein quaking maintains endothelial barrier function and affects VE-cadherin and  $\beta$ -catenin protein expression. *Scientific Reports* 6, 21643 (2016).
- 32 Hall, M. P. et al. Quaking and PTB control overlapping splicing regulatory networks during muscle cell differentiation. *Rna* 19, 627-638 (2013).
- 33 van der Veer, E. P. et al. Quaking, an RNA-binding protein, is a critical regulator of vascular smooth muscle cell phenotype. *Circulation research* 113, 1065-1075, doi:10.1161/CIRCRESAHA.113.301302 (2013).
- 34 Wang, Y., Vogel, G., Yu, Z. & Richard, S. The QKI-5 and QKI-6 RNA binding proteins regulate the expression of microRNA 7 in glial cells. *Molecular and cellular biology* 33, 1233-1243 (2013).
- 35 Zong, F.-Y. et al. The RNA-binding protein QKI suppresses cancer-associated aberrant splicing. *PLoS genetics* 10, e1004289 (2014).
- 36 de Bruin, R. G. et al. Quaking promotes monocyte differentiation into pro-atherogenic macrophages by controlling pre-mRNA splicing and gene expression. *Nature communications* 7, 10846, doi:10.1038/ncomms10846 (2016).
- 37 Bijkerk, R. et al. Silencing of microRNA-132 reduces renal fibrosis by selectively inhibiting myofibroblast proliferation. *Kidney Int* 89, 1268-1280, doi:10.1016/j.kint.2016.01.029

- 38 Bijkerk, R. et al. Silencing of Pericyte MicroRNA-132 Reduces Renal Fibrosis and Myofibroblast Proliferation and is Associated with Altered Sirt1 and Cox2 Expression. *MicroRNAs in Kidney Health and Disease*, 103 (2013).
- 39 Humphreys, B. D. et al. Fate tracing reveals the pericyte and not epithelial origin of myofibroblasts in kidney fibrosis. *The American journal of pathology* 176, 85-97 (2010).
- 40 Li, Z. et al. Defective smooth muscle development in qkl-deficient mice. *Development, growth & differentiation* 45, 449-462 (2003).
- 41 Sidman, R. L., Dickie, M. M. & Appel, S. H. Mutant mice (quaking and jimpy) with deficient myelination in the central nervous system. *Science* 144, 309-311 (1964).
- 42 Odegaard, J. I. et al. Macrophage-specific PPAR $\alpha$  controls alternative activation and improves insulin resistance. *Nature* 447, 1116-1120 (2007).
- 43 Engel, D. R. et al. CX3CR1 reduces kidney fibrosis by inhibiting local proliferation of profibrotic macrophages. *Journal of immunology* 194, 1628-1638, doi:10.4049/jimmunol.1402149 (2015).
- 44 Matsuoka, Y., Li, X. & Bennett, V. Adducin: structure, function and regulation. *Cellular and molecular life sciences : CMLS* 57, 884-895, doi:10.1007/PL00000731 (2000).
- 45 Winograd-Katz, S. E., Fassler, R., Geiger, B. & Legate, K. R. The integrin adhesome: from genes and proteins to human disease. *Nature reviews. Molecular cell biology* 15, 273-288, doi:10.1038/nrm3769 (2014).
- 46 Imhof, B. A. & Aurrand-Lions, M. Adhesion mechanisms regulating the migration of monocytes. *Nature reviews. Immunology* 4, 432-444, doi:10.1038/nri1375 (2004).
- 47 Hou, J. et al. PTPRO plays a dual role in hepatic ischemia reperfusion injury through feedback activation of NF-kappaB. *Journal of hepatology* 60, 306-312, doi:10.1016/j.jhep.2013.09.028 (2014).
- 48 Martinez, F. O. & Gordon, S. The M1 and M2 paradigm of macrophage activation: time for reassessment. *F1000prime reports* 6, 13, doi:10.12703/P6-13 (2014).
- 49 Waddell, S. J. et al. Dissecting interferon-induced transcriptional programs in human peripheral blood cells. *PloS one* 5, e9753, doi:10.1371/journal.pone.0009753 (2010).
- 50 Bossi, D. et al. Functional characterization of a novel FGFR1OP-RET rearrangement in hematopoietic malignancies. *Molecular oncology* 8, 221-231, doi:10.1016/j.molonc.2013.11.004 (2014).
- 51 Qin, H., Wu, Q., Cowell, J. K. & Ren, M. FGFR1OP2-FGFR1 induced myeloid leukemia and T-cell lymphoma in a mouse model. *Haematologica* 101, e91-94, doi:10.3324/haematol.2015.137695 (2016).
- 52 Ballerini, P. et al. RET fusion genes are associated with chronic myelomonocytic leukemia and enhance monocytic differentiation. *Leukemia* 26, 2384-2389, doi:10.1038/leu.2012.109 (2012).
- 53 Giannandrea, M. & Parks, W. C. Diverse functions of matrix metalloproteinases during fibrosis. *Disease models & mechanisms* 7, 193-203 (2014).
- 54 Hemmann, S., Graf, J., Roderfeld, M. & Roeb, E. Expression of MMPs and TIMPs in liver fibrosis—a systematic review with special emphasis on anti-fibrotic strategies. *Journal of hepatology* 46, 955-975 (2007).
- 55 Vernon, M. A., Mylonas, K. J. & Hughes, J. in *Seminars in nephrology*. 302-317 (Elsevier).
- 56 Duffield, J. S. et al. Selective depletion of macrophages reveals distinct, opposing roles during liver injury and repair. *The Journal of clinical investigation* 115, 56-65 (2005).

- 57 Atabai, K. et al. Mfge8 diminishes the severity of tissue fibrosis in mice by binding and targeting collagen for uptake by macrophages. *The Journal of clinical investigation* 119, 3713-3722 (2009).
- 58 Lucattelli, M. et al. Collagen phagocytosis by lung alveolar macrophages in animal models of emphysema. *European Respiratory Journal* 22, 728-734 (2003).
- 59 Madsen, D. H. et al. M2-like macrophages are responsible for collagen degradation through a mannose receptor-mediated pathway. *The Journal of cell biology* 202, 951-966 (2013).
- 60 Yang, L. et al. Vascular endothelial growth factor promotes fibrosis resolution and repair in mice. *Gastroenterology* 146, 1339-1350 e1331, doi:10.1053/j.gastro.2014.01.061 (2014).
- 61 Fallowfield, J. A. et al. Scar-associated macrophages are a major source of hepatic matrix metalloproteinase-13 and facilitate the resolution of murine hepatic fibrosis. *The Journal of Immunology* 178, 5288-5295 (2007).
- 62 Ramachandran, P. et al. Differential Ly-6C expression identifies the recruited macrophage phenotype, which orchestrates the regression of murine liver fibrosis. *Proceedings of the National Academy of Sciences* 109, E3186-E3195 (2012).
- 63 Aldigier, J. C., Kanjanbuch, T., Ma, L.-J., Brown, N. J. & Fogo, A. B. Regression of existing glomerulosclerosis by inhibition of aldosterone. *Journal of the American Society of Nephrology* 16, 3306-3314 (2005).
- 64 Fioretto, P., Steffes, M. W., Sutherland, D. E., Goetz, F. C. & Mauer, M. Reversal of lesions of diabetic nephropathy after pancreas transplantation. *New England Journal of Medicine* 339, 69-75 (1998).
- 65 Pichaiwong, W. et al. Reversibility of structural and functional damage in a model of advanced diabetic nephropathy. *J Am Soc Nephrol* 24, 1088-1102, doi:10.1681/ASN.2012050445 (2013).
- 66 Sugimoto, H. et al. Activin-like kinase 3 is important for kidney regeneration and reversal of fibrosis. *Nature medicine* 18, 396-404 (2012).
- 67 Kanasty, R., Dorkin, J. R., Vegas, A. & Anderson, D. Delivery materials for siRNA therapeutics. *Nature materials* 12, 967-977 (2013).
- 68 Shu, D., Shu, Y., Haque, F., Abdelmawla, S. & Guo, P. Thermodynamically stable RNA three-way junction for constructing multifunctional nanoparticles for delivery of therapeutics. *Nature nanotechnology* 6, 658-667, doi:10.1038/nnano.2011.105 (2011).
- 69 Shu, Y., Cinier, M., Shu, D. & Guo, P. Assembly of multifunctional phi29 pRNA nanoparticles for specific delivery of siRNA and other therapeutics to targeted cells. *Methods* 54, 204-214 (2011).
- 70 Sundaram, P., Kurniawan, H., Byrne, M. E. & Wower, J. Therapeutic RNA aptamers in clinical trials. *European Journal of Pharmaceutical Sciences* 48, 259-271 (2013).
- 71 Yu, Z., Chen, T., Hebert, J., Li, E. & Richard, S. A mouse PRMT1 null allele defines an essential role for arginine methylation in genome maintenance and cell proliferation. *Molecular and cellular biology* 29, 2982-2996, doi:10.1128/MCB.00042-09 (2009).
- 72 Blanc, R. S., Vogel, G., Chen, T., Crist, C. & Richard, S. PRMT7 Preserves Satellite Cell Regenerative Capacity. *Cell Rep* 14, 1528-1539, doi:10.1016/j.celrep.2016.01.022 (2016).



# CHAPTER

Discussion & Future Directions

# 10

## Discussion and future directions

### Quaking mediates cellular phenotype

The cardiovascular system is comprised of a wide variety of cell types that possess the capacity to modulate their phenotype in response to acute and chronic injury. Transcriptional and post-transcriptional mechanisms play a key role regulating remodelling and regenerative responses to damaged cardiovascular tissues. Simultaneously, insufficient regulation of cellular phenotype is tightly coupled with the persistence and exacerbation of cardiovascular disease. Recently, RBPs have emerged as pivotal regulators of these functional adaptations in the cardiovascular system by guiding a wide-ranging number of post-transcriptional events that dramatically impact RNA fate, including alternative splicing, stability, localization and translation of both protein-coding and non-coding RNA species. While the focus of this thesis is the RNA-binding protein Quaking, Chapter 2 commences by reviewing the diverse functions of RBPs in the setting of cardiovascular disease. This examination of RBP function in healthy and diseased cardiomyocytes, ECs, VSMCs and monocytes/macrophages points towards a pivotal role for RBPs in the genome-wide processing of RNA species. A particularly striking observation is the fact that in response to injury, cardiomyocytes adopt a regenerative or adaptive phenotype that is coupled with the selective activation of an RNA expression profile that is highly similar to the foetal transcriptome. This suggests that alongside transcriptional changes, RBPs and other post-transcriptional pathways assume starring roles in orchestrating this response. Identifying the key regulators responsible for driving this transcriptome editing, and comparing them to developmental regulators, could reveal important clues as to the role of such RBPs in tissue regeneration following injury. Evidence suggesting that RBPs indeed play a critical role in this regenerative response can be derived from the fact that the homozygous disruption of RBP genes is oftentimes associated with cardiac- and/or vascular complications (see chapter 2 of this thesis).

A careful examination of QKI expression developmentally reveals clear vascular defects as a result of dysfunctional VSMCs, ECs, and cells of the myeloid lineage. Whether similar post-transcriptional pathways are involved on a single-cell level in embryologic development remains to be investigated. However, given the overlap in splicing between e.g. cancer cells and myeloid cells (such as alternative splicing of the ADD3 pre-mRNA<sup>1,2</sup>) and the spatial distribution of QRE ACUAA motifs proximal to cassette exons in monocytes/macrophages and muscle cells<sup>1,3</sup>, it is plausible to assume that similarities would exist in developmental and disease biology in QKI deficient embryos. Cell type-specific disruption of QKI in conditional knockout mice, as generated by Darbelli et al.<sup>4</sup>, could provide valuable insight into these questions.

A clear example of this phenotypic dichotomy in the vessel wall is the provided by the VSMC. The arterial vasculature harbours abundant VSMCs that serve to provide vascular tone, regulate vessel diameter and control blood flow<sup>5</sup>. Upon injury to the vessel wall, medial VSMCs are activated by serum factors that induce their proliferation, migration and production of extracellular matrix, enabling the VSMC



to aid in the repair of the damaged portion of the artery wall<sup>5-7</sup>. These proliferative VSMCs however are not terminally differentiated and possess the capacity to reversibly modulate their phenotype from the less differentiated 'synthetic state' and the differentiated 'contractile' state<sup>6,8</sup>. Importantly, the unabated proliferation of synthetic VSMCs can lead to rapid luminal narrowing that endangers peripheral tissues by impairing arterial blood flow<sup>5</sup> or perturb haemodialysis<sup>9,10</sup>. The reversible cellular state has historically been described to be regulated at the transcriptional level, most importantly in response to cooperative binding of the transcriptional co-activator Myocardin (Myocd)<sup>8,11-16</sup>. Although reports investigating gene-expression modulation by miRNAs in VSMCs are abundant<sup>17,18</sup>, other post-transcriptional regulators of VSMC phenotype plasticity are scarce. For example, hallmark genes encoding the contractile apparatus proteins of VSMCs have been described to be generated through alternative splicing<sup>19-24</sup>, but the RBPs responsible for these events have yet to be identified and studies testing for RBPs involved in generating these splicing patterns could enhance our understanding of VSMC plasticity. In chapter 3 of this thesis, we demonstrated that QKI critically mediates this functional transition by post-transcriptionally guiding Myocd splicing, a protein that by driving contractile apparatus protein expression<sup>12,13,15,25-27</sup> has been extensively described to be the master regulator of VSMC phenotype and homeostasis. The generation of alternative transcripts from the Myocd locus is of particular interest as these had previously been deemed to be either cardiac- or VSMC-enriched<sup>28,29</sup>. However, the QKI-mediated splicing of the 'exon 2a' (which contains an ACUAA motif at the most 5'-region of this alternative exon) prompted us to further investigate whether differential QKI expression could impact splice site recognition. Interestingly, inclusion of this exon generates a mature mRNA that encodes a premature stop-codon that had previously been described to influence cardiomyocyte and VSMC contractile apparatus protein expression<sup>20</sup>.

Our studies in healthy, quiescent VSMCs revealed low levels of QKI expression, suggesting that the RNA-binding properties of QKI are of limited utility in contractile VSMCs. In contrast, QKI expression is strongly induced in VSMCs in response to vascular injury, a biology that was observed both *in vitro* using primary human and mouse smooth muscle cells, as well as immunohistochemically in healthy versus restenotic artery. Importantly, this augmentation of QKI increases the likelihood that it can bind to RNA targets, one of which we demonstrated to be the Myocd pre-mRNA. This interaction affects the splicing of the alternative exon 2a, an event that markedly affects the balance of the MYOCD\_v1 and MYOCD\_v3 protein isoforms. Although both isoforms serve as co-transcriptional activators of Serum Response Factor (SRF), the N-terminal portion of MYOCD\_v1 confers this isoform with the unique capacity to also interact with the myocyte enhancing factor 2 (MEF2) family of transcription factors. This gain-of-function facilitates the transcriptional induction of a distinct subset of MYOCD\_v1-controlled genes as a result of MEF2-mediated DNA binding, facilitating the shift to the proliferative phenotype. To further validate this, future studies could include chromatin-IP and RNA-sequencing experiments to determine which genes are selectively induced

by MYOCD\_v1 and MYOCD\_v3 in healthy and diseased VSMCs (and cardiomyocytes).

Moreover, the alternative N-terminal region of Myocd that is either included or excluded by QKI-mediated alternative splicing, also encodes two out of three RPEL domains that allow for interaction with cytoplasmic free G-actin. This directly couples cytoskeletal dynamics to the nuclear availability of RPEL domain-containing proteins. Upon RhoGTPase activation, a transition from G-Actin to F-actin stress fibers is induced, diminishing the cytoplasmic G-actin pool, allowing RPEL domain-containing proteins to translocate to the nucleus<sup>30</sup>. Whether these RPEL domains in Myocd influence VSMC phenotype modulation has, to our knowledge, not yet been demonstrated. It could be argued that in contractile VSMCs, the 'proliferative' MYOCD\_v1 (containing 3 RPEL domains), is sequestered to the cellular cytoplasm by the abundant G-actin, effectively inhibiting MYOCD\_v1 from exerting co-transcriptional effects in the nucleus, limiting the induction of proliferative gene expression profiles. Upon vascular injury however, the rapid formation of cytoskeletal F-actin would deplete cytoplasmic G-actin reserves. As a consequence, MYOCD\_v1 would be released from cytoplasmic sequestration, allowing it to translocate to the nucleus and activate the reparative response. Moreover, the contractile MYOCD\_v3 isoform, described to contain but one RPEL domain<sup>30</sup>, would be less susceptible to this mode of cytoplasmic sequestration, prompting MYOCD\_v3 to be present in the cellular nucleus where it facilitates the constitutive expression of contractile genes required for VSMC function.

Within this thesis, we provide evidence that QKI is induced amidst conversion to the proliferative VSMC phenotype. Indeed, inspection of chromatin-IP data in the ENCODE database for SRF<sup>31</sup> indicates that SRF binds to the QKI promoter region, suggesting that MYOCD\_V1/SRF complex could augment QKI expression upon vascular injury, which could subsequently further favour the alternative splicing of the proliferative MYOCD\_v1 variant. Collectively, this would represent a positive-feedback loop for QKI-mediated VSMC phenotype switching. In contrast, a negative feedback loop upon completion of the reparative response could include the induction of miRNAs. Interestingly, miRNA-214 is induced in proliferating VSMCs<sup>32,33</sup>, and has also been demonstrated to target the QKI mRNAs<sup>34</sup>. We postulate that upon completion of the reparative response, miR214 could reduce QKI protein levels, thereby again favouring the alternative splicing of the Myocd\_v3, reverting the VSMC to the contractile phenotype, but this hypothesis remains to be tested.

Alongside the artery wall, VSMCs also serve critical roles in the (patho)physiological functioning of the venous circulation. While the role for QKI in these cells was not directly investigated, alterations in QKI expression in venous VSMCs could play a regulatory role in vascular complications such as maturation failure of venous bypasses or arteriovenous fistulas for coronary/peripheral artery disease or haemodialysis, respectively<sup>5,9,35-39</sup>. In conclusion, our findings imply that QKI is

a critical regulator of the functional plasticity that is required for VSMC function under both physiological and pathophysiological conditions.

The development and chronic progression of atherosclerotic lesions throughout life is the main driver of ischemic events such as myocardial infarction, insufficient peripheral arterial circulation and cerebral stroke. Collectively, these cardiovascular manifestations represent the leading cause of death worldwide<sup>40</sup>. In chapter 4 we illustrate how QKI plays a pivotal role in guiding RNA fate during the conversion of circulating monocytes into macrophages and foam cells, cells that form the bulk of cellular content within atherosclerotic plaques. More recently, the primary contributor to atherosclerotic plaque-composition and growth has become the subject of debate, as alongside the active recruitment of monocytes from the circulation, intra-plaque proliferation of macrophages has been described and attributed an important role in plaque progression<sup>41</sup>. Interestingly, we demonstrated that 1) the plaque-residing macrophage potently expresses QKI and 2) that the amount of QKI expressing cells in atherosclerotic lesions is correlated to disease burden. Our subsequent experiments showed perturbed adhesion, migration, differentiation and lipid phagocytosis of QKI deficient monocytes and macrophages, suggesting that QKI mediates atherosclerotic plaque composition through these pathways. However, the previous well-documented role of QKI in cellular proliferation and cell-cycle regulation<sup>42-48</sup> also suggests that QKI could potentially influence the proliferative capacity of local macrophages. By discovering QKI-dependant alternative splicing in monocytes and macrophages, events that are linked with a shift to the pro-inflammatory macrophage, we provide evidence that a targeted reduction of QKI could be beneficial for reducing atherosclerotic burden. The consequences of the identified QKI-dependent splicing events on protein function however, such as those observed in gamma-adducin (ADD3), Fc-gamma receptor 2B (FCGR2B) and very low-density lipoprotein receptor (VLDLR) are unknown and are currently being investigated. The identification of disease-advancing splice variants and ensuing proteins could be targeted by a single-gene approach using RNA-therapeutics. This rapidly expanding field is now developing and implementing numerous RNA-based approaches to target at a cell type- and sequence-specific level detrimental RNA species, including naked or lipid-encapsulated siRNA, exon-skipping oligonucleotides and RNA-aptamers. Importantly, these technologies have been employed in clinical trials, and have proven to possess good efficiency- and safety-profiles<sup>49-57</sup>.

Moreover, the data presented in chapter 6 of this thesis indicates that a monocyte-specific reduction of QKI ameliorates the macrophage-induced interstitial fibrosis of the kidney, further demonstrating a anti-inflammatory phenotype of QKI deficient monocytes/macrophages. In a collaborative effort with Dr. G.T.M. Wagenaar, we have also performed pioneering experiments to ameliorate the inflammation-induced damage in a model of pulmonary arterial hypertension by providing decoy RNAs as a substrate to saturate QKI and inhibit QKI activity. By doing this, we have progressed through the first steps to translate our initial insights to selectively ameliorate RBP activity in vivo.

During our progressing studies regarding the expression of QKI in the vasculature, we observed high levels of QKI protein being expressed in healthy ECs of both the macro- and microvasculature. In contrast to the role of microRNAs in ECs, little is known regarding the post-transcriptional regulation of RNA species by RBPs in ECs. The defining feature of these cells is their capacity to create a high resistance barrier that is selectively permeable for solutes, but also dictates the location and rate of leukocyte recruitment and diapedesis in response to local injury. As detailed in chapter 5 of this thesis, we showed that the abrogation of QKI expression perturbs EC-monolayer integrity, likely by interfering with the translation of the VE-cadherin and  $\beta$ -catenin mRNAs. Whether other potential target genes are involved, either through perturbation of QKI-mediated splicing events, or by affecting mRNA translatability or mRNA expression, remains to be elucidated. The recent identification that QKI-5 mediates the differentiation of human induced-pluripotent stem cells (iPSCs) to ECs is also noteworthy<sup>58</sup> and further substantiates our hypothesis that QKI is essential in EC homeostasis. Genome-wide analyses through RNA-sequencing of normal and QKI deficient human ECs, for example using blood-outgrowth or iPSC-derived ECs from the QKI haplo-insufficient patient and sisters, complemented by mouse studies using the conditional VE-cadherin Cre-recombinase, could be worth pursuing to fully determine the QKI-orchestrated transcriptome in ECs.

The realisation that QKI is a central governor of mRNA expression, alternative splicing and circular RNA formation, strongly suggests that QKI is a broad regulator of EC function, and is not selectively affecting the expression of a small subset of genes. However, the identification that QKI mediates the translatability of the mRNAs of VE-cadherin and CTNNB1, without significantly affecting mRNA levels, does illustrate an underappreciated role for RBPs in ECs, and for QKI in particular. Complementing the proposed RNA-sequencing analyses with proteomic analyses could identify many candidate genes that are regulated on the translational- but not the mRNA level. Moreover, the proteome in settings where alternative splicing is rampant has yet to occur for most studies, and could provide key insight into the functional consequences of splicing in ECs.

### **Have we overlooked the proteome?**

The collective studies within this thesis demonstrate a pivotal role for QKI in orchestrating the cellular transcriptome in a diverse variety of vascular cells in health and disease. While beyond the scope of this thesis, one could argue that a glaring omission in this biology is how these post-transcriptional events impact the cellular proteome. In particular, chapter 3 of this thesis illustrates significant changes in Myocd protein structure as a direct result of QKI-mediated splicing of the Myocd pre-mRNA. Moreover, we also demonstrate striking effects of these protein isoforms on cellular phenotype (contraction and proliferation of VSMCs) and the handling of vascular damage, further stressing the relevance of investigating the QKI-mediated cellular proteome in general. Perhaps the most striking example of this phenomenon is conferring the non-contractile and highly proliferative HITA2 VSMC<sup>59</sup> with the capacity to functionally contract upon a targeted

reduction of QKI concomitant with the induction of the 'contractile' MYOCD\_V3 isoform. Moreover, many of the QKI-induced alternative splicing events could very well induce translational frameshifts, resulting in truncated or non-functional proteins that are likely to be targeted for decay. The alternative splicing within and alternative poly-adenylation of 3'-UTRs further emphasises the importance of investigating mRNA translation. Given the physiological functioning of QKI within heterogeneous ribo-nucleoprotein complexes, one might also assume that the RNA-sequencing-based target genes could also be affected by a plethora of other RNA-interacting partners that influence mRNA translation. Similar to the Pumilio RBPs 60, preliminary studies have indeed demonstrated that QKI competes with miRNAs for binding to their designated binding motif which could thereby alter the efficiency with which target mRNAs are translated. The presence of stable, unspliced pre-mRNAs in circulating platelets, that are spliced and only translated after platelet activation<sup>61-64</sup> opens another promising avenue of investigation. Moreover, the reported enrichment of circular RNAs<sup>65</sup>, which have previously been proposed to be generated by QKI<sup>66</sup>, make QKI a strong candidate to influence platelet function. Initial studies within our lab indeed show expression of QKI within platelets and the effects of QKI depletion on platelet function are currently under investigation.

Collectively, the ongoing development of methodologies that will enhance the efficiency with which cellular proteomes can be elucidated, will undoubtedly yield more in-depth insight into the cellular proteome orchestrated by QKI, thereby expanding our knowledge insight into the role of QKI in cellular biology in health and disease.

### **Coupling RNA-recognition to other protein functions**

Many RBPs have been described to harbour a variety of distinct RNA-binding domains, mainly to enhance target affinity and sequence specificity<sup>67</sup>. Similarly, the co-existence of RBDs with other protein domains, including catalytic or domains that facilitate protein-protein interactions, add another level of biological regulation commonly attributed to RBPs<sup>68</sup>. An excellent example of this biological phenomenon is the bacterial Cas9 nuclease that first binds to a guide RNA that in turns binds in a sequence complementary fashion to DNA, thereby activating Cas9 catalytic properties that leads to the introduction of double-stranded DNA (dsDNA) breaks<sup>69</sup>. Moreover, given that these guide RNAs can be readily designed and synthesized, they provide new opportunities to introduce targeted dsDNA breaks. This relatively novel means of editing the cellular genome<sup>70,71</sup> holds great therapeutic potential for genetic diseases<sup>72,73</sup>.

Interestingly, a striking enrichment of DNA-binding properties have also been attributed to RBPs<sup>74</sup>. In some cases this is due to the presence of separate DNA- and RNA-binding motifs within one protein, but other examples include RBDs that do not readily discriminate between RNA and DNA. These domains should therefore be termed DNA/RNA-binding domains and the proteins that contain these arguably DNA/RNA-Binding Proteins (DRBPs)<sup>74</sup>.

Examples of this particular subgroup of DRBDs include the KH-domain <sup>75</sup> (which is also present in QKI) and the RRM <sup>76</sup>, both described to preferably bind the nucleic acid bases and not the ribose-phosphate backbone of single-stranded DNA or RNA<sup>77</sup>. The functionality of this “cross-reactivity” is easily illustrated by the DRBP TDP-43, for which crystal structures of the RRM in complex with DNA and RNA have been generated <sup>76</sup>. As such, TDP-43 has been attributed both RNA-splicing roles as evidenced by interactions with pre-mRNAs <sup>78</sup>, along with DNA-binding properties as a transcriptional repressor as a consequence of interactions with DNA motifs<sup>79</sup>. Intuitively, the binding motifs are quite similar (DNA motif: GTGTGT and the RNA motif: UGUGU.), although it should be noted that this motif similarity between DNA- and RNA-binding sites is not always so clear. Evidence for this ambiguous binding of the RRM to DNA and RNA is the NonO protein<sup>80,81</sup> where the RNA- and DNA-binding motifs are strikingly different (RNA motif: AGGGA<sup>80</sup>, DNA motif: ATGCAAAT<sup>82</sup>). These examples indicate that the regulation of DNA versus RNA recognition could potentially involve post-translational protein modifications. Indeed, the RNA-binding capacity of NonO seems to be affected by phosphorylation and is itself regulated by CDK180. Moreover, subcellular or subnuclear localization has also been reported to be affected by post-translational modifications that confer designated proteins with “multipurpose molecular scaffold” functions<sup>83</sup>.

In contrast, this promiscuous DNA- or RNA-binding has also been described to be relevant for traditional transcription factors such as NF- $\kappa$ B, which in turn is of great importance to the biology described in chapters 4 and 6 of this thesis<sup>84,85</sup>. Initial experiments designed to inhibit the DNA-binding function of this transcription factor demonstrated that RNA-aptamers display similar binding affinity for the NF- $\kappa$ B subunits p50/p65 as the protein to DNA<sup>86</sup>. The paradoxical finding that a DNA-aptamer, with an identical sequence as the functional RNA-aptamer, cannot bind to the p50 subunit is still not fully understood<sup>87</sup>. Moreover, crystal structures of DNA<sup>88</sup> and RNA<sup>89</sup> in complex with the p50 subunit have been generated, showing that RNA-aptamers with little sequence resemblance to their DNA counterparts both interact with similar protein interfaces. Collectively, it appears that the nucleic-acid binding domain of the NF- $\kappa$ B subunits can bind both DNA or RNA in an sequence-independent manner.

## Concluding remarks

In conclusion, although originally discovered by chance through the striking phenotype of the quaking mouse, leading to several decades of investigation regarding the role of the RBP QKI in nervous system development and function post-natally, it is now clear that QKI is a pivotal director of RNA fate in numerous physiological and pathophysiological settings.

In this respect, this thesis has contributed to:

- 1) The understanding of the RBP QKI in general.
- 2) The role of QKI in CVD by elucidating how QKI guides RNA fate in monocytes/macrophages, ECs and VSMCs.
- 3) The groundwork to translate our post-transcriptional insights into therapeutic strategies for CVDs in the future.

In concert with many collaborators, and fellow QKI research groups worldwide, the function of QKI has been broadened from myelin disorders to cardiovascular diseases, inflammatory and fibrotic responses to injury, schizophrenia, and cancer, including a striking role in paediatric angiocentric glioma.

From a highly personal perspective, in light of our expanding insight into the complexity of the human genome, as well as the critical role played by an ever-expanding number of RBPs involved in processing RNA, I firmly believe that we have only scratched the surface with respect to truly understanding the complexity of the human genome. In particular, I feel that the ever-accelerating developments within the field of biomedical sciences aimed at further elucidating RNA regulatory pathways in disease, and their eventual translation into therapeutic modalities will improve healthcare and will represent real advances to the clinicians toolkit.



## References

- 1 de Bruin, R. G. et al. Quaking promotes monocyte differentiation into pro-atherogenic macrophages by controlling pre-mRNA splicing and gene expression. *Nature communications* 7, 10846, doi:10.1038/ncomms10846 (2016).
- 2 Zong, F.-Y. et al. The RNA-binding protein QKI suppresses cancer-associated aberrant splicing. *PLoS genetics* 10, e1004289 (2014).
- 3 Hall, M. P. et al. Quaking and PTB control overlapping splicing regulatory networks during muscle cell differentiation. *Rna* 19, 627-638 (2013).
- 4 Darbelli, L., Vogel, G., Almazan, G. & Richard, S. Quaking Regulates Neurofascin 155 Expression for Myelin and Axoglial Junction Maintenance. *The Journal of neuroscience : the official journal of the Society for Neuroscience* 36, 4106-4120, doi:10.1523/JNEUROSCI.3529-15.2016 (2016).
- 5 Lacolley, P., Regnault, V., Nicoletti, A., Li, Z. & Michel, J.-B. The vascular smooth muscle cell in arterial pathology: a cell that can take on multiple roles. *Cardiovascular research* 95, 194-204 (2012).
- 6 Owens, G. K., Kumar, M. S. & Wamhoff, B. R. Molecular regulation of vascular smooth muscle cell differentiation in development and disease. *Physiological reviews* 84, 767-801, doi:10.1152/physrev.00041.2003 (2004).
- 7 Hoofnagle, M. H., Thomas, J. A., Wamhoff, B. R. & Owens, G. K. (Am Heart Assoc, 2006).
- 8 Shankman, L. S. et al. KLF4-dependent phenotypic modulation of smooth muscle cells has a key role in atherosclerotic plaque pathogenesis. *Nature medicine* 21, 628-637, doi:10.1038/nm.3866 (2015).
- 9 Roy-Chaudhury, P. et al. Neointimal hyperplasia in early arteriovenous fistula failure. *Am J Kidney Dis* 50, 782-790, doi:10.1053/j.ajkd.2007.07.019 (2007).
- 10 Wong, C. Y. et al. Vascular remodeling and intimal hyperplasia in a novel murine model of arteriovenous fistula failure. *Journal of vascular surgery* 59, 192-201 e191, doi:10.1016/j.jvs.2013.02.242 (2014).
- 11 Kumar, M. S. & Owens, G. K. Combinatorial control of smooth muscle-specific gene expression. *Arteriosclerosis, thrombosis, and vascular biology* 23, 737-747 (2003).
- 12 McDonald, O. G., Wamhoff, B. R., Hoofnagle, M. H. & Owens, G. K. Control of SRF binding to CArG box chromatin regulates smooth muscle gene expression in vivo. *The Journal of clinical investigation* 116, 36-48 (2006).
- 13 Miano, J. M. Myocardin in biology and disease. *J Biomed Res* 29, 3-19, doi:10.7555/JBR.29.20140151 (2015).
- 14 Wamhoff, B. R., Bowles, D. K. & Owens, G. K. Excitation-transcription coupling in arterial smooth muscle. *Circulation research* 98, 868-878 (2006).
- 15 Creemers, E. E., Sutherland, L. B., Oh, J., Barbosa, A. C. & Olson, E. N. Coactivation of MEF2 by the SAP domain proteins myocardin and MASTR. *Molecular cell* 23, 83-96, doi:10.1016/j.molcel.2006.05.026 (2006).
- 16 Rensen, S. et al. Expression of the smoothelin gene is mediated by alternative promoters. *Cardiovascular research* 55, 850-863 (2002).
- 17 Kang, H. & Hata, A. MicroRNA regulation of smooth muscle gene expression and phenotype. *Current opinion in hematology* 19, 224-231 (2012).
- 18 Pujol-López, M. et al. miRNA Update: A Review Focus on Clinical Implications of miRNA in Vascular Remodeling. *AIMS MEDICAL SCIENCE* 4, 99-112 (2017).



- 19 Byrne, B., Kaczorowski, Y., Coutu, M. & Craig, S. Chicken vinculin and meta-vinculin are derived from a single gene by alternative splicing of a 207-base pair exon unique to meta-vinculin. *Journal of Biological Chemistry* 267, 12845-12850 (1992).
- 20 Ilagan, R. M. et al. Smooth muscle phenotypic diversity is mediated through alterations in myocardin gene splicing. *Journal of cellular physiology* 226, 2702-2711 (2011).
- 21 Lenz, S., Lohse, P., Seidel, U. & Arnold, H. The alkali light chains of human smooth and nonmuscle myosins are encoded by a single gene. Tissue-specific expression by alternative splicing pathways. *Journal of Biological Chemistry* 264, 9009-9015 (1989).
- 22 Nabeshima, Y., Nonomura, Y. & Fujii-Kuriyama, Y. Nonmuscle and smooth muscle myosin light chain mRNAs are generated from a single gene by the tissue-specific alternative RNA splicing. *Journal of Biological Chemistry* 262, 10608-10612 (1987).
- 23 Nagai, R., Kuro-o, M., Babij, P. & Periasamy, M. Identification of two types of smooth muscle myosin heavy chain isoforms by cDNA cloning and immunoblot analysis. *Journal of Biological Chemistry* 264, 9734-9737 (1989).
- 24 Ruiz-Opazo, N. & Nadal-Ginard, B. Alpha-tropomyosin gene organization. Alternative splicing of duplicated isotype-specific exons accounts for the production of smooth and striated muscle isoforms. *Journal of Biological Chemistry* 262, 4755-4765 (1987).
- 25 Chen, J., Kitchen, C. M., Streb, J. W. & Miano, J. M. Myocardin: a component of a molecular switch for smooth muscle differentiation. *Journal of molecular and cellular cardiology* 34, 1345-1356 (2002).
- 26 Wang, Z. et al. Myocardin and ternary complex factors compete for SRF to control smooth muscle gene expression. *Nature* 428, 185-189 (2004).
- 27 Yoshida, T. et al. Myocardin is a key regulator of CArG-dependent transcription of multiple smooth muscle marker genes. *Circulation research* 92, 856-864 (2003).
- 28 Imamura, M., Long, X., Nanda, V. & Miano, J. M. Expression and functional activity of four myocardin isoforms. *Gene* 464, 1-10 (2010).
- 29 Wang, D.-Z. et al. Activation of cardiac gene expression by myocardin, a transcriptional cofactor for serum response factor. *Cell* 105, 851-862 (2001).
- 30 Olson, E. N. & Nordheim, A. Linking actin dynamics and gene transcription to drive cellular motile functions. *Nature reviews. Molecular cell biology* 11, 353 (2010).
- 31 Gerstein, M. B. et al. Architecture of the human regulatory network derived from ENCODE data. *Nature* 489, 91-100 (2012).
- 32 Wu, Y. et al. MicroRNA-214 regulates smooth muscle cell differentiation from stem cells by targeting RNA-binding protein QKI. *Oncotarget* 8, 19866 (2017).
- 33 Sahoo, S. et al. MEF2C-MYOC and Leiomodin1 suppression by miRNA-214 promotes smooth muscle cell phenotype switching in pulmonary arterial hypertension. *PLoS one* 11, e0153780 (2016).
- 34 van Mil, A. et al. MicroRNA-214 inhibits angiogenesis by targeting Quaking and reducing angiogenic growth factor release. *Cardiovascular research* 93, 655-665, doi:10.1093/cvr/cvs003 (2012).
- 35 Lee, T. et al. Severe venous neointimal hyperplasia prior to dialysis access surgery. *Nephrology Dialysis Transplantation* 26, 2264-2270 (2011).
- 36 Lee, T. et al. in *Seminars in dialysis*. 592-595 (Wiley Online Library).
- 37 Rothuizen, T. C. et al. Arteriovenous access failure: more than just intimal hyperplasia? *Nephrology, dialysis, transplantation : official publication of the European Dialysis and Transplant Association - European Renal Association* 28, 1085-1092, doi:10.1093/ndt/

- gft068 (2013).
- 38 de Vries, M. R., Simons, K. H., Jukema, J. W., Braun, J. & Quax, P. H. Vein graft failure: from pathophysiology to clinical outcomes. *Nature Reviews Cardiology* 13, 451-470 (2016).
  - 39 Libby, P. Mechanisms of acute coronary syndromes and their implications for therapy. *New England Journal of Medicine* 368, 2004-2013 (2013).
  - 40 Mendis, S., Puska, P. & Norrving, B. Global atlas on cardiovascular disease prevention and control. (World Health Organization, 2011).
  - 41 Robbins, C. S. et al. Local proliferation dominates lesional macrophage accumulation in atherosclerosis. *Nature medicine* 19, 1166-1172, doi:10.1038/nm.3258 (2013).
  - 42 Biedermann, B., Hotz, H.-R. & Ciosk, R. The Quaking family of RNA-binding proteins: coordinators of the cell cycle and differentiation. *Cell cycle* 9, 1929-1933 (2010).
  - 43 Casaccia-Bonnel, P. et al. Loss of p27Kip1 function results in increased proliferative capacity of oligodendrocyte progenitors but unaltered timing of differentiation. *Development* 126, 4027-4037 (1999).
  - 44 Fu, X. & Feng, Y. QKI-5 suppresses cyclin D1 expression and proliferation of oral squamous cell carcinoma cells via MAPK signalling pathway. *Int J Oral Maxillofac Surg* 44, 562-567, doi:10.1016/j.ijom.2014.10.001 (2015).
  - 45 He, B. et al. MicroRNA-155 promotes the proliferation and invasion abilities of colon cancer cells by targeting quaking. *Mol Med Rep* 11, 2355-2359, doi:10.3892/mmr.2014.2994 (2015).
  - 46 Yang, G. et al. RNA-binding protein quaking, a critical regulator of colon epithelial differentiation and a suppressor of colon cancer. *Gastroenterology* 138, 231-240.e231-235, doi:10.1053/j.gastro.2009.08.001 (2010).
  - 47 Yang, G. et al. E2F1 and RNA binding protein QKI comprise a negative feedback in the cell cycle regulation. *Cell cycle* 10, 2703-2713, doi:10.4161/cc.10.16.15928 (2011).
  - 48 Zhang, R. L. et al. RNA-binding protein QKI-5 inhibits the proliferation of clear cell renal cell carcinoma via post-transcriptional stabilization of RASA1 mRNA. *Cell cycle* 15, 3094-3104, doi:10.1080/15384101.2016.1235103 (2016).
  - 49 Aartsma-Rus, A. New Momentum for the Field of Oligonucleotide Therapeutics. *Molecular therapy : the journal of the American Society of Gene Therapy* 24, 193-194, doi:10.1038/mt.2016.14 (2016).
  - 50 Fitzgerald, K. et al. Effect of an RNA interference drug on the synthesis of proprotein convertase subtilisin/kexin type 9 (PCSK9) and the concentration of serum LDL cholesterol in healthy volunteers: a randomised, single-blind, placebo-controlled, phase 1 trial. *Lancet* 383, 60-68, doi:10.1016/S0140-6736(13)61914-5 (2014).
  - 51 Gaur, R. K. RNA interference: a potential therapeutic tool for silencing splice isoforms linked to human diseases. *Biotechniques Suppl*, 15-22 (2006).
  - 52 Kanasty, R., Dorkin, J. R., Vegas, A. & Anderson, D. Delivery materials for siRNA therapeutics. *Nature materials* 12, 967-977 (2013).
  - 53 Shu, D., Shu, Y., Haque, F., Abdelmawla, S. & Guo, P. Thermodynamically stable RNA three-way junction for constructing multifunctional nanoparticles for delivery of therapeutics. *Nature nanotechnology* 6, 658-667, doi:10.1038/nnano.2011.105 (2011).
  - 54 Siva, K., Covello, G. & Denti, M. A. Exon-skipping antisense oligonucleotides to correct missplicing in neurogenetic diseases. *Nucleic acid therapeutics* 24, 69-86, doi:10.1089/nat.2013.0461 (2014).
  - 55 Sundaram, P., Kurniawan, H., Byrne, M. E. & Wower, J. Therapeutic RNA aptamers in

- clinical trials. *European Journal of Pharmaceutical Sciences* 48, 259-271 (2013).
- 56 Weinberg, M. S. Therapeutic aptamers march on. *Molecular therapy. Nucleic acids* 3, e194, doi:10.1038/mtna.2014.46 (2014).
- 57 Yla-Herttuala, S. Gene Therapy for Heart Failure: Back to the Bench. *Molecular therapy : the journal of the American Society of Gene Therapy* 23, 1551-1552, doi:10.1038/mt.2015.158 (2015).
- 58 Cochrane, A. et al. Quaking Is a Key Regulator of Endothelial Cell Differentiation, Neovascularization, and Angiogenesis. *STEM CELLS* 35, 952-966 (2017).
- 59 Li, S. et al. Innate diversity of adult human arterial smooth muscle cells. *Circulation research* 89, 517-525 (2001).
- 60 HafezQorani, S. et al. Modeling the combined effect of RNA-binding proteins and microRNAs in post-transcriptional regulation. *Nucleic acids research* 44, e83-e83 (2016).
- 61 Denis, M. M. et al. Escaping the nuclear confines: signal-dependent pre-mRNA splicing in anucleate platelets. *Cell* 122, 379-391, doi:10.1016/j.cell.2005.06.015 (2005).
- 62 Schubert, S., Weyrich, A. S. & Rowley, J. W. A tour through the transcriptional landscape of platelets. *Blood* 124, 493-502 (2014).
- 63 Schwertz, H. et al. Signal-dependent splicing of tissue factor pre-mRNA modulates the thrombogenicity of human platelets. *Journal of Experimental Medicine* 203, 2433-2440 (2006).
- 64 Shashkin, P. N., Brown, G. T., Ghosh, A., Marathe, G. K. & McIntyre, T. M. Lipopolysaccharide is a direct agonist for platelet RNA splicing. *The Journal of Immunology* 181, 3495-3502 (2008).
- 65 Alhasan, A. A. et al. Circular RNA enrichment in platelets is a signature of transcriptome degradation. *Blood* 127, e1-e11 (2016).
- 66 Conn, S. J. et al. The RNA binding protein quaking regulates formation of circRNAs. *Cell* 160, 1125-1134 (2015).
- 67 Lunde, B. M., Moore, C. & Varani, G. RNA-binding proteins: modular design for efficient function. *Nature reviews. Molecular cell biology* 8, 479-490 (2007).
- 68 Gerstberger, S., Hafner, M. & Tuschl, T. A census of human RNA-binding proteins. *Nature Reviews Genetics* 15, 829-845 (2014).
- 69 Jinek, M. et al. Structures of Cas9 endonucleases reveal RNA-mediated conformational activation. *Science* 343, 1247997 (2014).
- 70 Garneau, J. E. et al. The CRISPR/Cas bacterial immune system cleaves bacteriophage and plasmid DNA. *Nature* 468, 67-71 (2010).
- 71 Jinek, M. et al. A programmable dual-RNA-guided DNA endonuclease in adaptive bacterial immunity. *Science* 337, 816-821 (2012).
- 72 Mali, P., Esvelt, K. M. & Church, G. M. Cas9 as a versatile tool for engineering biology. *Nature methods* 10, 957-963 (2013).
- 73 Savić, N. & Schwank, G. Advances in therapeutic CRISPR/Cas9 genome editing. *Translational Research* 168, 15-21 (2016).
- 74 Hudson, W. H. & Ortlund, E. A. The structure, function and evolution of proteins that bind DNA and RNA. *Nature reviews. Molecular cell biology* 15, 749-760, doi:10.1038/nrm3884 (2014).
- 75 Braddock, D. T., Louis, J. M., Baber, J. L., Levens, D. & Clore, G. M. Structure and dynamics of KH domains from FBP bound to single-stranded DNA. *Nature* 415, 1051-1056 (2002).
- 76 Kuo, P. H., Doudeva, L. G., Wang, Y. T., Shen, C. K. & Yuan, H. S. Structural insights

- into TDP-43 in nucleic-acid binding and domain interactions. *Nucleic acids research* 37, 1799-1808, doi:10.1093/nar/gkp013 (2009).
- 77 Allers, J. & Shamoo, Y. Structure-based analysis of protein-RNA interactions using the program ENTANGLE. *J Mol Biol* 311, 75-86, doi:10.1006/jmbi.2001.4857 (2001).
- 78 Tollervay, J. R. et al. Characterizing the RNA targets and position-dependent splicing regulation by TDP-43. *Nat Neurosci* 14, 452-458, doi:http://www.nature.com/neuro/journal/v14/n4/abs/nn.2778.html#supplementary-information (2011).
- 79 Lalmansingh, A. S., Urekar, C. J. & Reddi, P. P. TDP-43 is a transcriptional repressor: the testis-specific mouse *acr1* gene is a TDP-43 target in vivo. *The Journal of biological chemistry* 286, 10970-10982, doi:10.1074/jbc.M110.166587 (2011).
- 80 Basu, A., Dong, B., Krainer, A. R. & Howe, C. C. The intracisternal A-particle proximal enhancer-binding protein activates transcription and is identical to the RNA-and DNA-binding protein p54nrb/NonO. *Molecular and cellular biology* 17, 677-686 (1997).
- 81 Yadav, S. P. et al. The transcription-splicing protein NonO/p54nrb and three NonO-interacting proteins bind to distal enhancer region and augment rhodopsin expression. *Human molecular genetics* 23, 2132-2144 (2014).
- 82 Yang, Y. et al. NonO, a non-POU-domain-containing, octamer-binding protein, is the mammalian homolog of *Drosophila* nonAdiss. *Molecular and cellular biology* 13, 5593-5603 (1993).
- 83 Knott, G. J., Bond, C. S. & Fox, A. H. The DBHS proteins SFPQ, NONO and PSPC1: a multipurpose molecular scaffold. *Nucleic acids research* 44, 3989-4004 (2016).
- 84 Baeuerle, P. A. & Henkel, T. Function and activation of NF-kappaB in the immune system. *Annual review of immunology* 12, 141-179 (1994).
- 85 Baker, R. G., Hayden, M. S. & Ghosh, S. NF-kB, inflammation, and metabolic disease. *Cell metabolism* 13, 11-22 (2011).
- 86 Wurster, S. E. & Maher, L. J., 3rd. Selection and characterization of anti-NF-kappaB p65 RNA aptamers. *Rna* 14, 1037-1047, doi:10.1261/rna.878908 (2008).
- 87 Lebruska, L. L. & Maher, L. J. Selection and characterization of an RNA decoy for transcription factor NF-kB. *Biochemistry* 38, 3168-3174 (1999).
- 88 Muller, C. W., Rey, F. A., Sodeoka, M., Verdine, G. L. & Harrison, S. C. Structure of the NF-kappa B p50 homodimer bound to DNA. *Nature* 373, 311-317, doi:10.1038/373311a0 (1995).
- 89 Huang, D. B. et al. Crystal structure of NF-kappaB (p50)<sub>2</sub> complexed to a high-affinity RNA aptamer. *Proceedings of the National Academy of Sciences of the United States of America* 100, 9268-9273, doi:10.1073/pnas.1632011100 (2003).





# CHAPTER

## Appendices

Curriculum Vitae

Bibliography

Dankwoord

# 11





## Curriculum vitae

The author of this thesis, Ruben Gosewinus de Bruin was born on the 7th of august 1987 in the Hague. Ruben attended primary school at “Wonnebald”, a school with a focus on creativity and the natural sciences. He subsequently continued his education at the “Sorghvliet” gymnasium in the Hague.

After graduating with honours in 2006 he pursued his ambition to study medicine at the Leiden University Medical Center. After his second year, Ruben enrolled in a simultaneous pre-master program in biomedical sciences to broaden his horizons and acquire expertise in molecular biology. He concomitantly interrupted his medical training and commenced with his Ph.D. training in vascular- and molecular biology within the department of Nephrology headed by prof. dr. A.J. Rabelink. Within the research group of prof. dr. A.J. van Zonneveld and under supervision of dr. E.P. van der Veer, Ruben worked on his doctoral research project for 4.5 years.

11

Within this period, Ruben assisted in the envisionment and development of a new ‘Heart and the Blood Vessels’ half-minor. This program was geared towards 3rd year medical students, providing them with an opportunity acquire state of the art knowledge and insight into the molecular pathways and novel therapeutics being developed within the field of cardiovascular medicine.

During his doctoral research project, Ruben was awarded several travel awards, including one from the Royal Netherlands Academy of Arts and Sciences (KNAW), which enabled him to present his research on international podia at the American Heart Association Scientific Sessions and the Kidney Week organised by the American Society of Nephrology. He also regularly attended the annual meetings of the RNA Society and the Dutch Endothelial Biology Society. During these meetings, strong collaborations with renowned international research groups were forged, including that of Prof. Dr. Manuel Ares Jr. at the University of Santa Cruz in California and Prof. Dr. Stéphane Richard at the Lady Davis Institute at McGill University, where he worked as a visiting scientist.

In 2015, Ruben resumed his medical studies by undertaking diverse clinical internships at hospitals in the Leiden and the Hague area. He graduated with honours from medical school in 2017 and continued working as a medical doctor in Gouda. He is now an internist in training at the Leiden University Medical Center with the goal of becoming an interventional-nephrologist.

## Bibliography

**de Bruin RG**, Rabelink TJ, van Zonneveld AJ, van der Veer EP. Emerging roles for RNA-binding proteins as effectors and regulators of cardiovascular disease. *European Heart Journal* 2017, May 7;38(18):1380-1388. PMID: 28064149

Bijkerk R, **de Bruin RG**, van Solingen C, van Gils JM, Duijs JM, van der Veer EP, Rabelink TJ, Humphreys BD, van Zonneveld AJ. Silencing of microRNA-132 reduces renal fibrosis by selectively inhibiting myofibroblast proliferation. *Kidney International* 2016, Jun;89(6):1268-80. Epub 2016 Apr 8. PMID: 27165825

HafezQorani S, Lafzi A, **de Bruin RG**, van Zonneveld AJ, van der Veer EP, Son YA, Kazan H. Modeling the combined effect of RNA-binding proteins and microRNAs in post-transcriptional regulation. *Nucleic Acids Research* 2016, May 19;44(9):e83. PMID: 2683757

**de Bruin RG**, Shiue L, Prins J, de Boer HC, Singh A, Fagg WS, van Gils JM, Duijs JM, Katzman S, Kraaijeveld AO, Böhringer S, Leung WY, Kielbasa SM, Donahue JP, van der Zande PH, Sijbom R, van Alem CM, Bot I, van Kooten C, Jukema JW, Van Esch H, Rabelink TJ, Kazan H, Biessen EA, Ares M Jr, van Zonneveld AJ, van der Veer EP. Quaking promotes monocyte differentiation into pro-atherogenic macrophages by controlling pre-mRNA splicing and gene expression. *Nature Communications* 2016, Mar 31;7:10846. PMID: 27029405

**de Bruin RG**, van der Veer EP, Prins J, Lee DH, Dane MJ, Zhang H, Roeten MK, Bijkerk R, de Boer HC, Rabelink TJ, van Zonneveld AJ, van Gils JM. The RNA-binding protein quaking maintains endothelial barrier function and affects VE-cadherin and  $\beta$ -catenin protein expression. *Nature Scientific Reports* 2016 Feb 24;6:21643 PMID: 26905650

Bijkerk R, van Solingen C, de Boer HC, van der Pol P, Khairoun M, **de Bruin RG**, van Oeveren-Rietdijk AM, Lievers E, Schlagwein N, van Gijlswijk DJ, Roeten MK, Neshati Z, de Vries AA, Rodijk M, Pike-Overzet K, van den Berg YW, van der Veer EP, Versteeg HH, Reinders ME, Staal FJ, van Kooten C, Rabelink TJ, van Zonneveld AJ. Hematopoietic microRNA-126 protects against renal ischemia/reperfusion injury by promoting vascular integrity. *Journal of the American Society of Nephrology* 2014 Aug;25(8):1710-22 PMID: 24610930

van der Veer EP, **de Bruin RG**, Kraaijeveld AO, de Vries MR, Bot I, Pera T, Segers FM, Trompet S, van Gils JM, Roeten MK, Beckers CM, van Santbrink PJ, Janssen A, van Solingen C, Swildens J, de Boer HC, Peters EA, Bijkerk R, Rousch M, Doop M, Kuiper J, Schaliij MJ, van der Wal AC, Richard S, van Berkel TJ, Pickering JG, Hiemstra PS, Goumans MJ, Rabelink TJ, de Vries AA, Quax PH, Jukema JW, Biessen EA, van Zonneveld AJ. Quaking, an RNA-binding protein, is a critical regulator of vascular smooth muscle cell phenotype.

*Circulation Research* 2013, Oct 12;113(9):1065-75. PMID: 23963726

Bijkerk R, **de Bruin RG**, van Solingen C, Duijs JM, Kobayashi K, van der Veer EP, ten Dijke P, Rabelink TJ, Goumans MJ, van Zonneveld AJ. MicroRNA-155 functions as a negative regulator of RhoA signaling in TGF- $\beta$ -induced endothelial to mesenchymal transition.

*Microna*. 2012;1(1):2-10. PMID: 25048084

## Dankwoord

Na ruim 4 jaar als fulltime onderzoeker te hebben gewerkt, zou ik graag iedereen bedanken die heeft bijgedragen aan het geweldige onderzoeksklimaat binnen de afdeling **Nierziekten** en het **Eindhoven Laboratorium**. Het was ontzettend leerzaam en leuk om samen te werken met een dynamische groep van gemotiveerde studenten, analisten, clinici, collega promovendi, postdocs en professoren vanuit het LUMC en daarbuiten. Dank voor de bereidheid om jullie kennis, kunde en inzichten met mij te delen. Dit proefschrift is tot stand gekomen met hulp van velen, graag zou ik van deze gelegenheid gebruik maken om enkelen in het bijzonder te bedanken.

11

**Anton-Jan**, allereerst zou ik je willen bedanken voor de enorme vrijheid waarin ik binnen jouw onderzoeksgroep aan mijn proefschrift heb mogen werken en de kansen welke jij mij hebt geboden. Je stuurde me bij waar nodig, was altijd enthousiast, ook over de kleinste resultaten en je was altijd bereid om mee te denken zonder daarbij directief te zijn. Ik vond het bijzonder te zien en te merken dat jouw deur *altijd* open stond voor iedereen, een mooie eigenschap! Dankzij jouw mentorschap heb ik geleerd om zelfstandig wetenschappelijke vraagstukken en het bijbehorend plan van aanpak te formuleren en uit te voeren, mijn dank daarvoor. Ik hoop dat onze paden nog vaak zullen kruisen in de toekomst.

**Eric**, zonder jouw onuitputtelijk enthousiasme, je doorzettingsvermogen en je geloof in ons Quaking onderzoek én in mij als persoon, zou mijn tijd als promovendus en het resultaat hiervan nooit zo mooi geweest zijn. Dank voor je vriendschap, de mooie jaren samen in het lab en alles wat ik van je heb geleerd op wetenschappelijk en persoonlijk vlak. Ik hoop dat het ons gegund is in de toekomst nogmaals samen te werken.

**Janine**, ik heb genoten van onze samenwerking en heb erg veel van je geleerd, mijn dank daarvoor. Een mooi hoofdstuk in dit proefschrift is het resultaat van onze geweldige samenwerking! Dank ook aan **alle co-auteurs** van de artikelen welke in dit proefschrift staan gedrukt. Zonder jullie bereidheid tot samenwerking waren de manuscripten lang niet zo mooi en compleet geweest. **Jurriën**, jij in het bijzonder dank voor je inzet en enorm scherpe analyses van de data, ik wens je succes met het afronden van je eigen promotie en je toekomstige carrière als wetenschapper.

**Ton**, ook jou wil ik hier graag bedanken, enthousiast wetenschapper, kundig arts en bestuurder maar vooral een motivator in hart en nieren. Ondanks je immer volle agenda dank ik je voor het vrijmaken van tijd voor mij, voor de vele inspirerende gesprekken die we hebben gehad en de mooie toekomstplannen die we samen hebben gesmeed. Ik hoop nog lang gebruik te mogen maken van je mentorschap.

**Stephane**, I have truly never felt so welcome in a foreign country. Your welcoming, warm, hyper-intelligent and often energetic character is one to aspire to. The great science in your lab, the home-dinners, the trips to Tremblant, the incredible restaurants you took me, thank you for the experience of a lifetime. I look forward to our continued friendship and sincerely hope that I can rely on your guidance for many years to come. Dear **Richard lab members**, thank you for making me feel at home in the lab in Montréal and the great times we had together. **Gillian**, thanks for all the work you did for me, you're an excellent researcher and above all a wonderful person.

**Melchior en Roel**, gewaardeerde paranimfen, wat gaaf om jullie naast me te hebben op deze dag. Met mijn eigen broer én mijn "broer in de wetenschap" aan mijn zijde kan ik alles op persoonlijk én wetenschappelijk vlak aan. Roel, dank voor de samenwerking de afgelopen jaren, ik hoop in de toekomst nog vaak met je te mogen samenwerken.

Lieve **familie**, dank voor jullie onvoorwaardelijke steun en vertrouwen in mij als mens, onderzoeker en dokter. Dankzij de stabiele basis die jullie me hebben gegeven, heb ik mij kunnen ontwikkelen tot wie ik nu ben. Lieve **Heleen**, inmiddels ruim twee jaar samen, vol vertrouwen en nieuwsgierigheid kijk ik uit naar onze toekomst samen, het voelt zo ontzettend goed!